

# Integrating Solar PV Systems into Residential Buildings in Cold-climate Regions: The Impact of Energy-efficient Homes on Shaping the Future Smart Grid

by

Hadia Awad

A thesis submitted in partial fulfillment of the requirements for the degree of

Doctor of Philosophy

in

Construction Engineering and Management

Department of Civil and Environmental Engineering

University of Alberta

© Hadia Awad, 2018

## **Abstract**

The integration of solar energy systems into residential buildings is an emerging trend worldwide and is an important method of mitigating the impact of housing on greenhouse gas (GHG) emissions. To achieve optimal energy performance, the generating capacity of solar photovoltaic systems (PVs) must be designed to match the electricity loads of a given building and the impacts of solar PVs on the utility grid must be investigated, particularly in cold-climate regions. As Net-zero Energy Homes (NZEHS) equipped with solar PVs gain market penetration, maintaining the resilience of the utility grid becomes an increasingly challenging task. In current NZEH practice, in order to minimise the GHG emissions, space heating and domestic hot water supply use electricity as energy source. Intrinsically, in cold climates, NZEHs consume 2–3 times the amount of electricity to that of a typical energy-efficient home (EEH). Large-scale implementation of NZEHs such as NZEH communities will further add dynamic complexities.

Hence, the research presented in this thesis aims to develop a generic roadmap to improve the solar PV self-consumption of sustainable communities and individual households by improving the PV design and prioritising its self-consumption. Accordingly, the present study aims to achieve the following objectives: (1) understand the local energy load and generation patterns and their impact on the grid, (2) develop a solar PV prediction model, (3) develop a load-match-driven PV

optimisation tool, and (4) simulate and optimise NZEH and EEH communities equipped with community shared solar PVs.

Results indicate that, in order to maximise the self-consumption of a PV system, it is necessary to consider the type of house being serviced. In general, provided that the present study is conducted in a high-latitude region, the tilt angle required for NZEHs is found to be higher than that for EEHs. On the other hand, the optimum azimuth angle for both NZEHs and EEHs is found to be south-west facing. It is also concluded that the implementation of community shared solar PVs can provide significant improvement in self-consumption and economic aspects compared with individual PVs following the current practice. The presented thesis also includes recommendations for future work.

## Preface

This thesis is an original work by Ms. Hadia Awad. Four chapters of this thesis have been published or submitted for journal publication. An additional conference proceeding is provided in the Appendix as a practical application to the research presented in this thesis, aiming for its expansion to become a future journal publication.

A version of Chapter 2 has been submitted for publication in *Applied Energy Journal*, as Awad H, Gül M, and Al-Hussein M “Long-term performance analysis and simulation of small-scale grid-tied residential Solar PV systems in Alberta, Canada”. Ms. Hadia Awad was responsible for the review of literature, long-term data monitoring and collection from the investigated sites (86 PV systems across Alberta), database development and information extraction using SQL queries, long-term energy performance analysis of the monitored solar PV systems, results validation, and manuscript composition. Dr. Mustafa Gül was the supervisory author and was involved in concept formation, analyses, and manuscript composition. Dr. Mohamed Al-Hussein was the supervisory author and was involved in concept formation, analyses, and manuscript composition.

A version of Chapter 3 has been published in the *International Journal of Sustainable Energy*, as Awad H, Gül M, Salim K M Emtiaz, and Yu H, “Predicting the Energy Production by Solar Photovoltaic Systems in Cold-climate Regions”. Ms. Hadia Awad was responsible for the development and structuring of the Artificial Neural Network model, collection of the relevant performance parameters, long-term data monitoring and collection from the investigated sites (85 PV systems across Alberta), database development and information extraction using SQL queries, long-term energy performance analysis of the monitored solar PV systems, development of clear-sky PV power output at any two-way tilted surface mathematical model, development of smart persistence model, model validation, and manuscript composition. Dr. Mustafa Gül was the supervisory author and was involved in

concept formation, analyses, and manuscript composition. Mr. K M Emtiaz Salim was responsible for the review of literature, long-term data monitoring and collection from the investigated sites, and long-term energy performance analysis of the monitored solar PV systems. Dr. Haitao Yu, the industry partner of the project by which this paper was developed, was the advisory author and was involved in parts of the concept formation and analyses.

A version of Chapter 4 has been submitted for publication in *Solar Energy Journal*, as Awad H and Gül M, “Load-match-driven Design of Solar PV Systems and Its Impact on the Grid”. Ms. Hadia Awad was responsible for the overall concept formation, review of literature, long-term data monitoring and collection from the investigated sites (85 PV systems across Alberta and 11 houses in Edmonton), development of clear-sky PV power output at any two-way tilted surface analytical model, development of a generalised reduced gradient (GRG) non-linear optimisation engine, model validation, and manuscript composition. Dr. Mustafa Gül was the supervisory author and was involved in concept formation, analyses, and manuscript composition.

A version of Chapter 5 has been submitted for publication in *Sustainable Cities and Society Journal* as Awad H and Gül M, “Optimisation of Community Shared Solar Application in Energy Efficient Communities using Monte Carlo Simulations”. Ms. Hadia Awad was responsible for the overall concept formation, review of literature, long-term data monitoring and collection from the investigated sites (11 houses in Edmonton), development of the Monte Carlo simulation model, implementation of the clear-sky PV power output at any two-way tilted surface analytical model developed in the previous paper, implementation of a generalised reduced gradient (GRG) non-linear optimisation engine developed in the previous chapter, model validation, and manuscript composition. Dr. Mustafa Gül was the supervisory author and was involved in concept formation, analyses, and manuscript composition.

Finally, a version of Appendix A has been presented and published in proceedings of *the 4<sup>th</sup> IEEE Conference on Technologies for Sustainability (SusTech)*, Phoenix,

Arizona, October 2016 as Awad H, Gül M, Ritter C, Verma P, Chen Y, Salim K, Al-Hussein M, Yu H, and Kasawski K, “Solar Photovoltaic Optimisation for Commercial Flat Rooftops in Cold Regions”. Ms. Hadia Awad was responsible for the concept formation, long-term data monitoring and collection from the investigated sites (48 PV sites in Edmonton), algorithm development, data analyses, and manuscript composition. Dr. Mustafa Gül was the supervisory author and was involved in concept formation, analyses, and manuscript composition. Ms. Chelsea Ritter was responsible for the optimisation model structure and development, data validation, and manuscript composition. Mr. Preshit Verma was responsible for the financial analysis section of the study and manuscript composition. Ms. Yuan Chen was responsible for the review of literature and manuscript composition. Mr. K M Emtiaz Salim was involved in the data collection and analysis process. Dr. Haitao Yu, the industry partner of the project by which this paper was developed, was the advisory author and was involved in parts of the concept formation and analyses. Mr. Kyle Kasawski, the industry partner of the project by which this paper was developed, was the advisory author and was involved in parts of the concept formation and analyses.

## **Dedication**

*To my beautiful, most adorable kids, Mariam and Yahia, without whom this thesis  
would have been completed one year earlier!*

## Acknowledgement

I would love to express my gratitude to my supervisors who have put trust and faith in me throughout my PhD journey and have given me unlimited opportunities to exceed my personal expectations. It has been an honour to conduct my PhD research project under the supervision of two amazing professors, *Dr. Mohamed Al-Hussein* and *Dr. Mustafa Gül*. Very special thanks to my direct supervisor, *Dr. Mustafa Gül*, who has taken every chance to mentor, guide, and support me and my family at the professional as well as the personal level. The knowledge and expertise I have gained from him are priceless and unforgettable. Without the trust and generous support that I received from *Dr. Mohamed Al-Hussein*, I would never be standing where I am now. His creative vision has always added a unique flavour to my research perspectives.

I would also love to thank my small family for supporting me throughout my long journey that sometimes felt like an emotional rollercoaster. My husband, *Nader Ibrahim*, is a one-of-a-kind husband, who has taken all my moments of success as his personal success and acknowledged my ups and downs with love and gratitude. My kids, *Mariam* and *Yahia*, have always been an endless source of joy and laughter, even in my most stressful moments. Despite their young age, they have appreciated the value behind their mom being busy studying instead of playing with them; moreover, they helped me focus on my work.

Words cannot describe my pride in my parents, *Mr. Awad Said* and *Mrs. Maha Gheith*. Since my birth, they have planted in me the seeds of curiosity, independence, and self-learning. At a very young age they introduced me to problem-solving strategies and encouraged me to make my own decisions and stand up for them. I owe a considerable amount of my success to my mother-in-law, *Mrs. Mervat Mohamed*, may her soul rest in peace, as she dedicated two years of her time to look after my kids during my course work, and without her help, my PhD would have never been a success.

Technical writing and administrative work are unsurprisingly part of the everyday routine for a graduate student. Having generous support from fine technical writing advisors such as *Ms. Claire Black* and *Mr. Jonathan Tomalty* has been a privilege that has added priceless value to my writing and presentation skills. I would also like to thank my peers who joined me during this phase of my life.

I am pleased to have worked closely with one of the amazing industry partners, *Landmark Group of Companies*, which provided me with data, market experience, and innovative solutions. Special thanks to *Dr. Haitao Yu* for the time and effort he provided to reinforce my academic research with his practical expertise.

Finally, this thesis has been written at the University of Alberta within the scope of a project entitled, “Integrating solar PV systems into residential buildings in cold-climate regions”. I would like to thank the *Natural Sciences and Engineering Research Council of Canada (NSERC)* for their funding of this research.

# Table of Contents

Abstract.....	ii
Preface.....	iv
Dedication.....	vii
Acknowledgement.....	viii
Table of Contents.....	x
List of Tables.....	xvi
List of Figures.....	xviii
List of Symbols.....	xxiv
Chapter 1: Introduction.....	1
1.1. Motivation.....	1
1.2. Statement of Problem.....	3
1.3. Background and Review of Literature.....	4
1.4. Research Gap.....	7
1.5. Hypothesis and Research Objectives and Scope.....	9
1.6. Organisation of Thesis.....	13
Chapter 2: Long-term Performance and GHG Emission Offset Analysis of Small-scale Grid-tied Residential Solar PV Systems in Northerly Latitudes.....	16
2.1. Overview.....	16
2.2. Introduction.....	17
2.2.1. Research Gap.....	21
2.2.2. Research Objectives and Scope.....	21
2.3. Data Collection.....	21
2.4. Impact of Performance Parameters on PV Output.....	25

2.4.1.	Geographical Location.....	27
2.4.2.	Tilt Angle and Azimuth Angle .....	28
2.4.3.	Meteorological and Soiling Parameters .....	34
2.5.	Validation.....	37
2.6.	GHG emission quantification.....	38
2.7.	Summary and Discussion.....	43
Chapter 3: Predicting the Energy Production by Solar Photovoltaic Systems in Cold-climate Regions.....		46
3.1.	Overview .....	46
3.2.	Introduction .....	46
3.2.1.	Literature Review.....	47
3.2.1.1.	Solar PV Prediction .....	47
3.2.1.2.	Solar PV Performance Parameters .....	48
3.2.1.3.	Snow Impact on PV Efficiency .....	48
3.2.2.	Research Gap .....	49
3.2.3.	Research Objectives.....	50
3.3.	Methodology .....	50
3.3.1.	Prediction of PV Daily Energy Generation using Artificial Neural Networks.....	50
3.3.2.	Clear-sky Index/Model .....	51
3.3.3.	PV Layout Configuration as Input Parameter.....	54
3.3.4.	Soiling Parameters .....	55
3.4.	Data Collection.....	59
3.4.1.	Historical Energy Output Data.....	59
3.4.2.	Meteorological Data.....	61

3.5.	Predictive Model Results .....	63
3.6.	Summary and Discussion .....	70
3.7.	Conclusions and Future Work.....	71
Chapter 4: Load-match-driven Design of Solar PV Systems and Its Impact on the Grid .....		72
4.1.	Overview .....	72
4.2.	Introduction .....	72
4.2.1.	Literature Review.....	73
4.2.1.1.	Recent Studies on Net-zero Energy and Energy-efficient Homes	74
4.2.1.2.	Review on Solar PV Design Optimisation .....	75
4.2.2.	Research Gap and Study Scope .....	77
4.3.	Method .....	79
4.4.	Proposed Optimisation Framework.....	82
4.4.1.	Net-zero Balance of Household Energy Performance .....	82
4.4.2.	Clear-sky PV Output at Two-way Tilted Surface.....	83
4.4.3.	Optimisation Framework .....	85
4.4.3.1.	Optimised Tilt Angle and Azimuth Angle .....	86
4.4.3.2.	Optimised System Sizing.....	86
4.4.3.3.	Other Applications.....	88
4.5.	Data Collection and Analysis.....	89
4.5.1.	Solar PV Data Analysis .....	89
4.5.2.	Household Energy Performance of Net-zero Energy Homes and Energy-efficient Homes.....	92
4.6.	Case Studies .....	95
4.6.1.	Energy-efficient Single-family Home (EEH) in Edmonton, Alberta ...	96

4.6.2.	Net-zero Energy Single-family Home (NZEH) in Edmonton, Alberta	100
4.7.	Results and Framework Validation	105
4.7.1.	Results	105
4.7.2.	Model Validation	113
4.8.	Discussion and Conclusion	118
4.8.1.	Discussion	118
4.8.2.	Conclusion	121
4.8.3.	Limitations and Recommendations for Future Work	122
Chapter 5: Optimisation of Community Shared Solar Application in Energy Efficient Communities using Monte Carlo Simulations		123
5.1.	Overview	123
5.2.	Introduction	124
5.2.1.	Literature Review	124
5.2.1.1.	Community Shared Solar Definition	124
5.2.1.2.	Current State-of-the-art Community Generation Models	125
5.2.1.3.	Community Shared Solar Challenges	127
5.2.1.4.	Net-zero definitions	129
5.2.2.	Research Gap and Objectives	129
5.3.	Method	131
5.4.	Data Collection and Analysis	134
5.4.1.	Household Energy Performance of Net-zero Energy Homes and Energy-efficient Homes	134
5.5.	Framework	139
5.5.1.	Simulation of Energy Demand	139

5.5.2.	PV Power Output at a Two-way Tilted Surface .....	143
5.5.3.	Net-zero Balance of Communities.....	145
5.5.4.	Optimisation Framework .....	146
5.5.5.	Model Validation .....	147
5.6.	Results .....	148
5.6.1.	Energy Demand Simulation Results .....	149
5.6.2.	Energy Generation Modelling Results.....	151
5.6.2.1.	Behind-the-meter Individual PV System.....	151
5.6.2.2.	Community-scale distributed generation PV system.....	154
5.6.3.	System Optimisation Results .....	155
5.7.	Discussion and Conclusion .....	160
5.7.1.	Summary and Discussion.....	160
5.7.2.	Conclusion, Limitations, and Recommendations .....	163
Chapter 6: Summary, Conclusions and Recommendations for Future Research .....		165
6.1.	Research Summary.....	165
6.2.	Research Contributions .....	167
6.3.	Limitations and Recommendations for Future Work.....	169
6.3.1.	Comments on Building Research in the Context of Smart Grids .....	171
References.....		174
Appendix A: Commercial Application– Solar Photovoltaic Optimisation for Commercial Flat Rooftops in Cold Regions.....		197
A. 1	Overview .....	197
A. 2	Introduction .....	197
A. 3	Proposed Methodology .....	199
A.3.1	Regulations .....	200

A.3.2	Shading Analysis and Sun Angles .....	201
A.3.3	Solar PV Generation in Edmonton .....	204
A.3.4	Snow Coverage Loss Factors.....	206
A. 4	Photovoltaic Array Layout Models .....	207
A. 5	Payback Period Analysis.....	210
A. 6	Analytic Heirarchy Process .....	214
A. 7	Discussion and Conclusion .....	214
A. 8	Future Recommendations.....	215
Appendix B:	List of Publications.....	217
B. 1	Journal papers.....	217
B. 2	Conference papers .....	218

## List of Tables

Table 2-1. Locations and grouping method of the cities where the PV systems are installed. ....	23
Table 2-2. Histogram of the tilt and azimuth angles of the PV systems. Roof pitch ratios and azimuth angle ranges are provided only in this table and can be referred to for the tables below. ....	25
Table 2-3. Correlation analysis between performance parameters and final yield. ....	35
Table 2-4. Measured PV potential (kWh/kW <sub>p</sub> ) of various PV system layouts located in Region I. Note: information on roof pitches and azimuth angle ranges are provided in Table 2-2. ....	36
Table 2-5. Assessment of estimated system losses. ....	37
Table 2-6. Summary of the life cycle energy component statistics of monocrystalline solar PV panels. (Source: Natural Resources Canada, 2015; Peng et al., 2013). ....	39
Table 2-7. Statistical results of the EPBT and GHG <sub>e-rate</sub> measures. ....	40
Table 3-1. Correlation analysis result between daily energy generated in all monitored PV systems and different performance parameters. ....	58
Table 3-2. Statistical weather data for Edmonton, Red Deer, and Calgary (Environment Canada, 2017). ....	61
Table 3-3. Parameters and their error statistics. ....	64
Table 4-1. List of monitored NZEHs and EEHs. ....	92
Table 4-2. Profile of sample single-family EEH. ....	98
Table 4-3. Profile of sample single-family NZEH. ....	102
Table 4-4. Summary of optimal array layouts concluded for the EEH. ....	106
Table 4-5. Summary of optimal array layouts concluded for the NZEH. ....	107
Table 4-6. Assessment of estimated system losses in PVWatts®. ....	114

Table 4-7. Validation summary of the proposed model for (a) EEH and (b) NZEH. .....	116
Table 5-1. List of monitored NZEHs (denoted with N-#####) and EEHs (denoted with E-#####). .....	135
Table 5-2. Assessment of estimated system losses in PVWatts®. ....	148
Table 5-3. Statistical analysis of simulation results and data validation. ....	150
Table 5-4. Single system per unit setting. ....	152
Table 5-5. Total EEH community optimisation results. ....	157
Table 5-6. Total NZEH community optimisation results. ....	158
Table 6-1. Disciplines and domains for Smart Grid research (Source: Hovd, 2015). .....	173
Table A-1. Summary of optimal array layouts.	211
Table A-2. Summary of solar panel costs and revenue (Energy Informative, 2016). .....	212
Table A-3. AHP rankings for the four optimal array layouts. ....	215

## List of Figures

Figure 1-1. Demonstration of (a) top ten countries in solar PV cumulative capacity versus Canada (2016 report) (source: NRCan, 2017a; Statista, 2017) and (b) the growth of micro-generators in Alberta (source: AESO, 2017).....	6
Figure 1-2. Demonstration of renewable energy setting of (a) small-scale behind-the-meter solar PV application and (b) mid-scale community shared solar applications.	11
Figure 1-3. Methodology proposed in this thesis.....	12
Figure 2-1. Geographic location of the monitored PV systems in longitude and latitude.....	22
Figure 2-2. Typical monitoring system of the PV systems: (a) is the PV array and micro-inverters hidden underneath; (b) is the bi-directional metering system where the AC from the PV system is connected to the grid; (c) is the Envoy system that monitors the data collected from the PV system; and (d) is a sample of the five-minute interval data.....	23
Figure 2-3. Statistical properties of the monitored PV sites including (a) panel efficiency, (b) panel capacity, (c) tilt angle, (d) azimuth angle, (e) year of installation, and (f) system size. ....	24
Figure 2-4. Annual energy generation of all monitored PV sites by year and average of all years.....	26
Figure 2-5. The (a) monthly and (b) annual energy generation of south-facing 27°-tilt PV systems in different cities. ....	28
Figure 2-6. (a) Mean daily profile for each month of the year for a PV system in Edmonton with 18° tilt and 180° azimuth angles; (b) the mean monthly power generation percentage; (c) the mean daily profile for each month of the year for a PV system in Edmonton with 60° tilt and 180° azimuth angles; (d) the mean monthly power generation percentage. ....	31

Figure 2-7. Correlation between the daily final yield from all monitored PV sites against the (a) system tilt angle and (b) inclination of the sun on the PV system’s receiving surface. ....	33
Figure 2-8. Annual final yield of PV systems placed at 30° tilt angle in Region I, Region II, and Region III. ....	34
Figure 2-9. Correlation between insolation and final yield. ....	36
Figure 2-10. Regression charts of (a) actual energy generation of all PV systems (abscissa) against RETScreen simulated systems (ordinate) and (b) actual energy generation of all PV systems (abscissa) against PVWatts simulated systems. ....	38
Figure 2-11. GHG emission rates by energy source in Canada. ....	41
Figure 2-12. Correlation analysis of the EPBT and $\text{GHG}_{\text{e-rate}}$ against (a) tilt angle, (b) azimuth angle, (c) latitude, and (d) panel efficiency; and statistical analysis of the (e) impact of panel brand on EPBT, (f) impact of panel brand on $\text{GHG}_{\text{e-rate}}$ , (g) impact of location on EPBT, (h) impact of location on $\text{GHG}_{\text{e-rate}}$ , (i) impact of tilt angle deviation from latitude on EPBT, and (j) impact of tilt angle deviation from latitude on $\text{GHG}_{\text{e-rate}}$ . ....	43
Figure 3-1. Data flow diagram of the proposed model structure. ....	52
Figure 3-2. Diurnal time-series plot of the historical clear-sky GHI (daily averages of July 1983–November 2016), clear-sky GHI model proposed by Berger-Duffie along with other models, and the absolute bias between actual data and proposed model. .	54
Figure 3-3. Five-minute time-series energy generation of maintained and unmaintained modules placed at 14° tilt in Edmonton on the spring, summer, fall, and winter equinox days. ....	56
Figure 3-4. Curve fitting of snow loss factors for each tilt angle based on an empirical study in Edmonton (May 2012–Aug. 2014) (NAIT, 2015). Continuous lines represent the actual efficiencies and dashed lines represent the fitted curves for efficiencies as a function of tilt angle and month of observation. ....	57

Figure 3-5. Location of the monitored PV systems: (a) on Alberta map; (b) in longitude and latitude.....	60
Figure 3-6. Daily snow on ground in Edmonton, Red Deer, and Calgary (Source: Environment Canada (2017)).....	62
Figure 3-7. Comparison of the diurnal (a) actual, clear-sky, and smart persistence GHI ( $\text{W}/\text{m}^2$ ) and (b) prediction results of a west-facing ( $270^\circ$ ), $30^\circ$ tilt PV system in Cochrane using actual GHI, smart-persistence GHI along with measured PV energy output ( $\text{kWh}/\text{kW}_p$ ).....	67
Figure 3-8. Regression charts of daily prediction of all tested PV systems against actual (measured) data for ‘with-soiling-factors’ data and ‘without-soiling-factors’ data for (a) no-snow seasons, (b) snow seasons, (c) all seasons, and (d) the absolute bias between measured and prediction data at each month of the year. ....	68
Figure 3-9. Demonstration of (a) monthly, and (b) annual energy generation prediction with and without soiling parameters compared to measured data and simulation results from PVWatts. PV system is located in Edmonton, south-facing with an $18^\circ$ tilt angle. ....	69
Figure 4-1. (a) Locations of monitored solar PV systems in Alberta, Canada; (b) exact coordinates of each site; and (c) one of the monitored sites in Edmonton. ....	82
Figure 4-2. Summary of the research method.....	82
Figure 4-3. Proposed optimisation framework. ....	88
Figure 4-4. Solar PV annual output efficiency at varying layout placements in Edmonton, Canada (Lat. $53.53^\circ$ N). ....	91
Figure 4-5. Summary of energy-component profiles of all 11 houses demonstrating the monthly (a) loads, (b) generation, (c) exported energy, (d) imported energy, and (e) solar energy used on site, while (f) represents the annual percentage of solar energy used on site in each house. ....	93

Figure 4-6. Pairwise comparison between the average annual energy performance of EEHs and NZEHs. ....	94
Figure 4-7. Schematic representation of the solar PV arrays placement of the EEH. ....	97
Figure 4-8. (a) Daily power profile on maximum PV power output, (b) daily power profile on peak load demand, (c) daily average year-long power profile, and (d) cumulative monthly breakdown of the household energy demand, imported energy from the grid, on-site self-consumed solar energy, generated energy, and the surplus energy exported to the utility grid.....	99
Figure 4-9. Peak daily load profile (kW) in (a) summer, (b) winter, (c) spring, and (d) fall. ....	100
Figure 4-10. Schematic representation of the solar PV arrays placement of the NZEH. ....	102
Figure 4-11. (a) Daily power profile on maximum PV power output, (b) daily power profile on peak load demand, (c) daily average year-long power profile, and (d) cumulative monthly breakdown of household energy demand, imported energy from grid, on-site self-consumed solar energy, generated energy, and surplus energy exported to utility grid. ....	103
Figure 4-12. Peak load profile (kW) in (a) summer, (b) winter, (c) spring, and (d) fall. ....	104
Figure 4-13. Sensitivity analysis demonstrating the impact of system size on (a) EEH and (b) NZEH in terms of LM, GI, yearly generation, and on-site solar use (as a percentage of yearly generation and as a percentage of yearly loads).....	112
Figure 4-14. Pairwise comparison between the monthly measured and predicated data along with PVWatts estimate for (a) EEH and (b) NZEH. The charts represent (a) an EEH with 3.64 kW <sub>p</sub> , tilt = 26.5°, azimuth = 182° and (b) an NZEH with 10.92 kW <sub>p</sub> , tilt = 26.5°, azimuth = 195°. ....	115
Figure 5-1. Proposed research method.....	133

Figure 5-2. Summary of average energy-component profiles of all 11 houses demonstrating average monthly profile of (a) EEHs and (b) NZEHs. ....	135
Figure 5-3. Pairwise comparison between the average annual energy performance of EEHs and NZEHs. ....	136
Figure 5-4. Sample energy performance of an EEH's (a) monthly profile, (c) cumulative monthly profile, and (e) daily profile on peak demand, and an NZEH's (b) monthly profile, (d) cumulative monthly profile, and (f) daily profile on peak demand.....	138
Figure 5-5. Statistical distribution of the energy load in January at 0:00 a.m. ....	142
Figure 5-6. Screen shot of the Monte Carlo simulation model for January.....	143
Figure 5-7. Simulation results of energy consumption of 42 (a) EEH and (b) NZEH dwellings. ....	150
Figure 5-8. Single system dwelling unit setting (green rectangle represents the backyard of each dwelling).....	152
Figure 5-9. Simulation results for individual dwellings based on scenario#1 for the (a) EEH and (b) NZEH community. Labels are assigned to the dwellings according to the orientation of the rooftop PV system; S: south, E: east, W: west, SE: south east, and SW: south west. ....	154
Figure 5-10. Energy profiles of the community dwellings after implementing the suggested solution for community shared solar PV application for the (a) EEH and (b) NZEH community.....	159
Figure A- 1. Proposed framework for flat rooftop optimisation model. ....	200
Figure A- 2. Solar panel layout and parameters for row spacing. ....	203
Figure A- 3. Solar altitude, declination, and daylight hour calculations in Edmonton over one year.....	203
Figure A- 4. A comparison between the annual actual PV generation and PVWatts (kWh/kW). ....	205

Figure A- 5. Solar PV system efficiency at different tilt angles and orientations in Edmonton.....	205
Figure A- 6. Actual and forecasted snow coverage efficiency factors of solar PV generation on different tilt angles. ....	208
Figure A- 7. Yearly total array generation based on panel tilt and row spacing for landscape-oriented panels. ....	209
Figure A- 8. Yearly generation per panel based on panel tilt and row spacing for landscape-oriented panels. ....	209
Figure A- 9. Yearly total array generation based on panel tilt and row spacing for portrait-oriented panels. ....	209
Figure A- 10. Yearly generation per panel based on panel tilt and row spacing for portrait-oriented panels. ....	209
Figure A- 11. Associated yearly costs and savings over 25 years of a photovoltaic system’s life (Energy Informative, 2016). ....	211
Figure A- 12. Payback period for various array layouts for landscape-oriented panels. ....	213
Figure A- 13. Payback period for various array layouts for portrait-oriented panels. ....	213
Figure A- 14. Payback period for the four previously-determined optimal layouts based on the year that the array is installed and the initial investment is made. ....	213

## List of Symbols

PV	Photovoltaic
ANN	Artificial neural network
MLP	Multilayer perceptron
GHG	Greenhouse gas emission
EEC	Electrical energy consumption
CCEMC	Climate Change and Emissions Management Corporation
$Y_f$	Final yield (kWh/kW <sub>p</sub> )
$E$	Energy generated (kWh)
$P_0$	PV system's size (kW <sub>p</sub> )
$\varphi$	Latitude of a site (°)
$Z$	Zenith angle of the sun (°)
$DOY$	Day of the year
SN	Solar noon (time, h)
ST	Solar time (time, h)
$z_t$	True zenith angle of the sun (°)
$\delta$	Declination angle (°)
$h$	Sun's elevation or altitude angle (°)
$\omega$	The hour angle (°)
EoT	Equation of time (min)
$I_0$	Extraterrestrial irradiance (W/m <sup>2</sup> )
DNI	Direct normal irradiance (W/m <sup>2</sup> )
Diffuse	Diffuse irradiance (W/m <sup>2</sup> )
GHI	Global horizontal irradiance (W/m <sup>2</sup> )
$k_t$	Clear-sky index
$\tau$	Insolation (kWh/m <sup>2</sup> /day)
$\beta$	Daylight hours (h)
HourSet	The sunset hour angle (°)
$\alpha$	The solar azimuth angle; sun's relation to due south (°)

INC	Incidence angle for south-facing planar surfaces (°)
INC <sub>N</sub>	Normalised incidence angle for south-facing planar surfaces
$\vartheta$	Surface tilt angle from horizontal (°)
$\alpha_s$	Surface azimuth angle from north (°) (0° N, 180° S)
$\alpha_{sN}$	Normalised surface azimuth angle from north (0° N, 180° S)
$m$	Month of the year
$\varepsilon$	Snow adjustment factor due to snow coverage (%)
$x$	Input vector
$l$	Output vector
$k$	$k^{\text{th}}$ iteration
$y, b$	Errors
$A_i$	$i^{\text{th}}$ actual energy generation
$F_i$	$i^{\text{th}}$ forecasted energy generation
$n$	Number of records
MAPE	Mean absolute percentage error (%)
MBE	Mean bias error (W/m <sup>2</sup> ; kWh/kW <sub>p</sub> )
MSE	Mean square error (W/m <sup>2</sup> ; kWh/kW <sub>p</sub> )
RMSE	Root mean square error (W/m <sup>2</sup> ; kWh/kW <sub>p</sub> )
$S$	Forecast skill
$U$	Uncertainty
$V$	Variability
$R^2$	Coefficient of determination
NZEH	Net-zero Energy Home
EEH	Energy-efficient Home
DEG	Distributed energy generation
LM	Load-match index
GI	Grid-interaction index
LMGI	Load-match and grid-interaction indexes
$IMP$	Imported energy
$EXP$	Exported energy

$L$	Energy load
$G$	Generated energy
$i$	Index
$m$	Monthly
$P_{cs,o}$	Clear-sky power output at the original layout placement
MPP	Maximum power point
$n_p$	Number of panels in the PV system
$l_p, l_m$	Length of the panel in the PV system
$w_p, w_m$	Width of the panel in the PV system
$C$	Nameplate peak capacity of the panel ( $W_p$ )
$e_p$	Panel efficiency
$e_s$	System losses
$P_{p,n}$	Predicted actual power output at the new layout placement
$P_{cs,n}$	Clear-sky power output at the new layout placement
GRG	Generalised reduced gradient
Beta	Beta probabilistic distribution
Gamma	Gamma probabilistic distribution
Triangular	Triangular probabilistic distribution
$\rho$	Shape1 in Beta distribution
$\psi$	Shape2 in Beta distribution
B	Beta function
$\Gamma$	Gamma function
$j$	Shape in Gamma distribution
$\gamma$	Scale in Gamm distribution
$a$	Lower limit
$b$	Upper limit
$c$	Mode
EPBT	Energy payback time (yr)
$E_{input}$	The primary energy input of PV module during its life cycle (MJ)
$E_{BOS}$	The energy required for the physical balance of system (MJ)

$E_{\text{output}}$	The annual primary energy offset due to PV system's electricity generation (MJ)
$\text{GHG}_{\text{e-rate}}$	The GHG emission rate per unit energy generated by the PV system (g CO <sub>2</sub> eq./kWh)
$\text{GHG}_{\text{e-total}}$	The total GHG emission produced by the PV system throughout its life cycle (g CO <sub>2</sub> eq.)
$E_{\text{LCA-output}}$	The total energy generated by the PV system throughout its life cycle (kWh)
$\text{GHG}_{\text{input}}$	The GHG emission corresponding to the energy requirements for the PV input (g CO <sub>2</sub> eq.)
$\text{GHG}_{\text{BOS}}$	The GHG emission corresponding to the energy requirements for the PV BOS (g CO <sub>2</sub> eq.)

## Chapter 1: Introduction

### 1.1. Motivation

Due to the rising awareness and movement toward carbon footprint mitigation as well as the crucial need to sustain our resources for future generations, the use of microgeneration as a clean source of energy has become increasingly popular within the residential as well as the commercial sectors. One advantage of solar photovoltaic (PV) energy as a renewable source of electricity is its minimal direct and lifecycle emissions compared to fossil-based electricity supply technologies such as coal and natural gas (Camacho et al., 2011). Thus, solar PVs are considered clean, safe, and additionally, noise-free sources of electricity (Schlomer et al., 2014). In 2005, the globally installed PV capacity was nearly 5.4 GW, while due to cost reductions and incentive policies in some countries, the globally installed PV capacity reached 40 GW in 2010 (Braun et al., 2011; Nowak, 2015). The year 2015 witnessed a significant increase in PV installations of nearly 50 GW reaching a total cumulative PV capacity of 227 GW, accounting for an increase of 25% in installed PV capacity compared to 2014 (Nowak, 2015). As per Tsao et al. (2006), the theoretical potential of the earth's renewable energy sources is 89,300 TW while the extractable potential of solar power is 58,300 TW, given that the amount of solar power reaching the earth's surface is approximately 86,000 TW (Camacho et al., 2011). In order to satisfy the current annual global energy consumption of 394,560 PJ (9,424 Mtoe or 109,601 TWh) (IEA, 2014a), covering 0.22% of our planet with solar collectors with an efficiency of 8% would sufficiently provide for the global energy needs (Camacho et al., 2011). In 2010, the global power demand was approximately 15 TW, while, as per the 2050 projections, the global power demand will reach 25–30 TW (EIA, 2016; Lewis, 2010).

On the other hand, several challenges accompany solar PV applications at the residential level, such as determining an optimum size and layout design for best on-

site system utilisation that conforms to the current local roof-sloping practice, especially in cold-climate (and intrinsically high-latitude) regions. In addition, solar PVs installed in high-latitude regions encounter other challenges, such as the seasonal variation in daylight hours and sun's path (in terms of azimuth and zenith angles) and soiling parameters such as snow coverage. Furthermore, greater challenges are encountered with the implementation of solar PVs into net-zero energy homes (NZEHS), which aim at not only generating as much as they consume during the course of the year, but also providing electricity for the entire household, as a method of mitigating the housing impacts on GHG emissions. The shortcomings encountered by NZEH practice result in two outcomes: (a) in winter, a minimal PV-generated energy and high energy demand (due to space heating and domestic hot water supply loads); and (b) in summer, PV over-generation (or penetration) and reduced energy demand. This current situation is typically called "*PV mismatch*" and its large scale (i.e., community-scale) application will threaten the grid stability as it results in the so-called "*duck-curve*" phenomenon. The duck-curve, as defined by the National Renewable Energy Laboratory (NREL), is one of the shortcomings of over-generation during the day and excessive loads that peak in the morning and late afternoon. In some jurisdictions with high PV penetration, PV curtailment is considered as a potential solution to avoid the increased risk of penetration due to over-generation. In this context, the traditional electric power utilities have indicated a crucial need for improvement. Aging infrastructures, concerns for environmental footprint, and the rising demand for electricity make the current practice a good candidate for improvement. One suggested solution is the implementation of integrated Smart Microgrids. Smart Microgrids are "*geographically compact units running autonomously from the main grid*" (NSERC Smart Microgrid Research Network, 2015).

Today there is a crucial need for emerging new technologies and models that are end-user centric and that recognise the potential of the Smart Grid to change the end-user's perspective on energy consumption. Buildings, if considered to be the micro level of the utility grid, should remain as passive and enduring as possible in that they

should (1) mitigate their energy demand, (2) avoid peak-demand hours, and (3) mitigate their PV penetration (Hovd, 2015). In light of this practice, a bottom-up viewpoint with focus on the role of building science in shaping the future Smart Grid will potentially provide insight on how Smart Grids can facilitate changes in consumption patterns in desired ways (Hovd, 2015).

As an initiative toward improving the current residential solar PV microgeneration practice, aiming for implementing these improvements into smart grid infrastructures in future work, the present research focuses on reducing the mutual negative impacts exchanged among NZEHs, solar PV microgeneration, and the utility grid by (a) improving the design of the solar PV system to increase the load-match with the household energy load patterns, and (b) developing a systematic framework to simulate the energy demand of residential communities and to optimise the design of their respective community shared solar PV systems.

## **1.2. Statement of Problem**

With the community-wide application of solar PV microgeneration paired with energy-efficient homes (EEHs) in general and net-zero energy homes (NZEHs) in particular, it is expected that the utility grid will be confronted by the risk of PV penetration and mismatch issues. However, from the building science point of view, the primary goal of NZEHs is to mitigate their carbon footprint by (1) replacing natural gas with electricity for clean energy, (2) reducing the overall energy consumption, and (3) generating as much energy as they consume during the course of the year. In fact, after analysing the annual household energy consumption of several EEHs and NZEHs, it is observed that, by replacing natural gas with electricity, NZEHs consume double to triple the amount of electricity required by an EEH. Challenges resulting from geographical location, climatological conditions, and end-user behaviour are additionally encountered, which basically result in uncertainties and thus lead to potential mismatch.

In this regard, the present study investigates the community-scale interaction between the utility grid, grid-connected solar PV microgeneration, and the household energy consumption of NZEHs and EEHs in search for potential improvement of the solar PV load-match-driven design framework, housing interaction with the grid, thereby providing the smart grid infrastructure with end-user-centric insights on shaping future sustainable smart communities.

### **1.3. Background and Review of Literature**

Currently, with the increasing number of renewable energy practices, harvesting renewable energy on a large-scale has become the primary challenge. The installed capacity of PV systems has recently increased much more quickly than the development of grid codes that are supposed to effectively and efficiently manage the PV penetrations within the distribution system (Braun et al., 2011). Thus, within the next few decades, the renewable energy harvesting problem must be addressed. One of the advantages to fossil energy is its availability and controllability, with the exception of wind and solar energies. These energy sources are not controllable and not always available when and where needed (Camacho et al., 2011). In this context, a coordinated effort is necessary, beginning from the planning stage all the way to power generation, distribution, and consumption.

Small-scale grid-integrated solar PV systems as one type of renewable energy application in residential buildings have been adopted by home builders as a responsible sustainability practice. Not only can positive environmental impacts be achieved, such as reducing air pollution and GHG emissions by replacing fossil fuels, but also the utilisation of the energy derived from natural resources can improve current energy security and provide a sustainable environment for future generations. The residential sector accounts for the largest energy consumption share in Canada, reaching 24% in 2015, and is also responsible for 19.1% of Canada's GHG emissions (Statistics Canada, 2017) This is equivalent to 4.0 tonnes of GHG emissions on a per capita basis (Statistics Canada, 2017). Cost-effective design of solar PV systems in

the residential sector has become a critical issue in speeding the deployment of renewable solar energy for self-consumption, and the Electrical Energy Consumption (EEC) in residential buildings is a key factor for manufacturing companies in designing the proper size of such systems. As per Natural Resources Canada (NRCan) (2015) the GHG intensity by electricity generated as a Canada average is 43.2 tonne/TJ, while that by natural gas is 49.68 tonne/TJ.

The goal of the Alberta Government (Alberta Government, 2015; Leach et al., 2015) is that by 2030, 30% of Alberta's electricity will be powered by renewable energy sources. A feasible plan has been set in motion in order to successfully install a capacity of 5,000 MW of renewables in Alberta by such time. Being part of the Climate Change and Emissions Management Corporation (CCEMC, 2016) created in 2009, this project aims to support Alberta's Climate Change Strategy (Leach et al., 2015) in creating energy-efficient and energy-resilient communities and enhancing technology and innovation.

Solar PV potential varies across Canada; coastal areas have lower potential than central regions, since increased cloud coverage affects coastal areas. Also, about half of Canada's residential electricity demand is met by installing grid-connected solar PV systems on the roofs of residential buildings (NRCan, 2016). Figure 1-1 indicates the top ten countries by cumulative capacity of the installed solar PV systems as of 2016 (NRCan, 2017a; Statista, 2017) and the cumulative capacity of micro-generators in Alberta as of January, 2017 (AESO, 2017). According to 2014 statistics, the residential sector in Canada consumes 35.2 Millions of tonnes of oil equivalent (Mtoe) (17.5%) of the total final consumption of 200.3 Mtoe for energy demand; of which 45% of the energy consumed comes from natural gas, 39% comes from electricity, 10% comes from biofuels and waste, and 5% comes from other sources (IEA, 2014; Poissant et al., 2015).

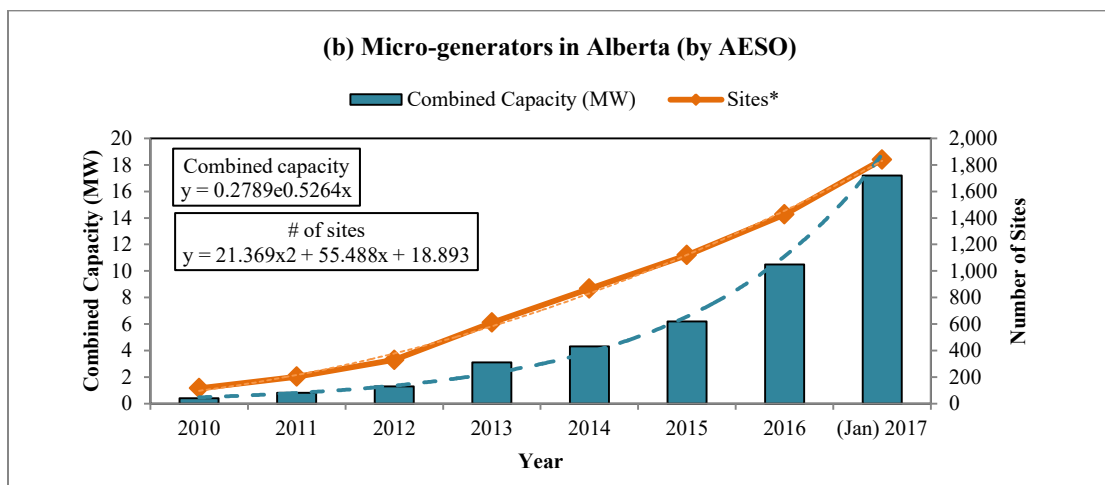
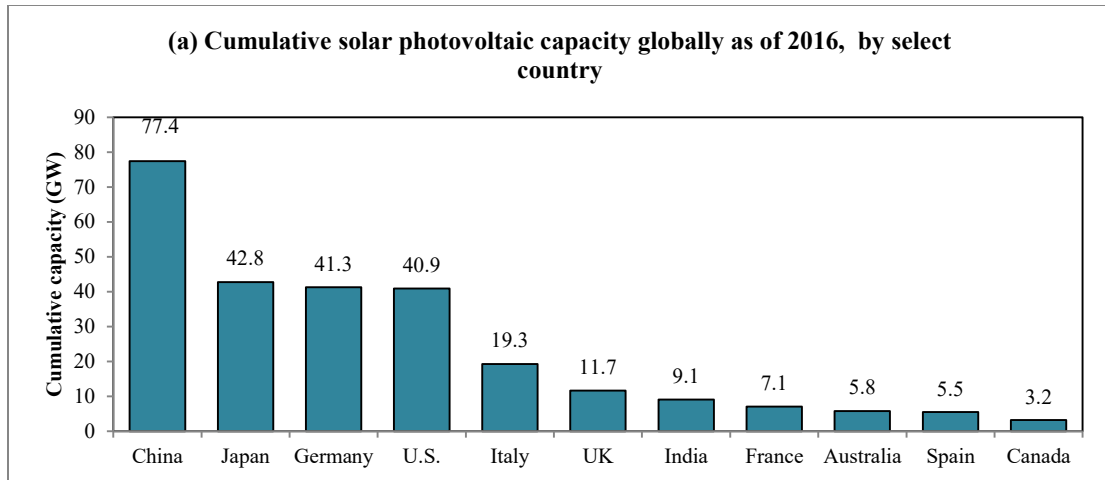


Figure 1-1. Demonstration of (a) top ten countries in solar PV cumulative capacity versus Canada (2016 report) (source: NRCan, 2017a; Statista, 2017) and (b) the growth of micro-generators in Alberta (source: AESO, 2017)

Several aspects of solar PVs which are relevant to the presented thesis are covered herein. A review of previous studies, including (1) the national solar PV application, (2) solar PV monitoring techniques and GHG emissions associated with solar PV installations, (3) solar PV forecasting techniques, (4) net-zero energy homes, and (5) community shared solar PV related to building science, has been carried out and summarised in the introduction of each of the following chapters in order to provide strong support for the current research study.

First, an overview of the potential of solar PV technology in Canada is discussed. Second, a full review on solar PV forecasting and/or prediction methods and algorithms is covered. Third, since the present study focuses on the mutual impact of the implementation of solar PV systems on net-zero energy homes in cold-climate regions, a review on net-zero energy home practices is provided in detail. Fourth, a review of community shared solar application is carried out and summarised to include the definition of community shared solar, state-of-the-art community solar models, and the challenges incurred by the implementation of community shared solar. Finally, a brief discussion of the literature review is presented and research gaps are identified.

#### **1.4. Research Gap**

As a conclusion from the review of literature, some research gaps have been identified and will be addressed in the presented thesis.

- (1) It is found that none of the previous studies (Marion et al., 2013, 2009, 2005, Mondol et al., 2005, 1998) have extensively quantified the impacts of the various performance parameters on the grid-tied residential solar PV performance, particularly in the northerly cold-climate regions. It is also found that, due to the solar PV market penetration in Canada, it is crucially important to provide a detailed performance analysis of the existing solar PV systems in the local meteorological and geographical conditions of Canada in general and in Alberta in specific.
- (2) Numerous studies have been conducted attempting to forecast solar PV energy output using various parameters (Alluhaidah et al., 2014; Antonanzas et al., 2016; Ding et al., 2011; Mellit and Pavan, 2010). Also, several algorithms and techniques have been used to develop and train the predictive model based on the given research approach. These models use historical data as an input parameter, but the sample size (or variability) of the PV systems is limited, not exceeding one or a few PV systems in any of the studies noted above.

Furthermore, snow coverage conditions in cold climate regions have not been well addressed in the existing literature. Existing studies on the effect of snow cover on PV systems are in agreement that PV systems with higher tilt angles are advantageous over those with lower tilt angles in the event of snow due to the natural sliding of snow off the PV modules. Thus, the statistical interpretation of the snow-related system efficiency can be implemented in PV modelling and forecasting.

- (3) Several studies propose methods by which to evaluate the performance of net-zero energy homes (Li et al., 2016; Salom et al., 2014b; Sartori et al., 2012). Other studies focus on investigating the optimum solar PV layout placement based on the objective of maximising the aggregated annual energy output. However, few studies address the optimum solar PV system layout placement to match household energy load and minimise its impact on the utility grid. Current solar PV design practice encompasses three primary objectives: (1) the installed solar PV system generates as much energy as the site consumes on an annual basis, (2) the annual energy aggregate from the solar PV system is maximised given that a south-facing installation satisfies this condition, and (3) the proposed PV system design can fit within the available roof area. (In addition, other financial, regulatory, and consumer-related aspects are considered; however, these aspects are beyond the scope of the present study). The current design method, although it satisfies the theoretical objectives of NZEH practice, fails to meet other aspects such as the PV system self-consumption, grid interaction, and economic viability from the end user's perspective.
- (4) Several studies have examined the definitions (Augustine, 2015; Hicks and Ison, 2018; Jones et al., 2017; Walker and Devine-Wright, 2008; Wiseman and Bronin, 2013) and legal implications (Romero-Rubio and de Andrés Díaz, 2015) of community shared solar application, while others have focused on developing simulation and decision-making models of solar shared communities (Cai et al., 2009b; Hachem-Vermette et al., 2016; Shakouri et

al., 2017). Furthermore, challenges associated with the application of community shared solar and its public acceptability have been addressed in studies from various countries and jurisdictions (Jones et al., 2017; Leuphana University, 2013). As the world is taking on the centralisation of distributed energy sources and the decentralisation of the utility grid and is also setting plans in place for the smooth transition from fossil-based energy sources (coal, gasoline, and natural gas) to renewable energy sources, it is critically important to investigate the grid-wise implications of the community-scale application of net-zero energy homes (NZEH) (i.e., highly energy-efficient homes that run independently of the natural gas grid) in comparison with the equivalent application of energy-efficient homes (EEH) (i.e., energy-efficient homes that rely on natural gas for space heating and hot water heating). This matter has hardly been addressed in previous studies, especially in northerly climates.

## **1.5. Hypothesis and Research Objectives and Scope**

The research presented herein is built upon the following hypothesis:

*“In search for sustainable communities, the optimum design of load-match-driven solar PV systems will improve the performance of energy-efficient homes on both individual and communal levels and, from the “bottom-up” viewpoint, will inherently provide better insight to stakeholders for the notable establishment of the future smart grid”.*

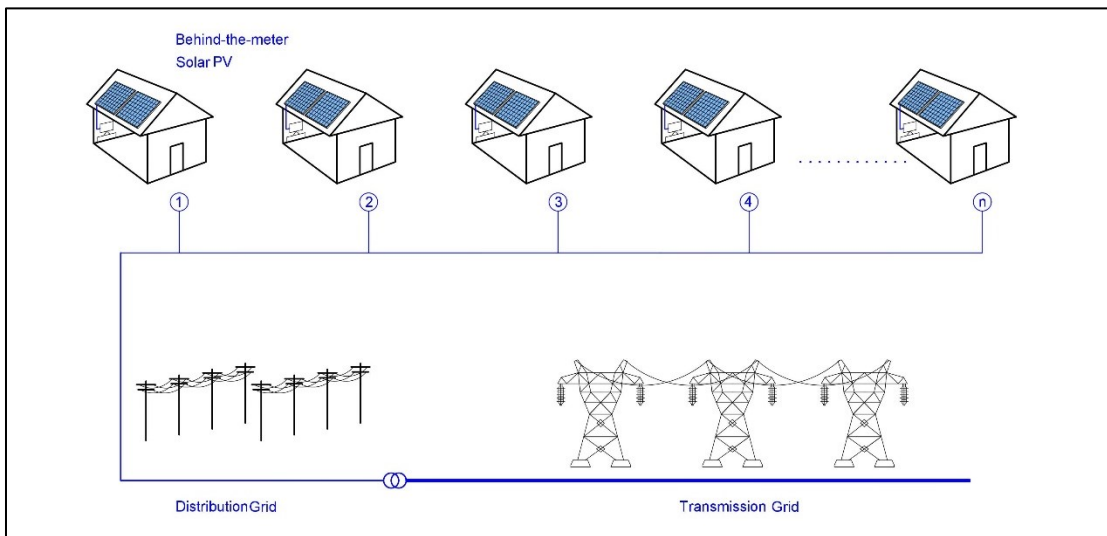
The primary goal of the research presented in this thesis is to provide a novel and generic framework that aims to leverage the large-scale interaction between energy-efficient buildings, solar PV microgeneration, and the utility grid from the energy-efficiency perspective of a building. This goal is met by investigating the load match and grid interaction for NZEHs and EEHs and their corresponding solar PVs, aiming at not only mitigating the GHG emissions, but also mitigating the negative impact of

these types of homes on the grid performance. To realise this underlying goal, the present research is divided into the following objectives:

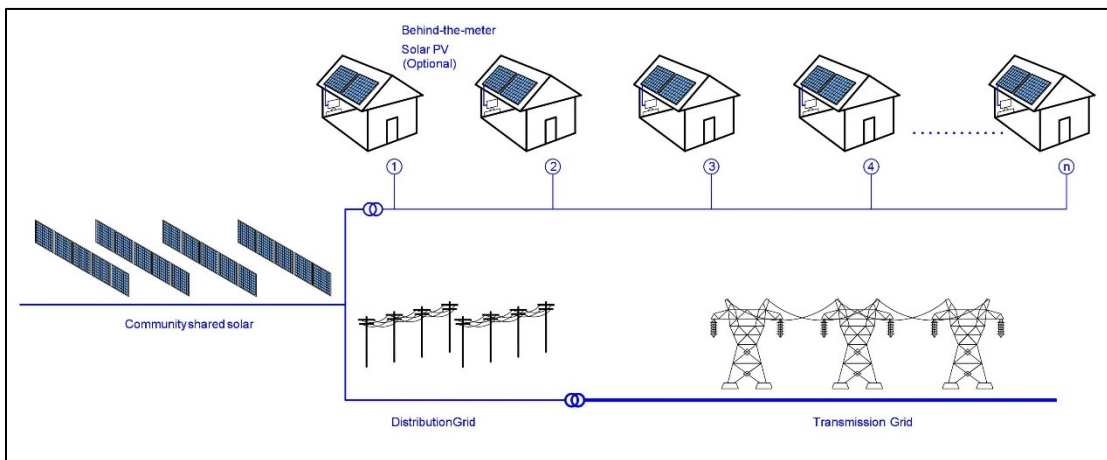
- (1) Investigate the long-term performance of household energy consumption and solar PV energy generation within the current housing practice of EEHs and NZEHs and then identify load and generation patterns within the local climatological, social, and cultural conditions within the locality of this study.
- (2) Identify the statistical properties of the energy load patterns of two housing types, EEHs and NZEHs, such as upper and lower boundaries of power demand and the probability distributions of the power demand of such housing types.
- (3) Quantify the load-match (LM) and grid-interaction (GI) indicators, as well as the net-zero balance of the current housing practice of EEHs and NZEHs.
- (4) Develop a prediction model for solar PV energy generation.
- (5) Develop an integrated evidence-based load-match-driven optimisation framework to identify the proper solar PV layout and sizing in order for this framework to maximise the solar PV self-consumption and environmental merits while minimising its initial cost (Figure 1-2a).

Provide a systematic framework for simulating the community-scale residential energy demand and optimising the size and layout of its corresponding community shared solar PV systems as demonstrated in Figure 1-2. In order to achieve this objective, the community-scale grid interaction of the individual households within the community and community-shared solar PV systems integrated into this community is investigated (Figure 1-2a). Individual households are then simulated by developing a Monte Carlo simulation prototype to simulate the energy loads of the entire community by obtaining data from only 11 households. Finally, the load-match-driven optimisation framework developed in objective (5) is applied at the community scale in order to identify the optimum PV design (Figure 1-2b). This study is performed based on a long-term data-monitoring approach in which 85 solar

PV systems in 8 major cities in Alberta have been monitored since July 2010 to date at a 5-minute temporal resolution.



(a)



(b)

Figure 1-2. Demonstration of renewable energy setting of (a) small-scale behind-the-meter solar PV application and (b) mid-scale community shared solar applications.

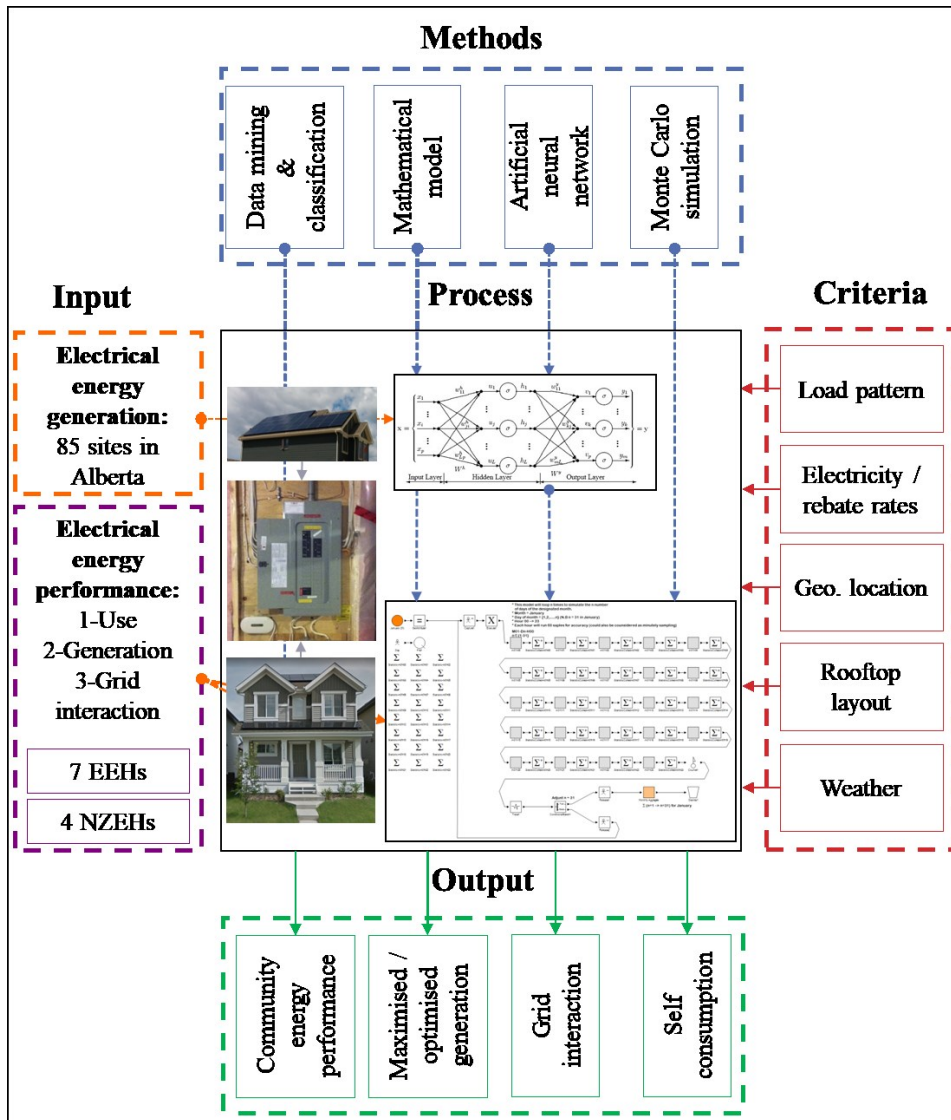


Figure 1-3. Methodology proposed in this thesis.

In addition, seven energy-efficient homes and four NZEHs located in Edmonton, Alberta have been monitored since May 2015 to date at a temporal resolution of 1 minute. Supplementary data such as meteorological and geographical data is also collected for analysis. Figure 1-3 summarises the methodology proposed in this thesis.

## 1.6. Organisation of Thesis

The thesis is organised into six chapters including this first introductory chapter, followed by two appendices.

*Chapter 2* presents a study conducted to evaluate the long-term energy performance of solar PV systems in cold-climate regions, specifically in Alberta, Canada. In this chapter, the performance of 86 solar PV systems located in 9 cities—Edmonton, Calgary, Red Deer, Airdrie, Cochrane, Leduc, Sherwood Park, Sylvan Lake, and Lakeland County—in Alberta is investigated by collecting at least three years' worth of data from each of the sites at a 5-minute temporal resolution. The dependency of a given solar PV's final yield on tilt angle, azimuth angle, and geographical location, and meteorological and soiling parameters is studied. The historical data is then validated by comparing the measured data against two solar PV prediction tools: RETScreen (Leng, 1998) and PVWatts (Dobos, 2014). In addition, energy payback time (EPBT) and GHG emission rates resulting from the monitored PV systems are identified, and the key parameters affecting the EPBT and GHG emissions are identified. Conclusions from this chapter are evidence based and are thus used as references for the developed algorithms in the following chapters. Some of these conclusions include, but are not limited to, the solar PV potential benchmarking in each of the cities where the study is conducted and the optimum layout placement in order to maximise the annual energy aggregate of PV systems and minimize the EPBT and GHG emissions.

*Chapter 3* presents a novel solar PV prediction model using an artificial neural network (ANN) that is developed to predict the daily energy generation from solar PV systems located in Alberta at large. The uniqueness of the developed model is that it accounts for the solar PV system's geographical location, tilt angle, azimuth angle, snow cover at any layout placement, and time of the year (with respect to the sun's altitude and azimuth). The model is considered a hybrid in the sense that it combines a mathematical model with historical data from 85 solar PV sites. Also, this study contributes to defining snow adjustment factors as a function of tilt angle and month

of the year. The ANN model is then validated by comparing the proposed model with a smart persistence model to identify the forecast skill of the proposed model. Finally, the proposed model is compared to PVWatts solar PV prediction tool, where it is concluded that the proposed model is more accurate than PVWatts.

*Chapter 4* demonstrates a generic solar PV optimisation model that focuses on maximising the grid-tied residential solar PV self-consumption rather than maximising its aggregated annual generation (as discussed in *Chapter 2*). This “*load-match-driven design of solar PV systems*” model is the first of its kind given that this concept is relatively novel in the design practice of residential solar PV systems. A generalised reduced gradient (GRG) non-linear optimisation algorithm is used to identify the optimum layout placement and sizing of a given solar PV system based on the household energy loads where the objective function is set to maximise the load-match (LM) indicator of the energy system (load, generation, grid). Four criteria are involved in the optimisation engine: layout placement, sizing for net-zero balance, regulatory, and economic criteria. Two case studies are also presented, one of which is an energy-efficient home and the other is a net-zero energy home. The model is finally validated by calculating the percent error between the model output with the historical data and with PVWatts.

*Chapter 5* presents a study conducted to evaluate the viability of community shared solar PV systems. Since this concept is relatively novel, it is found that no commercial tool has been developed to support such a purpose. Also, no community prototype is available within the locality of this study for evaluation. Thus, in order to simulate an entire community of diverse users by owning historical data from only 11 households, a Monte Carlo simulation model is developed to simulate the hourly energy load patterns of an entire community using probabilistic distribution of the available data samples rather than the deterministic values. Two communities of energy-efficient homes (EEHs) and net-zero energy homes (NZEHs) are simulated at the hourly interval. In order to evaluate the new conception of community shared solar, two scenarios are developed: (1) scenario 1 represents the current practice of solar PV installation, in other words, behind-the-meter individual systems connected

directly to their respective dwellings; and (2) scenario 2 demonstrates the installation of one large solar PV system that is connected to the entire community and is evenly distributed among the end-users. An optimisation model (discussed in *Chapter 4*) is applied at the community scale to identify the optimum layout placement of the solar PV system and its size in order to achieve maximum self-consumption.

*Chapter 6* summarises the findings of the studies presented in the other chapters along with conclusions and offers recommendations for future research.

*Appendix A* presents a study conducted on the design optimisation of commercial flat rooftop solar PV systems. This study is introduced as a practical application of the research presented in this thesis, since its scope is less related to the original scope of the thesis. On flat rooftops, solar PV systems are installed in arrays consisting of rows, while each row is tilted at a specific slope potentially resulting in the self-shading of the successive rows. The lower the tilt angle the shorter the shadow length, and the higher the tilt angle the more energy is generated (in high latitude regions). In this regard, this study focuses on developing an optimisation framework that identifies the optimum tilt angle and inter-row spacing while satisfying two possible criteria: (1) maximum aggregated annual generation, or (2) maximum per panel energy generation. Analytical hierarchy process (AHP) is then used to identify the market preferences of the two possible criteria and to find the optimum solution.

*Appendix B* presents the list of research publications conducted during the PhD research program.

## **Chapter 2: Long-term Performance and GHG Emission Offset Analysis of Small-scale Grid-tied Residential Solar PV Systems in Northerly Latitudes<sup>1</sup>**

### **2.1. Overview**

In the present research the energy generation of solar photovoltaic (PV) sites in northerly latitudes is analysed to investigate their actual long-term energy performance considering various performance parameters. Solar PV systems with various layout configurations are investigated based on the long-term monitored historical data collected from 86 small-scale grid-connected PV systems located in 9 cities in Alberta, Canada. The impacts of various performance parameters on the solar PV energy generation are studied in detail. The real-time solar PV performance of the sites under investigation is then verified by comparing the measured data against two commercially available online solar PV prediction tools in order to validate the data reliability. Energy payback time (EPBT) and greenhouse gas (GHG) emissions of the monitored PV systems are determined and key parameters affecting the EPBT and GHG emissions are identified. A review of the performance parameters of the monitored PV systems is undertaken and potential results are obtained and validated. Some of the conclusions include, but are not limited to, the solar PV potential benchmarking in each of the cities where the study is conducted and the optimum layout placement in order to maximise the annual energy aggregate of PV systems and minimize the EPBT and GHG emissions.

---

<sup>1</sup> A version of this chapter has been submitted for publication in *Applied Energy Journal* as Awad H, Gül M, and Al-Hussein M, *Long-term Performance and GHG Emission Offset Analysis of Small-scale Grid-tied Residential Solar PV Systems in Northerly Latitudes*.

## 2.2. Introduction

Small-scale grid-integrated solar PV systems as one type of renewable energy application in residential buildings have been adopted by home builders as a responsible sustainability practice. Not only can positive environmental impacts be achieved, such as reducing air pollution and GHG emissions by replacing fossil fuels, but also the utilisation of the energy derived from natural resources can improve current energy security and provide a sustainable environment for future generations. The residential sector accounts for the largest energy consumption share in Canada, reaching 24% in 2015, and is also responsible for 19.1% of Canada's GHG emissions (Statistics Canada, 2017) This is equivalent to 4.0 tonnes of GHG emissions on a per capita basis (Statistics Canada, 2017). Cost-effective design of solar PV systems in the residential sector has become a critical issue in speeding the deployment of renewable solar energy for self-consumption, and the Electrical Energy Consumption (EEC) in residential buildings is a key factor for manufacturing companies in designing the proper size of such systems. As per Natural Resources Canada (NRCan) (2015) the GHG intensity by electricity generated as a Canada average is 43.2 tonne/TJ, while that by natural gas is 49.68 tonne/TJ.

Several studies on solar PV technology have been conducted over the past 30 years. Some of which have covered the electrical and thermal performance of PV modules (Bernardo et al., 2011; Bhargava et al., 1991; Fujisawa and Tani, 1997; Huang et al., 2001; Kraemer et al., 2011; Kumar and Rosen, 2011; Marion et al., 2005; Raman and Tiwari, 2009; Sopian et al., 2000; Wolf, 1976), numerical simulation (da Silva and Fernandes, 2010; Dobos, 2014; Kalogirou, 2001; Leng, 1998; Naraghi, 2016; Skoplaki and Palyvos, 2009; Yang et al., 2012), integration to building subsystems (Delisle and Kummert, 2014; Hestnes, 1999; Katiraei, 2011; Román et al., 2008; Yin et al., 2013), configuration of various types of solar collector and PV systems (Braunstein and Kornfeld, 1986; Cox and Raghuraman, 1985; Ibrahim et al., 2011; Sopian et al., 2000; Ueda et al., 2009), and review of residential solar power systems (Chow, 2010; Iwafune et al., 2010; Leloux et al., 2012; Parida et al., 2011; Ramos et

al., 2010; Riffat and Cuce, 2011; Vivar et al., 2012). Additionally, previous studies on snow-coverage loss factors have been conducted by Andrews et al. (2013), Marion et al. (2013), NAIT (2015), and Awad et al. (2017a).

Decker and Jahn (1997) investigate the performance of 172 rooftop grid-tied solar PV systems in Northern Germany using AC electricity counters and PV power integrators to measure the irradiance on site where all PV systems are south facing and at tilt angles of 22°–50°. Their study reveals that the final yield in Northern Germany varies between 750 kWh/kW<sub>p</sub> and 850 kWh/kW<sub>p</sub>. Sugiura et al. (2003) investigate the residential solar PV performance characteristics in Japan in order to obtain knowledge required for solar PV optimisation. Jahn and Nasse (2003) analyse the performance of grid-tied solar PV systems in international energy agency (IEA) countries where data from 334 PV sites located in different 14 countries is collected and compared in terms of performance ratio (PR). Their results indicate that the average annual PR of the monitored PV systems is 75%. Hussein et al. (2004) study the performance of mono-crystalline silicon type solar PV modules at various tilt angles and orientations in Cairo, Egypt. In their study, a prediction model using Fortran® computer subprogram is developed and compared with the real-time PV performance. According to the geographical location and meteorological conditions of Cairo, the optimum layout placement for maximized aggregated annual generation is found to be south-facing at a tilt angle of 20°–30°. Mondol et al. (2007, 2006, 2005) simulate and validate the long-term electrical and thermal performance of a building-integrated solar PV system in Northern Ireland by comparing the simulation results with the actual measured data. Their study reveals that the error between the measured and the simulated PV output is 6.79%. Marion et al. (2005) focus on defining the performance parameters for grid-connected solar PV systems with respect to the variability of design, technology, and geographical location. In this regard, they conclude that, according to the scope of the study, the four primary performance parameters to consider are the PV system's final yield, reference yield, performance ratio, and PVUSA rating. Joshi et al. (2009) conduct a review study on the performance analysis of solar PV systems with a focus on electrical, thermal,

energy, and exergy efficiency aspects. Another review study conducted by Leloux et al. (2012) focus on the performance of residential solar PV systems in Belgium by analyzing the operational data of 993 PV sites. Their study concludes that in Belgium, the average annual yield is 892 kWh/kW<sub>p</sub> and the performance ratio is 78%. Ayompe et al. (2011) investigate the performance of a solar PV system installed on a flat rooftop of a mid-rise building located in Dublin, Ireland. Their study concludes that, despite the low insolation levels in Ireland, the annual final yield from the monitored PV system, 885.1 kWh/kW<sub>p</sub>, is higher than that recorded from Germany, Portland, and Northern Ireland due mainly to the relatively high wind speed and low ambient temperature. In developing countries, the solar power sector development is confronted by the shortage of reliable long-term global irradiance data; the performance analysis of solar PV installations thus becomes a great challenge. In this context, Purohit and Purohit (2018) monitor and evaluate the techno-economic performance of 39 solar PV systems located in India where they compare the measured data with irradiance data from several databases.

The residential sector accounts for the largest energy consumption share in Canada, reaching 24% in 2015, and is also responsible for 19.1% of Canada's GHG emissions (Statistics Canada, 2017). This is equivalent to 4.0 tonnes of GHG emissions on a per capita basis (Statistics Canada, 2017). Cost-effective design of solar PV systems in the residential sector has become a critical issue in speeding the deployment of renewable solar energy for self-consumption, and the Electrical Energy Consumption (EEC) in residential buildings is a key factor for manufacturing companies in designing the proper size of such systems. As per Natural Resources Canada (NRCan) (2015) the GHG intensity by electricity generated as a Canada average is 43.2 tonne/TJ, while that by natural gas is 49.68 tonne/TJ. Several studies have covered methods of quantifying the energy payback time (PV) and life cycle GHG emissions resulting from solar PV technology referring back to the last 40 years (Celik et al., 2018; Laleman et al., 2011; Louwen et al., 2016; Nugent and Sovacool, 2014; Peng et al., 2013). Knapp and Jester (2000; 2001) investigate the EPBT for crystalline silicon photovoltaic panels by conducting an empirical study and find that,

in general, these panels achieve an energy break-even in 3–4 years. Bhandari et al. (2015) conduct a systematic review and meta-analysis of EPBT and energy return on energy invested (EROI) metrics while focusing on crystalline silicon and thin film solar PV panels. Kato et al. (1998) quantify the environmental impacts in terms of EPBT and life cycle GHG emissions for various solar PV module technologies such as mono-crystalline, poly-crystalline, and amorphous silicon modules, where their study reveals that mono-crystalline silicon modules are accompanied by the shortest EPBT and GHG emission compared to other PV technologies. Peng et al (2013) conduct a review study on the assessment of EPBT and GHG emissions of various solar PV systems. In their study, results indicate that the average life cycle energy requirement for mono-crystalline solar PV modules varies between 2860 MJ/m<sup>2</sup> and 5253 MJ/m<sup>2</sup> and that the EPBT varies between 1.7 yr to 2.7 yr.

In a previous study, Awad et al. (2017) develop a prediction model that predicts the daily energy generation of solar PV systems through a generic framework, taking into account snow adjustment factors, tilt angle, azimuth angle, and geographical location. This study reveals that higher-mount solar PV systems (i.e., 50°–60°) improve the performance of the solar PV systems in high-latitude regions. Another study by Awad et al. (2017b) proposes a generic framework to improve the self-consumption of solar PV systems based on the household energy consumption patterns of energy-efficient homes located in Edmonton, Canada. Results indicate that a south-west facing solar PV system tilted at approximately 40° maximises the load-match of the solar PV system significantly. However, in commercial flat rooftop solar PV applications, other measures should be taken into consideration in order to maximise the roof space productivity such as self-shading, inter-row spacing for fire, safety, maintenance purposes, and the user's preferences of whether to maximise the annual aggregated energy or to maximise the productivity of each panel in the system. For example, Awad et al. (2016) propose an analytical hierarchy process to optimise the layout placement of a solar PV system in terms of tilt angle and inter-row spacing.

### 2.2.1. *Research Gap*

As a conclusion from the literature review, it is found that previous studies have primarily focused on the electrical components of solar PV systems and have hardly quantified or correlated the combined impacts of the various performance parameters such as geographical location, climatological conditions, tilt angle, and azimuth angle on the grid-tied residential solar PV performance, EPBT, and GHG emissions, particularly in the northerly cold-climate regions. It is also found that, due to the solar PV market penetration in Canada, it is crucially important to provide a detailed performance analysis of the existing solar PV systems in the local meteorological and geographical conditions of Canada in general and Alberta in specific.

### 2.2.2. *Research Objectives and Scope*

- (1) The scope of this study highlights the actual long-term performance of residential grid-tied solar PV systems located in northerly latitudes. Four specific questions will be answered in this chapter: (1) what is the actual performance of solar PV systems in cold-climate regions? (2) what is the impact of geographical location, tilt angle, azimuth angle, and weather conditions on the solar PV performance? (3) how accurate are the commercially available solar PV prediction software compared to the real-time data? and (4) what is the “energy payback time” and GHG emission rates accompanied by the installed solar PV systems?

## 2.3. **Data Collection**

Eighty-six solar PV systems across Alberta are monitored on the long term. All of the monitored PV systems are fixed monocrystalline silicon solar PV panels of various brands (Canadian Solar, 2013; Conergy, 2016; Hyundai, 2010; JA Solar, 2015; Sanyo, 2014) and capacities ( $225W_p$ – $260W_p$ ). The tilt angles of those PV systems vary between  $9^\circ$  and  $60^\circ$  and the azimuth angles vary between  $60^\circ$  and  $279^\circ$ . The PV systems, as presented in Figure 2-1, are located in nine cities in Alberta, namely,

Airdrie, Calgary, Cochrane, Red Deer, Edmonton, Sherwood Park, Leduc, Sylvan Lake, and Lakeland County, where the longitude varies between 114.5° W and 111.9° W and the latitude varies between 50.8° N and 54.7° N. In the context of this study, the cities within the same 1° latitude range are grouped into one region and given a region number. For example, Edmonton, Leduc, and Sherwood Park, having latitudes of 53.631°, 53.258°, and 53.541°, respectively, are grouped into one region and named as Region III. Table 2-1 demonstrates the locations where the PV systems are installed and the method by which the cities are grouped into four regions: Region I to Region IV.

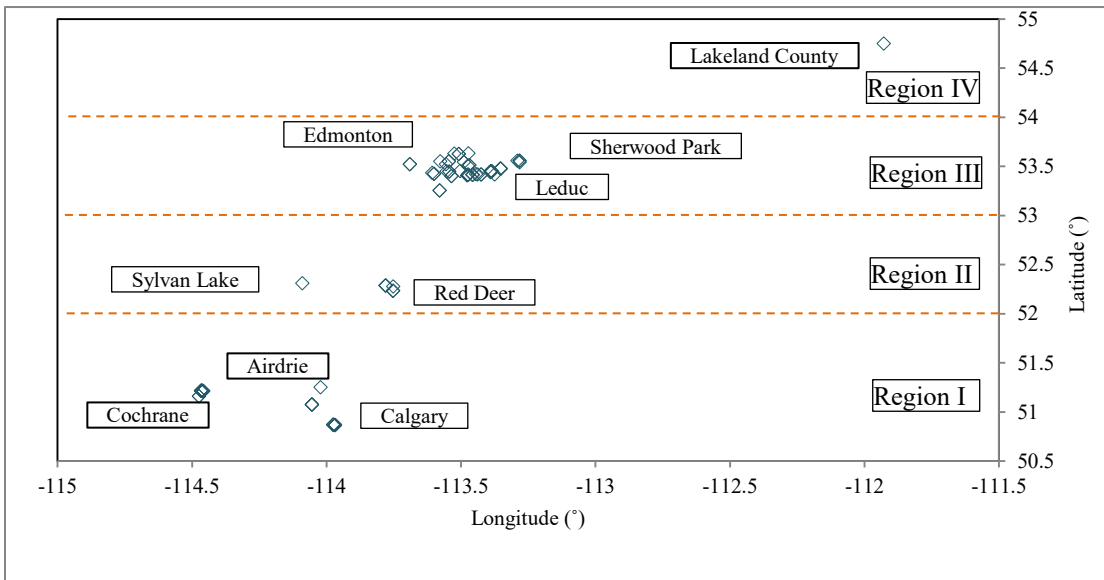


Figure 2-1. Geographic location of the monitored PV systems in longitude and latitude.

Each PV system module is connected to a micro-inverter (Figure 2-2a). DC current is then converted into AC current and sent to the utility grid through the bi-directional metering system (Figure 2-2b). The energy generation data is then collected and monitored by the Envoy data monitoring system (Enphase System, 2017) (Figure 2-2c) where data is stored in the cloud-based management system, Enphase Energy (2016). Finally, data from all monitored PV systems are collected and stored in an in-house data warehouse developed by the research team for analysis (Figure 2-2d).

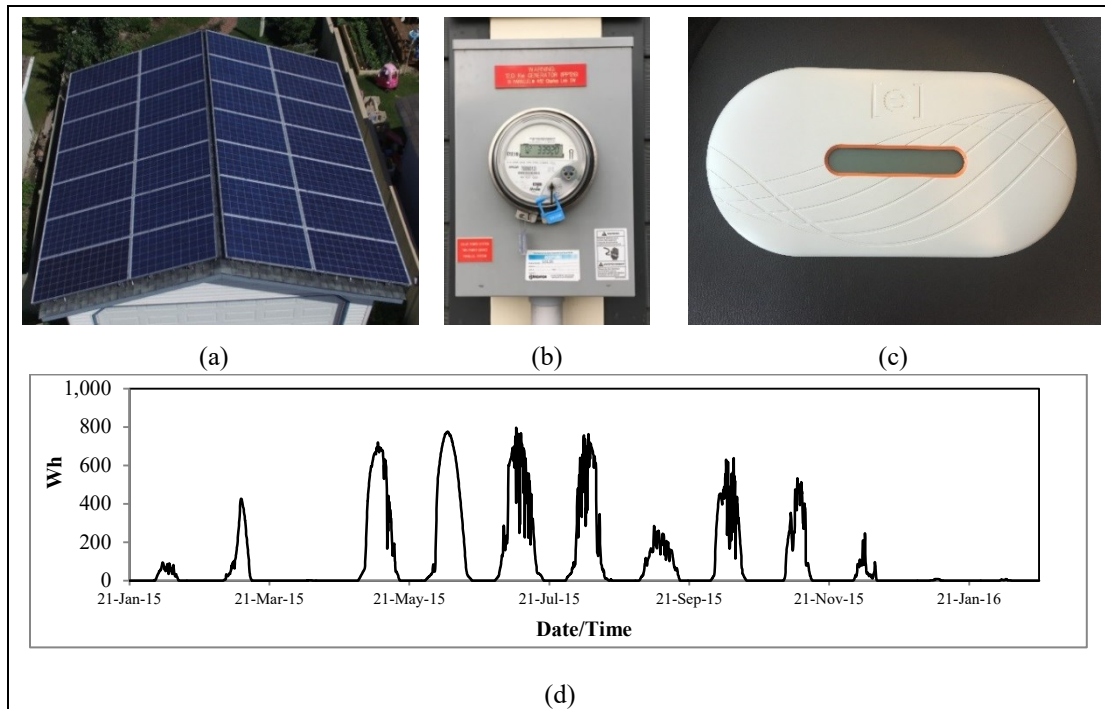


Figure 2-2. Typical monitoring system of the PV systems: (a) is the PV array and micro-inverters hidden underneath; (b) is the bi-directional metering system where the AC from the PV system is connected to the grid; (c) is the Envoy system that monitors the data collected from the PV system; and (d) is a sample of the five-minute interval data.

Table 2-1. Locations and grouping method of the cities where the PV systems are installed.

City	Qty of PVs	Lat. (° N)	Long. (° W)	Region	Lat. range (° N)	Total
Airdrie	1	51.286	113.999			
Calgary	13	51.131	114.011	Region I	51.00 – 51.99	30
Cochrane	16	51.197	114.472			
Red Deer	6	52.268	113.811	Region II	52.00 – 52.99	7
Sylvan Lake	1	52.312	114.087			
Edmonton	42	53.631	113.324			
Leduc	2	53.258	113.550	Region III	53.00 – 53.99	48
Sherwood Park	4	53.541	113.295			
Lakeland County	1	54.750	111.928	Region IV	54.00 – 54.99	1

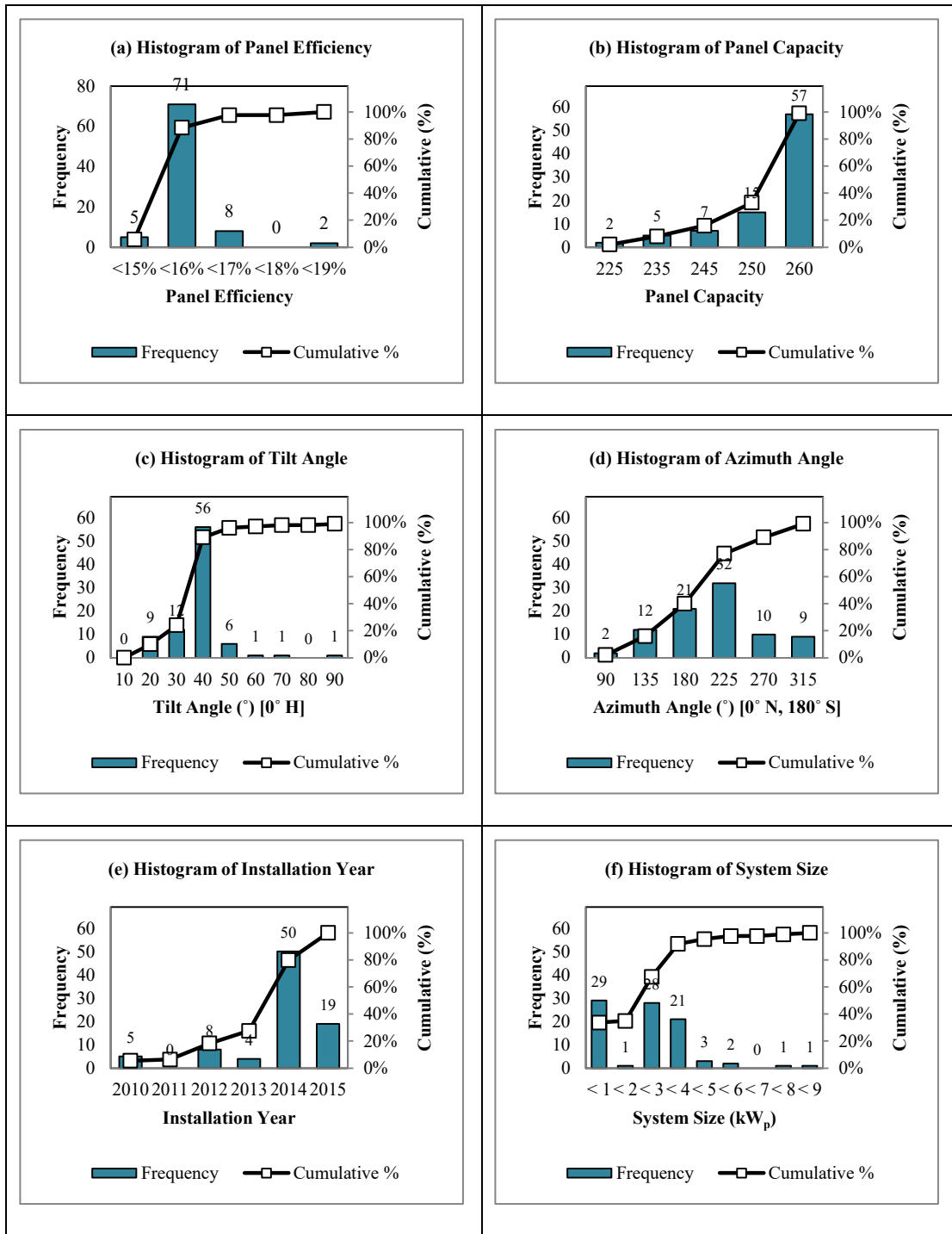


Figure 2-3. Statistical properties of the monitored PV sites including (a) panel efficiency, (b) panel capacity, (c) tilt angle, (d) azimuth angle, (e) year of installation, and (f) system size.

Figure 2-3 summarises the statistical properties of the monitored PV sites in terms of histogram and cumulative distributions by (a) panel efficiency, (b) panel capacity, (c) tilt angle, (d) azimuth angle, (e) installation year, and (f) system size. For simplicity and regarding the fact that the monitored PV systems are installed at a wide range of azimuth angles, these angles are systematically divided into eight bins. Each bin is 45° wide and divided evenly around the true directions of north (0°), northeast (45°), east (90°), etc., as demonstrated in Table 2-2. In addition, a wide range of tilt angles is also investigated in this study, including 2:12 (9°), 3:12 (14°), 4:12 (18°), 5:12 (23°), 6:12 (27°), 7:12 (30°), 8:12 (34°), 9:12 (37°), 10:12 (40°), and 21:12 (60°).

Table 2-2 presents the distribution of tilt and azimuth angles deployed in the present study. Similar to the majority of pitched roof conventional practice in North America, 74% of the monitored houses are constructed at slope ratios of 6:12, 7:12, and 8:12, and 32% of these slopes are south oriented.

Table 2-2. Histogram of the tilt and azimuth angles of the PV systems. Roof pitch ratios and azimuth angle ranges are provided only in this table and can be referred to for the tables below.

Roof pitch ratio (#:12)		2	3	4	5	6	7	8	9	10	11	Total	%	
Tilt angle (°)		9	14	18	23	27	30	34	37	40	60			
Azimuth angle (°)	22.5~67.5	NE	-	-	-	1	-	-	-	-	-	1	1.2	
	67.5~112.5	E	-	-	2	-	-	7	3	-	1	13	15.1	
	112.5~157.5	SE	1	-	-	1	3	2	-	2	1	10	11.6	
	157.5~202.5	S	-	1	5	-	7	11	10	-	3	1	38	44.2
	202.5~247.5	SW	-	-	-	-	-	8	2	1	-	-	11	12.8
	247.5~292.5	W	-	-	1	-	-	8	3	-	1	-	13	15.1
	292.5~337.5	NW	-	-	-	-	-	-	-	-	-	0	0	
	337.5~22.5	N	-	-	-	-	-	-	-	-	-	0	0	
Total		1	1	8	2	10	36	18	3	6	1	86	100	
%		1.2	9.3	2.3	11.6	41.9	20.9	3.5	7	1.2	100	1.2		

#### 2.4. Impact of Performance Parameters on PV Output

Since this study investigates systems of various locations, tilt and azimuth angles, panel models and capacities, and number of panels, the data is normalised to its final

yield (Eq. 2-1) to better serve the analytical purpose of the study (Marion et al., 2005).

$$Y_f = \frac{E}{P_0} (kWh/kW_p) \quad (2-1)$$

Where  $E$  is the energy generated by the PV system (kWh) and  $P_0$  is the system size as a product of the number of the systems modules and the module capacity ( $kW_p$ ). Data is collected at a five-minute interval resolution to investigate the daily power generation profiles; however, the daily energy generation is used to match the time resolution of the currently available meteorological data collected from the National Aeronautics and Space Administration (NASA, 2017). Figure 2-4 presents the annual final yield of the monitored PV sites by year and by average of all years. Providing that most of the systems (82% as per Figure 2-3e) were installed between 2014 and 2015, it is observed that in majority of the systems the annual final yield is maximised in 2015, followed by 2016, and then 2017. As discussed later, a correlation analysis is provided in order to demonstrate the key drivers of the systems' generating potential.

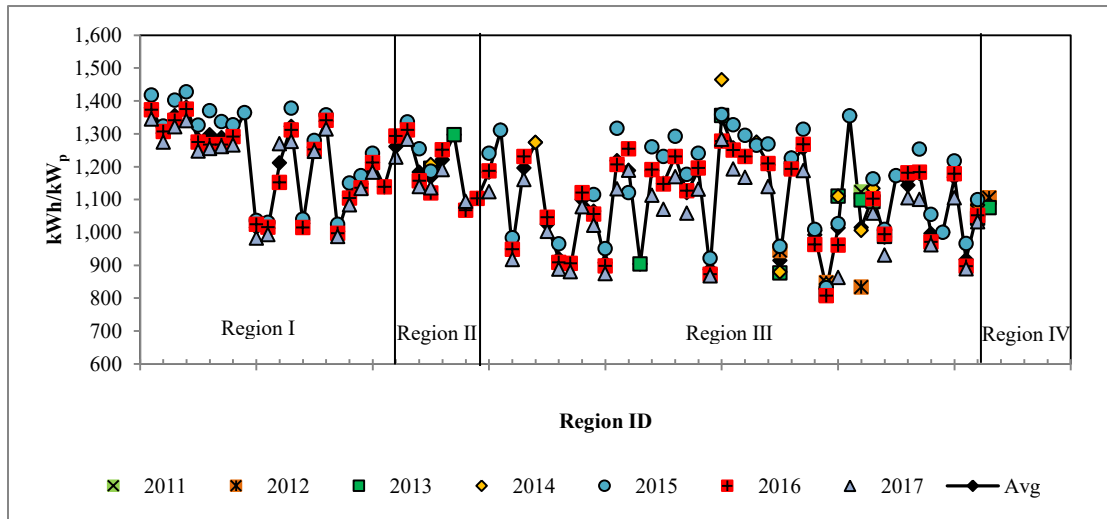
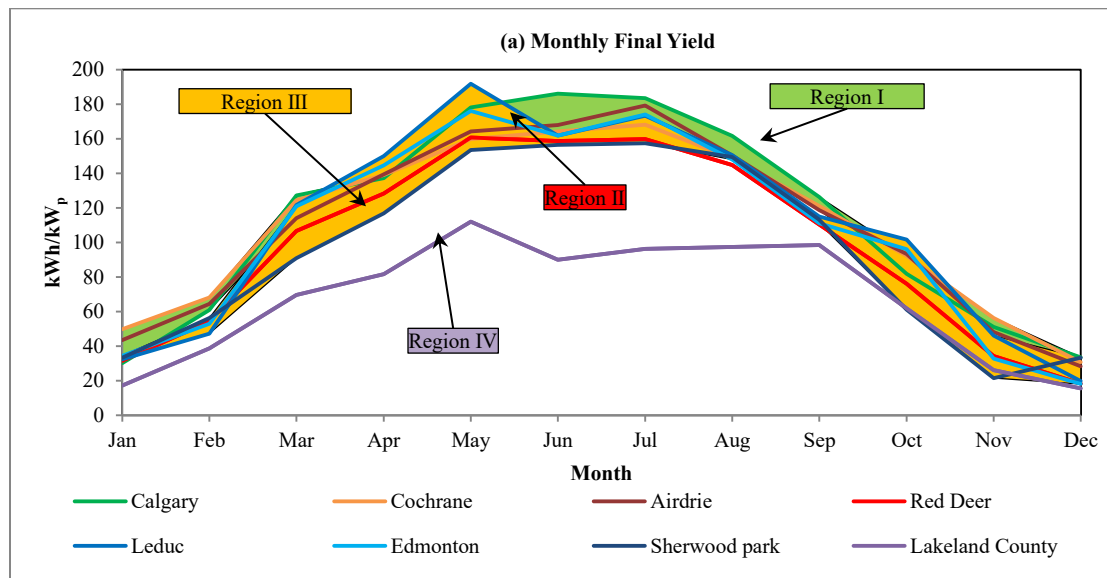


Figure 2-4. Annual energy generation of all monitored PV sites by year and average of all years.

### 2.4.1. Geographical Location

To determine the impact of various parameters on PV performance, each parameter will be investigated separately by fixing the other parameters. For instance, the impact of location on PV performance will be determined by investigating PV systems of the same tilt and azimuth angles in the various locations. Figure 2-5a presents an example of the monthly profile of the energy generated by south-facing 27°-tilt PV systems in different cities from September 2015 to August 2016 while Figure 2-5b indicates the annual energy generated in these cities. Since Airdrie, Cochrane, and Calgary are located within the same region (Region I), the annual energy generation of these three cities is comparable at 1,311.4 kWh/kW<sub>p</sub>, 1,322.5 kWh/kW<sub>p</sub>, and 1,357.2 kWh/kW<sub>p</sub>, respectively. Similarly, Edmonton Sherwood Park, and Leduc (Region III) have annual energy generations of 1,270.4kWh/kW<sub>p</sub>, 1,143.4 kWh/kW<sub>p</sub>, and 1,311.2 kWh/kW<sub>p</sub>, respectively. Red Deer (Region II), located between Region I and Region II, has an annual energy generation of 1,183.8.0 kWh/kW<sub>p</sub>, unexpectedly a lesser generation than both surrounding regions. Lakeland County (Region IV), located northeast of Region III is observed to have the least generation of all locations of 804.8 kWh/kW<sub>p</sub>.



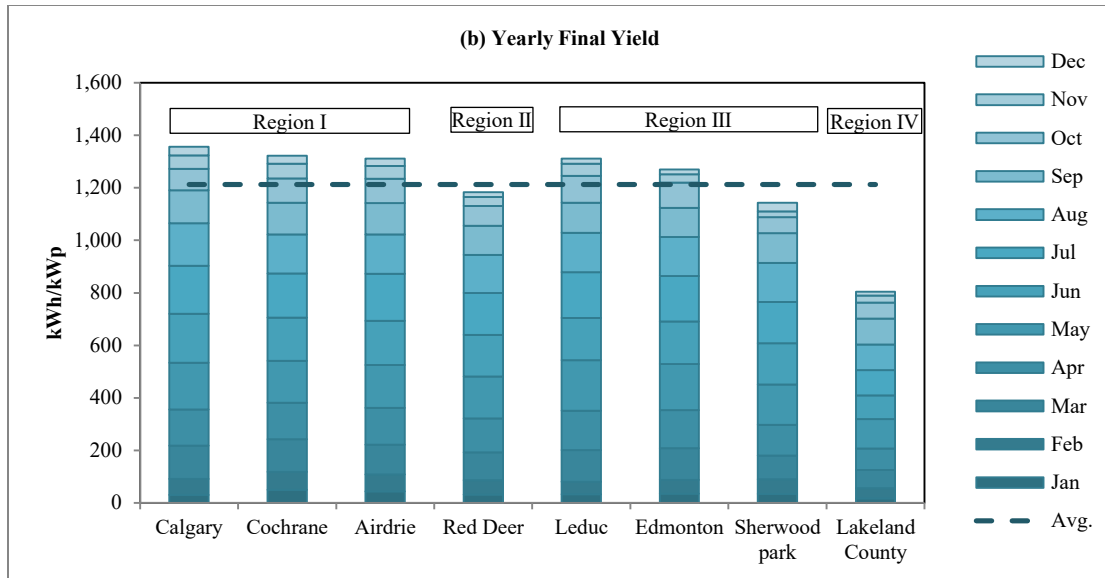


Figure 2-5. The (a) monthly and (b) annual energy generation of south-facing 27°-tilt PV systems in different cities.

The mean energy generation of all cities at the same layout placement (i.e., south-facing at 27° tilt angle) is 1,213.10 kWh/kW<sub>p</sub>, while the standard deviation is found to be 180.4 kWh/kW<sub>p</sub>. This drives a conclusion that location has an average impact of 15% on energy generation within the 4° -latitude interval. It is also apparent that Region I (especially Cochrane), due to the larger number of sunny hours and lesser amounts of snow, has a higher PV potential than the other cities. It is also observed that in Region III and Region IV, the energy generation in May is larger than that of June, despite the fact that daylight hours peak globally in June with respect to the northern hemisphere. This is due mainly to the increased cloud cover and precipitation in June.

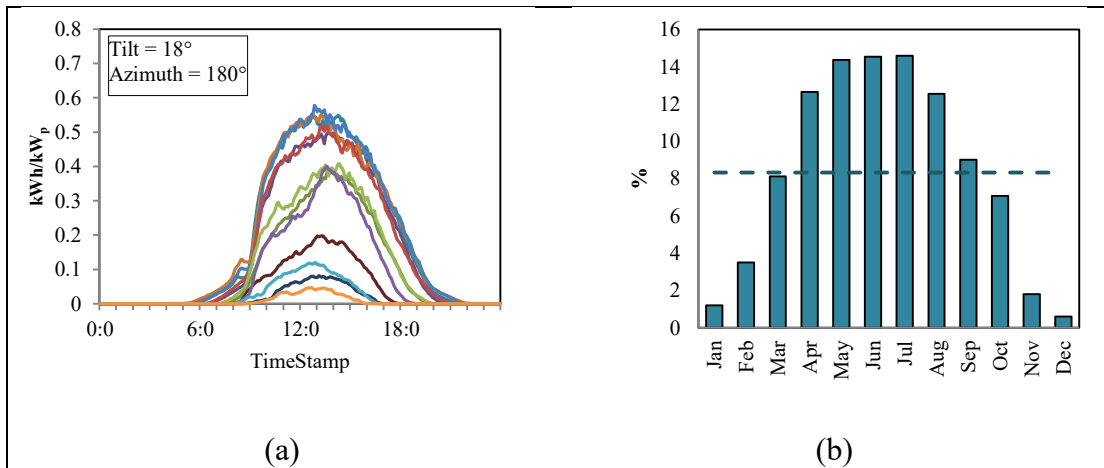
#### 2.4.2. Tilt Angle and Azimuth Angle

A PV system's tilt angle has a strong influence not only on the daily power generation profile but also its monthly energy generation profile and distribution. Figure 2-6 demonstrates another example comparing a common-practice south-facing 27°-tilt PV system (Figure 2-6c and Figure 2-6d) against two south-facing PV

systems located in the same city, Edmonton (in Region III), where the first example (Figure 2-6a and Figure 2-6b) is tilted at 18° and the second example (Figure 2-6d and Figure 2-6e) is tilted at 60°. Figure 2-6a, Figure 2-6c, and Figure 2-6e are plots of the mean daily profile for each month of the year to demonstrate the impact of daylight hours, amount of irradiance received throughout the year, latitude angle of the sun, and also the local tilt angle of the PV system (which correlates to the local in-plane irradiance of each PV system). Figure 2-6b, Figure 2-6d, and Figure 2-6f demonstrate the mean monthly energy generation percentage for the 18°, 27°, and 60°-tilt PV systems, respectively. By comparing the three bar-charts, it is observed that the energy generation for the PV system with 18° tilt angle is maximised in July (14.6%), followed by June (14.5%) and May (14.4%), and is minimised in December (0.59%) while that of the PV system with 60° tilt angle is maximised in May (11.3%), followed by August (10.9%) and July (10.6%), and is minimised in December (2.55%). The energy generation of the 27° tilt is maximised in May (14.4%), followed by July (13.6%) and June (13%), and is minimised in December (1.09%). Overall, the energy generation of the 60°-tilt PV system has less standard deviation (3.0%) throughout the year than the 18°- and the 27°-tilt PV systems, having standard deviations of 5.2% and 4.7%, respectively. This is indicative of the high local latitude in Alberta; thus high-mount PV systems become more capable of receiving sun rays throughout the year, especially during shoulder and winter seasons where the sun's altitude angle is relatively low. Even though the current practice of pitched roofs in North America is between 27° and 34°, it is advisable to install the south-oriented PV systems at high tilt angles such as 50°–60°. The annual final yield of these PV systems is calculated as 1,066 kWh/kW<sub>p</sub>, 1,235 kWh/kW<sub>p</sub>, and 1,314 kWh/kW<sub>p</sub> for the 18°, 27°, and 60°-tilt angles, respectively. This concludes that changing the tilt angle from 18° to 60° incurs variability of 127 kWh/kW<sub>p</sub>—approximately 10% of the mean annual energy generation of these PV systems. Also, leveraging the amount of energy generated in winter months has an advantage in paying for the higher energy consumption in winter due to excessive electricity usage for heating, hot water

heating, and lighting as a result of a small number of daylight hours, etc. (Li et al., 2016).

In order to quantify the impact of a given system's tilt angle ( $\theta$ ) on its generating capacity, knowing the daily and seasonal variability of the sun's angle of incidence on the receiving surface, it is found that the tilt angle, as a fixed value, can be misleading, especially in case of investigating multiple systems at once. In this context, the PV system's tilt angle is re-defined as the inclination of the sun on the receiving surface (*INC*) at a given time. In order to do so, a mathematical model is developed to track the sun's path according to the geographical locations of the monitored sites. Solar geometry calculations for each day of the year (*DOY*)—including solar zenith ( $z$ ) (Reno et al., 2012), declination ( $\delta$ ) (Allen, 2005; Reno et al., 2012), solar time (ST) (Allen, 2005; Reno et al., 2012), hour angle ( $\omega$ ) (Kreider et al., 1989; Reno et al., 2012), true zenith ( $z_t$ ), daylight hours ( $\beta$ ) (Kreider et al., 1989), the sun's degree angle from due south at sunset (Hourset) (Kreider et al., 1989), and the sun's azimuth angle ( $\alpha$ ) (Kreider et al., 1989)—are derived from Eq. 2-2 to Eq. 2-13.



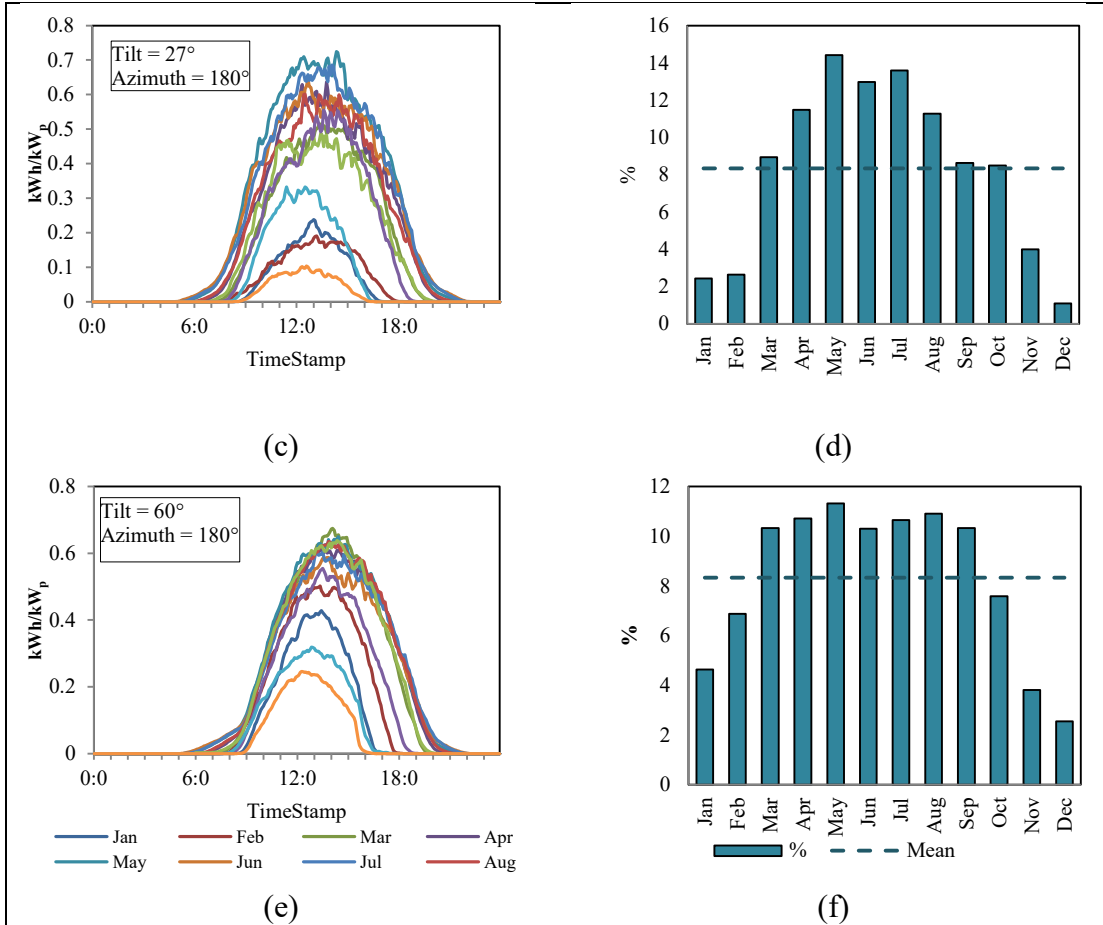


Figure 2-6. (a) Mean daily profile for each month of the year for a PV system in Edmonton with 18° tilt and 180° azimuth angles; (b) the mean monthly power generation percentage; (c) the mean daily profile for each month of the year for a PV system in Edmonton with 60° tilt and 180° azimuth angles; (d) the mean monthly power generation percentage.

$$z = \begin{cases} \varphi, & DOY = 80 \text{ or } DOY = 264 \\ \varphi - \delta, & \text{Otherwise} \end{cases} \quad (2-2)$$

$$\delta = 23.45 \times \sin(x) \quad (2-3)$$

$$\text{with } x = 360^\circ/365 \times (DOY - 81) \quad (2-4)$$

$$ST = Local\ Time + (Standard\ Meridian - Local\ Meridian) \times 4' + EoT \quad (2-5)$$

$$\text{with } EoT (\text{minutes}) = 9.87 \times \sin(2x) - 7.53 \times \cos(x) - 1.5 \times \sin(x) \quad (2-6)$$

$$\omega^\circ = (ST (\text{hours}) - 12) \times 15 \quad (2-7)$$

$$z_t^\circ = \cos^{-1} [\cos(\varphi) \times \cos(\delta) \times \cos(\omega) + \sin(\varphi) \times \sin(\delta)] \quad (2-8)$$

$$\beta = 2 \times HourSet / 15 \quad (2-9)$$

$$\text{with } HourSet (\text{ }^\circ) = \cos^{-1} [-\tan(\delta) \times \tan(\varphi)] \quad (2-10)$$

$$\alpha = \sin^{-1} [\cos(\delta) \times \sin(\omega) / \cos(h)] \quad (2-11)$$

$$\text{with the sun's elevation } h = 90 - z_t \quad (2-12)$$

In this regard, the tilt angle ( $\vartheta$ ) at a specific site ( $\varphi$ ) on a specific *DOY* is processed to define the sun's angle of inclination on that specific tilted surface as a function of declination ( $\delta$ ), latitude ( $\varphi$ ), and hour angle ( $\omega$ ) (Kreider et al., 1989) as per Eq. 2-13

$$INC = \sin(90 - \cos^{-1} [\cos(\delta) \times \cos(\varphi - \vartheta) \times \cos(\omega) + \sin(\delta) \times \sin(\varphi - \vartheta)]) \quad (2-13)$$

Figure 2-7 demonstrates the correlation between the daily final yield of all monitored systems located at various sites against each system's corresponding tilt angle (Figure 2-7a) and against the inclination of the sun on each system's receiving surface (Figure 2-7b) calculated at solar noon. Since the tilt angle is a fixed parameter accompanied with the a given PV system's layout setting while the sun's angle of incidence varies within the daily as well as the seasonal context, and since the tilt angle intrinsically incurs variable impacts while considering the variation of geographical location, a system's tilt angle solely is non-intuitive. Instead, the degree inclination of the sun on the receiving surface by combining the geographical location and the system's tilt angle is greatly important to drive meaningful conclusions. It is thus observed that the latter setting is recommended in order to quantify the impact of tilt angle on a PV system's final yield accurately (Awad et al., 2017a). The impact of the deviation of azimuth angle from the south direction on the yearly final yield of PV systems is also investigated. The final yield of PV systems having a tilt angle of  $30^\circ$  in each area is

plotted in Figure 2-8 for Region I, Region II, and Region III. The impact of the deviation of a PV system from the true south by  $90^\circ$  on its energy generation is approximately 20%. By comparing  $30^\circ$  mount south-facing PV systems in the various locations, it is concluded that the PV potential of these systems are 1,311.4 kWh/kW<sub>p</sub>, 1,322.5 kWh/kW<sub>p</sub>, and 1,357.2 kWh/kW<sub>p</sub>, 1,270.4kWh/kW<sub>p</sub>, 1,143.4 kWh/kW<sub>p</sub>, and 1,311.2 kWh/kW<sub>p</sub>, 1,183.8, kWh/kW<sub>p</sub> and 804.8 kWh/kW<sub>p</sub> for Airdrie, Cochrane, Calgary, Edmonton, Sherwood Park, Leduc, Red Deer, and Lakeland County, respectively, having an average of 1,213.10 kWh/kW<sub>p</sub>, and a standard deviation of 180.4 kWh/kW<sub>p</sub>.

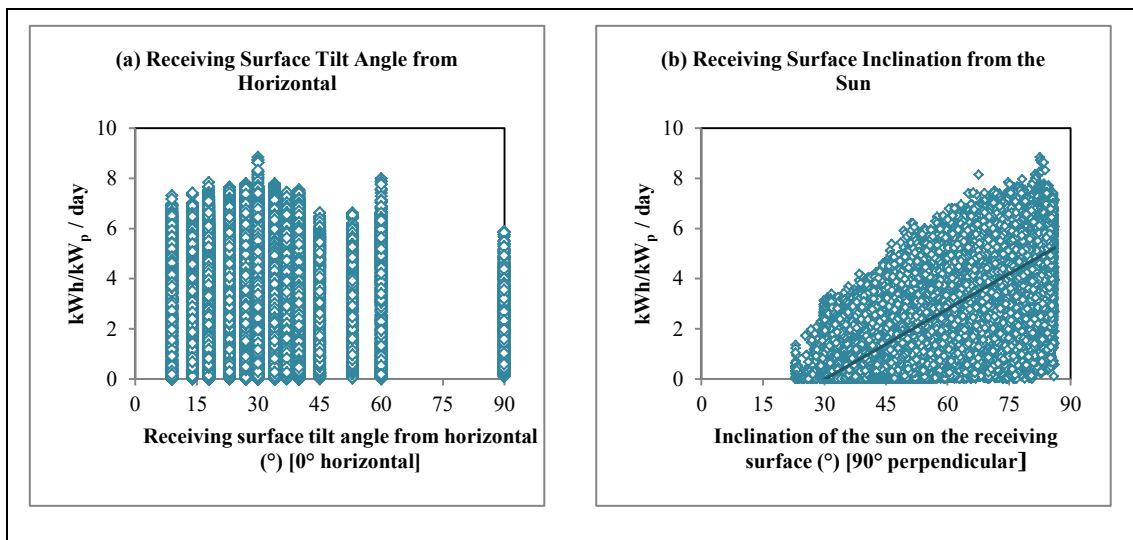


Figure 2-7. Correlation between the daily final yield from all monitored PV sites against the (a) system tilt angle and (b) inclination of the sun on the PV system's receiving surface.

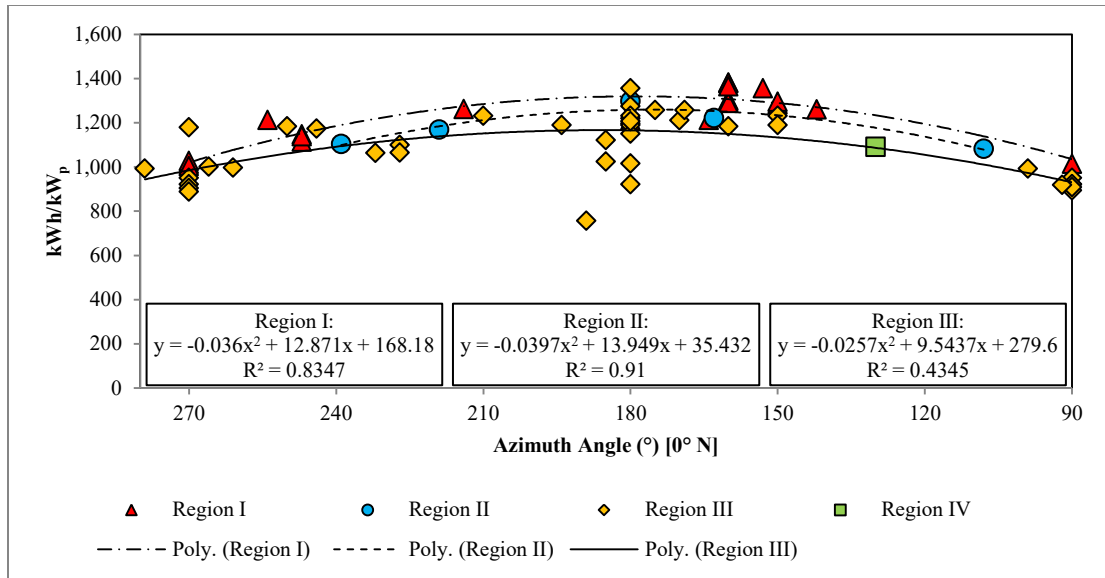


Figure 2-8. Annual final yield of PV systems placed at 30° tilt angle in Region I, Region II, and Region III.

### 2.4.3. Meteorological and Soiling Parameters

Several studies have previously been conducted to determine the key performance parameters of a solar PV system; however, due to the extreme weather conditions in Alberta, especially in winter, parameters such as irradiance are highly correlated with final yield, yet are not enough to achieve a highly accurate prediction of the solar PV productivity. In addition to the significantly low temperature and snow coverage during winter, the sun's altitude angle becomes very low in winter, at about 13.6° in December, and increases in summer, reaching only 60.0° in June. Furthermore, daylight hours fluctuate drastically between winter and summer. Therefore, energy generation in winter is relatively insignificant whereas energy generation in summer is comparatively high. A correlation analysis is conducted, and, accordingly, the effective performance parameters are identified and summarized in Table 2-3, while more details can be found in a study conducted by Awad et al. (2017a).

As discussed previously, tilt angle, orientation, and geographical location in terms of latitude are effective parameters on solar PV performance; however, it is observed that by comparing the various meteorological (variable) parameters with the location

and layout (fixed) parameters, the “daily” energy generation is significantly affected by the varying meteorological conditions that fluctuate significantly rather than the fixed parameters that can affect the overall performance by a relatively low degree of fluctuation. As a demonstration, Figure 2-9 visualises the correlation between the solar PV systems’ final yield and local insolation. Here it is observed that there is a linear correlation between the daily final yield and the daily insolation for the events of daylight hours having an average of 8.9 hours, while, on the other hand, with events of daylight hours with an average of 14.6 hours, the correlation between the daily final yield and daily insolation become non-linear, particularly logarithmic.

Theoretically and empirically (Moghadam et al., 2011), a PV system’s annual energy generation is maximised if the system is installed at a tilt angle equivalent to the local latitude of the system and oriented to the south with a little allowance (e.g., 15°) (Moghadam et al., 2011). In this context, analysis is conducted to investigate and compare the PV annual energy generation in each city with regard to the various tilt and azimuth angles. Table 2-4 presents the annual final yield (kWh/kW<sub>p</sub>) of all the PV systems installed in Region I, Region II, and Region III and discusses the amount of loss due to system design compared to its PV potential. A south-facing PV system installed at a 60° tilt angle at latitude of 53.45°N has a PV potential of 1,314 kWh/kW<sub>p</sub>.

Table 2-3. Correlation analysis between performance parameters and final yield.

Parameter	Correlation [0-1]	Parameter	Correlation [0-1]
GHI_Actual	0.8778	Downward Longwave Radiation Flux	-0.6763
Altitude	0.7387	Snow Adjustment Factors	0.5246
Hourset	0.7360	Clear-sky Index	0.5057
Relative Humidity	-0.7315	Snow on Ground	-0.4364
True Zenith	-0.7312	Solar Time	-0.2518
Declination	0.7297	Hour Angle	-0.2518
Daylight hours	0.7274	El Nino Index	-0.1643
Direct Normal Irradiance	0.7183	Wind Speed	-0.1545
Extraterrestrial Irradiance	-0.7119	Total Precipitation	-0.1134
Inclination	0.6909	Azimuth	0.1011
Temperature	0.6868	Age	-0.0452

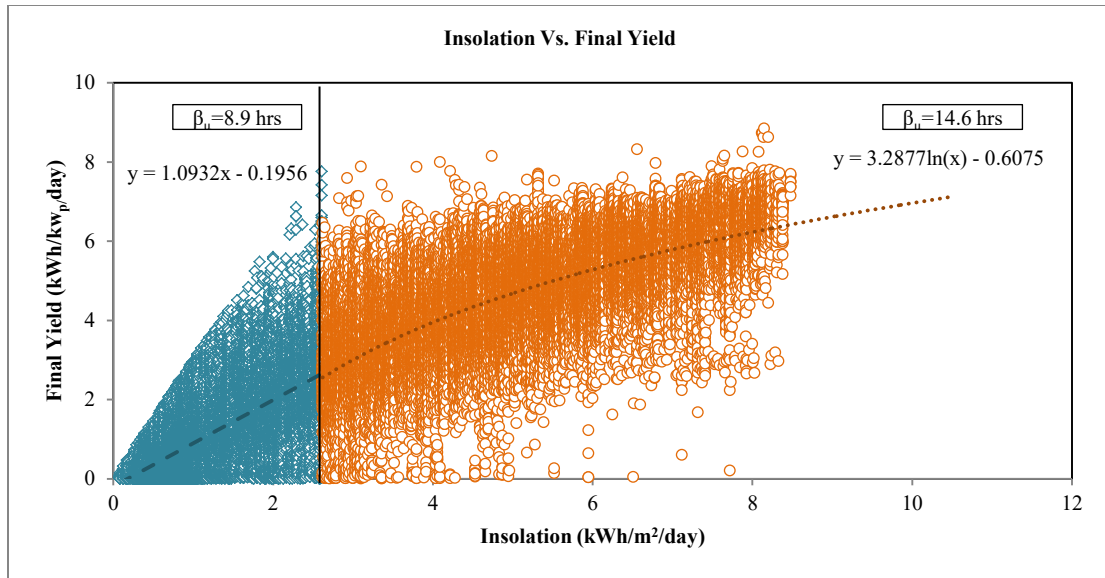


Figure 2-9. Correlation between insolation and final yield.

Unlike Region III, some PV array layouts are missing for Region I, Region II, and Region IV due to the low population of the PV systems in those regions (e.g., no PV systems with 60° tilt angle are installed in Region I, Region II, or region IV)).

Table 2-4. Measured PV potential (kWh/kW<sub>p</sub>) of various PV system layouts located in Region I. Note: information on roof pitches and azimuth angle ranges are provided in Table 2-2.

Tilt angle (°)		9	14	18	23	27	30	34	37	40	60
E	RI	-	-	933	-	-	1,016	-	-	-	-
	RII	-	-	-	-	-	-	-	-	-	-
	RIII	-	-	832	-	-	979	932	-	1,129	-
SE	RI	-	-	-	-	1,345	1,262	-	1,304	1,373	-
	RII	989	-	-	-	1,194	-	-	-	-	-
	RIII	-	-	-	1,216	-	1,259	-	-	-	-
S	RI	-	1,072	-	-	1,364	1,176	1,355	-	1,389	-
	RII	-	-	-	-	1,218	1,347	-	-	-	-
	RIII	-	-	1,066	-	1,235	1,259	1,275	-	-	1,314
SW	RI	-	-	-	-	-	1,208	-	-	-	-
	RII	-	-	-	-	-	1,208	1,172	-	-	-
	RIII	-	-	-	-	-	1,229	1,136	-	-	-
W	RI	-	-	909	-	-	1,026	-	-	-	-
	RII	-	-	-	-	-	-	-	-	-	-
	RIII	-	-	-	-	-	1,010	984	-	696	-

## 2.5. Validation

In order to conclude the PV potential of a wider range of PV layouts that have not been tested in field, first, all the monitored PV systems are simulated and validated by using two online simulation tools namely, PVWatts (Dobos, 2014) and RETScreen (Leng, 1998). Table 2-5 summarises the system losses estimated for simulations. Figure 2-10 presents the linear regression correlation between the actual and simulated energy generation of the monitored PV systems. It is observed that both PVWatts and RETScreen prediction results are greater than the actual field data. This may refer to the excess amount of snow that covers the PV systems in winter months (November to March) and precipitation in summer months (June and July). Prediction results obtained from RETScreen are observed to be over-optimistic compared to PVWatts in such a way that higher mean absolute percentage error (MAPE) (Eq.2-14) (Jin et al., 2005) is determined. The measured MAPE for PVWatts and RETScreen against the annual actual energy generation are 9.28% and 12.6%, respectively

$$MAPE \% = \frac{1}{k} \sum_{i=1}^k \left( \left| \frac{A_i - E_i}{A_i} \right| * 100 \right) \quad (2-14)$$

where  $A_i$  is the  $i^{th}$  actual energy generation,  $E_i$  is the  $i^{th}$  estimated energy generation and  $k$  is the number of PV systems.

Table 2-5. Assessment of estimated system losses.

Parameter	Loss Factor (%)
Soiling	2
Shading (based on location)	3
Snow	5
Mismatch	2
Wiring	2
Connections	0.5
Light-induced Degradation	1.5
Nameplate Rating	1
Age	0.5
Availability	3
Estimated system losses	18.78

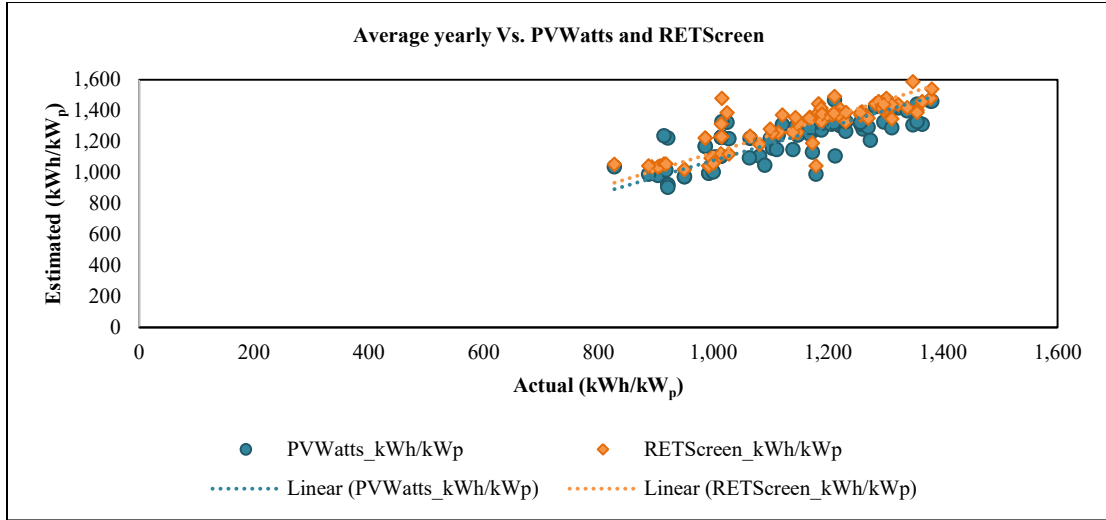


Figure 2-10. Regression charts of (a) actual energy generation of all PV systems (abscissa) against RETScreen simulated systems (ordinate) and (b) actual energy generation of all PV systems (abscissa) against PVWatts simulated systems.

## 2.6. GHG emission quantification

In this section, the energy payback time (EPBT) and GHG emissions are quantified by PV location and layout placement. Within the scope of this study, quantification methods of EPBT and GHG emissions and empirically driven values of energy required to manufacture and install solar PVs that are currently available in the market at the time of writing this thesis are adopted from the review study provided by Peng et al. (2013). On the other hand, local GHG emission factors and statistics resulting from the local grid electricity usage are implemented from Statistics Canada (2017), NRCan (2015), and Elliot (2017). Quantification method of EPBT and life cycle GHG emissions are given in Eq. 2-15 and Eq. 2-16 respectively.

$$EPBT = \frac{E_{input} + E_{BOS}}{E_{output}} \quad (2-15)$$

$$GHG_{e-rate} = \frac{GHG_{e-total}}{E_{LCA-output}} = \frac{GHG_{input} + GHG_{BOS}}{E_{LCA-output}} \quad (2-16)$$

where  $E_{input}$  (MJ) is the primary energy input of PV module during its life cycle which includes the energy required for the module manufacturing, transportation, installation, operation and maintenance, and recycling;  $E_{BOS}$  (MJ) is the energy required for the physical balance of system (BOS) which includes mounting structures, cabling, electronic components, and inverters;  $E_{output}$  (MJ) is the annual primary energy offset due to PV system's electricity generation;  $GHG_{e-rate}$  (g CO<sub>2</sub>-eq./kWh) is the GHG emission rate per unit energy generated by the PV system;  $GHG_{e-total}$  (g CO<sub>2</sub>-eq.) is the total GHG emission produced by the PV system throughout its life cycle;  $E_{LCA-output}$  (kWh) is the total energy generated by the PV system throughout its life cycle;  $GHG_{input}$  and  $GHG_{BOS}$  (g CO<sub>2</sub>-eq.) are the GHG emission components corresponding to the energy requirements for the PV input and BOS respectively.

In the current study, all PV systems are mono-crystalline PV panels with varying mechanical and electrical parameters; information on each system is collected from data sheets available online, including panel length, width, efficiency, and capacity. It is assumed that the average lifetime of PV systems is 25 years for all systems. As per NRCan (2015) the GHG emissions intensity per unit of electricity generated in Canada (from the end-use electricity consumption viewpoint) is 43.20 tonnes CO<sub>2</sub>-eq./TJ (155.52 g CO<sub>2</sub>-eq./kWh) unlike natural gas emissions intensity, which is 49.68 tonnes CO<sub>2</sub>-eq./TJ (178.85 g CO<sub>2</sub>-eq./kWh). On the other hand, the EPBT measures in terms of  $E_{input}$  and  $E_{BOS}$  are statistically adopted from the several studies summarised by Peng et al. (2013) as presented in Table 2-6.

Table 2-6. Summary of the life cycle energy component statistics of monocrystalline solar PV panels. (Source: Natural Resources Canada, 2015; Peng et al., 2013).

E (MJ/m <sup>2</sup> )	Min	Max	Average
Input	2,860	5,253	4,057
BOS	43	2,030	916

In order determine the EPBT components in terms of kWh/kW<sub>p</sub>, Eq. 2-17 is used for conversion between MJ/m<sup>2</sup> and kWh/kW<sub>p</sub> and vice versa.

$$E_{input}, E_{BOS} \left( \frac{kWh}{kW_p} \right) = \frac{E_{input}, E_{BOS} (MJ/m^2) \times l_m \times w_m \times 1000}{C(W_p) \times 3.6} \quad (2-17)$$

where  $l_m$  (m) and  $w_m$  (m) are the length and width of the panel, respectively,  $C$  is the panel peak capacity ( $W_p$ ). The GHG emissions corresponding to the EPBT components are calculated by multiplying each component by the local GHG intensity per unit of electricity generated (i.e., 155.52 g CO<sub>2</sub>-eq./kWh). Computation results indicate that the EPBT of the monitored PV systems varies between 6.10 years and 10.73 years with an average of 7.93 years. On the other hand, the GHG<sub>e-rate</sub> varies between 37.93 g CO<sub>2</sub>-eq./kWh and 66.78 g CO<sub>2</sub>-eq./kWh with an average of 49.33 g CO<sub>2</sub> eq./kWh. If compared with the GHG intensity per unit of generated electricity generated in Canada, as demonstrated in Figure 2-11, it is found that a minimum, maximum, and average of 88.74 g CO<sub>2</sub>-eq./kWh, 117.58 g CO<sub>2</sub>-eq./kWh, and 106.189 g CO<sub>2</sub>-eq./kWh respectively can be offset by considering solar energy implementation into the energy generation utilities. Table 2-7 summarises the statistical results of the EPBT and GHG<sub>e-rate</sub> measures of the monitored PV systems. In comparison with the current GHG emission intensity from electricity generation in Canada, it is found that the implementation of solar PV systems can offset the GHG emissions by an average of 121.15 kg CO<sub>2</sub>-eq. per kW<sub>p</sub> of installed capacity annually.

Table 2-7. Statistical results of the EPBT and GHG<sub>e-rate</sub> measures.

	Min	Average	Max
Final Yield (kWh/kW <sub>p</sub> )	893.35	1,380.95	1,132.48
EPBT (Yr)	6.10	7.93	10.73
GHGe-rate (g CO <sub>2</sub> -eq./kWh)	37.93	49.33	66.78
GHGe-rate (Kg CO <sub>2</sub> -eq./kW <sub>p</sub> /Yr)	51.15	54.98	60.40
Offset of GHGe-rate (g CO <sub>2</sub> -eq./kWh)	88.74	106.19	117.59
Offset of GHGe-rate (Kg CO <sub>2</sub> -eq./kW <sub>p</sub> /Yr)	80.26	121.15	158.57

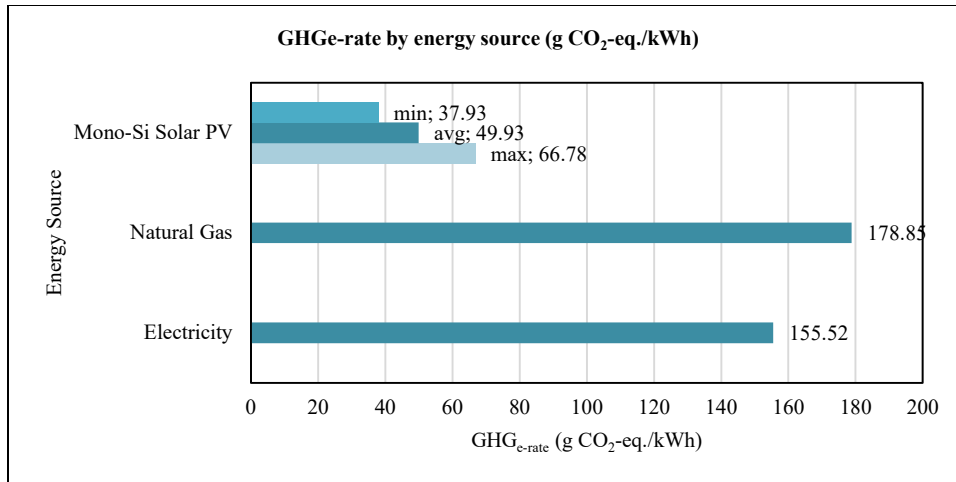
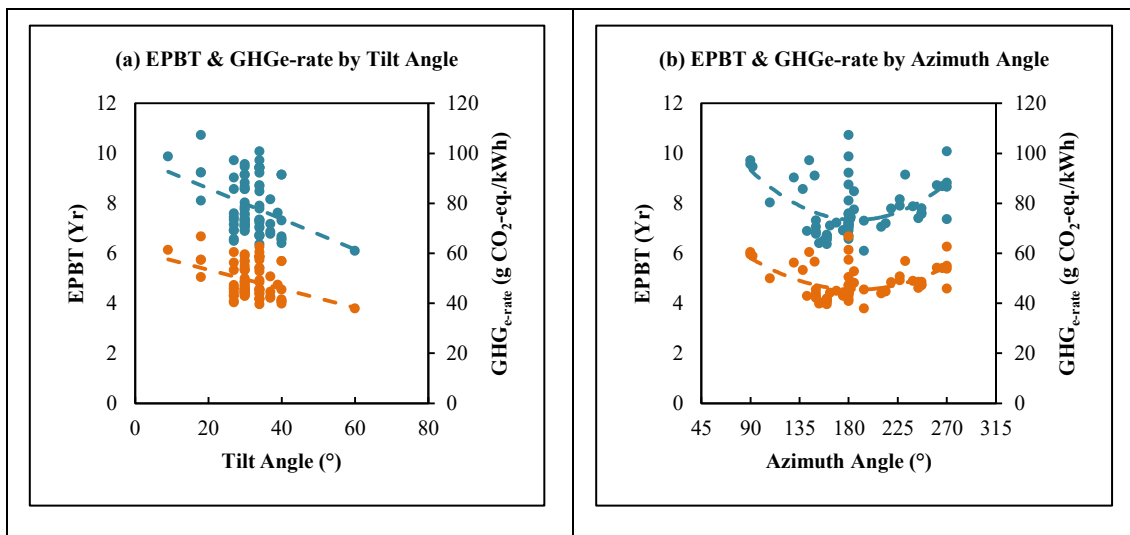
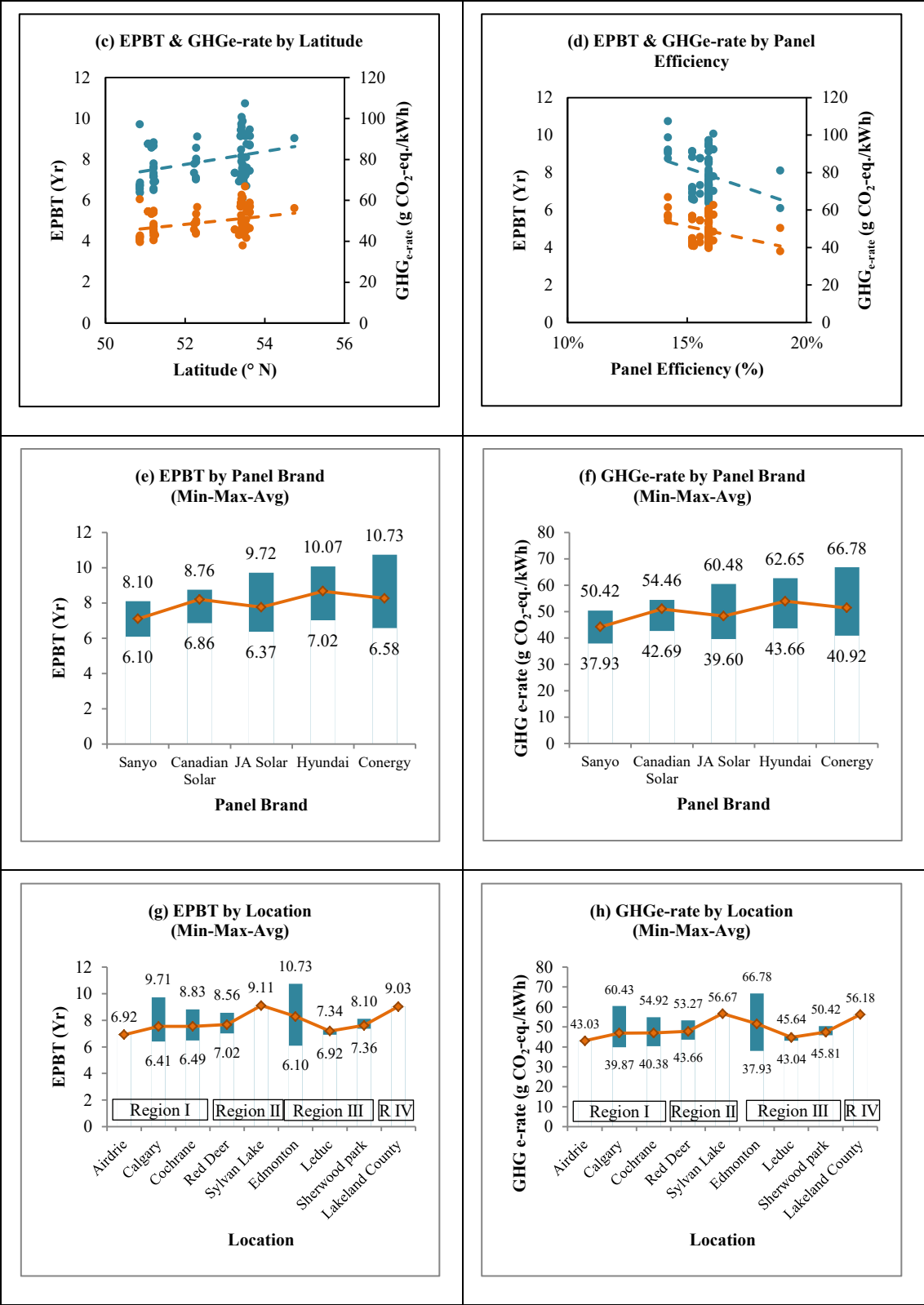


Figure 2-11. GHG emission rates by energy source in Canada.

Figure 2-12 presents the EPBT and  $\text{GHG}_{\text{e-rate}}$  resulting from the monitored PV sites in correlation with several aspects of these PV systems such as tilt angle, azimuth angle, latitude, panel efficiency, panel brand, location, and finally the deviation of the receiving surface from the local latitude (i.e., tilt angle – latitude). It is observed that some of the above mentioned aspects provide a considerable trend with EPBT and  $\text{GHG}_{\text{e-rate}}$  such as tilt angle, azimuth angle, and panel efficiency; however, it is also observed that by combining the system’s tilt angle (Figure 2-12a) with the system’s local latitude (Figure 2-12c), a significantly stronger correlation can be obtained as presented in Figure 2-12i and Figure 2-12j for EPBT and  $\text{GHG}_{\text{e-rate}}$  respectively.





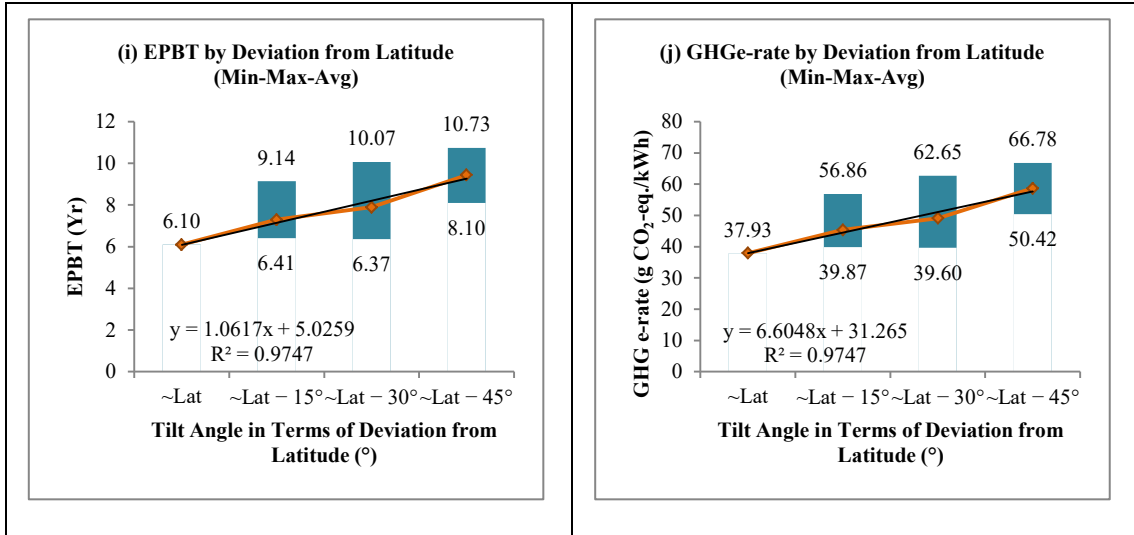


Figure 2-12. Correlation analysis of the EPBT and  $\text{GHG}_{e\text{-rate}}$  against (a) tilt angle, (b) azimuth angle, (c) latitude, and (d) panel efficiency; and statistical analysis of the (e) impact of panel brand on EPBT, (f) impact of panel brand on  $\text{GHG}_{e\text{-rate}}$ , (g) impact of location on EPBT, (h) impact of location on  $\text{GHG}_{e\text{-rate}}$ , (i) impact of tilt angle deviation from latitude on EPBT, and (j) impact of tilt angle deviation from latitude on  $\text{GHG}_{e\text{-rate}}$ .

In this regard, it is can be perceived that the layout placement with regards to the local latitude is one of the most important aspects that not only maximises the PV system's aggregated annual energy generation, but also minimises its EPBT and  $\text{GHG}_{e\text{-rate}}$ .

## 2.7. Summary and Discussion

The objectives of the study presented in this chapter include an overview of the performance analysis of the monitored PV systems, discussion of the performance parameters of those systems through correlation analysis, and finally quantification of the energy payback time and GHG emissions resulting from the solar PV practices in northerly latitudes based on the real-time performance of these systems. There is a non-significant impact of location on the PV potential of the installed systems for the

considered monitoring sites. Within the 4° latitude range of the cities where the PV systems are monitored, a variability of 15% in the aggregated annual energy generation is obtained. Tilt angle has a higher impact on energy generation than location. A changing of a south-facing PV system's tilt angle from 18° to 60° results in a variability of 127 kWh/kW<sub>p</sub> (15%) of the annual energy generation. On the other hand, rotating a PV system by 90° away from the true south direction while maintaining its tilt angle at 30° results in a loss of 20% in energy generation.

In addition to the maximised annual energy generation, one of the advantages of a high-mount (i.e., 60° tilt) PV system is that it generates a semi-uniform amount of energy during most of the year (from March to September) compared to a low-mount (i.e., 18° tilt) PV system whose energy generation fits into a bell-shaped normal distribution. Another advantage is the mitigated impact of snow coverage since snow slides off the PV modules. Even though daylight hours, and consequently the daily global horizontal irradiance, peak in June, it is observed that energy generation peaks in July and May for the 18°-, 27°-, and 60°- tilt angle PV systems, respectively. This is because precipitation, and thus cloudiness, is maximised in June. Higher tilt angles such as 50° or 60° are recommended in northerly altitudes, not only because of the location characteristics, but also because of the uniform distribution of the energy generation throughout the year, and also for the less impact of snow coverage energy generation loss. Additionally, due to the above mentioned location characteristics and adverse weather conditions, household energy demand in winter is increased significantly as previously concluded by Awad et al. (2017b) and Li et al. (2016). In this context, the flattened energy generation resulting from recommended high-mount tilt angle can also enhance the load match between household energy demand and energy generation (Awad et al., 2017b).

Based on the final yield of the monitored PV systems and information on life cycle energy components of mono-crystalline PV panels adopted from literature, it is found that the EPBT of the mono-crystalline PV systems under investigation vary between a minimum, maximum, and average of 6.10 yr, 10.73 yr, and 7.93 yr respectively.

Inherently, the GHG emission rates of these systems vary between a minimum, maximum, and average of 37.93 g CO<sub>2</sub>-eq./kWh, 66.78 g CO<sub>2</sub>-eq./kWh, and 49.33 g CO<sub>2</sub>-eq./kWh respectively (compared to 155.52 g CO<sub>2</sub>-eq./kWh from electricity generation in Canada). In this context, on average, the per-kW<sub>p</sub> of solar PV installed capacity in Alberta is accompanied with a yearly GHG emission rate of only 54.98 Kg CO<sub>2</sub>-eq./kW<sub>p</sub>/year, resulting in a GHG<sub>e-rate</sub> saving of 121.15 Kg CO<sub>2</sub>-eq./kW<sub>p</sub>/year. It is also found that the most effective factor for minimizing the EPBT and GHG emissions resulting from solar PVs is the tilt angle, or in other words, the inclination of the receiving surface from the local latitude; the closer the tilt angle to the latitude the lesser the EPBT and GHG emissions, and the greater the aggregated annual energy generation. Provided that the most-likely North American roof-sloping practice varies between 30° (7:12) and 40° (10:12), a range which is approximately below the local latitude by 15° to 25°, it is concluded that by changing the solar PV system's tilt angle from the current practice to a tilt angle that is equal to the local latitude, the EPBT and GHG emission rate decreases by 29.48%.

Future work will include the analysis of EPBT and GHG emissions on residential buildings accompanied with grid-tied solar PV systems to include energy consumption patterns and the mutual impacts associated with the interaction between solar PV generation at various layout placements, household energy consumption, and the utility grid, where typically, houses in Canada use natural gas for space heating and domestic hot water supply. Two types of homes will be investigated: net-zero energy homes and typical energy-efficient homes. The work will then be expanded to the community shared solar applications.

## Chapter 3: Predicting the Energy Production by Solar Photovoltaic Systems in Cold-climate Regions<sup>2</sup>

### 3.1. Overview

One challenge in designing a photovoltaic (PV) system is to predict its generation, given parameters such as location, meteorological conditions, and layout. A greater challenge is to predict the generation of such a system under snow-cover condition. Publicly available snowfall data provide records for horizontal surfaces. However, the effect of snow accumulated on a tilted PV module remains unknown. Hence, irradiance is insufficient for predicting the output of PV systems having any given layout configuration. The research in this chapter aims to predict the daily generation of PV systems through the development of a predictive model flexible enough to accommodate different layout configurations based on long-term monitoring data collected from 85 sites. Snow coverage loss factors are derived empirically to enhance the performance of the model. A feed-forward backpropagation artificial neural network model is developed and implemented with snow adjustments (snowfall data and snow coverage loss factors). Promising results are obtained and validated.

### 3.2. Introduction

Small-scale grid-integrated solar PV systems have been adopted by home builders as a sustainable solution for residential construction. Not only can positive environmental impacts be achieved through the use of renewable and cleaner energy sources in place of fossil fuels, but the use of renewable energy resources can improve energy security. Cost-effective design of solar PV systems in the residential

---

<sup>2</sup> A version of this chapter has been published in the International Journal of Sustainable Energy as Awad H, Gül M, Salim K, and Yu H, *Predicting the Energy Production by Solar Photovoltaic Systems in Cold-climate Regions*. doi: 10.1080/14786451.2017.1408622.

sector has become a critical issue in speeding the deployment of renewable solar energy for self-consumption.

### 3.2.1. *Literature Review*

#### 3.2.1.1. *Solar PV Prediction*

The use of ANN or MLP in solar PV prediction is explained thoroughly in studies by Al-Amoudi and Zhang (2000), Braun (2012), Casaca de Rocha Vaz (2014), Coit et al. (1998), Ding et al. (2011), Krenker et al. (2011), and Yona et al. (2013). An ANN involves computing non-linear functions of the scalar product of the input nodes and weighted vectors (Al-Amoudi and Zhang, 2000). Hassan et al. (2011) propose a framework for modelling solar energy in the city of Calgary, Canada, using high spatial resolution remote-sensing images to determine the effective roof area for installing PV cells. In their study, the authors assume a solar PV cell efficiency of 11–15%. Krömer et al. (2015) estimate the harvestable solar energy in the Canadian province of Alberta using support vector regression, an extension method of support vector machines based on statistical learning theory where surface pressure is deployed as the main input parameter, in addition to other parameters such as downward shortwave flux and instantaneous downwelling clear-sky shortwave flux. Solar PV power output can also be forecast by different methods such as stochastic learning, sky imaging, solar radiometers, or power output. Stochastic-learning methods such as the time series based method include both regression techniques such as ARIMA, and non-linear techniques such as ANNs (Coimbra et al., 2013). For interested readers, other solar PV forecasting studies using artificial intelligence techniques – which are not directly relevant to this study – can be found in studies by Ding et al. (2011), Sulaiman et al. (2012), Almonacid et al. (2011), Zhang et al. (2015), Chen et al. (2011), Mandal et al. (2012), Rana et al. (2015), Ramsami and Oree (2015), and Do et al. (2016).

### 3.2.1.2. Solar PV Performance Parameters

One of the advantages of ANN-based forecasting algorithms is that they offer the user the ability to select and increase the number of inputs to improve the performance of the forecast (Azadeh et al., 2009). Coimbra et al. (2013) provide an overview of the PV forecast parameters and methods of performance evaluation. In their book chapter, the authors suggest the use of global irradiance for a medium forecast skill and global irradiance, air temperature, and wind for higher forecast skills. Mellit (2008) and Mellit and Pavan (2010) suggest using relative humidity, daylight hours, air temperature, and irradiance (diffuse, DNI, and GHI) to add precision to solar PV forecasting. Mellit and Pavan (2010) propose a practical method for solar irradiance forecast using ANN. The developed multilayer perceptron MLP-model forecasts 24-h-ahead solar irradiance using the present values of the mean daily solar irradiance and air temperature. Ding et al. (2011) use minimum, average, and maximum daily temperature as inputs for the improved back propagation learning algorithm to predict its 24-h-ahead energy generation at half-hour time intervals. Askarzadeh (2013) uses solar irradiance, temperature, and electric current to predict the voltage of a PV system in Iran. Alluhaidah et al. (2014) conduct a study to determine the most influential variables for solar radiation forecasting in Saudi Arabia using ANN. Inman et al. (2013), Antonanzas et al. (2016), and Engerer and Mills (2015) all provide comprehensive overviews of solar forecasting methods for renewable energy integration as well as PV performance models with reference to clear-sky models.

### 3.2.1.3. Snow Impact on PV Efficiency

Previous studies on snow coverage loss factors have been conducted by Andrews, Pollard, and Pearce (2013), Andrews and Pearce (2012), Becker et al. (2006), Marion et al. (2013), NAIT (2015), and Powers et al. (2010). Researchers at the Northern Alberta Institute of Technology (NAIT, 2015) analyse the long-term impact of snow on the energy generation of south-facing PV systems with different tilt angles in the local conditions of Edmonton and Grand Prairie, Alberta. Annual loss factors due to snow are found in their study to vary between 1% and 5% depending on the PV

module's tilt angle. The present study capitalises on the findings of the NAIT study as discussed in the following sections. In Marion et al. (2013), several PV systems in Wisconsin and Colorado are investigated in order to evaluate PV system energy losses from snow where parameters such as snow depth, plane of array irradiance, and air temperature are measured and actual losses are compared against modelled losses. They conclude that higher tilt angles result in increased snow sliding. Powers et al. (2010) build and monitor a test bed in California with three common tilt angles to measure the energy loss due to snow. Becker et al. (2006) describe the operational performance of a PV system under snow conditions in Germany for the winter of 2005–2006 and quantify the impact of these conditions. Andrews, Pollard, and Pearce (2013) propose a new method to quantify the effects of hydrodynamic surface coatings on the snow cover effectiveness of solar PV systems with different tilt angles in Ontario, Canada. Finally, Marion, Rodri, and Pruet (2013) suggest the installation of two useful instruments to reduce uncertainty in PV performance prediction during snow events in northern latitudes: (1) a pyranometer with a heater and (2) a digital camera for remote detection of the presence of snow on the PV system modules.

### 3.2.2. *Research Gap*

As can be seen from the literature review, numerous studies have been conducted attempting to forecast solar PV energy output using various parameters. Also, several algorithms and techniques have been used to develop and train the predictive model based on the given research approach. These models use historical data as an input parameter, but the sample size (or variability) of the PV systems is limited, not exceeding one or a few PV systems in any of the studies noted above. Furthermore, snow coverage conditions in cold climate regions have not been well addressed in the existing literature. Existing studies on the effect of snow cover on PV systems are in agreement that PV systems with higher tilt angles are advantageous over those with lower tilt angles in snow events due to the natural sliding of snow off the PV modules. Thus, the statistical interpretation of the snow-related system efficiency can be implemented in PV modelling and forecasting.

### 3.2.3. *Research Objectives*

The research in this chapter aims to develop a forecast model to predict the daily energy generation of PV systems in the cold climate of Central Alberta, Canada, while satisfying the following objectives:

- the proposed model should be designed to be flexible enough to accept the varying layout configurations (tilt and orientation) of any PV system;
- the proposed model should account for generation loss due to snow coverage and precipitation; and
- the proposed framework should be generic in its structure so that it can be reproducible in other jurisdictions by applying the local relevant parameters and input data.

## 3.3. **Methodology**

### 3.3.1. *Prediction of PV Daily Energy Generation using Artificial Neural Networks*

This study presents a data-driven approach based on Artificial Neural Networks developed by using a portion of the collected data as input parameters in the training phase (80%) and validation phase (10%) with input and target data, while the other portion of the data (10%) is reserved for the testing of the network. Eighty-five small-scale residential rooftop grid-connected solar PV systems located in eight different cities in Alberta, Canada (Airdrie, Calgary, Cochrane, Edmonton, Leduc, Red Deer, Sherwood Park, and Sylvan Lake) are studied. In addition to the five-minute-interval historical data, geographical location, system layout configuration, system size (capacity), and relevant meteorological and climatological data are collected for each PV system. A predictive model is then developed using the ANN technique. The ANN consists of a pair of input and output vectors,  $x(k)$  and  $l(k)$ , respectively, for training, where  $k$  refers to the  $k$ th iteration (not to be mistaken with the clear-sky index,  $k_t$ , which will be discussed later in this chapter), while the network output and error,  $y(k)$  and  $b(k)$ , respectively, are defined in Eq. 3-1. The error,  $e(k)$ , is then used

as an objective function to optimise network weights and recalculate the output vector  $d(k + 1)$  accordingly (Braun, 2012). An ANN is characterised by its static behaviour, in that the network is uni-directional rather than being continuously modified based on feedback during the process (Casaca de Rocha Vaz, 2014; Coit et al., 1998).

$$b(k) = l(k) - y(k) \quad (3-1)$$

Due to the non-linear transformation of output of the hidden-layer neurons of an ANN, the output layer is defined by the sigmoid (or hyperbolic tangent) function in Eq. 3-2 (Yona et al., 2013).

$$f(x) = \frac{2}{1 + \exp(-2x)} - 1 \quad (3-2)$$

where  $x$  is the input data. The selected input parameters to the proposed ANN model will be discussed in detail later in this chapter. Using trial and error, it is found that 2 layers and 33 nodes provide the optimum results in terms of both accuracy and computation time. The data flow diagram presented in Figure 3-1 summarises the structure of the proposed framework.

### 3.3.2. *Clear-sky Index/Model*

Since this study investigates systems of varying locations, tilt and azimuth angles, panel models and capacities, and numbers of panels, the data is normalised to its final yield (Eq. 3-3) to better serve the analytical purpose of the study, as per Marion et al. (2005).

$$Y_f (kWh/kW_p) = \frac{E}{P_0} \quad (3-3)$$

where  $E$  is the energy generated by the PV system (kWh) and  $P_0$  is the system size as a product of the number of the system modules and the module capacity ( $kW_p$ ). Data is collected at a five-minute interval resolution to investigate the daily power generation profiles; the daily energy generation is used to match the temporal resolution of the currently available meteorological data collected from the National Aeronautics and Space Administration (NASA, 2017).

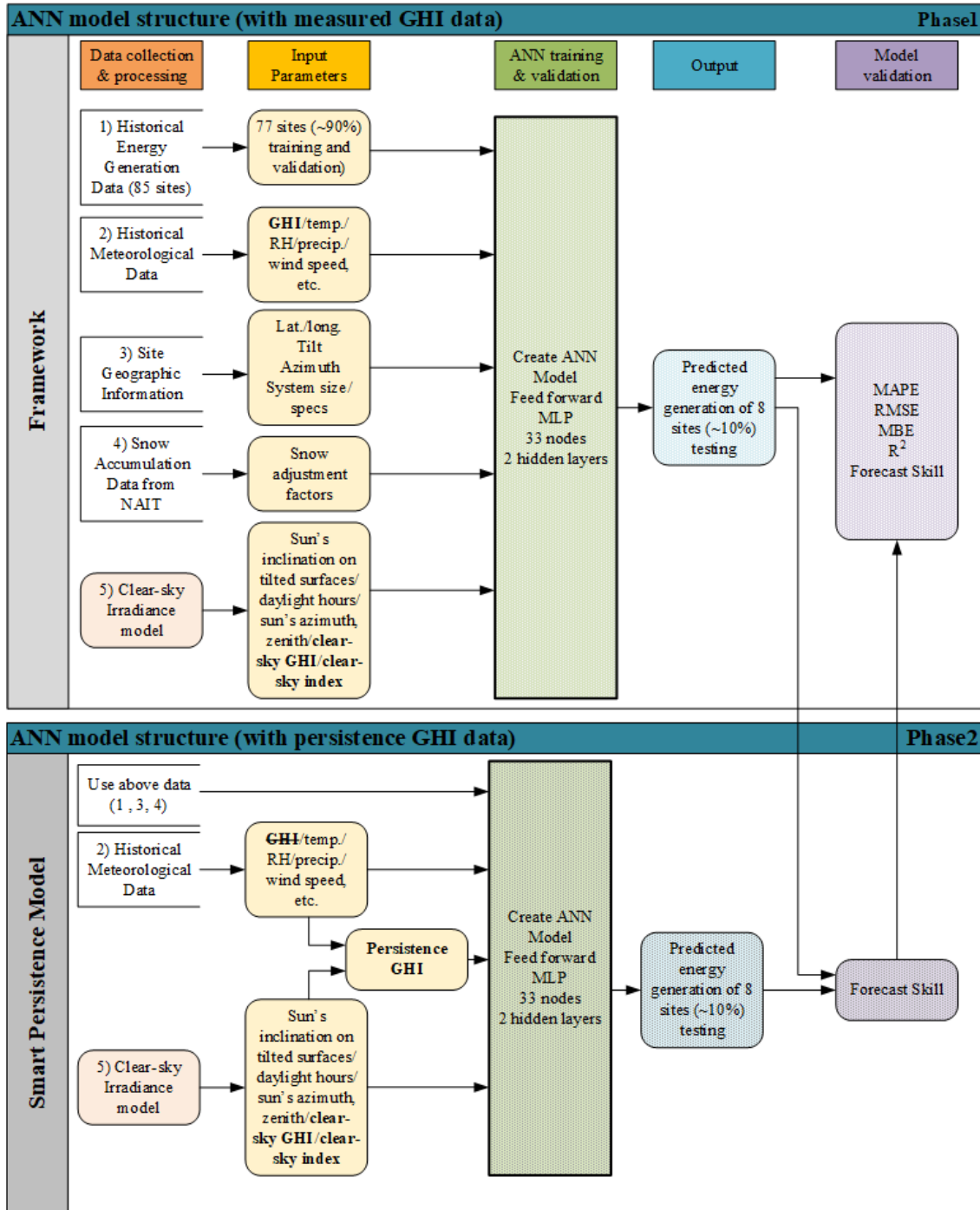


Figure 3-1. Data flow diagram of the proposed model structure.

It is necessary that the meteorological characteristics be considered independent of the site under investigation by factoring the clear-sky conditions into the evaluation of

the forecast skill of the proposed model. Accordingly, an important input parameter is the clear-sky index,  $k_t$ , as expressed in Eq. 3-4 (Coimbra et al., 2013; Engerer and Mills, 2015; Mathiesen and Kleissl, 2011). Eq. 3-5 is used to convert the measured insolation data (kWh/m<sup>2</sup>/day) into GHI (W/m<sup>2</sup>). Note 1: In cases where the GHI data is readily available, Eq. 3-5 may be disregarded. Note 2: If the reader has no interest in creating a GHI persistence model, then Eq. 3-2 and Eq. 3-3 may be disregarded.

$$k_t = \text{GHI}_{\text{Measured}} / \text{GHI}_{\text{cs}} \quad (3-4)$$

$$\text{GHI}_{\text{Measured}} (\text{W/m}^2) = \tau (\text{kWh/m}^2/\text{day}) \times 1000/\beta (\text{hr}) \quad (3-5)$$

where  $k_t$  is the clear-sky index,  $\text{GHI}_{\text{Measured}}$  is the satellite-measured GHI, and  $\text{GHI}_{\text{cs}}$  is the clear-sky GHI,  $\tau$  is the daily insolation data and  $\beta$  is the daylight hours (Eq. 3-9). Solar geometry calculations for each day of the year (DOY)—including solar zenith ( $z$ ) (Reno et al., 2012), declination ( $\delta$ ) (Allen, 2005; Reno et al., 2012), solar time (ST) (Allen, 2005; Reno et al., 2012), hour angle ( $\omega$ ) (Kreider et al., 1989; Reno et al., 2012), true zenith ( $z_t$ ) (Reno et al., 2012), extraterrestrial irradiance ( $I_0$ ) (Spencer, 1971), direct normal irradiance (DNI) (Daneshyar, 1978; Paltridge and Proctor, 1976) (Eq. 3-6), diffuse irradiance (diffuse) (Eq. 3-7) (Daneshyar, 1978; Paltridge and Proctor, 1976), clear-sky global horizontal irradiance ( $\text{GHI}_{\text{cs}}$ ) (Badescu, 1998), daylight hours ( $\beta$ ) (Kreider et al., 1989), the sun's degree angle from due south at sunset (Hourset) (Kreider et al., 1989), and the sun's azimuth angle ( $\alpha$ ) (Kreider et al., 1989)—can be found in the relevant literature.

$$\text{DNI} (\text{W/m}^2) = 950.2 \times (1 - \exp(-0.075(90 - z_t))) \quad (3-6)$$

$$\text{Diffuse} (\text{W/m}^2) = 14.29 + 21.04 \times \left(\frac{\pi}{2} - z_t \times \pi/180\right) \quad (3-7)$$

Numerous methods exist, ranging from simple to highly complex, by which to determine the GHI on a clear day, including those published by SANDIA Laboratory (Reno et al., 2012), Marquez and Coimbra (2012), and Rigollier et al. (2000). In the present study, these models are investigated and compared against the historical clear-sky irradiance data collected between 1983 and 2016 from NASA (2017). It is found that the Berger-Duffie (BD) model (Badescu, 1998) expressed in Eq. 3-8 has the least

bias with reference to the local climatological conditions covered by the present study as shown in Figure 3-2.

$$GHI_{cs} (W/m^2) = I_0 * 0.70 \times \cos(z_t) \quad (3-8)$$

$$\beta = 2 \times HourSet/15 \quad (3-9)$$

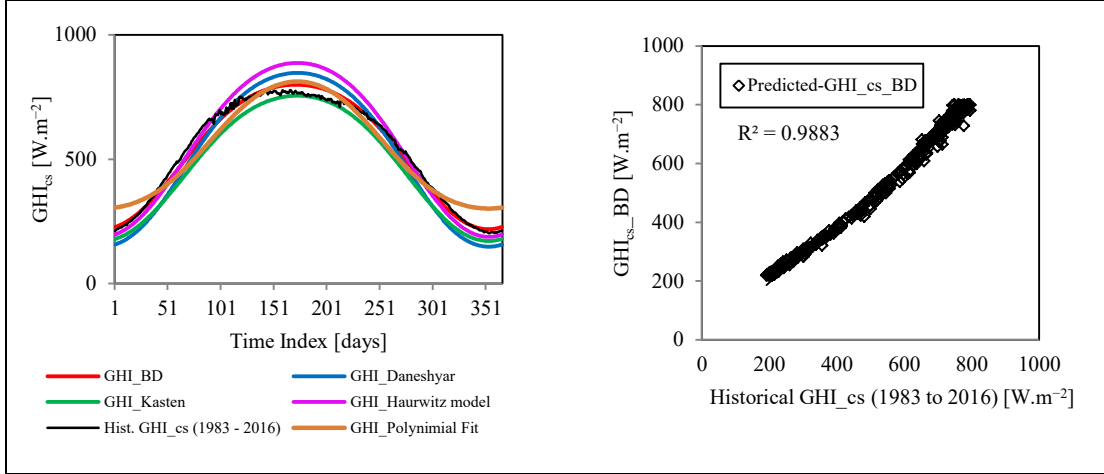


Figure 3-2. Diurnal time-series plot of the historical clear-sky GHI (daily averages of July 1983–November 2016), clear-sky GHI model proposed by Berger-Duffie along with other models, and the absolute bias between actual data and proposed model.

### 3.3.3. PV Layout Configuration as Input Parameter

Because the PV systems used in the predictive model have a variety of tilt and azimuth angles and are located on different sites, it is crucial to pre-process the tilt and azimuth angles of the receiving surfaces in a manner reflective of their impact on the PV power output. In this context, the tilt angle ( $\vartheta$ ) at a specific site ( $\varphi$ ) on a specific DOY is processed to define the sun's angle of inclination on that specific tilted surface as a function of declination ( $\delta$ ), latitude ( $\varphi$ ), and hour angle ( $\omega$ ) (Kreider et al., 1989) as per Eq. 3-10.

$$INC = \sin(90 - \cos^{-1}[\cos(\delta) \times \cos(\varphi - \vartheta) \times \cos(\omega) + \sin(\delta) \times \sin(\varphi - \vartheta)]) \quad (3-10)$$

#### 3.3.4. *Soiling Parameters*

It is hypothesised that adding soiling parameters—snow coverage in winter and rain (also referred to as precipitation) in summer—as input parameters can improve the precision of the predictive model. Precipitation in general, and snow coverage in particular, have a significant impact on solar PV energy generation as they block the sun’s rays from reaching the modules of a PV system, and thus the amount of snow cover is considered a dominant factor in winter months. In fact, historical snow data only accounts for the snow falling on each specific day on a horizontal surface, whereas the accumulated snow varies depending on the PV layout, particularly the tilt angle.

Consequently, snow adjustment factors are introduced to the predictive model according to each PV system’s tilt angle and month of observation. These adjustment factors are derived from the open-source data collected from a study conducted by the Northern Alberta Institute of Technology (NAIT, 2015). The impact of snow coverage on south-facing PV systems of various tilt angles is investigated by installing and monitoring two typical PV systems, where the first system (referred to as ‘Maintained’ in Figure 3-3) is cleared after every heavy snowfall, and the second system (referred to as ‘Unmaintained’ in Figure 3-3) remains undisturbed to allow only the clearing that occurs naturally due to sun and wind. Each system consists of six PV modules with tilt angles of 14°, 18°, 27°, 45°, 53° (Edmonton latitude) / 55° (Grand Prairie latitude), and 90°.

In this research, the monthly impact of snow coverage in winter (i.e., snow season—November to March) is analysed and added to the predictive model as a snow adjustment factor, while in other months (non-snow season—April to October) a factor of solid-one is used to indicate that no loss in efficiency is incurred due to snow. The example in Figure 3-3 shows the discrepancy between the maintained (cleared of heavy snow events) and unmaintained (cleared naturally by the sun’s heat and wind) modules placed at a 14° tilt.

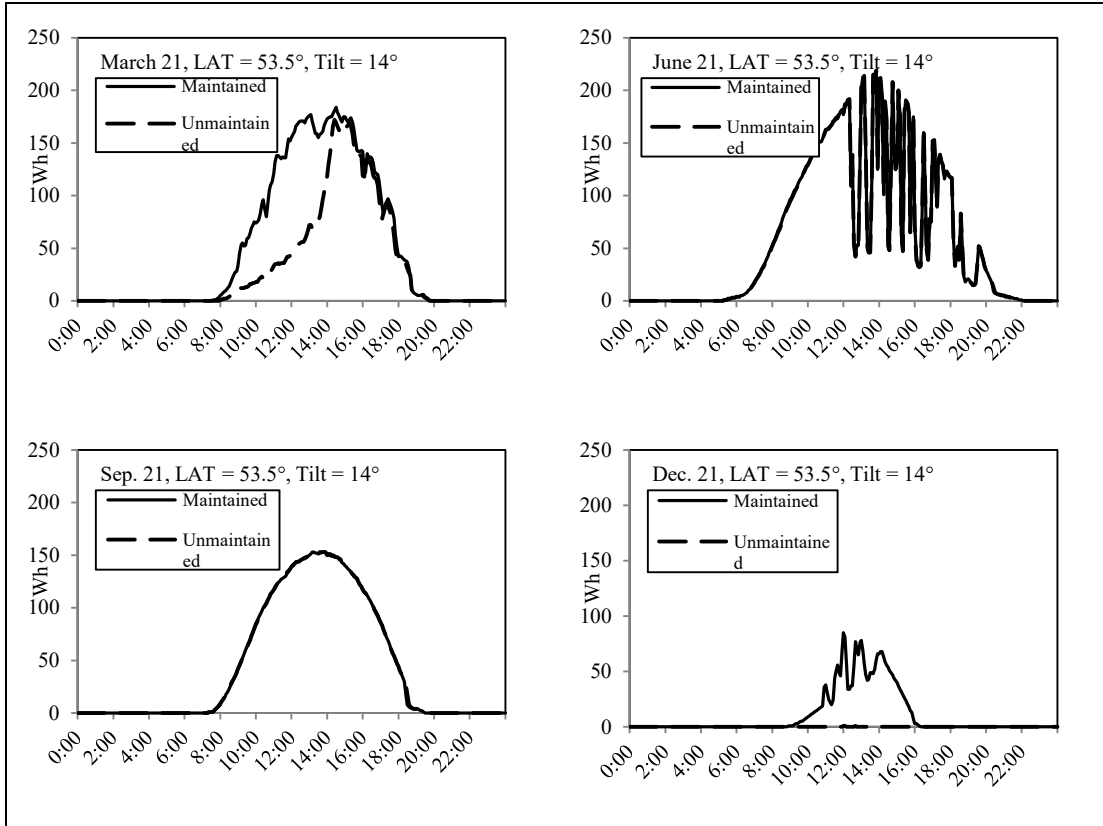


Figure 3-3. Five-minute time-series energy generation of maintained and unmaintained modules placed at 14° tilt in Edmonton on the spring, summer, fall, and winter equinox days.

Figure 3-4 shows the derived energy generation loss for winter months in PV systems for each tilt angle in Edmonton. Within the period, April to October, the snow adjustment efficiency factor is input as 100%. During winter, the module's efficiency varies according to the month and the module surface's tilt angle. Eq. 3-11 expresses the general empirical formula derived by the authors of the present study to determine the snow loss factor as a function of tilt angle and month of observation using the curve-fitting technique.

$$\varepsilon(m) = \begin{cases} \sin(\vartheta) + a \times \frac{[\cos(\vartheta)]^2}{2}, & m \in \{Nov:Mar\} \\ 1, & otherwise \end{cases} \quad (3-11)$$

where  $\varepsilon$  is the PV system's snow coverage module efficiency factor due to snow in winter months,  $m$ , (from November to March);  $\vartheta$  is the PV system's tilt angle; and  $a$  is an empirically-derived coefficient that varies according to the month of observation, where  $a$  is equal to 0.46, 0.23, 1.14, 1.16, and 0.93 for November, December, January, February, and March, respectively, and the average is 0.78. It is worth mentioning that these coefficients are dependent on the local conditions and the period of study. As with the results reported by Marion et al. (2013), then, it can be noted that higher tilt angles are advantageous over lower tilt angles because they see less snow accumulation, due primarily to the gravitational force (weight of snow) and, to a lesser extent, to wind.

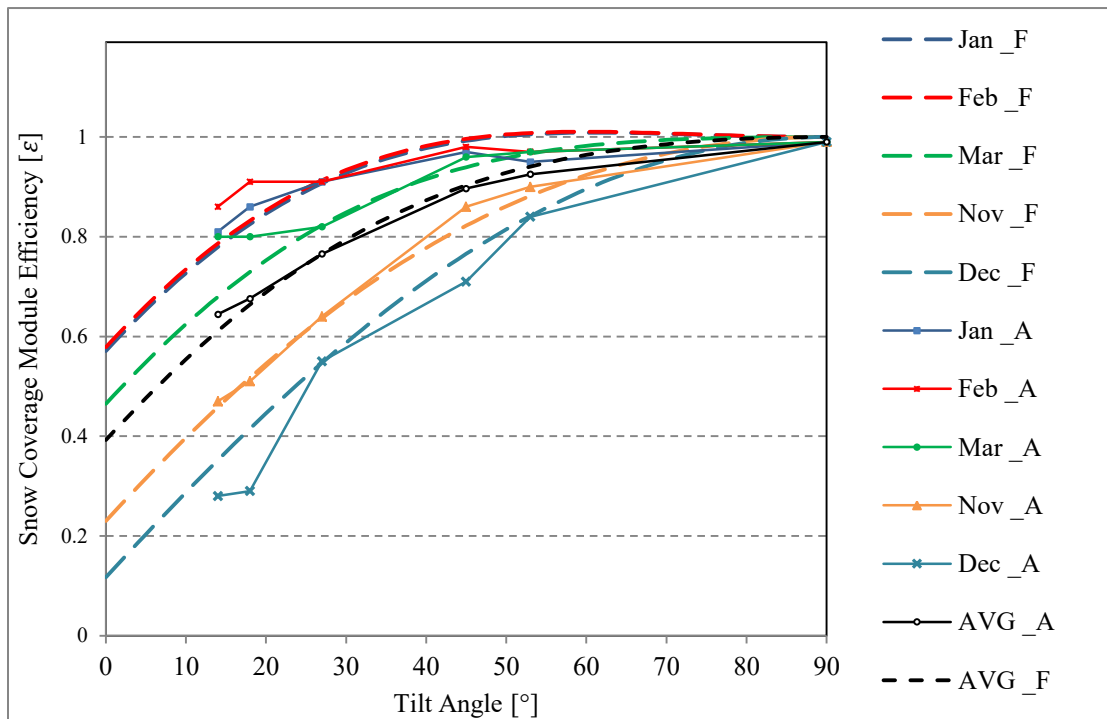


Figure 3-4. Curve fitting of snow loss factors for each tilt angle based on an empirical study in Edmonton (May 2012–Aug. 2014) (NAIT, 2015). Continuous lines represent the actual efficiencies and dashed lines represent the fitted curves for efficiencies as a function of tilt angle and month of observation.

Due to the extreme climate conditions in Alberta, a correlation analysis is conducted, and, accordingly, the effective performance parameters of the predictive model are selected. Table 3-1 offers insight into the correlation analysis results pertaining to the parameters that have a direct impact on the daily energy generation of the 85 PV systems under study. The parameters provided in this table are the result of shortlisting a large number of parameters in order to identify the most relevant input parameters.

Table 3-1. Correlation analysis result between daily energy generated in all monitored PV systems and different performance parameters.

Parameter	Energy output (kWh/kW <sub>p</sub> )	Parameter	Energy output (kWh/kW <sub>p</sub> )
GHI_Actual	0.878	Air Temperature	0.687
GHI_cs_BD	0.741	Downward Longwave Radiative Flux	-0.676
Relative Humidity	-0.731	Snow Adjustment	0.525
Diffuse Irradiance	0.731	Snow on Ground	-0.436
True Zenith	-0.731	Wind Speed	-0.155
Daylight hours	0.727	TotalPrecip	-0.113
Direct Normal Irradiance	0.718	Azimuth	0.101
Extraterrestrial Irradiance	-0.712	PV system's age	-0.045
Sun's Inclination on tilted Surface	0.691		

As discussed previously, tilt angle (redefined as the sun's inclination toward the tilted surface), orientation, and geographical location in terms of solar geometry are suitable parameters for assessing solar PV performance. However, it is noted that, in comparing the different meteorological (stochastic) parameters with the location and layout (fixed) parameters, the 'daily' energy generation is influenced more by fluctuating meteorological conditions (as a result of the presence of gases in the atmosphere) than by fixed parameters, which are subject to a relatively low degree of fluctuation (Badescu, 2008; Coimbra et al., 2013). Given that the objective of the proposed predictive model is to determine the energy generation of PV systems regardless of the layout, the tilt and azimuth angles are used as input parameters to the predictive model in addition to meteorological and solar geometry parameters.

### 3.4. Data Collection

#### 3.4.1. *Historical Energy Output Data*

Eighty-five solar PV systems installed in various locations across the Canadian province of Alberta are monitored for the purpose of this study. All of the monitored systems are fixed monocrystalline silicon solar PV panels of different models (Canadian Solar, 2013; Conergy, 2016; Hyundai, 2010; JA Solar, 2015; Sanyo, 2014) and capacities (ranging from 235 W to 260 W). The tilt angles of these PV systems vary between 9° and 60° (0° horizontal) and the orientations vary between 60° and 279° (0° N). The PV systems, as shown in Figure 3-5, are located in eight cities in Alberta—Airdrie, Calgary, Cochrane, Edmonton, Leduc, Red Deer, Sherwood Park, and Sylvan Lake—where the longitude varies between 114.5° W and 113.3° W and the latitude varies between 50.8° N and 53.6° N. In the context of this study, the cities within the same one-degree latitude range are grouped into one region and named after the major city within this range. For example, Edmonton, Leduc, and Sherwood Park, having latitudes of 53.631°, 53.258°, and 53.541°, respectively, are grouped into one region referred to as ‘Edmonton’ (the major city within this range). Table 2-1 presents a list of the locations where the PV systems are installed and demonstrates the method by which the cities are grouped into three regions—Calgary, Red Deer, and Edmonton.

The layout designs of the systems under study are random and unevenly distributed in terms of the diversity and sample size of location, tilt, and directional orientation. The dominant factors pertaining to rooftop PV layout design include the common practice of residential roof pitch angles and the orientation of the house within the street. Taking this into account, a detailed analysis of the impact of tilt, orientation, and location is undertaken on the configurations with higher density and diversity, such as PV systems located in Edmonton with 27° tilt angle and 180° azimuth angle.

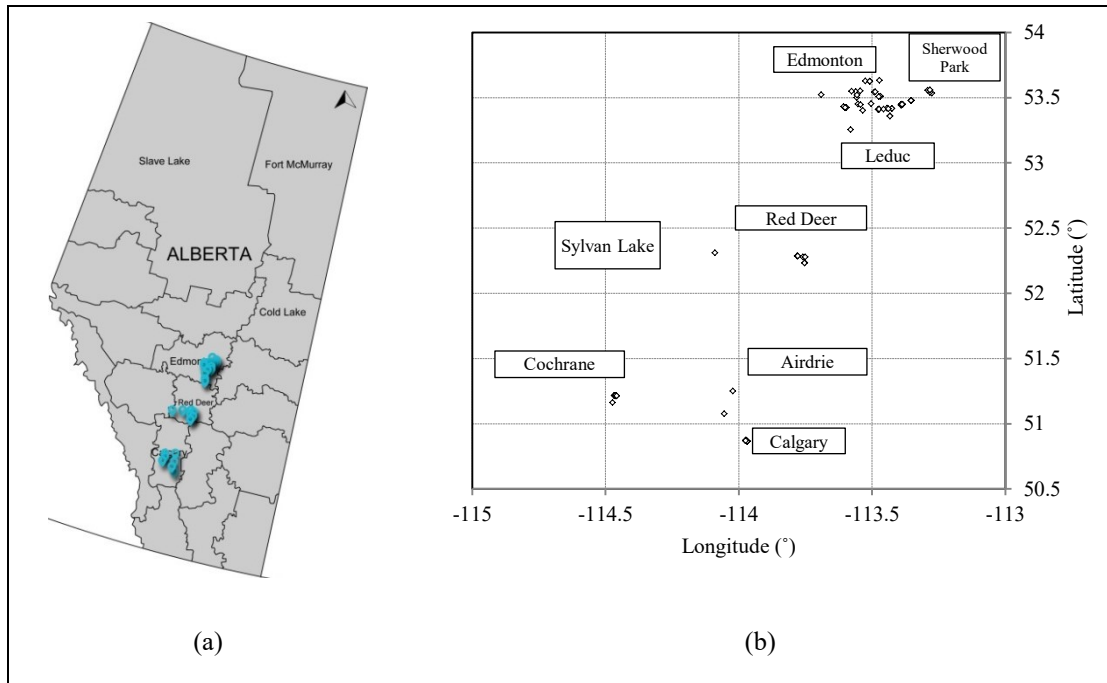


Figure 3-5. Location of the monitored PV systems: (a) on Alberta map; (b) in longitude and latitude.

For simplicity and given that the monitored PV systems are installed at a wide range of azimuth angles, these angles are systematically divided into eight bins. Each bin is  $45^\circ$  wide and divided evenly around the directions of true north ( $0^\circ$ ), northeast ( $45^\circ$ ), east ( $90^\circ$ ), etc., as demonstrated in Table 2-2. Additionally, a wide range of tilt angles is investigated in this study, including 2:12 ( $9^\circ$ ), 3:12 ( $14^\circ$ ), 4:12 ( $18^\circ$ ), 5:12 ( $23^\circ$ ), 6:12 ( $27^\circ$ ), 7:12 ( $30^\circ$ ), 8:12 ( $34^\circ$ ), 9:12 ( $37^\circ$ ), 10:12 ( $40^\circ$ ), and 21:12 ( $60^\circ$ ). Table 2-2 shows the distribution of tilt and azimuth angles deployed in this study. In keeping with conventional practice in North America for roof pitch, 74% of the monitored houses are constructed at a slope ratio of 6:12, 7:12, or 8:12, and 32% of these slopes are south-oriented. For the purpose of testing the developed forecast model, rare tilts and orientations are hidden during the training of the model and are instead reserved for later testing. The purpose of this is to validate the hypothesis that the proposed model is capable of predicting the PV performance of varying layouts and locations and for the prediction model to avoid the risk of memorising/overlearning.

Historical energy output data is verified for its quality and reliability by simulating all monitored systems using two commercially available software tools: the Clean Energy Management Software system, RETScreen (Leng, 1998), and the National Renewable Energy Laboratory’s PVWatts calculator (Dobos, 2014).

### 3.4.2. Meteorological Data

Many studies have been conducted to determine the key performance parameters of a solar PV forecast model. However, due to the extreme weather conditions in Alberta, especially in winter, parameters such as irradiance, though strongly correlated with solar PV output, are not sufficient to achieve a highly accurate predictive model. In addition to the low temperatures and snow coverage during winter, the sun’s altitude angle decreases in winter, to approximately 13.6° on December 21<sup>st</sup> at solar noon (and increases in summer, reaching 59.9° on June 21<sup>st</sup> at solar noon). Furthermore, daylight hours vary drastically between winter and summer in Alberta, resulting in insignificant amounts of energy generation in winter, and comparatively high energy generation in summer. Statistical weather data for Edmonton, Calgary, and Red Deer are provided in Table 3-2 (Environment Canada, 2017).

Table 3-2. Statistical weather data for Edmonton, Red Deer, and Calgary (Environment Canada, 2017).

	Lat.	Long.	Jan. avg. temp.	Jul. avg. temp.	Avg. monthly snowfall	Avg. monthly rainfall
	(° N)	(° W)	(° C)	(° C)	Oct. – Apr. (cm)	Apr. – Sep.(mm)
Edmonton	53.53	113.45	-13.9	17.4	6 – 26	24 – 88
Red Deer	52.3	113.8	-11.6	16.3	6 – 22	14 – 92
Calgary	51.1	114.0	-8.9	16.2	10 – 22	2 – 80

The potential for snowfall in winter and precipitation in summer that can cover the panels and consequentially reduce the generation of energy, it should be noted, are important factors to consider when planning the layout for a solar PV system in a cold climate. Figure 3-6 shows snow accumulation in Edmonton, Calgary, and Red Deer during the period of monitoring. Although temperature, insolation, and precipitation

follow similar patterns in the three major cities, there is a significant variation in the amount of snowfall, especially between Edmonton and Calgary. In light of this, it is crucial to include both (a) snowfall data in order to define the real-time local meteorological conditions and (b) the proposed snow adjustment factors in order to identify the actual impact of the snowfall on a tilted surface at a specific site. It is advantageous that the climatic conditions within the three regions are similar in nature, despite the variations in magnitude, and thus it is concluded that a single predictive model is sufficient for all PV systems within Central Alberta. In addition to snow and precipitation, satellite-measured daily insolation, extraterrestrial insolation, longwave radiative flux, relative humidity, wind speed, and air temperature data are collected for all sites. The temporal resolution of the prediction model has then been constrained to the highest available temporal resolution of the meteorological parameters (one day in the present thesis), even though this given resolution might affect the accuracy of the entire prediction model in the sense that the energy output is not able to identify the daily fluctuation of irradiance, temperature, relative humidity, etc. In this regard, it is worth mentioning that mean values of meteorological parameters are used in the model, while the output defines the aggregated daily energy output of solar PV.

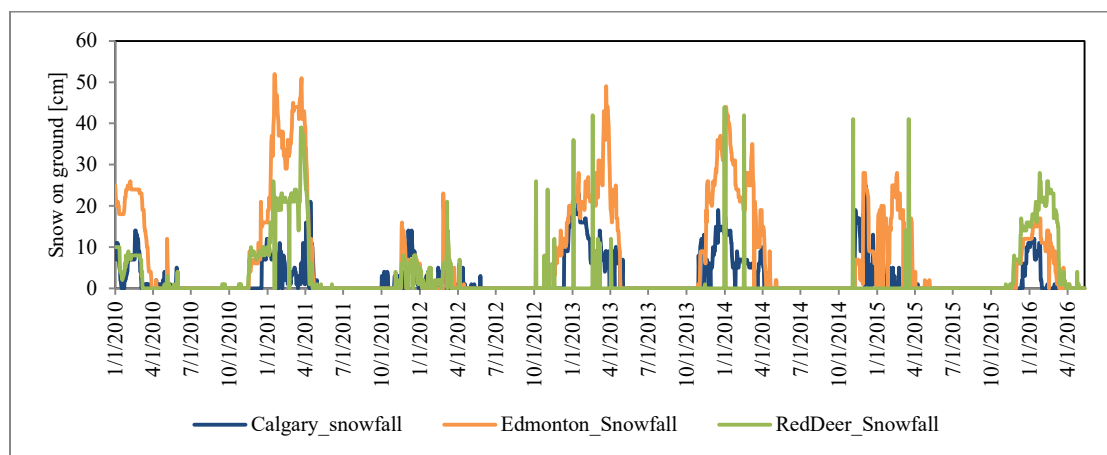


Figure 3-6. Daily snow on ground in Edmonton, Red Deer, and Calgary (Source: Environment Canada (2017)).

### 3.5. Predictive Model Results

Eight out of 85 PV systems, representing approximately 10% of the monitored systems—two PV systems from each of Calgary, Cochrane, Edmonton, Red Deer—are reserved for testing. These systems are not seen by the ANN in the training set. The other 77 PV systems, representing approximately 90% of the monitored systems, are used for training and validation. The objective of this approach is to validate the hypothesis that the energy generation of any unseen PV system with any tilt-azimuth configuration within Alberta can be predicted using the proposed ANN model. Input parameters to the final ANN include tilt angle, azimuth angle, solar geometry and meteorological parameters, precipitation, snow accumulation, and efficiency factors due to snow coverage. Here, the persistence of the clear-sky index is introduced to the validation process as a normalised method of evaluating the proposed model. Clear-sky persistence is defined by Marquez and Coimbra (2012) as having the clear sky conditions persist for the next time-step, where the clear-sky index is the ratio between the measured irradiance and the clear-sky irradiance. The clear-sky model previously mentioned in Eq. 3-8 is implemented in the validation as a function of mean absolute percent error (MAPE) (%) (Eq. 3-12), root mean square error (RMSE) (kWh/kW<sub>p</sub>, W/m<sup>2</sup>) (Eq. 3-13), mean bias error (MBE) (kWh/kW<sub>p</sub>, W/m<sup>2</sup>) (Eq. 3-14), coefficient of determination ( $R^2$ ) (Eq. 3-15), and forecast skill ( $S$ ) (Eq. 3-16) (Coimbra et al., 2013; Marquez and Coimbra, 2012), as summarised in Table 3-3.

$$\text{MAPE (\%)} = \frac{1}{n} \sum_{i=1}^n \left( \left| \frac{A_i - F_i}{A_i} \right| \times 100 \right) \quad (3-12)$$

$$\text{RMSE (kWh/kW}_p, \text{ W/m}^2) = \sqrt{\sum_{i=1}^k \frac{(A_i - F_i)^2}{k}} \quad (3-13)$$

$$\text{MBE (kWh/kW}_p, \text{ W/m}^2) = \frac{1}{n} \sum_{i=1}^n (A_i - F_i) \quad (3-14)$$

$$R^2 = 1 - \frac{\sigma^2(F_i - A_i)}{\sigma^2(A_i)} \quad (3-15)$$

$$S = 1 - \text{RMSE}_{PV} / \text{RMSE}_{\text{smart-persistence}}, S = 1 - U/V \quad (3-16)$$

where  $A_i$  is the  $i^{\text{th}}$  actual energy generation,  $F_i$  is the  $i^{\text{th}}$  forecasted energy generation, and  $k$  is the number of PV systems. The uncertainty ( $U$ ) and variability ( $V$ ) are the forecast skill measures. For interested readers, further details can be found in Coimbra et al. (2013) and Marquez and Coimbra (2012). In order to test the forecast skill of the proposed predictive model, the aforementioned smart persistence model is developed. A comparative analysis between two predictive models is performed: the first model uses the actual GHI,  $\text{GHI}_{\text{actual}}$  ( $\text{W}/\text{m}^2$ ), while the second model uses the persistence GHI,  $\text{GHI}_{\text{persistence}}$  ( $\text{W}/\text{m}^2$ ) in addition to the other input variables. In this case the forecast skill ( $S$ ) of the predictive model is  $\sim 1 - \text{RMSE}_{\text{actual}}/\text{RMSE}_{\text{persistence}}$ , where  $\text{RMSE}_{\text{actual}}$  results from the model fed with  $\text{GHI}_{\text{actual}}$ , and  $\text{RMSE}_{\text{persistence}}$  results from the model fed with  $\text{GHI}_{\text{persistence}}$ . Table 3-3 summarises the various validation techniques for the predictive model with reference to the smart persistence model. In this table the MSE, RMSE, MBE, MAPE,  $R^2$ , and  $S$  are presented for the eight tested PV systems. These systems are selected based on the criteria of (1) covering all major locations and (2) capturing outlier system layouts (tilt and azimuth angles).

Table 3-3. Parameters and their error statistics.

City	Lat.	Tilt	Azimuth	Sample Size	MSE		RMSE		MBE		MAPE	$R^2$	RMSE_PVcs	S
					kWh/kW	W/m <sup>2</sup>	kWh/kW	W/m <sup>2</sup>	kWh/kW	W/m <sup>2</sup>				
1	53.45	18	180	1711	0.23	37.89	0.48	6.16	0.14	1.40	5.53	0.96	101.94	0.37
2	50.87	37	150	572	0.23	43.20	0.48	6.57	-0.02	-0.47	0.47	0.95	113.43	0.45
3	51.21	30	270	435	0.19	33.14	0.43	5.76	0.03	0.72	0.25	0.94	110.51	0.30
4	52.29	27	138	384	0.28	60.33	0.53	7.77	-0.07	0.45	1.26	0.92	105.76	0.28
4	52.23	27	180	419	0.31	67.49	0.56	8.22	-0.08	-1.09	0.68	0.93	105.34	0.29
2	50.87	40	160	344	0.25	55.05	0.50	7.42	0.12	1.73	0.28	0.95	110.46	0.40
3	51.21	27	157	343	0.32	71.46	0.56	8.45	0.25	3.55	0.24	0.94	110.38	0.30
1	53.45	60	194	809	0.54	99.00	0.74	9.95	0.19	2.68	0.42	0.88	122.22	0.15

1: Edmonton; 2: Calgary; 3: Cochrane; 4: Red Deer.

It is observed that the largest contributor to the forecast skill ( $S$ ) is the location, followed by the tilt angle, and, finally, the azimuth angle. Also, the RMSE of the predictive model shows a strong positive correlation with the PV system location, but weaker correlations with the azimuth and tilt angles, respectively. On the other hand, the MAPE is strongly correlated to the sample size, where the highest MAPE belongs to the system with the highest sample size, with weaker correlations observed between MAPE and tilt angle, location, and azimuth angle, respectively. As expected, the coefficient of determination ( $R^2$ ) (where 1 indicates the greatest degree of precision) inversely correlates with tilt angle and azimuth angle, but positively correlates with location and sample size.

Figure 3-7a plots the actual irradiance data ( $GHI_{\text{actual}}$ ) in a pairwise comparison with the persistence irradiance ( $GHI_{\text{persistence}}$ ) along with the clear-sky GHI model. Here, the bias, measured as the difference between the actual and the persistence irradiances, is significantly higher in summer than in winter. This is indicative of (1) the highly-fluctuating cloud cover conditions in the summer, and (2) the significantly high irradiance as well as daylight hours in summer in comparison with winter.

Figure 3-7b presents a sample diurnal prediction result of a PV system located in Cochrane (16 of the 85 PV systems are located in Cochrane) having a tilt angle of  $30^\circ$  and a west-facing orientation ( $270^\circ$ ) (validation details can be found in the third row in Table 3-3). In this figure, the two predictive models—PV output prediction with  $GHI_{\text{actual}}$  and PV output prediction with  $GHI_{\text{persistence}}$ —are presented, along with the measured PV output, given in  $\text{kWh.kW}^{-1}$ . The prediction result confirms the model's ability to predict the module's output in the highly-fluctuating summer meteorological conditions, as well as in low-fluctuating-snow-covered conditions.

The error charts in Figure 3-8 offer a comparison between the performances of the predictive model without soiling parameters (precipitation, snowfall data, and snow adjustment factors) (in asterisk-shaped symbols) and the predictive model with soiling parameters (precipitation, snowfall data, and snow adjustment factors) as an additional input (in diamond-shaped symbols). In Figure 3-8a and Figure 3-8b a

segregation of the ‘non-snow’ season (April to October) and the ‘snow’ season (November to March) demonstrates the varying impact of adding the soiling parameters to the base model. It is evident that the forecast skill of the ‘snow’ season (Figure 3-8b) shows more improvement in terms of  $R^2$  than that of the ‘non-snow’ season. Further improvement can be observed on the upper-right tail of the regression chart in Figure 3-8b; those values which belong to the PV systems with higher tilt angles (i.e.,  $> 40^\circ$ ) are indicative of more energy being generated in winter and shoulder seasons than in summer due to the sun’s low altitude angle (discussed earlier in this chapter).

In addition to the observation that using the soiling parameters as inputs helps the ANN model learn that the ‘snow’ season generates less energy than the ‘non-snow’ season, it is also observed that this approach helps the model to learn that higher tilt angles perform better than lower tilt angles under the same climatological and meteorological conditions. This explains the improved performance (and higher energy generation) in the ‘snow’ season. Overall, looking at the ‘non-snow’ and ‘snow’ seasons combined, the overall efficiency of the forecast model is improved from an  $R^2$  value of 0.93 to 0.95, as in the regression chart in Figure 3-8c. Figure 3-8d shows the bias measured in terms of the absolute difference between the measured and predicted values in both models: base model without soiling parameters and model with soiling parameters. Here, the lower the error values are, the better the model performance will be. In other words, the greater the discrepancy between the two plots, the greater the improvement achieved by the new model will be.

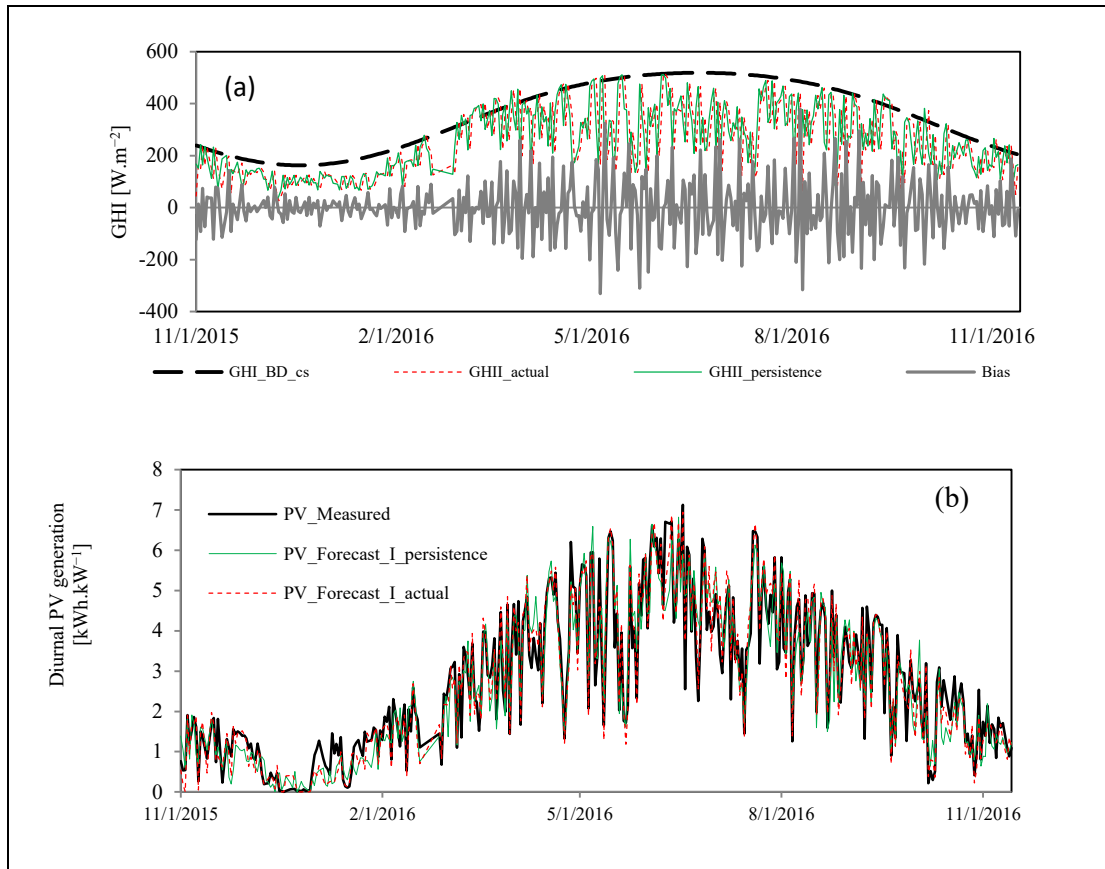


Figure 3-7. Comparison of the diurnal (a) actual, clear-sky, and smart persistence GHI ( $\text{W}/\text{m}^2$ ) and (b) prediction results of a west-facing ( $270^\circ$ ),  $30^\circ$  tilt PV system in Cochrane using actual GHI, smart-persistence GHI along with measured PV energy output ( $\text{kWh}/\text{kW}_p$ ).

The model with soiling parameters is found to have improved significantly in the ‘snow’ season (since significantly lower errors on the tails of the plot are observed) in addition to a modest improvement in the ‘non-snow’ season. This improvement is a direct result of the added dimension of precipitation. (For future applications, it is recommended that the input data to the ANN be divided into two separate models for summer and winter seasons due to the variability of the PV performances in different seasons of the year for northerly latitudes.)

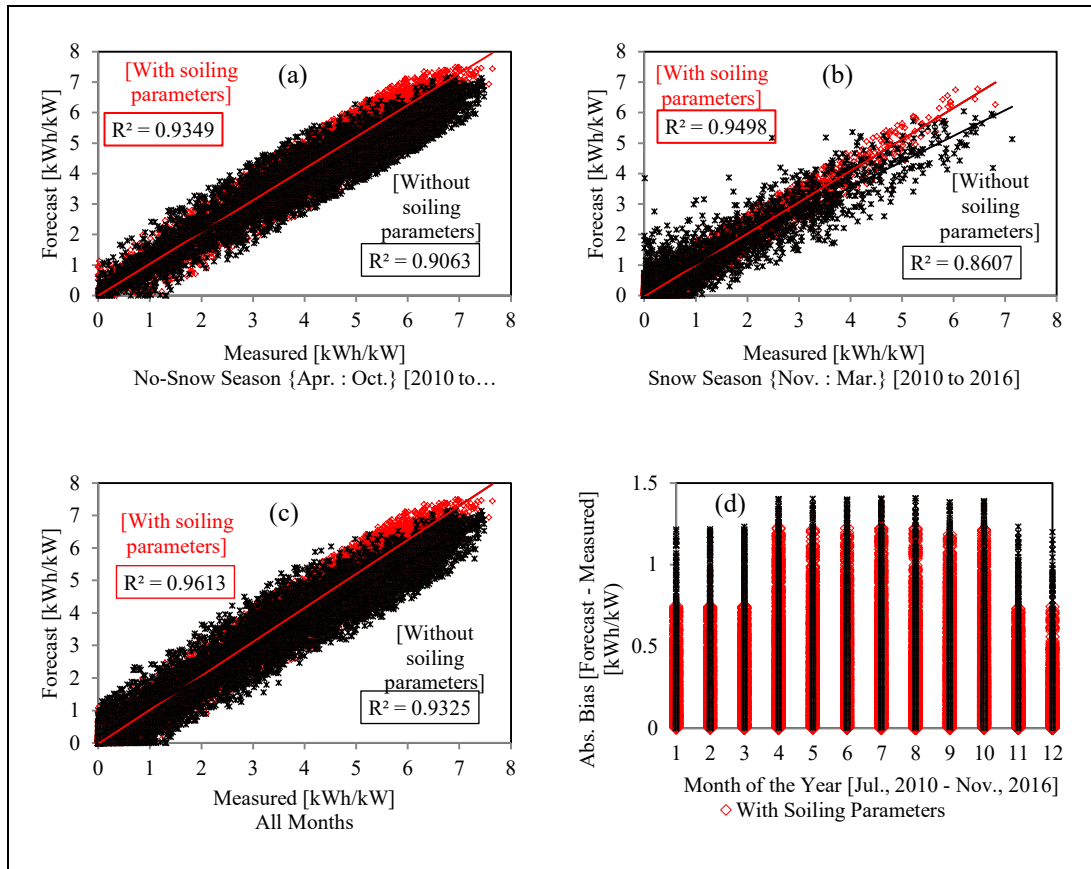


Figure 3-8. Regression charts of daily prediction of all tested PV systems against actual (measured) data for ‘with-soiling-factors’ data and ‘without-soiling-factors’ data for (a) no-snow seasons, (b) snow seasons, (c) all seasons, and (d) the absolute bias between measured and prediction data at each month of the year.

To highlight the results of the predictive models—models with and without snow parameters—one of the eight tested sites is sampled to demonstrate the monthly and yearly aggregates of both models and of commercially available solar PV estimate tools. Figure 3-9 presents a comparison of the monthly (Figure 3-9a) and annual (Figure 3-9b) energy generation output of the measured data, predictive model without soiling parameters, prediction with soiling parameters, and PV system simulation results from PVWatts software (Dobos, 2014). This example considers a south-facing, 18°-tilt PV system located in Edmonton. Input parameters to the PVWatts software include location, system size, tilt angle, azimuth angle, mounting

type, module type, and losses (14% by default). The MAPE values for prediction without soiling parameters, prediction with snow parameters, and PVWatts PV simulation tool (Dobos, 2014) against measured data are 6%, 1%, and 12%, respectively.

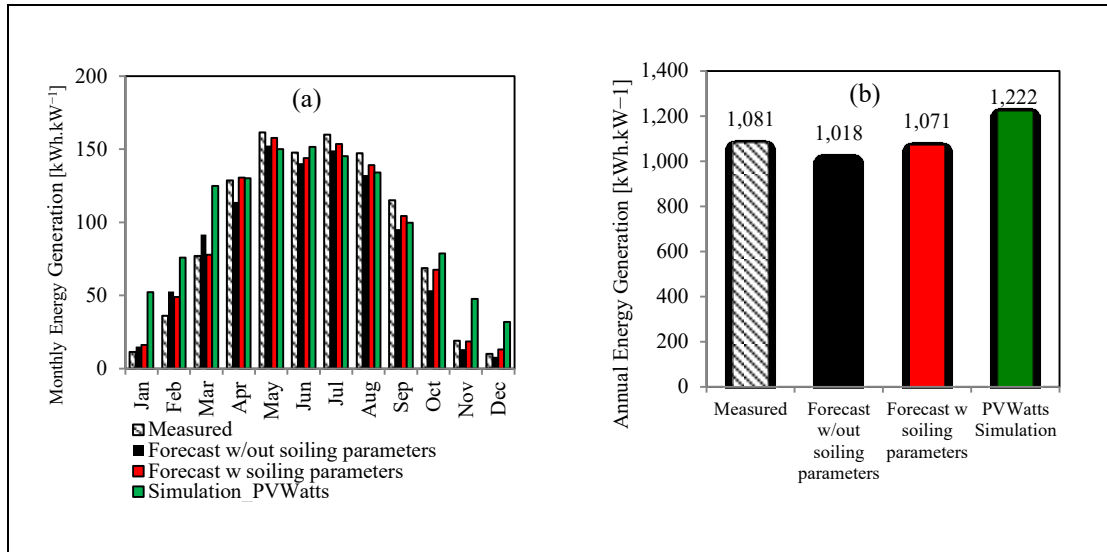


Figure 3-9. Demonstration of (a) monthly, and (b) annual energy generation prediction with and without soiling parameters compared to measured data and simulation results from PVWatts. PV system is located in Edmonton, south-facing with an 18° tilt angle.

The predictive model with soiling parameters is the model with the most accurate values (with accuracy determined by comparing predicted values to measured values in both seasons), followed by the model without soiling parameters. The relatively higher error scored by the PVWatts simulation results is primarily due to the impact of snow cover on the PV system’s efficiency having been overlooked. This oversight, in turn, results in an over-estimation of the PV system’s energy generation in winter months (November through March). For the summer months, a smaller discrepancy in error is observed between the three models against the measured data. Typically, this smaller discrepancy is due to the absence of soiling effects during this time of year.

### 3.6. Summary and Discussion

In order to ensure that the efficiency of the proposed model is not inhibited by any cloud cover-related local conditions, a clear-sky energy generation (smart persistence) model is developed and used for model validation. The model is based on Berger-Duffie's GHI model since it is found to be the closest match to the local clear-sky GHI historical data collected between the years of 1983 and 2016.

- In addition to the maximised annual energy generation, one of the advantages of a high-mount (i.e., 60° tilt) PV system is that it generates a reasonably uniform amount of energy throughout much of the year (from March to September) compared to a low-mount (i.e., 18° tilt) PV system, whose energy generation fits into a bell-shaped normal distribution. Another advantage is the mitigated impact of snow coverage, since the snow will be more likely to clear off naturally (i.e., slide off the PV modules) in the case of the high-mount system.
- The results from the proposed ANN show an average forecast skill of 0.31 after testing eight unseen PV systems in four different cities in Central Alberta. Different tilt and azimuth angles are tested, some of which, such as the 60° tilt angle, have never before been trained. East-, west-, and south-oriented PV systems are also tested by the proposed model. The predictive model results are grouped into monthly and annual aggregates and cross-checked with other simulation tools. The MAPE values for predicted annual energy generation by the ANN without and with soiling parameters are found to be 6% and 1%, respectively, while the PVWatts estimates result in a MAPE of 12%.
- The addition of soiling parameters due to rain and snow is found to significantly improve the predictive model. As a result of the improved model, the coefficient of determination ( $R^2$ ) is found to have increased from 0.93 to 0.96 for the daily energy generation of all tested PV systems.

### 3.7. Conclusions and Future Work

This study successfully meets its goal in predicting the daily energy generation of various PV systems located in cold-climate regions, with an emphasis on improving the forecast skill under soiling conditions in general, and snow coverage conditions in particular. Although the ANN model is able to accurately predict the daily energy generation of PV systems with varying locations, tilt angles, and orientations, even though some of the layouts are unseen by the ANN, it is recommended to add more variety of panel layouts, especially for the less common tilt angles.

In the proposed model, a feed-forward backpropagation model is used for its simplicity, short computational time, and high accuracy; however other several techniques can also be implemented such as radial basis function (RBF), support vector machine (SVM), decision trees, etc. depending on the complexity of the given model. Future work will consider higher temporal resolution input parameters in order for the prediction model to obtain energy output with a higher resolution.

Higher tilt angles such as  $50^\circ$  or  $60^\circ$  are recommended, not only because of the northerly latitude, but also because they offer a more uniform distribution of energy generation throughout the year and are less vulnerable to energy generation loss due to snow coverage.

It is recommended that the input data to the ANN be divided into two separate models for summer and winter seasons due to the variability of the PV systems in different seasons of the year for northerly latitudes. More accurate and higher space and time resolution of meteorological data is strongly recommended for better training of the network. It is also recommended to implement a wider range of tilt angles and orientations to better serve the purpose of the predictive model.

Analysis of the electrical energy consumption of the houses on which the monitored PV systems are located will be conducted and predictive models that combine both consumption and generation will be developed in future research. Load match and peak load analyses on NetZero and NetZero-ready homes will also be undertaken.

## Chapter 4: Load-match-driven Design of Solar PV Systems and Its Impact on the Grid<sup>3</sup>

### 4.1. Overview

Several challenges accompany the deployment of solar photovoltaic (PV) technology in residential construction, such as determining an optimum size and layout design for on-site utilisation that conforms to local roof-sloping practice. Common solar PV installation practice tends to prefer the south-facing orientation due to its maximised energy aggregate regardless of household load patterns. Solar PV applications in high-latitude regions encounter other challenges, such as significant seasonal variations in daylight hours and in the sun's path. These challenges result in a PV mismatch: (a) in winter, minimal PV-generated energy and high energy demand (due to space and hot-water heating), and (b) in summer, PV over-generation and reduced energy demand. This study aims to provide a generic framework that identifies the best possible layout placement and size by applying the generalised reduced gradient nonlinear optimisation algorithm. In this regard, the energy performance of eleven single-family homes in Edmonton, Canada is monitored at one-minute intervals, some of which are net-zero energy homes and others of which are energy-efficient homes. The results show that a south-west facing solar PV system installed at a tilt angle  $10^\circ$  above or below the local latitude can significantly improve the self-consumption compared to common installation practice.

### 4.2. Introduction

The integration of solar energy systems into residential buildings is emerging as an important method for mitigating the greenhouse gas emissions of the housing

---

<sup>3</sup> A version of this chapter has been submitted for publication in Solar Energy Journal as Awad H and Gül M, *Load-match-driven Design of Solar PV Systems and Its Impact on the Grid*.

industry. To achieve optimal energy performance, the generation capacity of the solar photovoltaic (PV) system installed on a building must be designed in such a manner as to match the electricity loads of the given building (and potentially avoid negative impacts on the grid). While the economics of PV systems is the primary factor affecting the buying decisions of investors and system owners, providing sufficient infrastructure and quantifying the impacts of solar PV systems on the utility grid are major concerns of developers, engineers, and utility providers. As Energy-efficient Homes (EEHs), Net-zero Energy Homes (NZEHs), and Distributed Energy Generation (DEG) systems gain market penetration, ensuring that the electricity distribution grid remains safe, reliable, and affordable is becoming an increasingly vexing challenge. NZEHs, electric cars, and energy storage will further add dynamic complexity to the problem. In current practice, for example, air-source heat pump equipment, which is widely used in NZEHs for space heating and domestic hot water (DHW) supply in order to minimise the energy usage in NZEHs, generally uses electricity rather than natural gas as the energy source. Intrinsically, NZEHs, not considering on-site DEG, consume 2.5 to 3 times the electricity consumed by a typical home, with a large portion of the increased demand occurring in winter. The large-scale application of grid-tied solar PV microgeneration thus results in the so-called “duck-curve” phenomenon. The duck-curve, as defined by the National Renewable Energy Laboratory (Denholm et al., 2015), is one of the shortcomings of over-generation during the day and excessive loads that peak in the morning and late-afternoon. Among the advantages of the solar PV application as a renewable source of electricity is its minimal direct and lifecycle emissions compared to fossil-based electricity supply technologies such as coal and natural gas (Camacho et al., 2011). Thus, solar PVs as an alternative are considered to be a clean, safe, and noise-free source of electricity (Schlomer et al., 2014).

#### 4.2.1. *Literature Review*

This section summarises the literature relevant to the scope of the present study and then identifies the research gap and study objectives. The first subsection presents recent studies carried out with respect to the application of NZEHs and EEHs and the

different strategies for energy reduction in the residential sector. The second subsection demonstrates a review on studies previously undertaken on several solar PV design optimisation frameworks.

#### *4.2.1.1. Recent Studies on Net-zero Energy and Energy-efficient Homes*

Sartori et al. (2012) provide a consistent framework for setting the Net-zero Energy Home (NZEH) definitions and methods of evaluation. As defined in the literature, an NZEH is a building with low energy demand that produces as much renewable energy as it consumes annually (Li et al., 2016; Sartori et al., 2012; Seljom et al., 2016). The research described in the present study is based on the hypothesis that the annual balance between the energy consumption and generation is not sufficient to fully characterise NZEHs. Other studies provide a comprehensive framework to identify the Load Match and Grid Interaction (LMGI) indicators of an NZEH (Salom et al., 2014a, 2011). Among these studies, Salom et al. emphasise the importance of reducing the overall annual demand of NZEHs in order to realistically match the on-site microgeneration energy supply. They propose a quantitative method to identify the LMGI indicators and net-zero balance through a weighting system that converts the physical units of different energy carriers into a uniform metric. This weighting system could be used to convert the exported and imported energy to the amount of corresponding CO<sub>2</sub> emissions. Luthander et al. provide a review on PV self-consumption in buildings in which they address a number of research questions/topics such as how to define self-consumption for a residential PV system, the amount of increase in self-consumption in response to installing a residential PV system, possible methods to increase self-consumption for a residential PV system, and knowledge gaps in the literature (Luthander et al., 2015). In their study, two methods are introduced to increase the household self-consumption: local storage technologies and demand side management (or demand-response). Li et al. (2016) and Li (2016) monitor, simulate, and investigate the long-term performance of ten NZEHs located in Edmonton, Alberta, under occupancy. These latter mentioned studies find that, in the application of NZEHs in cold-climate regions, space heating

and cooling accounts for 56.77% of the annual energy consumption, DHW heating is the second-highest energy consumer, accounting for 12.9%, while the clothes dryer represents only 3.5%. Farahbakhsh et al. (1998) investigate methods to reduce the CO<sub>2</sub> emissions from the residential sector in Canada using the Canadian Residential Energy End-use Model (CREEM), a residential energy model. Stoll et al. (2013) investigate the interaction between the so-called “Active House” electricity consumer (resident) and the utility in Stockholm, Sweden. Their concept aims at reducing electricity use (and resultant CO<sub>2</sub> emissions), engaging the customer in consumption control, reducing the overall electricity loads, and stimulating local microgeneration. Seljom et al. (2016) study the effect of net Zero Energy Buildings (ZEBs) on cost-optimal investments in the Scandinavian energy system using the stochastic TIMES model. The results from their study indicate the direct impact of the ZEBs on reducing the investments in non-flexible hydropower, wind power, and combined heat and power while increasing the reliability on direct electric heating and electric boilers. Reka and Ramesh (2016) study the demand response modelling for residential consumers in a smart grid environment and develop a game theory-based algorithm—a generalised tit-for-tat dominant game-based energy scheduler. In the demand-response concept, both the end users (consumers) and utility grids become key players, and consumers must be tech-savvy to ensure economical and environmentally-friendly occupancy (Reka and Ramesh, 2016). Additionally, Deng et al. (2014) provide a framework to evaluate the performance of NZEHs through a life cycle assessment, and Widén (2014) studies the improved on-site utilisation of solar PV systems resulting from appliance scheduling in 200 single-family homes.

#### *4.2.1.2. Review on Solar PV Design Optimisation*

Several studies have been performed to investigate the optimal layout placement within a specific site or jurisdiction. For example, Kaddoura et al. (2016) investigate the optimum PV panel tilt angles for various cities in Saudi Arabia. In this study, the horizontal solar radiation data is collected from NASA and then an optimisation framework is developed in a MATLAB<sup>®</sup> platform where the objective function is set

to maximise the solar radiation. Darhmaoui and Lahjouji (2013) develop a latitude-based model for tilt-angle optimisation for solar collectors in the Mediterranean region. In their study, a mathematical model is developed to calculate the optimal tilt angle based on the daily global solar radiation on a horizontal surface. To support the mathematical model, data from 35 sites in different Mediterranean countries spanning four years is investigated and fed to the model. Yi-da (2013) studies a method to maximise PV power generation based on solar radiation data, and the concept of utility factor per area is introduced. To achieve the goals of their study, dynamic programming algorithm is used to maximise the number of cells per unit area. The author also considers the lifetime total profit of the PV system in addition to the annual energy generation. Other studies (Kacira et al., 2004; Mahmoud and Nabhan, 1990) suggest installing PV systems at a tilt angle that is above or below the local latitude by  $15^\circ$  (latitude  $\pm 15^\circ$ ) at a south-facing orientation (for the Northern Hemisphere, and a north-facing orientation for the Southern Hemisphere). Naraghi (2016) investigates the optimum solar panel tilt angle for maximum annual irradiation based on the clear-sky model provided by the American Society of Heating, Refrigerating, and Air-Conditioning Engineers (ASHRAE). The study highlights the significant effect of ground reflectivity on the optimum solar panel tilt angle. Naraghi concludes that a panel's optimum tilt angle is nearly equal to the local latitude, with a variation of  $\pm 3^\circ$ . Awad et al. (2017b) study the design improvement of residential rooftop solar PV systems resulting from the use of a hybrid data-driven-analytical optimisation framework. They apply a GRG nonlinear optimisation algorithm to identify the optimum tilt and azimuth angle of a PV system in order to achieve the highest possible PV self-consumption while the system size remains unchanged. Awad et al. (2016) develop a generic framework to optimise the layout placement of commercial flat rooftops in cold regions, aiming to identify the optimum placement taking into account tilt angle, inter-row spacing, snow coverage, shade effect, and the system's lifetime cost-effectiveness. Two solutions are proposed in their study: (1) an economical solution that maximises the per-panel annual output (and minimises the overall system's payback period), and (2) a solution that maximises the overall

system's annual output by placing as many panels as possible while avoiding any shading effect.

Furthermore, the economics of distributed energy generation has been investigated. For example, Darghouth et al. (2011) investigate the value of the bill savings under different mechanisms while focusing on net-metering mechanism against alternative PV compensation mechanisms. Freitas et al. (2018) study the community-scale combined effect of aggregating demand, photovoltaic generation and electricity storage, on-site consumption of PV and its impact on the grid using real-time aggregated data. Two storage strategies were investigated in this study: one of which that maximised self-consumption and the other of which that reduced the net load variance. This study concludes that, from the prosumer's point of view a PV system can be viable with no or small storage system, while from the grid point of view, higher storage capacities are vital to the reduction of unmanageable load variance and consequent costs. Litjens et al. (2017) study the impact of load patterns on the orientation of PV systems using historical Dutch demand patterns of 48 residential buildings and 42 commercial buildings. This study concluded that the PV self-consumption was maximised in residential buildings in the Netherlands with a tilt angle of  $26^\circ$  and an azimuth angle of  $212^\circ$ , while that of commercial buildings was maximised by implementing a tilt angle of  $17^\circ$  and  $188^\circ$ .

#### 4.2.2. *Research Gap and Study Scope*

Several studies propose methods by which to evaluate the performance of NZEHs. Other studies focus on investigating the optimum solar PV layout placement based on the objective of maximising the aggregated annual energy output. However, few studies address the optimum solar PV system layout placement to match household energy load and minimise its impact on the utility grid. Current solar PV design practice is premised on three main objectives: (1) the installed solar PV system generates as much energy as the site consumes on an annual basis, (2) the annual energy aggregate from the solar PV system is maximised given that a south-facing installation satisfies this condition, and (3) the proposed PV system design can fit

within the available roof area. (In addition, other financial, regulatory, and consumer-related aspects are considered; however, these aspects are out of the scope of the current study). The current design method, although it satisfies the theoretical objectives of NZEH practice, fails to meet other aspects such as the PV system self-consumption, grid interaction, and economic viability from the end user's perspective. The present study aims to develop an improved design framework for residential grid-tied small-scale solar PV micro-generators using a data-driven approach that focuses on maximising the household load-match rather than maximising the annual solar PV energy production. The scope of the study is limited to finding methods of improvement for existing PV systems, with the intent that the findings from this research will be applied in future solar PV installations.

In light of the emergence of smart technologies and the demand for economical building and distributed energy generation (DEG) practices, the primary goal of the research presented in this chapter is to provide a novel framework that aims to leverage the large-scale interaction between energy-efficient buildings, DEG, and the utility grid in order to improve energy efficiency. This entails investigating the load-match and grid interaction between DEG and household energy consumption, aiming at not only mitigating the greenhouse gas emissions resulting from these homes but also mitigating their negative impact on grid performance.

Within the context of the present study and as per the local practices where this study is conducted, an NZEH is defined as a house that has low energy demand, relies on the electricity as a sole source of energy, and generates as much energy as it consumes over the course of the year (Li et al., 2016). An EEH is referred to as a house that has low energy demand, relies on natural gas for space heating and domestic hot water (DHW) heating, can optionally be equipped with a solar PV system, but does not necessarily achieve a yearly net-zero balance.

### 4.3. Method

First, an investigation of the long-term energy performance of 85 solar PV systems installed on homes in various locations in Alberta, Canada (ongoing since 2010) is conducted as plotted in Figure 4-1a and Figure 4-1b where the scope of the portion of this study is focused on the dependency of the yield of such systems on the various tilt and azimuth angles. These systems are installed at various tilt angles and orientations, where a heat map can be generated that identifies the impact of the variation of location, tilt angle, and azimuth angle on the annual PV performance by applying a 5<sup>th</sup>-degree by 5<sup>th</sup>-degree polynomial fit function in a MATLAB® platform as explained in Subsection 4.5.1. The sensitivity of the annual energy output of a PV system installed in Alberta, Canada, is identified as a function of tilt angle and azimuth angle. In this context, the following research question is addressed: What is the LMGI performance of a specific grid-tied building-integrated PV system, and what is the impact of PV systems coupled with various types of residences such as NZEHs and EEHs, on the central grid? Here, in addition to the 85 sites mentioned earlier, complete household energy monitoring is performed on seven EEHs and four NZEHs (Figure 4-1c) (ongoing since 2015). LMGI measures proposed by Salom et al. (2014) are used to quantify the LMGI indicators and to identify the net-zero balance of the sites under investigation using the collected real-time data. Building on this, the following research question is addressed: *Is the current know-how for residential PV system design sufficient to provide the optimum design in terms of environmental impact, economy, and on-site PV self-consumption and its impact on the grid?* To answer this question, a novel hybrid framework that combines the inputs from real-time data with an analytical model is proposed. First, the analytical model is developed to determine the clear-sky solar PV power output at any given two-way tilted surface at any location around the globe at a one-minute temporal resolution. This model is highly beneficial for data analysis and data mining purposes given that it can predict the theoretical clear-sky irradiance at any given latitude at the desired temporal resolution (secondly, minutely, daily, etc.). The clear-sky irradiance is used

as a denominator to predict the clear-sky index, where the nominator is the real-time power generation of a given PV module. It is thus possible to estimate the clear-sky energy aggregate of a given PV system at any layout placement and at the desired temporal resolution. However, due to the varying weather conditions, especially cloud cover, it is crucial to determine the clear-sky index of the site under investigation at the specified temporal resolution (minutely in the current case). One site that is south-facing and tilted at  $26.5^\circ$  is then selected as a reference based upon which the minutely clear-sky index is calculated (as the ratio between the actual power output and the clear-sky power output at the same layout placement) to be used as a multiplier for any other layout placement. This method will later be explained in detail and validated. Two sites, an NZEH and an EEH, are selected as case studies to validate the framework. A Generalised Reduced Gradient (GRG) nonlinear optimisation algorithm is then developed to identify the best PV system layout placement and size. The optimisation framework is set to facilitate the objective function of maximising the minutely load-match between the household energy loads and the proposed PV system. Finally, the research results and findings from the case studies are summarised and the actual practice is compared to the recommended future practices. Figure 4-2 summarises the research methodology used to achieve the stated objectives. To meet both environmental goals (i.e., load-match and net-zero balance) and economic goals, the model is run three times to handle one goal at a time. The first run addresses the load-match goal by identifying the optimum PV orientation to match the household energy consumption patterns. The variables include the solar PV tilt angle (between horizontal and vertical) and azimuth angle (between east and west) while the system size (capacity and number of panels) remains unchanged. Once the model has identified the best possible layout placement, the second run is set. The objective of the second run is to achieve the net-zero balance of the site under investigation. The net-zero balance means that the annual load becomes equal to the annual generation—and similarly the yearly imported energy becomes equal to the exported energy. Therefore, the objective function is to equalise the load-generation balance to zero (or near zero). Here, the tilt and azimuth

angles are fixed at the preferred solution from the first run and the variable is changed to include only the system size. Solutions from the first and second runs may be environmentally sound, yet uneconomical and unfeasible. Some jurisdictions set strict regulations on microgeneration sizing, and thus the over-sizing of a PV system may pose problems in terms of procuring profit from microgeneration. This may impact some rewards programs and may also result in a lengthy payback period. To capture economic implications, the model is run a third time, setting the objective function in such a manner as to minimise the system's cost (or payback) while achieving the preferred load-match (LM) indicator and net-zero balance. The variable for this run is set as the system size.

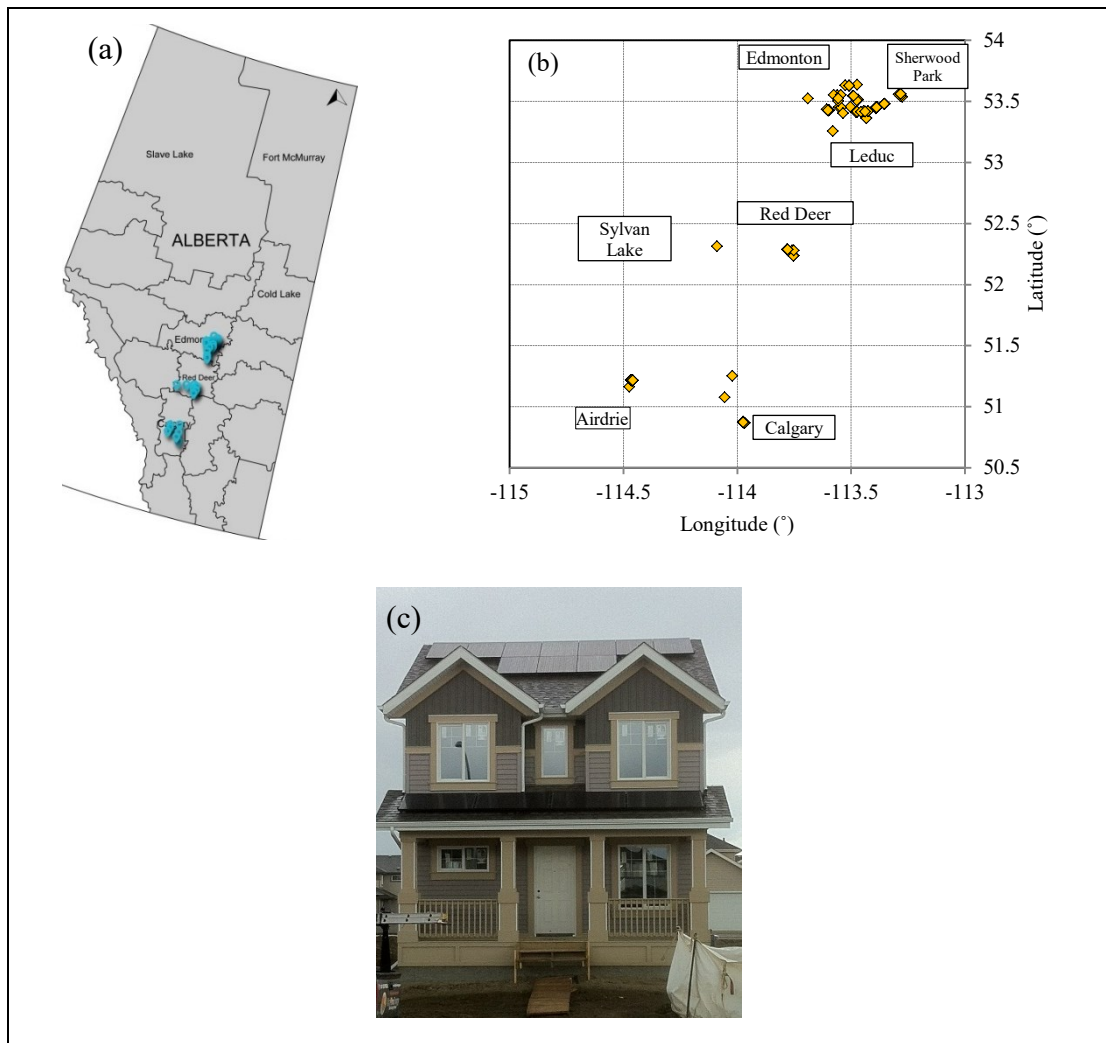


Figure 4-1. (a) Locations of monitored solar PV systems in Alberta, Canada; (b) exact coordinates of each site; and (c) one of the monitored sites in Edmonton.

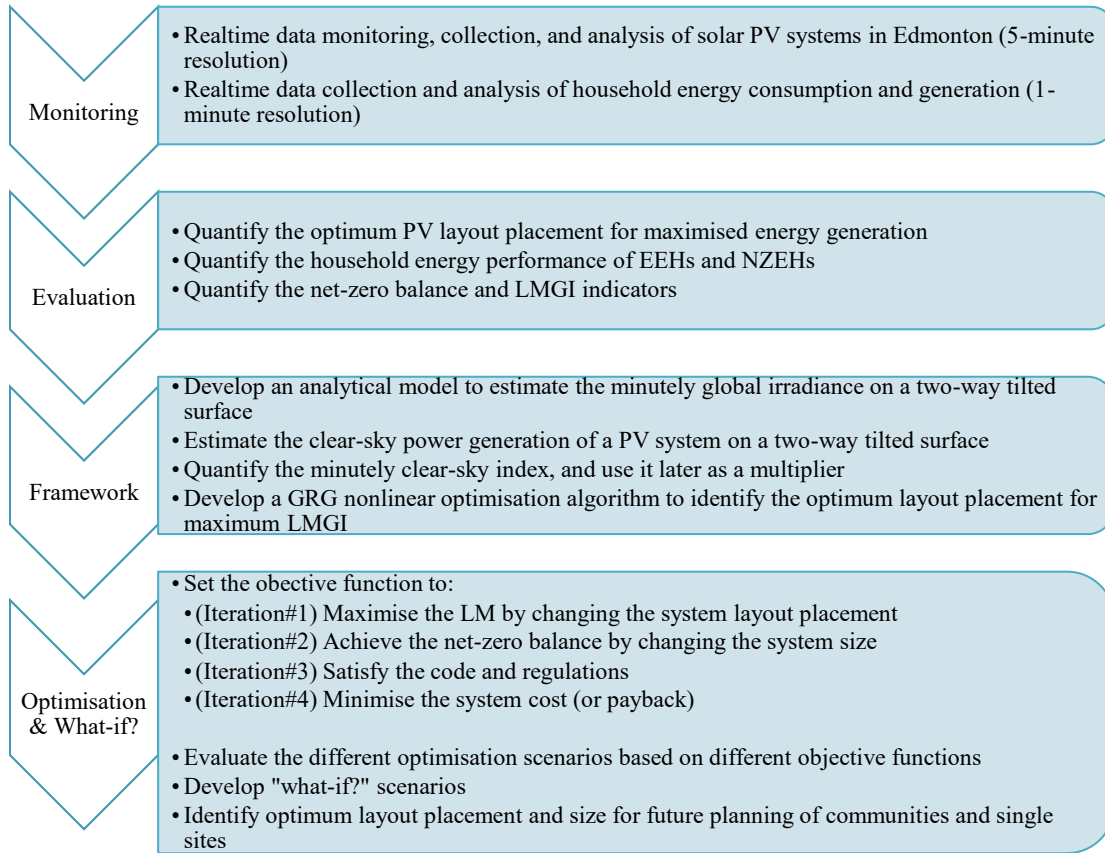


Figure 4-2. Summary of the research method.

#### 4.4. Proposed Optimisation Framework

##### 4.4.1. Net-zero Balance of Household Energy Performance

The first step of the proposed optimisation framework is to analyse the energy performance of NZEHs and EEHs located in cold-climate regions and quantify their load-match and grid-interaction (LMGI) indicators. In this regard, Eq. 4-1 to Eq. 4-9, as per Salom et al. (2014), are applied. In their study (Salom et al., 2014a), they suggest using weighting factors ( $w_x$ ) to evaluate several aspects of the net-zero

balance of a house rather than the energy performance alone; for example, these weighting factors may represent political, economic, or even environmental aspects of an NZEH. In the present study, though, the author focuses on the net-zero balance in terms of energy performance only, and thus the weighting factors corresponding to these other aspects is disregarded.

$$\sum_x exp_x - \sum_x imp_x = EXP - IMP \geq 0 \quad (4-1)$$

$$\sum_x g_x - \sum_x l_x = G - L \geq 0 \quad (4-2)$$

$$g_{m,x} = \sum_m \max[0, g_x(m) - l_x(m)] \quad (4-3)$$

$$l_{m,x} = \sum_m \max[0, l_x(m) - g_x(m)] \quad (4-4)$$

$$\sum_x g_{m,x} - \sum_i l_{m,x} = G_m - L_m \geq 0 \quad (4-5)$$

$$f_{load,x} = \frac{1}{N} \sum_{year} \min[1, g_x(t)/l_x(t)] \quad (4-6)$$

$$f_{grid} = net\ grid / \max|net\ grid| \times 100(\%) \quad (4-7)$$

$$\text{with } net\ grid = exp_x - imp_x \quad (4-8)$$

$$f_{grid,yr} = STD(f_{grid,i}) \quad (4-9)$$

where  $exp$  is the exported energy to the grid;  $imp$  is the imported energy from the grid;  $x$  is the energy carrier (solar PV energy in this study);  $g$  is the generation;  $l$  is the load;  $m$  is monthly resolution;  $f$  is the index;  $t$  is the time interval; and  $N$  is number of data samples. The net-zero balance of a given building should be achieved by satisfying the above set of equations. In other words, the exported energy should be greater than or equal to the imported energy (at the yearly and monthly time intervals). Similarly, the generated energy should be greater than or equal to the load on the yearly interval.

#### 4.4.2. Clear-sky PV Output at Two-way Tilted Surface

The importance of developing an analytical model for clear-sky global irradiance (and PV power output) is twofold: first, and most importantly, the clear-sky global

irradiance model is used in the assessment of the clear-sky index ( $k_t$ ) as the ratio between the actual power output and the clear-sky PV power output (Eq. 4-10). The purpose of the implementation of  $k_t$  into the optimisation framework is to determine the impact of cloud cover on the power output of the solar PV system under investigation at any two-way tilted surface. In such case, the actual power output can thus be determined with a considerable degree of accuracy. It is worth mentioning that the impact of cloud cover on a given PV system's orientation has been assumed to be fixed. Second, this model is used to support the learning of the optimisation framework since several solar PV systems with varying layouts and locations can be introduced to the generic model. Hence, it is vital to provide the model with sufficient information (i.e., the sun's location and expected angle of incidence on the given PV system at any given time of day). The clear-sky model is used to analytically predict the clear-sky solar PV power output on a two-way tilted surface at the highest possible temporal resolution (i.e., monthly, daily, hourly, or minutely). This information becomes helpful in cases where historical data with high temporal resolution is not available. In this study, clear-sky PV power output is used to calculate the minutely clear-sky index ( $k_t$ ) as well as to leverage the calculated index later in predicting the solar PV power output at any desired layout placement as a factor of tilt and azimuth angles. Solar geometry calculations for each day of the year (*DOY*), including solar zenith ( $z$ ) (Reno et al., 2012), declination ( $\delta$ ) (Reno et al., 2012; Walter et al., 2012), solar time ( $ST$ ) (Reno et al., 2012; Walter et al., 2012), hour angle ( $\omega$ ) (Kreider et al., 1989; Reno et al., 2012), true zenith ( $z_t$ ) (Reno et al., 2012), extraterrestrial irradiance ( $I_0$ ) (Spencer, 1971), direct normal irradiance ( $DNI$ ) (Eq. 4-11) (Daneshyar, 1978; Paltridge and Proctor, 1976), diffuse irradiance (*diffuse*) (Eq. 4-12) (Daneshyar, 1978; Paltridge and Proctor, 1976), clear-sky global horizontal irradiance ( $GHI_{cs}$ ) (Eq. 4-13) (Badescu, 1998), daylight hours ( $\beta$ ) (Kreider et al., 1989), the sun's degree angle from due south at sunset (*Hourset*) (Kreider et al., 1989), and the sun's azimuth angle ( $\alpha$ ) (Kreider et al., 1989), can be found in the relevant literature.

$$k_t = GHI_{measured}/GHI_{cs} \quad (4-10)$$

$$DNI (W/m^2) = 950.2(1 - \exp(-0.075(90 - z_t))) \quad (4-11)$$

$$Diffuse (W/m^2) = 14.29 + 21.04 \left( \frac{\pi}{2} - z_t \times \pi/180 \right) \quad (4-12)$$

$$GHI_{cs} (W/m^2) = I_0 * 0.70 \times \cos(z_t) \quad (4-13)$$

The angle of incidence of the sun on a two-way tilted surface ( $\theta_i$ ) is defined in Eq. 4-14 as

$$\begin{aligned} \cos \theta_i = & \sin(\delta) \sin(\varphi) \cos(\vartheta) + \sin(\delta) \cos(\varphi) \sin(\vartheta) \cos(\alpha) + \\ & \cos(\delta) \cos(\varphi) \cos(\vartheta) \cos(\omega) - \cos(\delta) \sin(\varphi) \sin(\vartheta) \cos(\alpha) \cos(\omega) - \\ & \cos(\delta) \sin(\vartheta) \sin(\alpha) \sin(\omega) \end{aligned} \quad (4-14)$$

The clear-sky power output is then identified by applying the following equation:

$$P_{cs,o} = \min(MPP, GHI_{cs} \times n_p \times l_p \times w_p \times e_p \times e_s/1000) \quad (4-15)$$

where  $\varphi$  is the latitude of the site under investigation;  $P_{cs,o}$  is the clear-sky power output at the original layout placement of the solar PV system;  $MPP$  is the Maximum Power Point of the PV system;  $n_p$  is the number of panels in the PV system;  $l_p$  and  $w_p$  are the length and width of the panel, respectively; and  $e_p$  and  $e_s$  are the module efficiency and system losses, respectively. The clear-sky index and the clear-sky power output having been determined earlier in this section, the power output at any two-way tilted surface can then be predicted as expressed in Eq. 4-16:

$$P_{p,n} = P_{cs,n} \times k_t \quad (4-16)$$

where  $P_{p,n}$  is the predicted actual power output at the new layout placement, and  $P_{cs,n}$  is the clear-sky power output at the new layout placement.

#### 4.4.3. Optimisation Framework

In this subsection the building of the optimisation framework is described based on the findings reported in the preceding subsections along with the collected real-time household energy consumption and generation data. In this regard, a generalised reduced gradient (GRG) nonlinear optimisation algorithm (Lasdon et al., 1974) is employed to identify the optimal solution. As demonstrated in Figure 4-3, four

iterations are run to identify the optimal PV layout and sizing satisfying the system's (1) load-match, (2) net-zero balance, (3) regulatory, and (4) economic criteria.

#### 4.4.3.1. Optimised Tilt Angle and Azimuth Angle

The next step in the proposed optimisation framework is to identify the optimum tilt and azimuth angles of the PV system, assuming that the PV system sizing remains unchanged. Here the objective function is to maximise the load-match index by changing the tilt and azimuth angles of the PV system, as expressed in Eq. 4-17 to Eq. 4-19, in order to maximise the load-match indicator (previously calculated in Eq. 4-6), considering that

$$f_{load,x} = f(\theta, \alpha_s) \quad (4-17)$$

Here, the objective function, taken from Lasdon et al. (1974), is defined as:

$$\text{maximise } f(\theta, \alpha_s) \quad (4-18)$$

and subject to

$$0^\circ \leq \theta_o \leq 90^\circ, 90^\circ \leq \alpha_{s,o} \leq 270^\circ \quad (4-19)$$

where  $\theta_o$  is the optimum PV system's tilt angle and  $\alpha_{s,o}$  is the optimum PV system's azimuth angle. It is assumed that the  $0^\circ$  and  $90^\circ$  tilt angles are horizontal and vertical placements, respectively. Similarly,  $90^\circ$  and  $270^\circ$  azimuth angles are east- and west-oriented placements, respectively, while true south is represented as  $180^\circ$ .

#### 4.4.3.2. Optimised System Sizing

A solar PV system's sizing in terms of nameplate capacity and overall efficiency varies based on two main drivers: the number of panels of which the system consists and the module's nameplate capacity. A group of PV panels form an array in which these panels are similar and placed according to the same layout (tilt and azimuth angles). A single PV system may consist of one or more arrays, while the mechanical features of a solar PV module—such as the module's dimensions (length, width, and thickness), nameplate capacity, and efficiency—vary in relation to its brand, model,

and age. Given that the aim of this study is to optimise solar PV sizing to achieve both the environmental and economic goals (by maximising on-site utilisation), it is found that, in the optimisation framework, setting up the module type as a variable necessitates providing the model with a complete database of module types and their relevant attributes such as module dimensions, nameplate capacity, and efficiency. Despite the expected high accuracy of the model with variable module type, the complexity of the model and its computational time can both be expected to increase significantly. Consequently, in this study, one module type is selected based on availability, affordability, and user preference, and it remains unchanged throughout the optimisation. Furthermore, in order for the optimisation framework to identify the optimum PV sizing, the only variable is the number of panels per PV system. The lower and upper limits of the number of panels ( $n_p$ ) are defined as zero (no PV system) and  $n_{p,t}$  (total number of panels), respectively. The upper limit varies from one site to another since it is mainly dependent on the roofing geometry and available space (assumed to be one array and thus one surface). If the geometry of the rooftop is rectangular, then the upper limit of the number of panels can be estimated using Eq. 4-20 as follows.

$$n_{p,t} = (l_r - 2 \times b)/l_p \times (w_r - 2 \times b)/w_p \quad (4-20)$$

where  $l_r$  is the length of the roof,  $b$  is the regulatory offset distance of the PV array from the roof edge, and  $w_r$  is the width of the roof. If the rooftop is non-rectangular in its geometry, then manual assessment or more complex algorithms are to be applied to identify the upper limit with regards to the number of panels.

Here, the objective function, taken from Lasdon et al. (1974), and constraints are defined in Eq. 4-21 and Eq. 4-22 and Eq. 4-23 respectively as

$$\text{maximise } f(\theta, \alpha_s) \quad (4-21)$$

and subject to

$$0 \leq n_p \leq n_{p,t} \text{ and } n_p \text{ is integer} \quad (4-22)$$

$$G \geq L \quad (4-23)$$

where  $n_p$  is the number of panels,  $n_{p,l}$  is the maximum possible number of panels based on the rooftop allowable space,  $G$  is the yearly generation, and  $L$  is the yearly load.

#### 4.4.3.3. Other Applications

The proposed optimisation framework can also be used for several purposes such as target pricing or target net-zero balance requirements (for example, 75% net-zero balance). It can also be used to modify a given solar PV design to conform to the local residential regulatory parameters (as discussed in Iteration#3 in Figure 4-3).

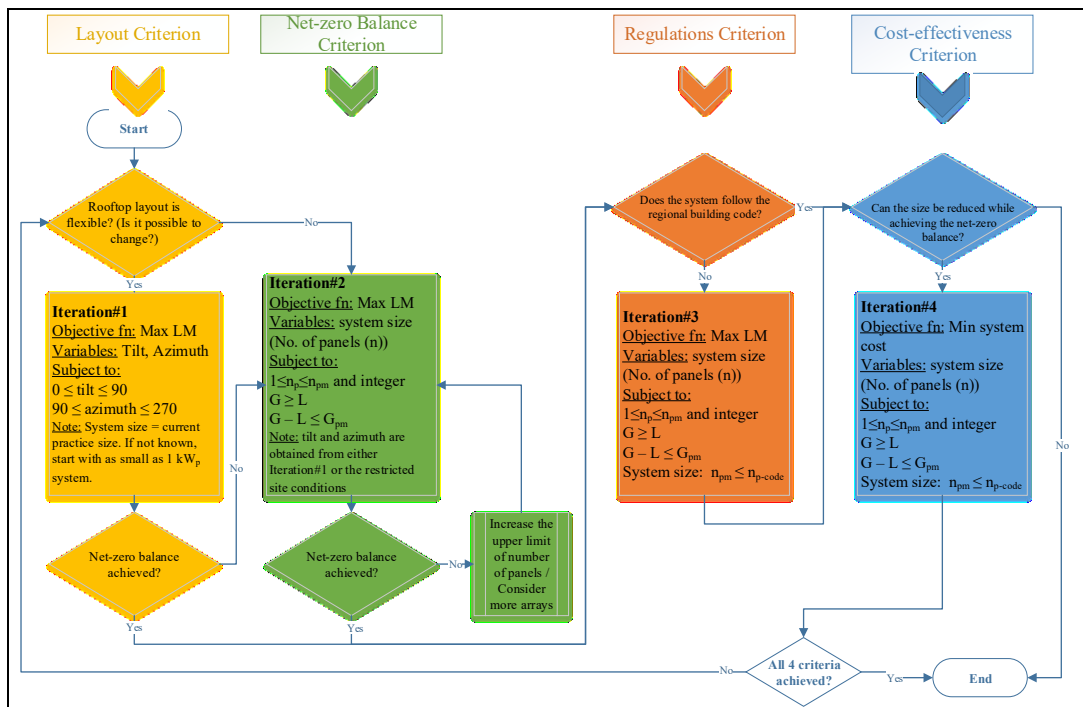


Figure 4-3. Proposed optimisation framework.

The regulatory and economic criteria are mainly structured to provide the reader with a holistic, generic and systematic framework that is applicable to any other jurisdictions. In this sense, the regulatory criterion manages the upper limit of a given PV system to override the net-zero balance criterion, if needed, since the regulatory criterion reflects the actual allowance for a PV system's size (capacity) as per the local governmental regulations of a given site. The economic criterion is set to run an

additional iteration for minimised system size (and initial cost) while meeting all other criteria (i.e., layout, net-zero balance, and regulatory criteria). In Iteration #3, the upper limit of the system size is set to correspond to the maximum PV sizing for residential applications. This model can also be used to identify the predicted generation and grid activity at any two-way tilted surface at any desired temporal resolution. Payback period can also become the end user's target of interest. In future applications of the model, Monte Carlo simulation technique will be used in the pre-processing stage of the minutely data in order to address the most-likely grid interaction scenarios. In the current form of the optimisation model, four consequent iterations are performed in order for each iteration to satisfy one of the given criteria, which may lead to potential sub-optimal rather than global solutions. The reasoning behind this current configuration is to learn the impact of satisfying each criterion and to perform a comparative analysis between the degrees of improvement incurred by each of the criteria. However, it is recommended to consider combining the net-zero balance and regulatory criteria as constraints under the layout placement (iteration #1) criterion in order to avoid possible sub-optimal solutions. Additionally, it is recommended to use weighted objective functions in order to prioritise specific criteria such as layout placement. In this context, future work will consider combining all four criteria by using weighted objective functions in order to avoid any possible sub-optimal solutions that could be obtained from the model in its current state.

## **4.5. Data Collection and Analysis**

### *4.5.1. Solar PV Data Analysis*

Long-term monitoring of PV systems from 85 sites across the province of Alberta, Canada is conducted, to investigate the performance of solar PVs in cold-climate regions, among which 48 systems are located in the city of Edmonton while focusing on the dependency of the yield of such systems on the various tilt and azimuth angles. Several parameters such as the system's tilt angle, orientation, and geographical location have been investigated in order to identify the sensitivity of such PV systems

to the above mentioned parameters (Awad et al., 2017a, 2017b, 2016). Within the scope of this chapter, the primary focus is on the data collected from Edmonton sites as a base case and consequently, the geographical location as a parameter itself has been scaled down to include sites from Edmonton solely. The impact of tilt angle and azimuth angle is then identified (as shown in Figure 4-4) by developing an empirical surface fitting formula (Eq. 4-25) where the inputs represent the tilt angle and azimuth angle, and the output represents the normalised annual energy generation (0–1) kWh/kW<sub>p</sub>. However, the proposed optimisation framework is generic and applicable to any other location within the Northern Hemisphere. For interested readers, this framework can be implemented for any other location by either (1) collecting the clear-sky index ( $k_t$ ) for the given location at the desired time interval, or (2) collecting the year-long power output data on a site near the desired location and then calculating the clear-sky index ( $k_t$ ) accordingly. Since this study investigates systems of different sizes, the data is normalised to its final yield,  $Y_{f,i}$ , (Eq. 4-24) to better serve the analytical purpose of the study (Marion et al., 2005).

$$Y_{f,i} = \frac{E_i}{P_{0,i}} (\text{kWh/kW}_p) \quad (4-24)$$

where  $Y_{f,i}$  is the final yield of a PV system,  $i$ ,  $E_i$  is the energy generated by the PV system (kWh), and  $P_{0,i}$  is the system size as a product of the number of the systems' panels and the panel capacity (kW<sub>p</sub>). Eq. 4-25 is empirically driven based on the actual energy generation data collected from the Edmonton sites; in order for it to be applied elsewhere, the equation must be customised for the site under investigation. The normalised annual energy output,  $Y_{f,i}$ , from all 48 PV systems, given that these systems are placed at tilt angles and orientations with a degree of variability, is used as the input to generate a polynomial surface fit in a MATLAB® platform where the coefficient of determination  $R^2$  is calculated as 0.96. The empirical equation below accounts for the dependency of the PV yield on the tilt and azimuth angles solely. In future works, other parameters such as various loss factors including wiring, shadow, soiling, etc. will be implemented. The annual PV potential at this specific placement is benchmarked in previous studies by Awad et al. at 1,350 kWh/kW<sub>p</sub> (Awad et al.,

2017a, 2017b, 2016). For interested readers, the impact of snow cover on the final yield of PV systems at a given month and tilt angle has been investigated in detail in Awad et al. (2017a).

$$\begin{aligned}
 Y_{f,\theta,\alpha_s} = & 1,350 \times [1.013 - 0.02661\theta - 0.006501\alpha_s + 0.0002649\theta^2 + \\
 & 0.0003459\alpha_s + 5.898 \times 10^{-5}\alpha_s^2 - 5.217 \times 10^{-7}\theta^3 - 4.17 \times 10^{-6}\theta^2\alpha_s - \\
 & 2.099 \times 10^{-7}\theta\alpha_s^2 - 2.246 \times 10^{-7}\alpha_s^3 + 2.151 \times 10^{-9}\theta^4 + 3.14 \times 10^{-9}\theta^3\alpha_s + \\
 & 1.199 \times 10^{-8}\theta^2\alpha_s^2 - 4.276 \times 10^{-9}\theta\alpha_s^3 + 2.963 \times 10^{-10}\alpha_s^4 - 5.417 \times \\
 & 10^{-12}\theta^5 + 3.412 \times 10^{-12}\theta^4\alpha_s - 1.074 \times 10^{-11}\theta^3\alpha_s^2 - 7.046 \times 10^{-13}\theta^2\alpha_s^3 + \\
 & 6.032 \times 10^{-12}\theta\alpha_s^4 + 3.593 \times 10^{-14}\alpha_s^5] \quad (4-25)
 \end{aligned}$$

where  $Y_{f,\theta,\alpha_s}$  is the annual final yield (kWh/kW<sub>p</sub>) at a specific tilt angle,  $\theta$ , and azimuth angle,  $\alpha_s$ . Although in order to maximise the annual PV output the placement of any solar PV system should be at a south-facing position with a tilt angle equal to the local latitude where the PV system is located, this study will demonstrate that the maximised annual energy aggregate may not be the optimum objective for on-site solar PV utilisation.

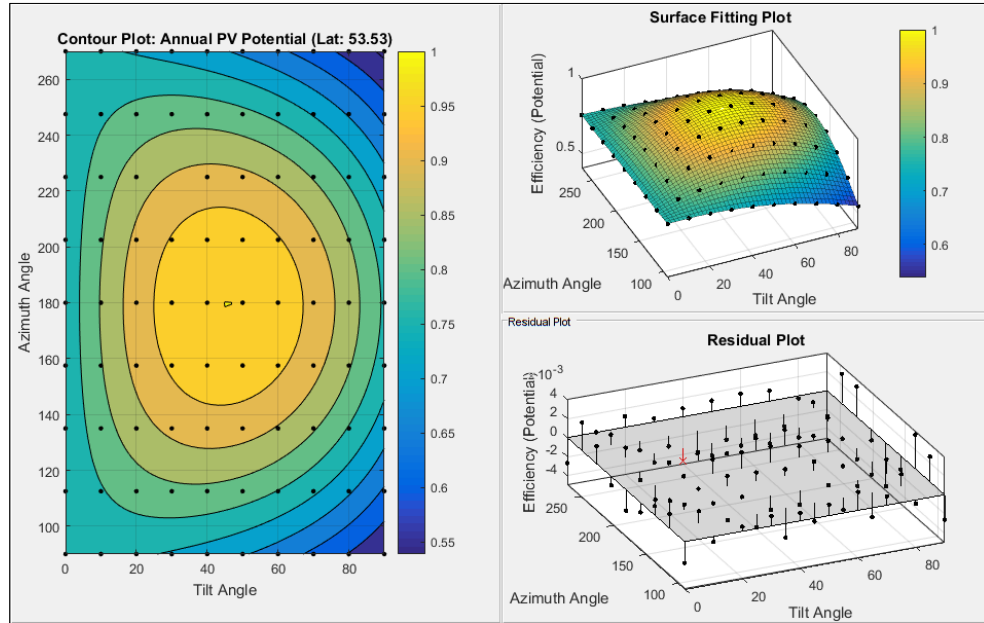


Figure 4-4. Solar PV annual output efficiency at varying layout placements in Edmonton, Canada (Lat. 53.53° N).

The purpose of this step was to better understand the sensitivity of the PV system’s final yield in terms of layout design and to later highlight the difference between the maximised generation and the maximised self-consumption. However, the empirical equation was not implemented into the optimisation framework by any means. Figure 4-4 shows the impact of tilt and azimuth angles on the efficiency of a given PV system’s annual energy generation. From the figure it is clear that the annual output is maximised at a south-facing orientation with a tilt angle of  $\pm 10^\circ$  from the local latitude in Edmonton (i.e.,  $53.53^\circ$  N).

#### 4.5.2. Household Energy Performance of Net-zero Energy Homes and Energy-efficient Homes

Data monitored and collected from 11 houses in Edmonton (Table 4-1) is analysed to investigate the energy performance of each house type (energy-efficient and net-zero), as well as the performance of different configurations of installed solar PV systems, with the focus on the net-zero balance, load-match, and grid interaction indicators of each house.

Table 4-1. List of monitored NZEHs and EEHs.

Type	Data Collection Starting Date	Tilt	Azimuth	No. of Panels	Panel Capacity ( $W_p$ )	System Size ( $kW_p$ )	Latitude ( $^\circ$ N)	Heating system	DHW heating
S-18356	20-May-15	27	182	14	260	3.640	53.62545	NG/ F <sup>1</sup>	NG
N-18366	29-May-15	27	195	39	280	10.92	53.51095	ASHP <sup>2</sup>	EHP <sup>3</sup>
S-18360	30-May-15	30	180	8	260	2.080	53.42344	NG/ F	NG
S-18357	2-Jun-15	30	201	8	260	2.080	53.62550	NG/ F	NG
S-18371	10-Jun-15	30	180 (2) – 270 (6)	8	260	2.080	53.40846	NG/ F	NG
S-18364	22-Jun-15	30	201	8	260	2.080	53.42183	NG/ F	NG
S-18358	23-Jun-15	34	130	8	260	2.080	53.62808	NG/ F	NG
N-18374	20-Aug-15	27	152	45	327	14.715	53.41930	ASHP	EHP
N-18361	26-Nov-15	10	165	39	345	13.455	53.51288	ASHP	EHP
S-18367	23-Apr-16	27 (18) – 30 (7)	180 (18) – 270 (7)	26	260	6.760	53.47755	NG/ F	NG
N-18365	17-Jun-16	23	180	51	280	14.280	53.52306	ASHP	EHP

<sup>1</sup>NG/F: natural gas / furnace; <sup>2</sup>ASHP: electric air source heat pump; <sup>3</sup>EHP: electric heat pump.

Figure 4-5a through Figure 4-5e summarise the monthly load, generation, exported energy, imported energy, and solar energy used on site (self-consumed) for the 11 monitored sites, respectively, while Figure 4-5f presents the percentage of the annual

self-consumption of the solar PV systems together with corresponding house type. Here, the green-coloured lines represent the four NZEHs (ID numbers in the legend starting with “N”), while the orange-coloured lines represent the seven EEHs (ID numbers in the legend starting with “S”).

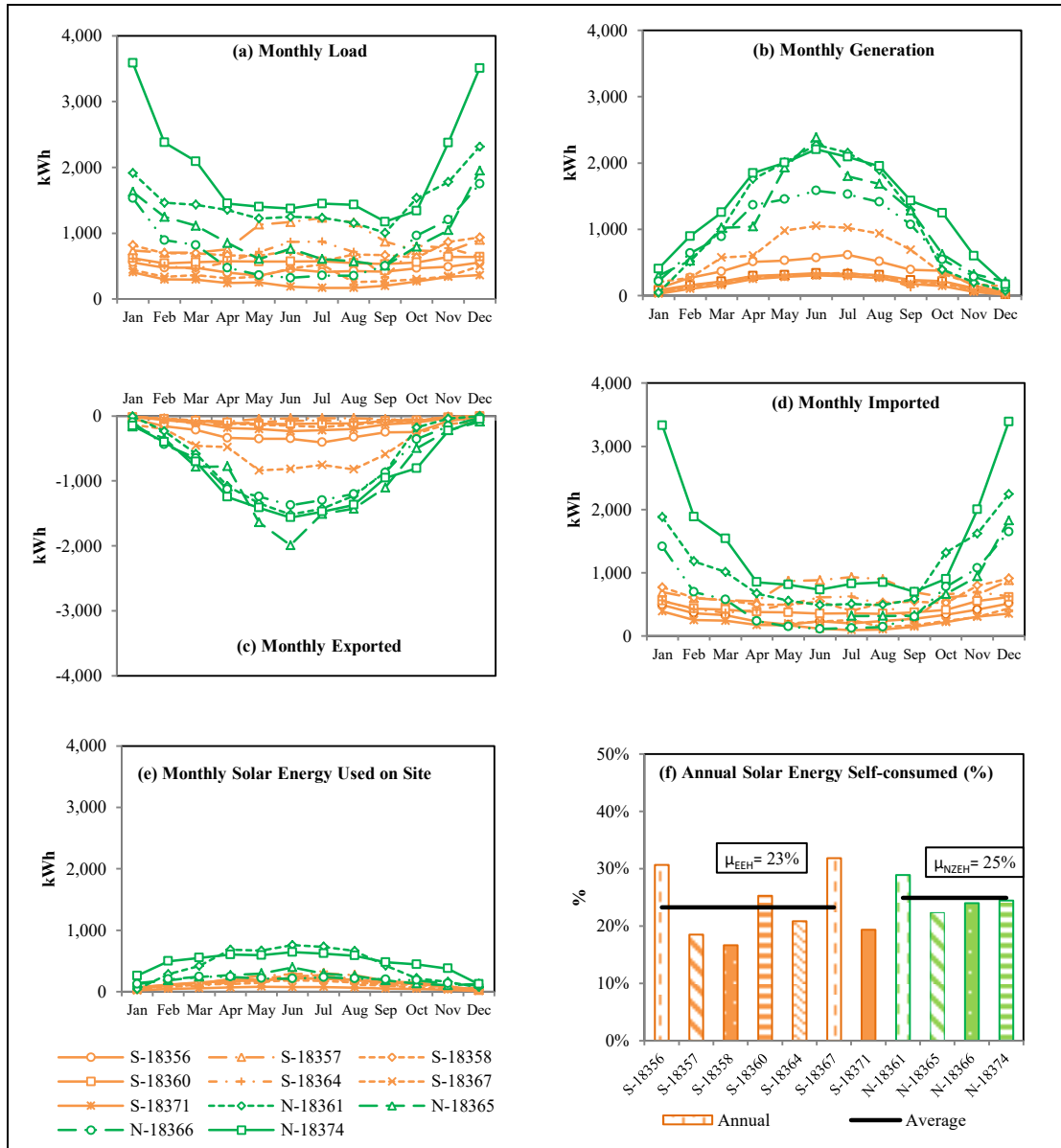


Figure 4-5. Summary of energy-component profiles of all 11 houses demonstrating the monthly (a) loads, (b) generation, (c) exported energy, (d) imported energy, and (e) solar energy used on site, while (f) represents the annual percentage of solar energy used on site in each house.

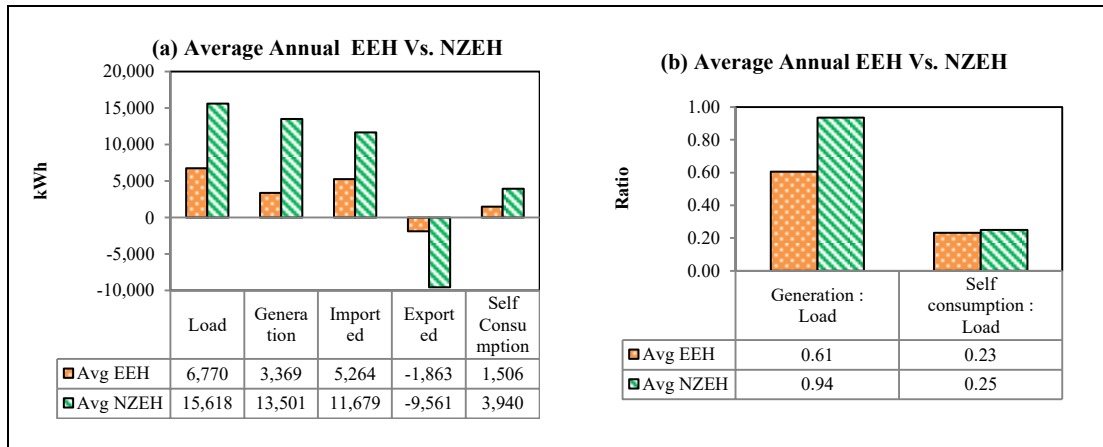


Figure 4-6. Pairwise comparison between the average annual energy performance of EEHs and NZEHs.

It can be observed in Figure 4-5a that NZEHs, due to being independent of the natural gas grid, consume significantly larger amounts of energy during colder months than do EEHs, particularly energy consumed for electricity-based space heating and DHW heating when the outdoor temperature falls below  $-15^{\circ}\text{C}$ . In this regard, relatively large solar PV systems are installed in the NZEHs to compensate for the inflated grid electricity demand. However, although these systems generate significantly larger amounts of electricity annually, they fail to match the real-time on-site energy demand, resulting in a PV mismatch in winter and PV penetration in summer as indicated in Figure 4-5b, Figure 4-5c, and Figure 4-5d. Although the sizing of a PV system should be designed to compensate for the household energy demand annually, it is demonstrated in Figure 4-5e and Figure 4-5f that, regardless of whether the PV system installed is over-, under-, or equally-sized, the results are an average of 23% and 25% of self-consumption for EEHs and NZEHs, respectively. This phenomenon points to the fact that most energy-consuming indoor household activities occur in the early morning or late afternoon hours when the sun is positioned at either the east or the west, respectively. In addition to the daily mismatch, due to the seasonal fluctuations in outdoor climatic conditions and daylight hours, the seasonal mismatch is considered as a critical environmental and economic issue in microgeneration practice, not to mention the expected challenges related to grid stability. Another

phenomenon to consider in regard to the PV self-consumption is the absence of solar power during night-time, especially in winter. However, PV designers tend to prefer south-facing solar PV installations that maximise the annual, or even daily, energy output rather than maximising the on-site PV utilisation.

It is also found that, on average, the annual household energy demand of an NZEH is 2.3 times that of an EEH, and, although the PV systems installed on NZEHs are 4 times the size of those installed on EEHs, the amounts of imported and exported energy of an average NZEH are found to be 2.2 and 5 times those of an average EEH, as presented in Figure 4-6a. Hence, existing NZEH technologies, specifically in cold climates, ought to be considered for re-evaluation and improvement. Nevertheless, it is worth mentioning the environmental benefits of NZEHs. Returning back to the original definition of NZEHs—homes that generate as much energy as they consume annually—on average the net-zero balance of the NZEHs and of the EEHs under investigation are found to be 94% and 61%, respectively, despite the fact that the self-consumption rates of those systems are 25% and 23%, respectively, as demonstrated in Figure 4-6b. Despite the proven environmental value of solar microgeneration practices due to reduced greenhouse gas emissions, though, the absence of affordable local storage systems in some jurisdictions and the ineffective application of Renewable Energy Credits (RECs) serve to diminish the economic viability of such systems.

#### **4.6. Case Studies**

As a case study the in-depth performance of two selected homes is investigated: an EEH (referred to as S-18356 in Table 4-1) and an NZEH (referred to as N-18366 in Table 4-1). Here, Eq. 4-1 to Eq. 4-9 are applied to assess the LMGI indicators. It is expected that, as the name implies, NZEHs should achieve net-zero balance on a yearly basis. As for EEHs, decisions made by home owners in regard to solar PV system sizing are dependent on their personal budgets, so the PV sizing is not necessarily dictated by the goal of achieving a net-zero balance. However, this study

aims to quantify the net-zero balance and LMGI of all monitored homes in order to improve future solar PV system design and installation for both EEHs and NZEHs while avoiding PV under- or over-sizing, an outcome which will benefit both the utility grid and system end users. Finally, methods of improvement by which to optimise utilisation of those systems are suggested based on household load patterns, such that the knowledge gained from this study can be considered in future community development as well as in individual installations, resulting in both environmental and economic benefits.

#### 4.6.1. *Energy-efficient Single-family Home (EEH) in Edmonton, Alberta*

This section discusses the application of the proposed optimisation framework to an existing energy-efficient single-family home (namely S-18356 in Table 4-1) in Edmonton, Alberta, under occupancy conditions. The house is located at 53.63° N latitude and 113.56° W longitude. Edmonton's climate is relatively cold, with an average temperature of -13.9 °C in January and 17.4 °C in July, an average monthly snowfall from October to April ranging from 6 cm to 26 cm, and average monthly rainfall from April to September ranging from 24 mm to 88 mm (Government of Canada, 2017). The house was built in 2014, whereas the solar PV system was installed in May 2015, at which point the house was set up for long-term monitoring and investigation. Data such as energy generation, household overall energy consumption, major appliance use, and grid interaction is monitored at a temporal resolution of one minute and collected via eGauge (eGauge Systems, 2017) data management system. The house is equipped with a grid-connected fixed monocrystalline silicon JA Solar (JAM 6(BK) 60-260/SI) PV system. The system consists of 14 panels (as illustrated in Figure 7) with nominal power capacity of 260 Wp and module efficiency of 15.90%. For interested readers, additional information on the panel specifications is available from JA Solar (JA Solar, 2015). The PV system is installed at a tilt angle of 26.5° (6:12)—a common slope in roofing practice in North America—and azimuth angle of 182° (i.e., near true south). The selection of the PV system's tilt angle traditionally conforms to the common roofing slope

practice in North America, which varies between 4:12 (14°) and 9:12 (37°), regardless of the performance of the installed PV system.

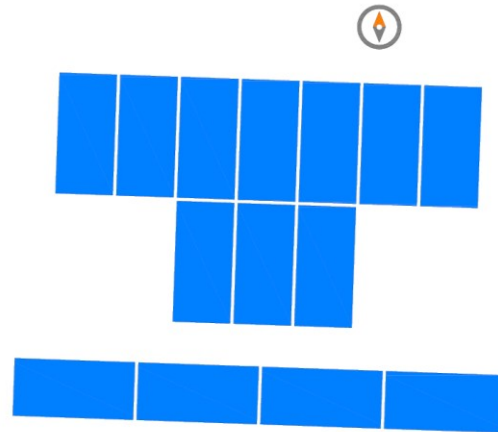


Figure 4-7. Schematic representation of the solar PV arrays placement of the EEH.

Table 4-2 summarises the profile of the EEH, including information on the solar PV system, MEP, and construction details. Figure 4-8a presents the maximum power output of the monitored PV system within the period of June 2015 to May 2017. Most of the generated energy is exported to the utility grid at a very low energy credit, resulting in an uneconomical situation for the end user. It is worth mentioning that due to the extremely cold weather in winter and mild weather in summer in this region, the energy and power demand peak in winter due to the extended hours of indoor activities and increased lighting consumption. Meanwhile, the use of air conditioners in summer is relatively uncommon in this region. The high-latitude location adds another dimension of impact on the residential energy profile. The variance of daylight hours and the sun's altitude, which ranges from 7.2 hr and 13.0° at winter solstice to 16.8 hr and 59.9° at summer solstice (Awad et al., 2016), has a direct impact on the end user's behaviour (e.g., lighting, number of hours spent indoors, etc.). Figure 4-8b represents the peak household power demand of the monitored house, while Figure 4-8c shows the daily average year-long energy profile of the monitored house. A large portion of the electricity generated by the solar PV system, peaking at 69%, is mismatched against the household energy loads and

exported to the utility grid, while only 31% of the generated electricity (representing 25% of the annual energy demand) is utilised on site, as demonstrated in the cumulative chart in Figure 4-8d.

Table 4-2. Profile of sample single-family EEH.

General Building Information	
Building type	Two-story single family house
Garage type	Detached
Roof orientation	Near-south (182°)
House volume	517.1 m <sup>3</sup>
Year completed	2014
Certification	Gold
Annual heating degree-days	5589
Latitude	53.63° N
Air tightness	0.79 ACH50
Energy monitoring system	eGauge
MEP Systems	
Space heating and cooling	Natural gas / Furnace
Heating distribution	Forced air ductwork, with ECM fan motor
Ventilation	HRV
Water heating	Natural gas / Instant
Solar PV Information	
Tilt angle	26.5° (0° horizontal – 90° vertical)
Orientation	182 ° (0° N – 180° S)
Number of panels (module capacity)	14 (260 Wp)
Array size	3.64 kWp

It is crucial for utility providers to also understand the household peak power demand patterns and the variations that occur due to seasonal and day type (i.e., weekday, weekend, holiday) changes. Unlike NZEHs, EEHs rely on natural gas as the energy source for space heating and DHW heating, so the majority of the energy consumed by EEHs is user-dependent—with the exception of the ventilation system and refrigerator, which are continuously operated independently regardless of the user’s behaviour. However, the climatic conditions and day type can have a significant impact on the user’s behaviour and activities. For example, on long weekends and holidays, end users tend to consume less power than normal. On weekdays, the power consumption peaks in the early morning and late afternoon hours.

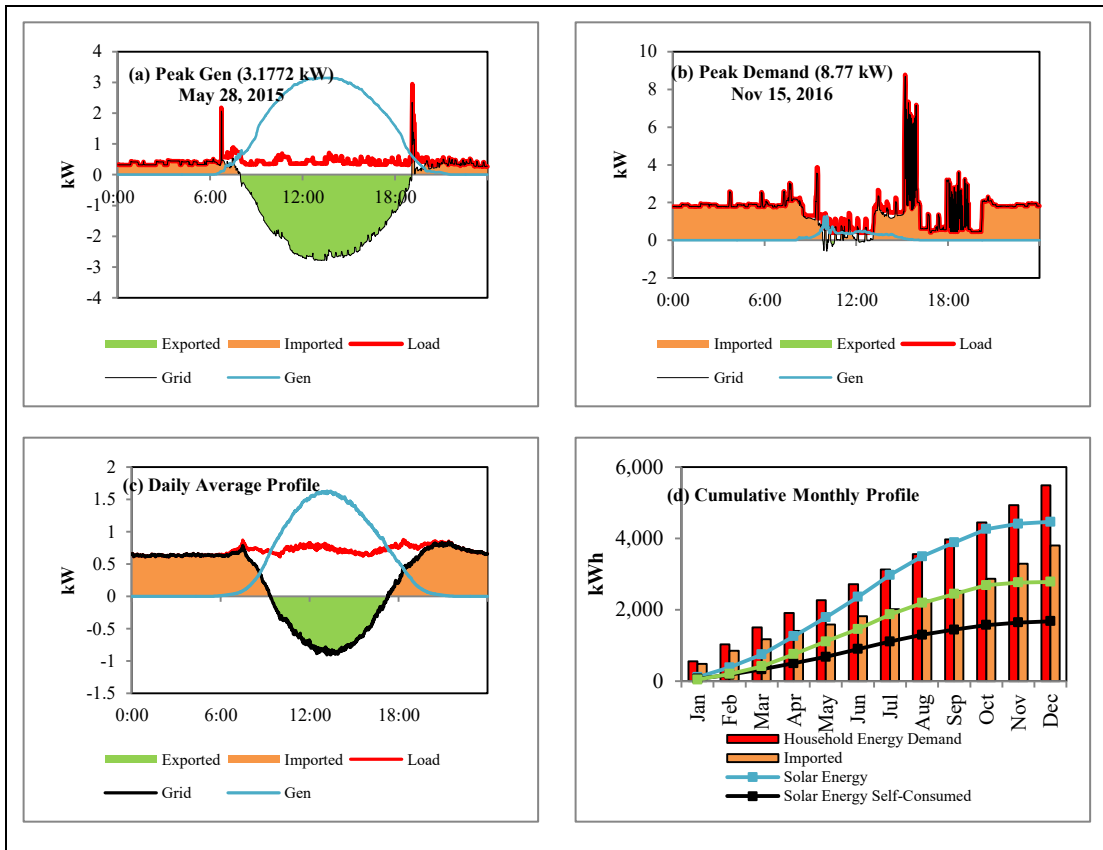


Figure 4-8. (a) Daily power profile on maximum PV power output, (b) daily power profile on peak load demand, (c) daily average year-long power profile, and (d) cumulative monthly breakdown of the household energy demand, imported energy from the grid, on-site self-consumed solar energy, generated energy, and the surplus energy exported to the utility grid.

In addition to the day type power demand patterns, it is observed that the power demand during winter and shoulder seasons (i.e., spring and fall) is significantly higher than that during the summer. Figure 4-9 demonstrates the peak power demand during the week days, weekends, and holidays in summer (Figure 4-9a), winter (Figure 4-9b), spring (Figure 4-9c), and fall (Figure 4-9d).

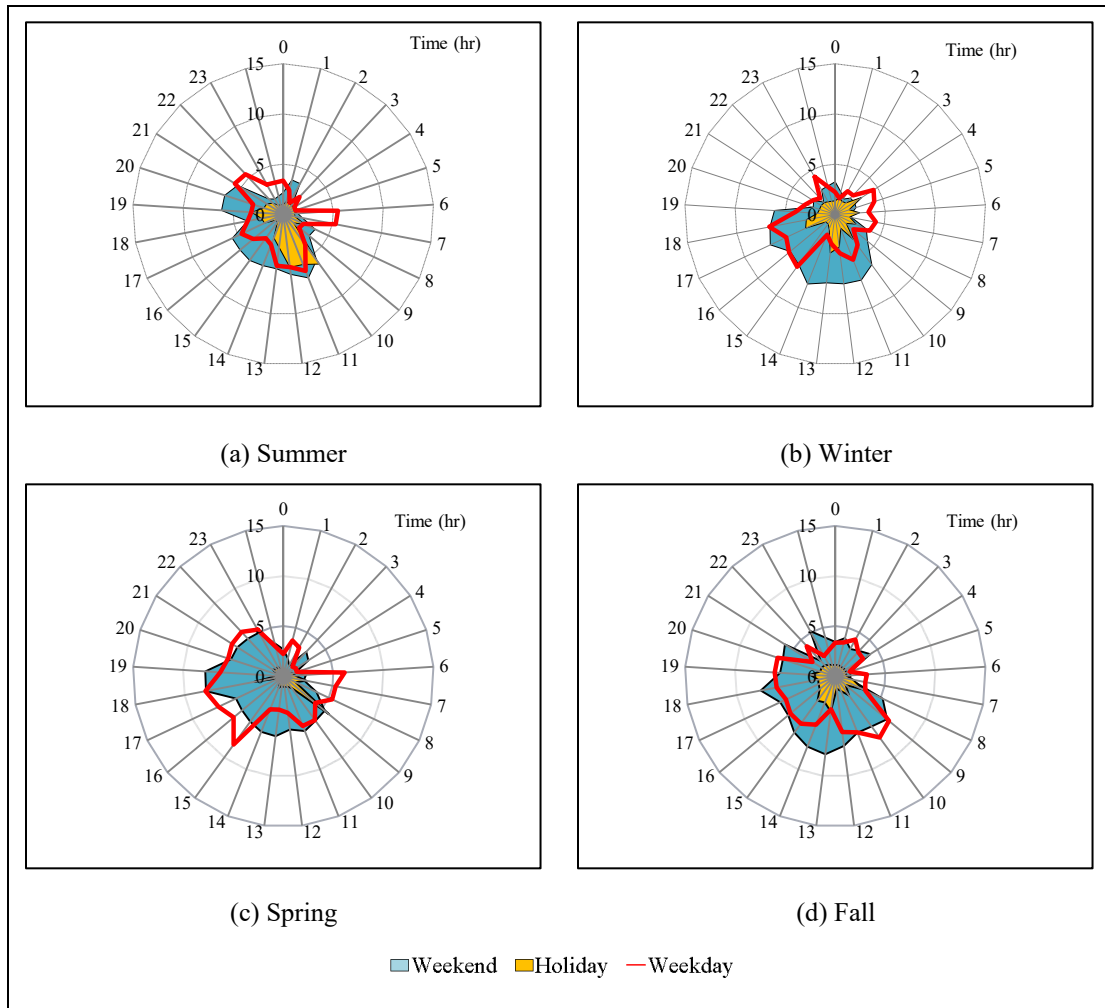


Figure 4-9. Peak daily load profile (kW) in (a) summer, (b) winter, (c) spring, and (d) fall.

It should be noted that Edmonton is located at a northerly latitude and its climate is considered severely cold in the winter and mild in the summer. In other jurisdictions with moderate-to-hot climate, these power demand patterns will differ primarily due to the use of air conditioners in summer.

#### 4.6.2. Net-zero Energy Single-family Home (NZEH) in Edmonton, Alberta

This section discusses the application of the proposed optimisation framework to an existing net-zero energy single-family home (namely N-18366 in Table 4-1) in Edmonton, Alberta, under occupancy conditions. The house is located at 53.51° N

latitude and 113.52° W longitude. The house was built in 2012, while the solar PV system was installed in May 2015, at which point the house was set up for long-term monitoring and investigation. The experimental set-up of this house is identical to that of the above-described EEH. The house is equipped with a grid-connected fixed monocrystalline silicon Heliene (Heliene 60 M 280p) PV system. The system consists of 39 panels (as illustrated in Figure 10) with nominal power capacity of 280 W<sub>p</sub> and module efficiency of 18.90%. For interested readers, additional information on the panel specifications is available from Heliene (Heliene Inc., 2017). Table 4-3 presents a summary of the profile of the NZEH, including information on the solar PV system, MEP, and construction details. Figure 4-11a presents the maximum power output of the monitored PV system within the period of June 2015 to May 2017. Although the sky condition shows partial clouds on the studied day, it can be observed that the PV system reaches its peak power output at 9.622 kW, given that the system's nominal size is 10.92 kW<sub>p</sub>. A situation in which an entire community consisting of 10 NZEHs is generating this amount of power at congruent times and patterns would pose a potential threat of damage or malfunction to the traditionally built utility grid. As previously highlighted, the primary difference between an EEH and an NZEH lies in the mechanical system's energy carrier. NZEHs use electrical air-source heat pumps for space heating and DHW heating, while EEHs use furnaces for space heating and water tanks for DHW heating, both appliances being powered by natural gas. In the present NZEH case, it can be clearly seen that there is a high fluctuation between the summer and winter supply and demand profiles. In Figure 4-11b, the peak power demand is used to identify the worst-case scenario of a high-demand profile. On the other hand, as noted above, in this region the use of air conditioners in summer is relatively uncommon, even in NZEHs. In addition to the impact of the user's behaviour on the household energy consumption (also known as user-dependent activities, as referred to by Li et al. (2016)), user-independent activities can be assessed as the key drivers of energy consumption profiles in NZEHs (Li et al., 2016). Examples of these activities are space heating and DHW heating. These two appliances account for high power demand especially when the outdoor temperature

falls below  $-15\text{ }^{\circ}\text{C}$ , independent of the user’s behaviour. Furthermore, these appliances cause significantly higher fluctuations to the net grid pattern due to their cyclic nature.

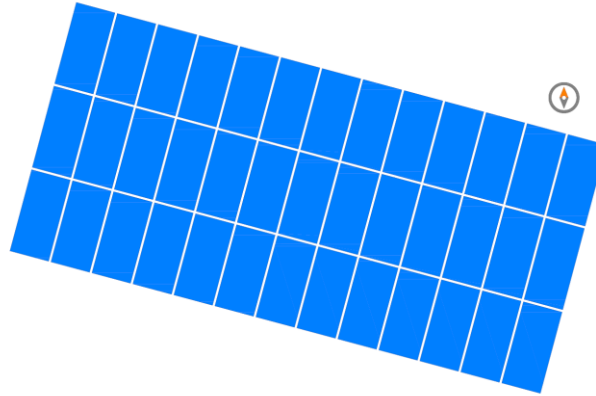


Figure 4-10. Schematic representation of the solar PV arrays placement of the NZEH.

Table 4-3. Profile of sample single-family NZEH.

General Building Information	
Building type	Two-story single family house
Garage type	Detached
Roof orientation	Near-south ( $195^{\circ}$ )
House volume	$762.1\text{ m}^3$
Year completed	2012
Certification	R-2000
Annual heating degree-days	5,589
Latitude	$53.51^{\circ}\text{ N}$
Air tightness	0.43 ACH50
Energy monitoring system	eGauge
MEP Systems	
Space heating and cooling	Air source heat pump: Cold climate ASHP 7.83 HSPF
Heating distribution	Forced air ductwork, with ECM fan motor
Ventilation	HRV
Water heating	Heat pump DHW tank $-3.27\text{ EF}$
Solar PV Information	
Tilt angle	$26.5^{\circ}$ ( $0^{\circ}$ horizontal – $90^{\circ}$ vertical)
Orientation	$195^{\circ}$ ( $0^{\circ}\text{ N} - 180^{\circ}\text{ S}$ )
Number of panels (module capacity)	39 ( $280\text{ W}_p$ )
Array size	$10.92\text{ kW}_p$

Figure 4-11b represents the peak household power demand of the monitored house. By comparing the peak power demand of the EEH and the NZEH shown in Figure 4-8b and Figure 4-11b, respectively, it can be seen that the NZEH exhibits much

higher grid fluctuations in winter than does the EEH. Figure 4-11c presents the daily average year-long energy profile of the monitored NZEH. A large portion of the generated electricity by the solar PV system, peaking at 80%, is mismatched against the household energy loads and exported to the utility grid, while only 20% of the electricity generated (representing 24% of the annual energy demand) is utilised on site, as demonstrated in the cumulative chart in Figure 4-11d.

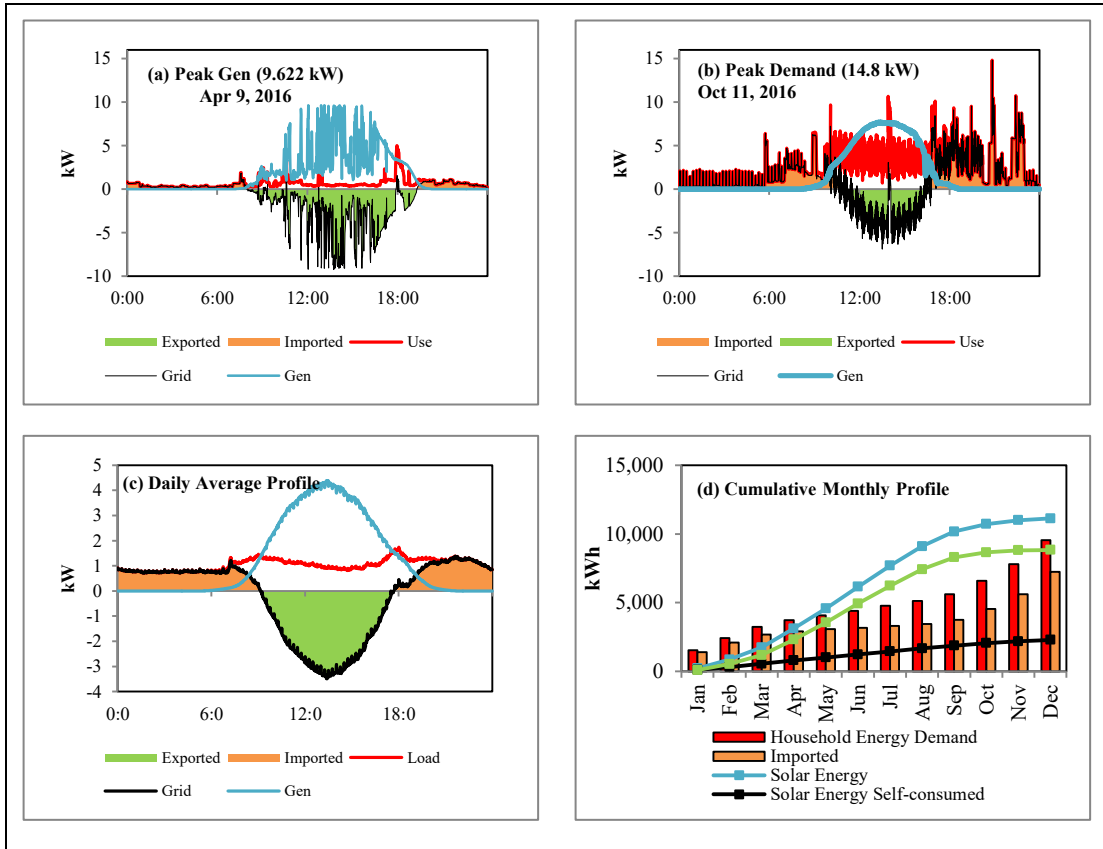


Figure 4-11. (a) Daily power profile on maximum PV power output, (b) daily power profile on peak load demand, (c) daily average year-long power profile, and (d) cumulative monthly breakdown of household energy demand, imported energy from grid, on-site self-consumed solar energy, generated energy, and surplus energy exported to utility grid.

As previously discussed, the household power demand in EEHs is user-driven, such that higher power demand is observed during the early mornings and late afternoons,

when end users are active in their use of high-consuming appliances such as wet appliances, cooking-related appliances, and lighting. These appliances are schedule-based appliances, meaning that their use tends to be dependent on the end user's specific schedule, and may vary from one household to another. NZEHs add another dimension to household consumption patterns in that their mechanical systems are weather-dependent.

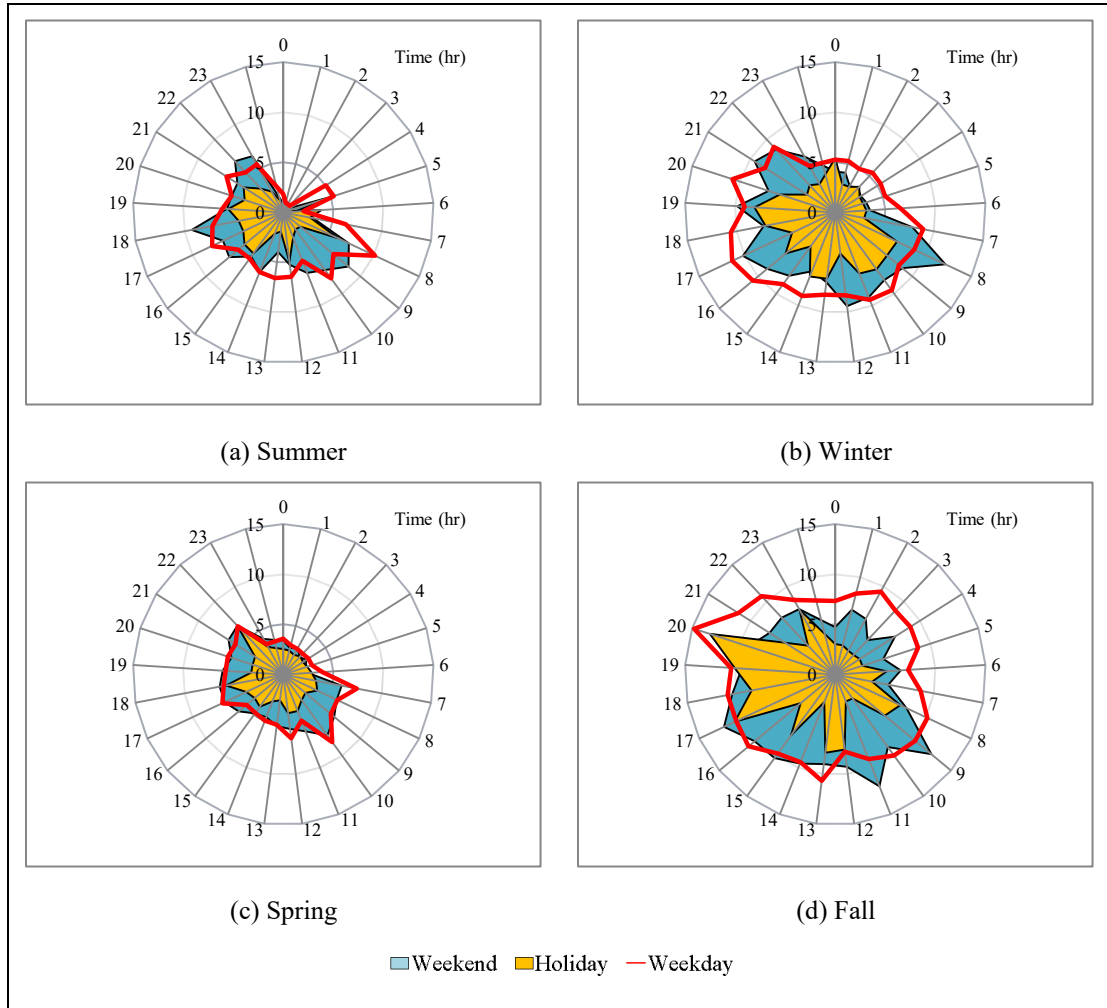


Figure 4-12. Peak load profile (kW) in (a) summer, (b) winter, (c) spring, and (d) fall.

This can be clearly seen in Figure 4-12. During the summer (Figure 4-12a) and spring (Figure 4-12c), the household power demand is dominated by the user-dependent consumption patterns; however, on colder days in the winter (Figure 4-12b) and fall

(Figure 4-12d), the household consumption significantly increases so that the power demand is increased throughout the 24-hour day, reaching approximately 15 kW.

## **4.7. Results and Framework Validation**

### *4.7.1. Results*

GRG nonlinear optimisation is applied in order to identify the optimal layout placement and sizing satisfying the proposed optimisation criteria. The base case from each of the investigated sites is considered as the “current practice” against which the optimised solutions will be compared. The current practice represents tilt and azimuth angles of  $26.5^\circ$  and  $182^\circ$ , respectively, with a system capacity of 3.64 kW<sub>p</sub> for the EEH, and tilt and azimuth angles of  $26.5^\circ$  and  $195^\circ$ , respectively, with capacity of 10.92 kW<sub>p</sub> for the NZEH. The optimal solutions are determined based on the four criteria presented in Figure 4-3; however, since no regulatory constraints have been introduced in Alberta as of the time of writing, the third iteration did not affect the results. This iteration can be implemented in future applications or in other jurisdictions.

For example, in Alberta, Renewable Energy Credits (RECs) have not yet been officially implemented as of the time of writing, and this market condition detracts from the economic feasibility of solar PV microgeneration practice. In such a scenario, end users endeavor to maximise the on-site solar PV utilisation in order to avoid large electricity bills. Table 4 4 and Table 4 5 summarise the load-match (LM) indicators in both the base case and optimised scenarios of the EEH and NZEH, respectively, where the LM and GI indicators are calculated using Eq. 4-1 to Eq. 4-9. Here, an assumption of a fixed electricity rate of 9.05 ¢/kWh and an REC of 3.9 ¢/kWh are made and applied.

Table 4-4. Summary of optimal array layouts concluded for the EEH.

Iteration	Current State		Step-wise Solutions			Final Solution	Implied Changes
	W/out Solar	Current Practice	It.#1 Layout Design	It.#2 Net-zero Balance	It.#3&4 Regulations & Cost-effectiveness		
State						Suggested Solution	Current Practice vs. Proposed Solution
Index		$S_0$	$S_1$	$S_2$	$S_{3,4}$	$S_f$	$(S_f - S_0) / S_0$
System Size (kW <sub>p</sub> )	-	3.64	3.64	4.94	4.94	4.94	35.7%
Number of Panels	-	14	14	19	19	19	35.7%
Module Nameplate Capacity (W <sub>p</sub> )	-	260	260	260	260	260	-
Tilt Angle (°)	-	26.5	38.9	38.9	38.9	38.9	-
Azimuth Angle (°)	-	182	189.8	189.8	189.8	189.8	-
Yearly Exported (kWh)	0	2,721	3,195	4,760	4,760	4,760	74.9%
Yearly Delivered (kWh)	6,347	4,767	4,721	4,564	4,564	4,564	-4.3%
Delivered/Exported Balance (kWh)	-6,347	-2,046	-1,526	196	196	196	-109.6%
Est. Clear-sky Generation (kWh)	0	8,970	9,869	13,394	13,394	13,394	49.3%
Yearly Generation (kWh)	0	4,301	4,822	6,544	6,544	6,544	52.2%
Yearly Loads (kWh)	6,347.0	6,347	6,347	6,347	6,347	6,347	0.0%
Load/Generation Balance (kWh)	-6,347	-2,046	-1,526	196	196	196	-109.6%
On-site Solar Energy Use (kWh)	0	1,580	1,627	1,784	1,784	1,784	12.9%
Minutely LM	0	33.2%	33.5%	35.5%	35.5%	35.5%	6.9%
Minutely LM (Night Values Removed)	0	65.8%	66.3%	70.3%	70.3%	70.3%	6.8%
Monthly LM	0	66.9%	69.8%	75.3%	75.3%	75.3%	12.6%
Yearly LM	0	67.8%	76.0%	100.0%	100.0%	100.0%	47.5%
Minutely GI	0	13.0%	14.0%	17.5%	17.5%	17.5%	34.6%
Yearly GI	0	57.0%	67.7%	100.0%	100.0%	100.0%	75.4%
Imported Grid Electricity (\$/year)	\$574	\$431	\$427	\$413	\$413	\$413	-4.3%
Export Revenue (\$/year)	\$0	\$106	\$125	\$186	\$186	\$186	74.9%
Balance (\$/year)	\$574	\$325	\$303	\$227	\$227	\$227	-30.1%
Balance Inc. Admin. Fees (%/year)	\$869	\$620	\$598	\$522	\$522	\$522	-15.8%

Table 4-5. Summary of optimal array layouts concluded for the NZEH.

Iteration	Current State		Step-wise Solutions			Final Solution	Implied Changes
			It.#1	It.#2	It.#3&4		
State	W/out Solar	Current Practice	Layout Design	Net-zero Balance	Regulations & Cost-effectiveness	Suggested Solution	Current Practice vs. Proposed Solution
Index	S <sub>0</sub>		S <sub>1</sub>	S <sub>2</sub>	S <sub>3,4</sub>	S <sub>f</sub>	(S <sub>f</sub> - S <sub>0</sub> ) / S <sub>0</sub>
System Size (kW <sub>p</sub> )	-	10.92	10.92	8.68	8.68	8.68	-20.5%
Number of Panels	-	39	39	31	31	31	-20.5%
Module Nameplate Capacity (W <sub>p</sub> )	-	280	280	280	280	280	-
Tilt Angle (°)	-	26.5	58.5	58.5	58.5	58.5	-
Azimuth Angle (°)	-	195.0	189.7	189.7	189.7	189.7	-
Yearly Exported (kWh)	0	8,852	9,665	7,477	7,477	7,477	-15.5%
Yearly Delivered (kWh)	9,594	7,327	7,254	7,403	7,403	7,403	1.0%
Delivered/Exported Balance (kWh)	-9,594	1,525	2,411	74	74	74	-95.1%
Est. Clear-sky Generation (kWh)	0	26,605	30,408	24,414	24,414	24,414	-8.2%
Yearly Generation (kWh)	0	11,119	12,007	9,671	9,671	9,671	-13.0%
Yearly Loads (kWh)	9,594	9,594	9,596	9,596	9,596	9,596	0.0%
Load/Generation Balance (kWh)	-9,594	1,525	2,411	74	74	74	-95.1%
On-site Solar Energy Use (kWh)	0	2,267	2,342	2,194	2,194	2,194	-3.2%
Minutely LM	0	36.3%	36.2%	34.8%	34.8%	34.8%	-4.2%
Minutely LM (Night Values Removed)	0	65.6%	65.3%	62.8%	62.8%	62.8%	-4.2%
Monthly LM	0	72.7%	77.8%	74.0%	74.0%	74.0%	1.8%
Yearly LM	0	100.0%	100.0%	100.0%	100.0%	100.0%	0.0%
Minutely GI	0	18.4%	19.8%	16.9%	16.9%	16.9%	-8.3%
Yearly GI	0	100.0%	100.0%	100.0%	100.0%	100.0%	0.0%
Imported Grid Electricity (\$/year)	\$868	\$868	\$868	\$868	\$868	\$868	0.0%
Export Revenue (\$/year)	\$0	\$345	\$377	\$292	\$292	\$292	-15.5%
Balance (\$/year)	\$868	\$523	\$492	\$577	\$577	\$577	10.3%
Balance Inc. Admin. Fees	\$1,163	\$818	\$787	\$872	\$872	\$872	6.6%

Administrative and grid-operation fees are also assumed to be at a flat rate of \$5.67/month and \$18.92/month, respectively, based on the local energy retailer fees; however, the initial cost of the solar PV system was not included in the net balance calculations. Although in the case of EEHs natural gas is used as an energy source for heating, the gas rates are not included in the calculations. Even though the cost of solar PV systems has dropped significantly within the last decade, the initial cost for residential solar PV installations is considered relatively high in terms of electricity rates and thus payback period, especially in the absence of effective incentive programs. It is observed that the payback period within the locality and current market conditions of the present study varies between 40 years and 44 years for EEHs and between 87 years to 95 years for NZEHs.

The layout placement solutions provided in the first iteration for both cases (EEH and NZEH) are indicative of the nature of the household energy demand for the given house type. For example, NZEHs consume significantly larger amounts of electricity, and, in addition, the high electricity demand is clustered in the winter months to meet mechanical system demand. Because the winter sun's altitude is relatively low in Edmonton, a higher-than-typical tilt angle is proposed by the optimisation framework—approximately  $60^\circ$  (about  $7^\circ$  higher than the local latitude). An EEH, as mentioned earlier, consumes natural gas for space heating and DHW heating, but has an energy-efficient building envelope. It is thus easier to achieve net-zero balance for this type of home than for an NZEH, provided that the PV system is sized properly. This explains the layout solution identified by the optimisation framework, which proposes a tilt angle of approximately  $40^\circ$  (about  $13^\circ$  lower than the local latitude). In both cases—EEH and NZEH—the azimuth angle is found to be approximately  $190^\circ$ , a value that is considerably close to the conclusions made by Litjens et al. (2017) where the preferred azimuth angle for residential buildings was deemed to be  $212^\circ$ . The reasoning behind this given solution is that the energy loads peak in the late afternoon hours (especially on weekdays), as demonstrated in Figure 4-9 and Figure

4-12. In case of implementing the proposed high-mount tilt angle (i.e.,  $60^\circ$ ), several practical aspects such as the structural health, building aesthetics, thermal performance, and cost should be considered in such context. The high-mount tilt angle practice could also be implemented by installing the solar PV system on top of flat rooftop modern homes, on walls, or by implementing community shared solar programs within communities where a large ground-mount solar PV system is installed and distributed among the community homes. The latter solution can provide a large degree of freedom with respect to layout placement and sizing, as discussed in the following chapter.

While the second iteration seeks to determine the PV sizing that satisfies the household net-zero balance, it is found that, in order for an EEH to achieve its net-zero balance, a  $4.94 \text{ kW}_p$  system is required (i.e., upgrading the existing system by  $1.3 \text{ kW}_p$ ), while, in order for an NZEH to achieve its balance, an  $8.68 \text{ kW}_p$  system is required (i.e., downgrading the existing system by  $2.24 \text{ kW}_p$ ), while still satisfying both regulatory and economic criteria.

As presented in Table 4 4, for the EEH, optimising the PV system's layout placement by raising its tilt angle by  $12.4^\circ$  and upgrading its size by 35.7% improves the annual LM by 47.5% and the annual GI by 75.4%, while the annual electricity bill is reduced by 15.8% and net-zero balance is achieved. The improvement of the LM indicators reflects the increased self-consumption and cohesively improved system economics. In other words, the LM improvement indicates a lesser generated electricity export and also a lesser grid electricity import. On the other side, the improvement of the GI indicators reflects the match between the demand and generation, or, in other words, the net-zero balance. In agreement with Salom et al. (2014), the net-zero balance achievement at lower temporal resolutions (i.e., monthly or yearly) is considerably easier than that of higher temporal resolutions, specifically in the absence of local storage systems. Due to the change in layout in the first iteration (from  $S_0$  to  $S_1$ ) while maintaining the system size unchanged, the system's energy generation has increased from 4,301 kWh to 4,822 kWh (+ 12.1%). In the second iteration (from  $S_1$  to  $S_2$ ), the system size was increased by 35.7% pursuant for net-zero balance, while maintaining

the layout unchanged, the yearly energy generation has increased by +35.7%. Overall, the total improvement in the yearly generation between the base case scenario and the final solution is found to be +52.2%. In the NZEH case presented in Table 4 5, the existing system is in fact over-sized to the point of being uneconomical. In such a case, the optimisation framework proposes to down-size the PV system in order to achieve its net-zero energy goals while still satisfying the given economic requirements. Here, the system's tilt angle is raised by 32° and its capacity is downsized by 20.5%, while the net-zero balance can still be achieved, and typically the annual LM and GI can be satisfied. On the other hand, the annual electricity bill is increased by 6.6% due to the lower export revenue than had been previously obtained from the over-sized system. The increase in the monthly LM is due mainly to the change in tilt angle. Since NZEHs rely on electricity as a sole source of energy, including space heating and DHW heating, and due to the severe weather conditions in Edmonton particularly in winter months, the employment of a high-mount PV system (i.e., 58.9° in this case) incurs significant improvement in the aggregated load match. This can be clearly seen in iteration#1 where the monthly LM was improved from 72.7% to 77.8% by only changing the layout. However, by reducing the system size, the monthly LM was decreased from 77.8% to 74.0%. On the other side, the reflection of the improvement in monthly LM cannot be seen in the minutely LM in coherence because (1) the monthly LM is obtained after the monthly aggregation, which makes it less accurate, but more informative on the high level (2) the minutely LM reflects the day-night mismatch between the demand and generation. This explains why the minutely LM was reduced by 8.3% while the monthly LM was increased by 1.8%.

Furthermore, in order to demonstrate the sensitivity of the load-match, grid-interaction, and on-site solar energy self-consumption against the PV system sizing, a “what-if?” scenario-based analysis is performed. At this point, it can be assumed that the layout placement is fixed at the optimum solution obtained from the first iteration (i.e., maximised LM criterion). It should also be noted that the household energy loads, against which the aim is to balance, are based on the real-time local data of the

two homes under investigation in Edmonton. For more robust findings, this work will expand in future studies to include more diverse locations and demand patterns. Figure 4-13 illustrates the impact on various aspects of the system's performance of changing the system size for (a) EEHs and (b) NZEHs. In the interest of brevity, only critical aspects such as the load match, grid interaction, and on-site solar PV utilisation as a percentage of loads and as a percentage of overall generated energy, are presented in this chapter. It is observed that for both the EEH and the NZEH most of the improvement in the LM, GI, and self-consumption is achieved at or before the net-zero balance point. A lesser degree of improvement is observed beyond this point. It is also found that the economic value of the PV system is deemed to be significantly higher on the under-sized side of the plot due to the maximised self-consumption and reasonable LMGI, while the system under-achieves in terms of environmental value due to its inability to compensate for its yearly household energy demand. On the other hand, the over-sizing of the PV system results in the environmental goals being far exceeded; however, the economical aspect and the ability of the grid to interact efficiently become unfeasible in this case, considering that the existing utility grid in Edmonton was designed and built decades ago in a traditional manner.

In accordance to the optimisation results discussed earlier, in regards to the optimum system size for the EEH and NZEH, it is observed that the net-zero balance of the NZEH is achieved at the 8.68 kW<sub>p</sub> mark while the EEH required a 4.94 kW<sub>p</sub> system. This significant difference in system size is due mainly to the high electricity demand in NZEHs, as they run off the natural gas grid, unlike EEHs, which are less challenged in achieving the net-zero balance of electricity loads, excluding space heating and DHW heating, which run on natural gas.

One other significant difference in the optimal layout of NZEHs and EEHs is that the electricity demand in NZEHs is weather-dependent in addition to its user-dependency, and thus peaks during severe winter months due to heating demand while air conditioning in summer is less common.

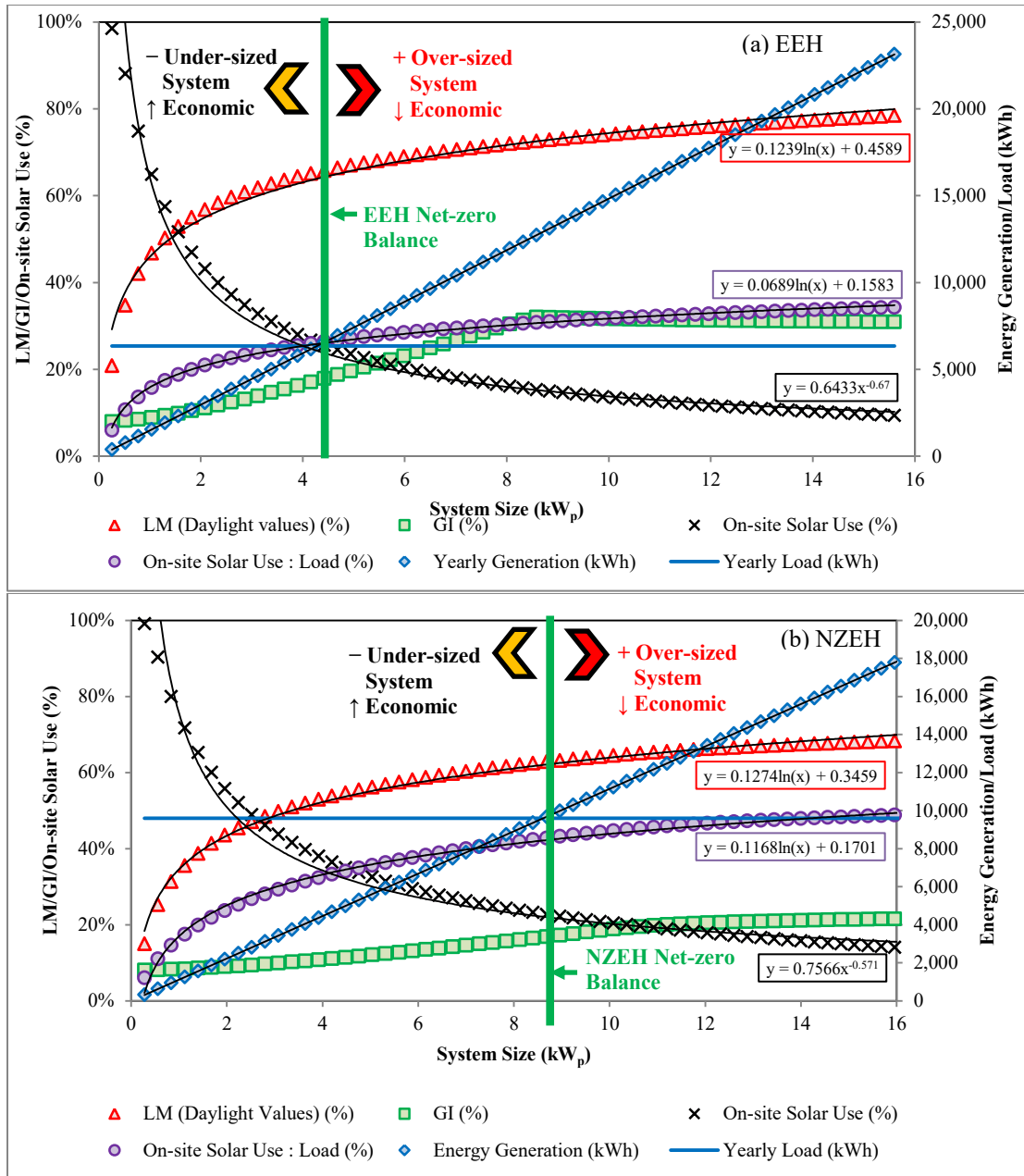


Figure 4-13. Sensitivity analysis demonstrating the impact of system size on (a) EEH and (b) NZEH in terms of LM, GI, yearly generation, and on-site solar use (as a percentage of yearly generation and as a percentage of yearly loads).

Consequently, a higher tilt angle and larger system is found optimal for self-consumption. On the other hand, the electricity demand in EEHs is solely user-dependent, since most of the electricity demand is based on scheduled and indoor

activities, thus a relatively lower tilt angle with a relatively smaller system size is found optimal in this case to cover the year-round seasonal electricity demand which, in turn, can be considered uniformly distributed in comparison with NZEHs.

Due to the limited availability of data and the unavailability of data from other locations nationally or internationally, this research did not include the impact of location on PV system size and layout with high levels or variability. However, future works will include data from multiple locations. Also, in future works, the authors will represent the household demand patterns in terms of probabilistic distributions to represent the most-likely demand scenarios based on the 11 households under investigation rather than individual households.

#### 4.7.2. *Model Validation*

The proposed model has been validated by simulating all the given solutions from the proposed model in PVWatts® simulation tool (Dobos, 2014). The system losses have been assessed according to the local climatic conditions in Edmonton as summarised in Table 2-5. Figure 4-14 visualises the comparison of the base case scenario of the (a) EEH and (b) NZEH between the monthly predicted energy generation from the proposed model against the measured data and PVWatts estimate (as a reference model). Percent error technique (Eq. 4-26 to Eq. 4-28) is applied here to validate the results from the proposed model. Here, the model is validated by, first, comparing the predicted output from the proposed model against the measured data at the base case scenario. Second, an estimate from a reference model (PVWatts in this case) is compared against the measured data. Third, the predicted model is compared against the PVWatts estimate. Since the suggested solution cannot be compared with any historical data and since it was found that there is a large percent error between the measured data and PVWatts estimate, an essential procedure is to calibrate the error of the predicted output with reference to the PVWatts estimate as presented in Eq. 4-29. The layout placements presented in this figure are the base cases of the EEH and NZEH.

$$\%error_{p,m} = \left| \frac{G_p - G_m}{G_m} \right| \times 100\% \quad (4-26)$$

$$\%error_{e,m} = \left| \frac{G_e - G_m}{G_m} \right| \times 100\% \quad (4-27)$$

$$\%error_{p,e} = \left| \frac{G_p - G_e}{G_e} \right| \times 100\% \quad (4-28)$$

$$\%error_{cal} = \left| \%error_{e,m} - \%error_{p,e} \right| \quad (4-29)$$

where the  $\%error_{p,m}$  is the percent error of the predicted output against the measured output,  $\%error_{e,m}$  is the percent error of the estimated output (from a reference model (PVWatts)) against the measured output,  $\%error_{p,e}$  is the percent error of the predicted output against the estimated output (from a reference model (PVWatts)) and  $\%error_{cal}$  is the calibrated error between the predicted output and the estimated output (from a reference model (PVWatts));  $G_p$  is the predicted output (from the proposed model),  $G_m$  is the measured generation (from a given base case scenario), and  $G_e$  is the estimated generation (from a reference model (PVWatts)). The logic behind the calibration of the percent error is to obtain a reference error margin in order to validate the suggested solutions, since the measured output is available only for the base case scenario.

Table 4-6. Assessment of estimated system losses in PVWatts®.

Parameter	Loss Factor (%)
Soiling	2
Shading (based on location)	3 (EEH) / 10 (NZEH)
Snow	5
Mismatch	2
Wiring	2
Connections	0.5
Light-induced Degradation	1.5
Nameplate Rating	1
Age	0.5
Availability	3
Estimated system losses	18.78 (EEH) / 28.61 (NZEH)

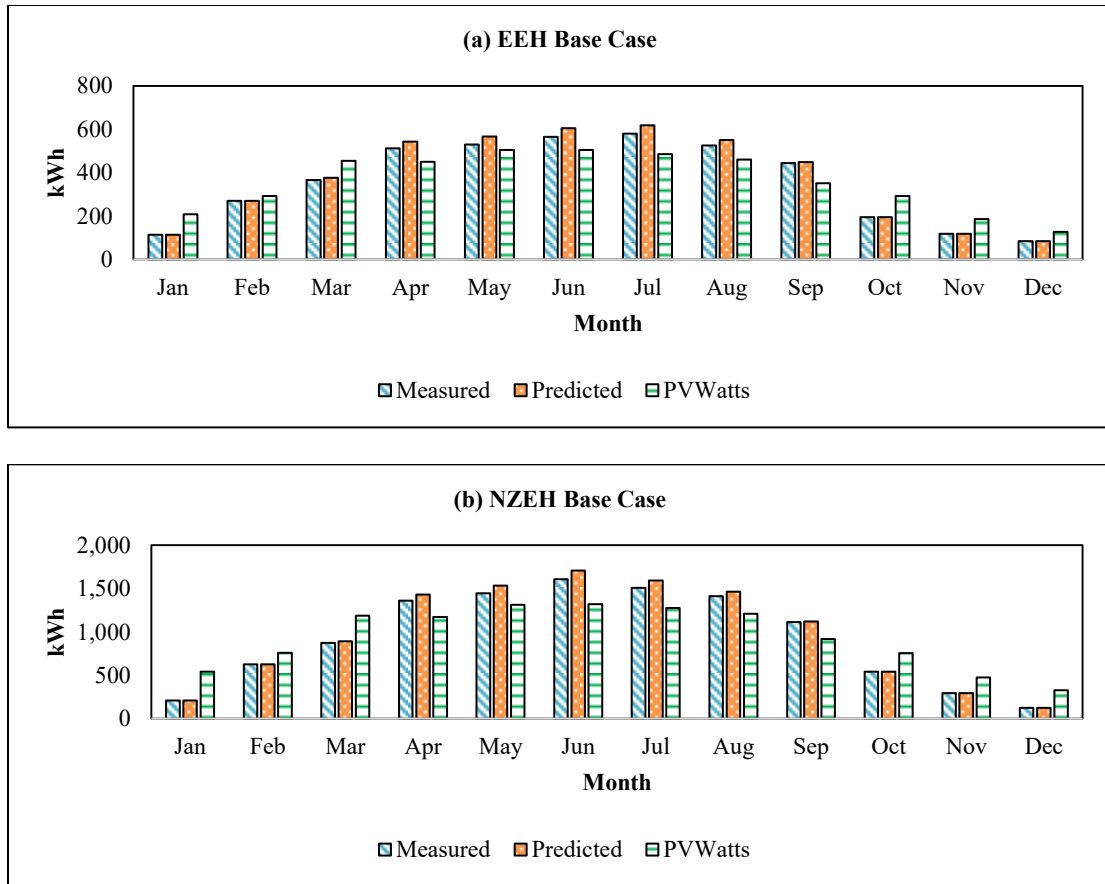


Figure 4-14. Pairwise comparison between the monthly measured and predicted data along with PVWatts estimate for (a) EEH and (b) NZEH. The charts represent (a) an EEH with 3.64 kW<sub>p</sub>, tilt = 26.5°, azimuth = 182° and (b) an NZEH with 10.92 kW<sub>p</sub>, tilt = 26.5°, azimuth = 195°.

Table 4-7 summarises the validation results of the base case scenario and the suggested solution for the (a) EEH and (b) NZEH. As demonstrated in Table 4-7, the annual percent error between the predicted model and the measured data for the base case scenario of the EEH and NZEH are 2.97% and 2.45% respectively. However, the percent error of the PVWatts estimate for the base case scenario of the EEH and NZEH are 29.24% and 49.27%. The calibrated percent error for the EEH and NZEH is deemed to be 4.60% and 16.60%. In terms of the suggested solution, the predicted model is validated by comparing the predicted output against the estimated output from PVWatts by means of the calibrated percent error method. In such case the

calibrated percent error of the predicted output for the EEH and NZEH are 2.40% and 14.55%, where these values are comparable to the calibrated percent errors from the base case scenario.

Table 4-7. Validation summary of the proposed model for (a) EEH and (b) NZEH.

House Type	(a) EEH										
Aspect	Base case							Solution			
System Size (kW <sub>p</sub> )	3.64							4.94			
Tilt Angle (°)	26.50							38.90			
Azimuth Angle (°)	182.00							189.80			
Data Source	Measured	Predicted	PV Watts	% <sub>error,p,m</sub>	% <sub>error,e,m</sub>	% <sub>error,p,e</sub>	Calibrated	Predicted	PV Watts	% <sub>error,e</sub>	Calibrated
Algorithm	G <sub>m</sub>	G <sub>p</sub>	G <sub>e</sub>	$\frac{ (G_p - G_m) }{G_m}$	$\frac{ (G_e - G_m) }{G_m}$	$\frac{ (G_p - G_e) }{G_e}$	$\frac{ \%_{error,p,e} - \%_{error,e} }{\%_{error,p,e}}$	G <sub>p</sub>	G <sub>e</sub>	$\frac{ (G_p - G_m) }{G_m}$	$\frac{ \%_{error,p,e} - \%_{error,e} }{\%_{error,p,e}}$
Measuring Unit / Monthly Output	kWh	kWh	kWh	%	%	%	%	kWh	kWh	%	%
Jan	113.30	113.30	208.52	0.00	84.04	45.66	38.38	187.84	335.34	43.98	40.06
Feb	270.54	270.59	291.45	0.02	7.73	7.16	0.57	428.93	449.37	4.55	3.18
Mar	365.11	375.88	454.59	2.95	24.51	17.31	7.19	570.70	664.62	14.13	10.38
Apr	511.76	543.02	449.36	6.11	12.19	20.84	8.65	784.40	614.39	27.67	15.48
May	529.33	565.93	504.76	6.91	4.64	12.12	7.48	779.46	663.04	17.56	12.92
Jun	564.44	604.61	504.32	7.12	10.65	19.89	9.23	815.17	655.33	24.39	13.74
Jul	580.49	618.04	485.39	6.47	16.38	27.33	10.95	843.49	637.57	32.30	15.91
Aug	525.23	550.73	459.81	4.85	12.46	19.77	7.32	787.09	624.52	26.03	13.57
Sep	443.78	449.14	351.61	1.21	20.77	27.74	6.97	698.29	495.02	41.06	20.30
Oct	194.77	194.77	292.65	0.00	50.26	33.45	16.81	313.63	433.85	27.71	22.55
Nov	117.56	117.56	185.21	0.00	57.54	36.52	21.02	193.19	287.13	32.72	24.83
Dec	84.47	84.47	126.48	0.00	49.73	33.21	16.52	141.65	202.20	29.95	19.78
Annual Output	4,300.79	4,488.05	4,314.16	2.97	29.24	25.08	4.16	6,543.84	6,062.38	26.84	2.40

House Type	(b) NZEH										
Aspect	Base case							Solution			
System Size (kW <sub>p</sub> )	10.92							8.68			
Tilt Angle (°)	26.50							58.50			
Azimuth Angle (°)	195.00							189.70			
Data Source	Measured	Predicted	PV Watts	% <sub>error,p,m</sub>	% <sub>error,e,m</sub>	% <sub>error,p,e</sub>	Calibrated	Predicted	PV Watts	% <sub>error,e</sub>	Calibrated
Algorithm	G <sub>m</sub>	G <sub>p</sub>	G <sub>e</sub>	$ (G_p - G_m)/G_m $	$ (G_e - G_m)/G_m $	$ (G_p - G_e)/G_e $	$ \frac{\%_{error,p,e} - \%_{error,p,e}}{\%_{error,p,e}} $	G <sub>p</sub>	G <sub>e</sub>	$ (G_p - G_m)/G_m $	$ \frac{\%_{error,p,e} - \%_{error,p,e}}{\%_{error,p,e}} $
Measuring Unit / Monthly Output	kWh	kWh	kWh	%	%	%	%	kWh	kWh	%	%
Jan	208.55	208.55	541.01	0.00	159.41	61.45	97.96	243.60	601.83	59.52	99.89
Feb	625.07	625.07	758.60	0.00	21.36	17.60	3.76	671.90	769.83	12.72	8.64
Mar	874.17	893.06	1,186.37	2.16	35.71	24.72	10.99	842.17	1,079.19	21.96	13.75
Apr	1,359.74	1,432.11	1,173.87	5.32	13.67	22.00	8.33	1,178.36	896.03	31.51	17.84
May	1,446.23	1,533.56	1,314.65	6.04	9.10	16.65	7.55	1,141.86	911.79	25.23	16.13
Jun	1,608.98	1,707.10	1,319.30	6.10	18.00	29.39	11.39	1,208.28	882.19	36.96	18.96
Jul	1,510.33	1,591.75	1,275.23	5.39	15.57	24.82	9.25	1,146.35	869.57	31.83	16.26
Aug	1,413.00	1,466.23	1,208.49	3.77	14.47	21.33	6.85	1,151.33	895.05	28.63	14.16
Sep	1,112.82	1,119.60	919.86	0.61	17.34	21.71	4.37	1,023.80	751.68	36.20	18.86
Oct	540.19	540.18	755.36	0.00	39.83	28.49	11.35	560.80	711.58	21.19	18.65
Nov	294.91	294.90	476.18	0.00	61.47	38.07	23.40	345.72	496.00	30.30	31.17
Dec	125.52	125.51	327.96	0.00	161.29	61.73	99.56	156.35	360.29	56.61	104.68
Annual Output	11,119.49	11,537.62	11,256.88	2.45	47.27	30.66	16.60	9,670.51	9,225.03	32.72	14.55

## 4.8. Discussion and Conclusion

### 4.8.1. Discussion

The present study aims to develop an improved design framework for residential grid-tied small-scale solar PV micro-generators using a data-driven approach that focuses on maximising the household load-match rather than either maximising the annual solar PV energy production (i.e., south-facing system with the local latitude as a tilt angle) or simply applying the current common practices that conform to the commonly constructed roof-sloping practices. The study focuses on finding methods of improvement for existing PV systems, with the intent that the findings from this research will be addressed in future individual solar PV installations as well as in smart community developments. In the research presented in this chapter, data of a minutely temporal resolution is used to feed the proposed framework; however, data of any available temporal resolution can be used. It should be taken into consideration that the higher the temporal resolution, the more accurate the results will be in the sense that data with higher temporal resolution, such as secondly, provides more accurate details on the grid-interaction profiles (i.e., exported versus imported energies, which are interpreted in negative and positive values, respectively). Having the grid data aggregated to a lower resolution such as minutely, hourly, or daily values, the positive and negative values cancel one another out and the resultant grid-interaction values may not represent the actual situation.

Based on the presented research, it is concluded that, despite their environmental and social merits, NZEHs account for higher fluctuations on the utility grid in terms of winter peak loads, energy demand, and energy export in cold-climate regions. Having said that, and, given that NZEHs rely on electricity for running the household mechanical equipment, these fluctuations in general are, to a great extent, dependent on outdoor weather conditions, be it high or low temperatures in hot or cold regions respectively. As for the present study, it is found that, on average, NZEHs consume 2.3 times the electrical energy consumed by EEHs. The net imported and exported energy of NZEHs from/to the grid are also 2.2 and 5 times, respectively, those of

EEHs. Intuitively, careful consideration of NZEH technologies should be taken to avoid any future complications to the utility grid. In addition, the sizing and layout placement of residential solar PV systems must be designed properly to avoid potential PV mismatch. In this study, the optimum solar PV layout placement is identified by developing the proposed generic framework.

Another notable finding is that the self-consumption does not exceed 25% of the generated energy on average for the homes under investigation. This issue points to the need for future work on reducing as well as flattening the electrical energy demand of NZEHs (Awad et al., 2017b; Freitas et al., 2018).

Having been tested on two of the monitored houses, the results from the proposed model are shown to be promising. Preliminary results indicate that a properly-sized southwest-oriented PV system improves the load-match indicator by increasing the PV energy utilised on site and reducing the grid power demand.

It should be noted that a PV system's tilt angle is dependent on the local latitude of the site under investigation; however, it is found that a tilt angle that is above or below the local latitude by approximately  $10^\circ$  coupled with a southwest-facing azimuth angle is the optimum scenario satisfying both environmental and economic criteria, regardless of geographic location. In specific, the optimal tilt angle for EEHs and NZEHs is found to be  $40^\circ$  (below the local latitude by  $13^\circ$ ) and  $60^\circ$  (above the local latitude by  $7^\circ$ ), respectively. Since NZEHs depend primarily on electricity (from either the grid or DERs) as the sole source of energy in which case the household demand peaks in winter, a relatively higher tilt angle was determined as the optimal solution for maximised self-consumption. It is also found that proper PV sizing is primarily dependent on the load/generation and import/export balance goals, secondarily taking into consideration criteria such as the given regulatory parameters and the economic feasibility of the system.

For the EEH, optimising the PV system's layout placement by raising its tilt angle by  $12.4^\circ$  and upgrading its size by 35.7% improves the annual LM by 47.5% and the annual GI by 75.4%, while the annual electricity bill is reduced by 15.8% and net-

zero balance is achieved. IN case of the NZEH, the system's tilt angle is raised by 32° and its capacity is downsized by 20.5%, while the net-zero balance can still be achieved, and typically the annual LM and GI can be satisfied. On the other hand, the annual electricity bill is increased by 6.6% due to the lower export revenue than had been previously obtained from the over-sized system.

It is concluded that the net-zero balance of the NZEH is achieved at the 8.68 kW<sub>p</sub> mark while the EEH required a 4.94 kW<sub>p</sub> system. This is due mainly to the high electricity demand in NZEHs, as they run off the natural gas grid, unlike EEHs, which are less challenged in achieving the net-zero balance of electricity loads.

The electricity demand in NZEHs is weather-dependent in addition to user-dependency, and thus peaks during severe winter months due to heating demand while air conditioning in summer is less common. Intuitively, a higher tilt angle and larger system is found optimal for self-consumption. On the other hand, the electricity demand in EEHs is solely user-dependent, since the household electricity demand of such homes is based on scheduled indoor activities, thus a relatively lower tilt angle with a relatively smaller system size is found optimal in this case to cover the year-round seasonal electricity demand which, in turn, can be considered uniformly distributed in comparison with NZEHs.

The model has also been validated by quantifying the percent error between the proposed model output and the measured data along with a reference model (PVWatts software). The percent error between the proposed model output and the measured data was deemed to be 2.97% and 2.45% for the EEH and NZEH respectively.

Intuitively, in order to ensure economical and environmentally-friendly energy usage in highly efficient self-consuming residences such as EEHs or NZEHs, consumers should be actively engaged in the energy-saving process. Several strategies can be suggested in this context, such as peak-shaving (or avoiding energy consumption at peak hours), applying delay/scheduled programs on wet appliances such as clothes dryers and washing machines and running them during peak generation hours, and considering smart devices such as sensor-based lighting and heating/cooling systems.

In this study, all sites were built in the year 2012 or later and are rated as highly energy-efficient building envelopes; however, it should be noted that, when studying the energy profiles of an older building, the building envelope should be investigated as it can be a major driver of high energy demand.

#### 4.8.2. *Conclusion*

The present study contributes to the following areas:

- Investigation of the energy performance of grid-connected solar PV systems in a cold-climate region, Edmonton, Canada, and quantification of the impact of layout placement on overall performance.
- Pairwise investigation and comparison of the energy performance of energy-efficient homes (EEHs) and net-zero energy homes (NZEHs).
- Quantification the LMGI indicators of EEHs and NZEHs.
- Development of a generic optimisation framework by which to identify a system's optimum layout placement and sizing.

The results of this study contribute to the accurate and systematic identification of the optimum solar PV system layout placement and sizing under any constraints pre-defined by the model user. In the proposed model, maximising the load-match and grid interaction is prioritised—in other words, on-site utilisation—of the PV system under design. Four criteria are considered in the present study: (1) layout placement, (2) net-zero balance, (3) code and regulations, and (4) cost-effectiveness. However, the model can accommodate other desired criteria.

This study leads to the conclusion, first, that it is crucial to perform an in-depth study of the load profile of the dwelling (or on similar existing dwellings if the optimisation is being conducted for a future home) on which a solar PV system is to be installed. Second, as a result, the solar PV system requirements for NZEHs differ in size and layout placement from those for EEHs. As mentioned previously, it is found that the optimum tilt angle for NZEHs is approximately 60°, while that of EEHs is approximately 40°, both southwest-oriented (where the local latitude is approximately

53.53° N). Third, in order to satisfy both environmental and economic criteria, the PV system's size should be near to the net-zero balance line. Elaborating on this, a smaller system is more economical due to its intensive on-site utilisation, but less environmentally-friendly due to its inability to compensate for the household annual energy demand. A larger system, in contrast, is less economical due to its under-utilisation (unless the demonstrated system is equipped with local storage solutions and/or effective RECs exist), but more environmentally-friendly due to its contribution in over-generation and in exporting clean energy and thereby playing a significant part in mitigating greenhouse gas emissions.

#### 4.8.3. *Limitations and Recommendations for Future Work*

It is important to mention that the solutions offered by this study are tailored toward addressing impracticalities such as the presence of prototype roofing slopes or a sub-optimal building orientation, both of which typically conform to the urban design of the community and street orientation. Nonetheless, the findings from this study are informative for academics and land developers and can easily be implemented for future research and in practice at the pre-planning phase in order to achieve greener net-zero communities and/or community generation applications. Local storage practices are also highly recommended for consideration as a second step toward flattening the load-generation balance and stimulating on-site energy utilisation.

As another limitation to the current optimisation framework, the authors have assumed that each house is an independent setting and that neighbouring PV systems (if any) do not incur any significant energy exchange or interference. However, future works will account for this issue. In addition, the impact of cloud cover on the PV system's orientation has been assumed to be fixed.

Future work will focus on multi-array layout placement at multiple orientations. The proposed model will be applied on all 11 houses and will also be generalised by running Monte Carlo simulations for energy consumption and artificial neural networks for energy generation.

## Chapter 5: Optimisation of Community Shared Solar Application in Energy Efficient Communities using Monte Carlo Simulations <sup>4</sup>

### 5.1. Overview

Integration of solar photovoltaic (PV) micro-generation into residential buildings is emerging rapidly as an effective method for mitigating the impact of housing on greenhouse gas (GHG) emissions. However, PV micro-generation is confronted with several challenges: (a) the average self-consumption does not exceed 25% in cold-climate regions; and (b) most of the generated energy during daytime is exported to the grid at a lower monetary rate per unit than that of imported energy. Governments and authorities envision the value of considering the integration of renewables at the community level rather than individual applications since this strategy can leverage self-consumption and increase its social impacts and economics. This research aims to develop a systematic framework that simulates and optimises community shared solar. The performance scenarios of two sustainable communities are simulated and presented as case studies. In the first scenario, each unit is connected to a small PV system. In the second scenario, all units are connected to a large PV system. Evidence-based Monte Carlo simulation is applied to ensure the stochasticity of the diverse household users. The hourly energy consumption and generation is simulated and an optimisation algorithm is then used to identify the optimum design of the community shared system.

---

<sup>4</sup> A version of this chapter has been submitted for publication in *Sustainable Cities and Society Journal* as Awad H. and Gül M, *Optimisation of Community Shared Solar Application in Energy Efficient Communities using Monte Carlo Simulations*.

## 5.2. Introduction

Renewable energy sources play a crucial role in mitigating GHG emissions by reducing the demand for fossil fuel (U.S. Energy Information Administration, 2017). Some widely used renewable energy sources include biomass, hydropower, geothermal, wind, and solar sources. With the exception of biomass, renewable energy sources do not directly emit GHGs. Renewable energy sources are also naturally replenishing but flow-limited (Wiseman and Bronin, 2013) due to uncertainties inherited from spatial and/or temporal variations (Cai et al., 2009b). Of the various types of renewable energy, solar and wind have become the most favourable when considering community-scale renewable applications, in addition to individual- and large-scale settings (Wiseman and Bronin, 2013).

As the residential solar PV applications within net-zero energy homes (NZEHS) and solar homes gain market penetration, maintaining the safety, reliability, and affordability of the electricity distribution grid becomes an increasingly challenging task especially in high-latitude regions. Individual behind-the-meter residential solar PV systems are confronted with several challenges (Awad et al., 2017b) such as PV mismatch in winter months, PV penetration in summer months, and poor economics in general. In this regard, governments and stakeholders seek alternative solutions that can possibly improve the economics of distributed energy generation. One of the potential solutions is the implementation of community shared solar PV systems. However, this concept is relatively novel and research work should be conducted to examine several aspects of this application (Nadkarni and Hastings-simon, 2017). In this context, this chapter focuses on developing a systematic framework that simulates and optimises community shared solar.

### 5.2.1. Literature Review

#### 5.2.1.1. Community Shared Solar Definition

Community shared solar has been defined by several researchers (Augustine, 2015; Hicks and Ison, 2018; Jones et al., 2017; Walker and Devine-Wright, 2008; Wiseman

and Bronin, 2013), one comprehensive definition of which is provided by Augustine (2015) as “*a solar photovoltaic project that delivers energy and/or economic benefit to multiple customers*”. The economic benefit here refers to the concept of the virtual net-metering setting, a setting which allows the customers to be credited for their share of the solar PV system that is not physically connected to their property (Augustine, 2015).

The community generation strategy responds to the sustainable development concept of “think globally and act locally” (Romero-Rubio and de Andrés Díaz, 2015). In addition to the environmental benefits of community generation, there are several economic and social benefits such as development of local and small businesses, job creation, public acceptance of the implementation of renewable energy sources within the community, citizen involvement, rational use of energy, and social cohesion and regeneration (Romero-Rubio and de Andrés Díaz, 2015). The vision of community energy generation contributes to public engagement and energy efficiency measures, which in turn favours and will accelerate the energy transition from fossil fuels towards clean renewable energy sources, from unintended energy wasting to wise energy use, and from centralised to decentralised production of energy (Romero-Rubio and de Andrés Díaz, 2015).

#### *5.2.1.2. Current State-of-the-art Community Generation Models*

Currently, there are more than fifty commercial solar PV design and simulation tools, as reviewed by Jakica (2018) and Sharma et al. (2014). However, since community shared solar is a relatively new trend, there are only a few tools that support, with limitations, the simulation, design, and analysis of large-scale community shared solar applications (Shakouri et al., 2017). For example, PVsyst (PVsyst, 2012) is a deterministic application that is widely used for the purpose of designing and simulating grid-tied standalone solar PV systems. On the other hand, the stochasticity and uncertainties associated with solar energy systems fall short of this type of application, and, this application focuses on the individual standalone aspect and therefore is unsuitable for designing community solar (Shakouri et al., 2017). Other

examples include Homer (Homer Energy, 2015), SAM (SAM, 2015), and NREL's Excel-based model, the Community Solar Tool (NREL, 2016). These tools provide rough estimates on solar PV applications; however, they are also associated with limitations such as geographic location, accuracy, or the number of systems that are simulated concurrently. For interested readers, additional details on the advantages and disadvantages of the abovementioned tools are described in a study by Shakouri et al. (2017).

Marique and Reiter (2014) propose a simplified framework to investigate the application of zero-energy buildings on the neighbourhood/community scale while considering two primary challenges: the impact of urban form on energy needs and on-site energy production, and the impact of location on transportation energy consumption. The study highlights the importance of energy mutualisation at the neighbourhood level. Hachem-Vermette et al. (2016) investigate building-integrated solar PV systems in mixed-use communities that combine residential and commercial buildings in Calgary, Canada from an urban development viewpoint. Their study accounts for primary energy demand, energy generation and GHG emissions using EnergyPlus and TRNSYS simulation platforms.

Cai et al. (2009a) develop a model that effectively addresses the dynamic interrelationships between renewable energy availability, economic penalties, and electricity generation deficiencies within a community scale. The study proposes an interval-parameter superiority-inferiority-based two-stage programming model for supporting community-scale renewable energy management (ISITSP-CREM). As an extension to this study, Cai et al. (2009b) develop an inexact community-scale energy model (ICS-EM) for supporting renewable energy management systems planning under uncertainty, incorporating both chance-constrained programming (CCP) and interval linear programming (ILP). Their study provides a decision-making framework to control and manage the various energy sources while considering the system reliability and costs. Li et al. (2017) develop a combined forecasting approach to model the net energy load (i.e., the differential value between generated and

consumed energy) in smart communities by which the forecast model can self-adjust its parameters online.

Shakouri et al. (2017) highlight the importance of implementing “randomness” while simulating the community-scale grid. For example, in their study, they focus on the economics of community shared solar PV applications by developing a probabilistic portfolio-based model for financial valuation of community solar in terms of payback period and return on investment.

Furthermore, the potential for community energy storage has recently been explored. For instance, Barbour et al. (2018) conduct a study in Cambridge, MA to simulate the community-level energy consumption and generation while adopting a community-level energy storage system in order to determine the battery economics; the developed model is then compared to that of an individual household scenario. Local energy storage has been introduced by previous studies as an effective method of allowing a larger fraction of demand to be met by PV generation (i.e., improving the self-consumption) (Barbour et al., 2018; Fthenakis et al., 2009; Luthander et al., 2015; Weniger et al., 2014).

Wiseman and Bronin (2013) identify three major areas of improvement that are necessary for substantial growth in community-scale renewables: (1) the willingness of communities to form business enterprises that regulate the purchase/share, installation, operation, and maintenance of the system infrastructure and sale of energy produced; (2) the acceptance of communities to facilitate the structure of the physical infrastructure, such as dwellings, public spaces, streets, and community buildings, that would house renewable generation; and (3) the utility-consumer relationship redefinition to accommodate this concept of community-scale generation, making it a reality.

#### 5.2.1.3. Community Shared Solar Challenges

Worldwide, the application of community shared solar is rapidly gaining popularity. For example, a study by Leuphana University (2013) reveals that, as of 2012, 46%

(34 GW) of the installed renewable energy capacity in Germany was owned by citizens (from urban areas and farmers), whereas the remainder belonged to energy suppliers (12%) and institutional and strategic investors (42%) (Leuphana University, 2013; Romero-Rubio and de Andrés Díaz, 2015). It can thus be concluded that there is strong potential for the implementation of community shared solar applications among citizens and communities. On the other hand, community shared solar is also associated with challenges (Jones et al., 2017). The application of community solar itself does not contribute to community resilience (Jones et al., 2017). For example, while the community solar arrays generate electricity to support the energy demands of the community and can be independent from the grid, when the grid is impacted by a power outage, the community solar facility is no more resilient than other fully-grid-supported communities. In their book chapter, Jones et al. (2017) recommend that future researchers target the technological and market forces in the implementation of community shared solar advances and to involve the community members along with policymakers, local utilities, and third-party suppliers to achieve the local energy goals.

Furthermore, the economic aspects of distributed energy generation have been investigated. Although the hardware costs of solar PVs have dropped substantially in the past decade, large-scale deployment of solar PVs is deemed to be challenging in terms of financial justification (Chan et al., 2017), especially in jurisdictions where the rate for purchasing electricity is considerably low and the reward programs are ineffective.

Darghouth et al. (2011) investigate the value of energy bill savings under various mechanisms while focusing on the net-metering mechanism against alternative PV compensation mechanisms. Freitas et al. (2018) study the community-scale combined effect of aggregating demand, photovoltaic generation, electricity storage, and on-site consumption of solar PV and its impact on the grid using real-time aggregated data. Two storage strategies are investigated in their study: one of which maximises self-consumption and the other of which reduces the net load variance; and in conclusion, from the prosumer's point of view, a PV system can be viable with little to no storage

system in place, while from the grid point of view, higher storage capacities are vital to the reduction of unmanageable load variance and consequent costs.

#### 5.2.1.4. Net-zero definitions

As demonstrated by Torcellini and Crawley (2006), there are currently four zero-energy-building (ZEB) definitions used which are incorrectly assumed to be interchangeable: (1) net zero source energy building; (2) net zero site energy building; (3) net zero energy cost building; and (4) net zero emissions building. In summary, in the present study, the net zero site energy building is the topic of interest and will be referred to as net-zero energy building (NZE) and more specifically as net-zero energy home (NZEH) for residential settings. An NZE/NZEH is defined as a building that produces as much energy as it uses when measured at the site (Salom et al., 2014a; Torcellini and Crawley, 2006).

Within the context of the present study and as per the local practices where this study is conducted, an NZEH is defined as a house that has low energy demand, relies on electricity as a sole source of energy, and generates as much energy as it consumes over the course of the year (Li et al., 2016; Torcellini and Crawley, 2006). An EEH is referred to as a house that has low energy demand, relies on natural gas for space heating and domestic hot water (DHW) heating, can optionally be equipped with a solar PV system, but does not necessarily achieve a yearly net-zero balance.

Also, within the context of the presented study the terms demand, consumption, and load are used interchangeably to convey the meaning of overall household electrical energy demand regardless of the energy source or carrier and not to be confused with delivered or imported energy, which refers to the delivered electricity from the utility grid.

#### 5.2.2. *Research Gap and Objectives*

Several studies have examined the definitions and legal implications of community shared solar, while others have focused on developing simulation and decision-

making models of solar shared communities. Furthermore, challenges associated with the application of community shared solar and its public acceptability have been addressed in studies from various countries and jurisdictions. As the world begins to consider the centralisation of distributed energy sources and the decentralisation of the utility grid and also prepare for the smooth transition from fossil-based energy sources to renewable energy sources, it is critically important to investigate the grid-wise implications of the community-scale application of net-zero energy homes (NZEH) (i.e., highly energy-efficient homes that function apart from the natural gas grid) in comparison with the equivalent application of energy-efficient homes (EEH) (i.e., energy-efficient homes that rely on natural gas for space heating and hot water heating). This matter has hardly been addressed in previous studies, especially in northerly climates. One of the focus areas of the present research is to develop a generic and systematic framework that analyses, simulates, and optimises community dwellings equipped with community shared solar PV systems, using statistical distributions since real-time energy consumption data is usually scarce and it is often difficult to obtain such data for a large number of dwellings. In order to support the proposed framework, a given example of a virtual community site of 42 dwellings is simulated and optimised by using the historical energy consumption and generation data from only 11 households. This chapter aims to address the grid-wise quantification of the implications associated with the community shared solar advances in both NZEHs and EEHs. In this regard, two types of communities, NZEH and EEH, are simulated in terms of energy demand, energy generation, self-consumption, and overall grid interaction in a Monte Carlo simulation environment with respect to the stochastic nature of energy demand. It is worth mentioning that energy storage is not considered within the context of this study; however, future work will include this aspect. The specific objectives and contributions of this study are summarised as follows:

- to develop a systematic model that simulates the household energy demand of multiple dwellings (community) based on statistical data (probabilistic

distributions) from one dwelling or a few dwellings by means of Monte Carlo simulation technique;

- to develop an optimisation framework that identifies the optimum community-shared solar energy system in terms of layout design and system size, and thereby quantify the improvements incurred by the optimised system against the current practice; and
- to quantify the energy performance measures of the simulated community scenarios in terms of hourly energy demand, energy generation, load match, and grid interaction.

### **5.3. Method**

The present study is carried out by means of three primary stages. First, long-term historical energy performance data (ongoing since 2015) is collected at a one-minute temporal resolution, which includes energy loads, generation, and grid interaction. This data is stored in an in-house database and then used later to generate probabilistic distribution curves for each hour of the day and month of the year. In order to simulate the household energy demand of multiple units with respect to the stochasticity and uncertainties of multiple users' behaviour, it is preferred to consider the random selection of demand activities rather than deterministic demand activities. In this context, the following research question is addressed: *What is the load-match and grid-interaction (LMGI) performance of a community integrated with a community shared solar PV system, and what is the impact of PV systems coupled with various types of residences, such as NZEHs and EEHs, on the central grid?* Here, the LMGI measures proposed by Salom et al. (2014) are used to quantify the LMGI indicators and to identify the net-zero balance of the community under investigation using the collected real-time data. Second, a Monte Carlo simulation prototype is developed to represent the hourly-interval energy demand. In this stage, for simplicity, it is assumed that demand patterns can change with respect to the hour of the day and the month of the year. Third, after simulating the energy demand of the

dwellings in the simulated community, an optimisation model is used to identify the optimum load-match-driven design of community-scale PV system layout and size for both EEHs and NZEHs. Building on this, the following research question is addressed: *Is the current know-how for the community-scale PV system design sufficient to provide the optimum design in terms of environmental impact, economy, and on-site PV self-consumption and its impact on the grid?* To answer this question, a novel hybrid framework previously developed by Awad et al. (2017a, 2017b) is applied in the present research that combines the inputs from real-time data with an analytical model. The analytical model is developed to determine the solar PV power output for any given two-way tilted surface at any location around the globe at a one-minute temporal resolution. This model is highly beneficial for data analysis and data mining purposes given that it can predict the theoretical clear-sky irradiance at any given latitude at the desired temporal resolution (secondly, minutely, daily, etc.). The clear-sky irradiance is used as a denominator to predict the clear-sky index, where the nominator is the real-time power generation of a given PV module. It is thus possible to estimate the clear-sky energy aggregate of a given PV system at any layout placement and at the desired temporal resolution.

However, due to the varying weather conditions, especially cloud cover, it is crucial to determine the clear-sky index of the site under investigation at the specified temporal resolution (minutely in the current case). A generalised reduced gradient (GRG) nonlinear optimisation algorithm is used to identify the optimal PV system layout placement and size. The optimisation framework is set to facilitate the objective function of maximising the load-match between the household energy loads and the proposed PV system. Finally, options analysis is carried out by conducting a pairwise comparison between two scenarios: (1) small single PV system per household, and (2) large system connected evenly to the entire community.

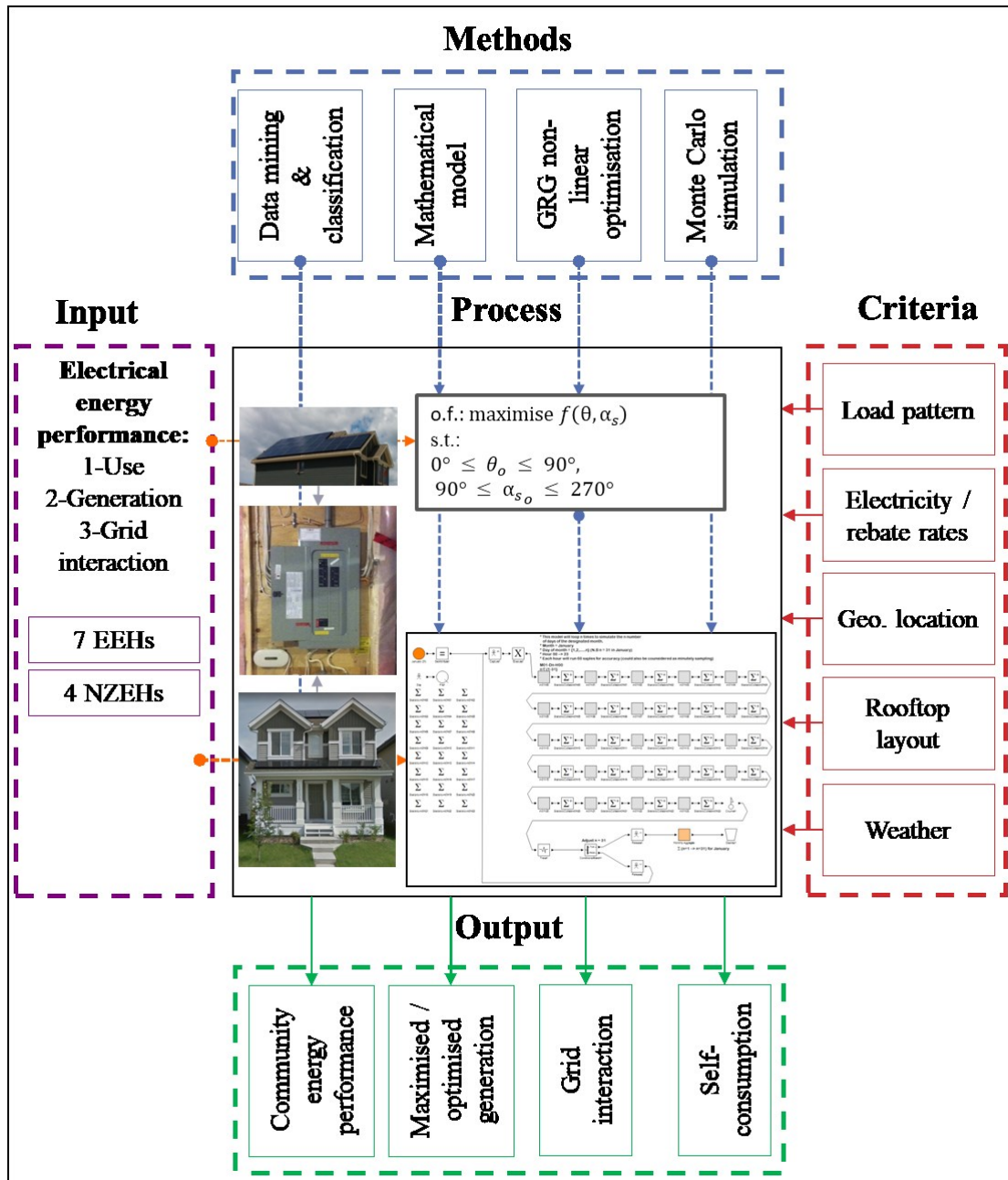


Figure 5-1. Proposed research method.

It is worth mentioning that all the models developed in the present study are generic in order to accommodate data from any location around the globe; however, findings from the present study are dependent on the local input data collected from 11 households located in Edmonton, Canada. It is well-acknowledged that demand

patterns differ significantly with the change of geographical location, weather, culture, technology, and social conditions. However, it is crucial for readers interested in replicating this work to collect their own sets of data in order for these models to reflect the local conditions of sites under investigation. Figure 5-1 summarises the proposed research method.

#### **5.4. Data Collection and Analysis**

In this chapter, a comparison between individual micro-generation systems (i.e., single PV system per household) and community shared PV systems is conducted. Evidence-based simulation of two types of communities is carried out in the case of EEHs and NZEHs located in Edmonton, Canada.

##### *5.4.1. Household Energy Performance of Net-zero Energy Homes and Energy-efficient Homes*

Data collected from 11 houses in Edmonton (Table 5-1) is analysed to investigate the energy performance of each house type (energy-efficient and net-zero), as well as the performance of various configurations of installed solar PV systems, with the focus on the net-zero balance, load-match, and grid interaction indicators of each house. Figure 5-2a and Figure 5-2b summarise the monthly load, generation, exported energy, imported energy, net electricity bill, and solar energy used on site (self-consumed) for the 11 monitored sites, respectively, while Figure 5-3 presents the percentage of the annual self-consumption of the solar PV systems together with the corresponding house type. For the net electricity bill presented in Figure 5-2, this calculation is based on the local energy retailer rates explained later in Section 5.3. It can be observed from Table 5-1 that the average PV system size for EEHs and NZEHs is 3.08 kW<sub>p</sub> and 13.39 kW<sub>p</sub>, respectively, since, unlike EEHs, NZEHs are required to achieve a yearly net-zero goal. Thus, the large PV sizing of NZEHs reflects the high electrical energy demand to be compensated on a yearly basis. However, it is difficult for the layout placement of both EEHs and NZEHs to follow a specific standard other than yielding to the current roof sloping practice in North

America and the building orientation with respect to the urban planning of the neighbourhood.

Table 5-1. List of monitored NZEHs (denoted with N-#####) and EEHs (denoted with E-#####).

Type	Data Collection Starting Date	Tilt (°)	Azimuth (°)	System Size (kW <sub>p</sub> )	Latitude (° N)	Heating system	DHW heating
E-18356	20-May-15	27	182	3.640	53.62545	NG/ F <sup>1</sup>	NG
N-18366	29-May-15	27	195	10.92	53.51095	ASHP <sup>2</sup>	EHP <sup>3</sup>
E-18360	30-May-15	30	180	2.080	53.42344	NG/ F	NG
E-18357	2-Jun-15	30	201	2.080	53.62550	NG/ F	NG
E-18371	10-Jun-15	30	180 (2) – 270 (6)	2.080	53.40846	NG/ F	NG
E-18364	22-Jun-15	30	201	2.080	53.42183	NG/ F	NG
E-18358	23-Jun-15	34	130	2.080	53.62808	NG/ F	NG
N-18374	20-Aug-15	27	152	14.715	53.41930	ASHP	EHP
N-18361	26-Nov-15	10	165	13.455	53.51288	ASHP	EHP
E-18367	23-Apr-16	27 (19) – 30 (7)	180 (19) – 270 (7)	6.760	53.47755	NG/ F	NG
N-18365	17-Jun-16	23	180	14.280	53.52306	ASHP	EHP

<sup>1</sup>NG/F: natural gas / furnace; <sup>2</sup>ASHP: electric air source heat pump; <sup>3</sup>EHP: electric heat pump.

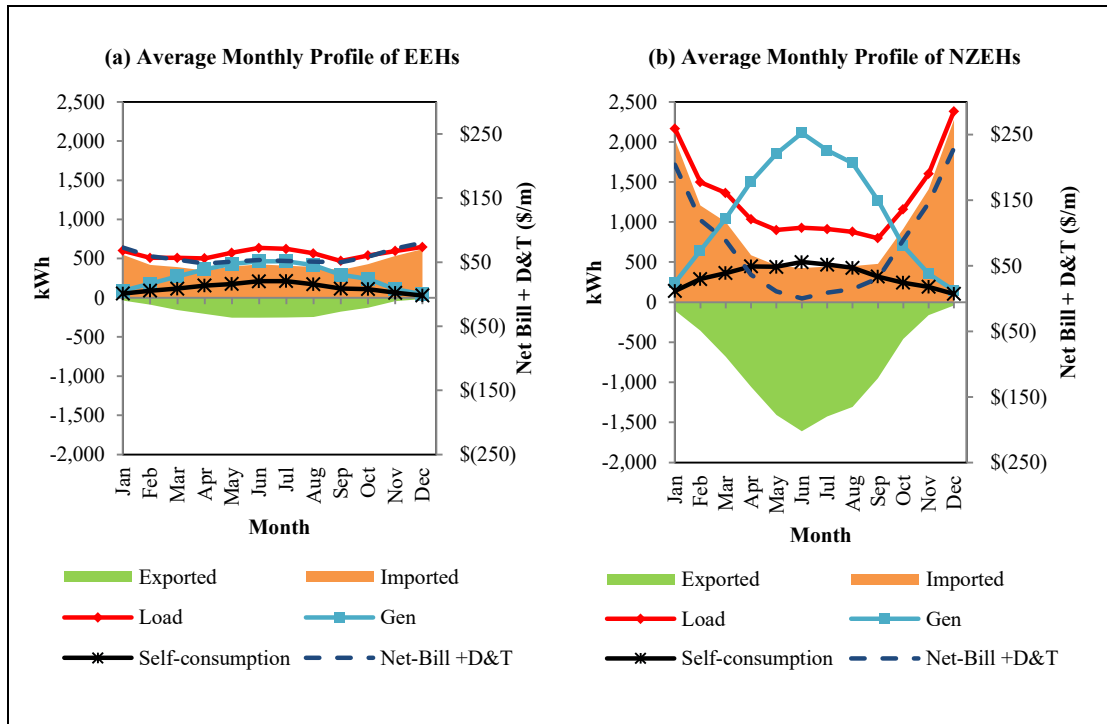


Figure 5-2. Summary of average energy-component profiles of all 11 houses demonstrating average monthly profile of (a) EEHs and (b) NZEHs.

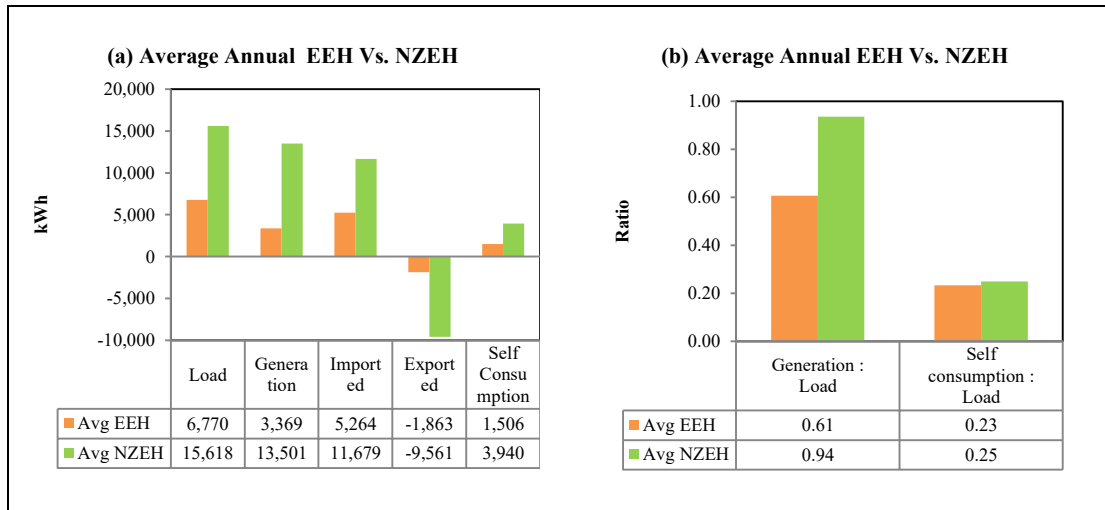


Figure 5-3. Pairwise comparison between the average annual energy performance of EEHs and NZEHs.

It can be observed in Figure 5-2b that NZEHs, due to being independent of the natural gas grid, consume significantly larger amounts of energy during colder months than do EEHs, particularly energy consumed for electricity-based space heating and DHW heating when the outdoor temperature falls below  $-15^{\circ}\text{C}$ . In this regard, relatively large solar PV systems are installed in the NZEHs to compensate for the inflated grid electricity demand. However, although these systems generate significantly larger amounts of electricity annually, they fail to match the real-time on-site energy demand, resulting in a PV mismatch in winter and PV penetration in summer as indicated in Figure 5-2a and Figure 5-2b. The detailed performance of the 11 households can be found in Awad et al. (2017b). Although the sizing of a PV system should be designed to compensate for the household energy demand annually, it is demonstrated in Figure 5-3b through f that, regardless of whether the installed PV system is over-, under-, or equally-sized, the results are an average of 23% and 25% of self-consumption for EEHs and NZEHs, respectively. This phenomenon underscores the fact that most energy-consuming indoor household activities occur in the early morning or late afternoon hours when the sun is positioned in either the east or the west, respectively.

It is also found that, on average, the annual household energy demand of an NZEH is 2.3 times that of an EEH, and, although the PV systems installed on NZEHs are 4 times the size of those installed on EEHs, the amounts of imported and exported energy of an average NZEH are found to be 2.2 and 5 times those of an average EEH, as presented in Figure 5-3a. Hence, existing NZEH technologies, specifically in cold climates, ought to be considered for re-evaluation and improvement. Nevertheless, it is worth mentioning the environmental benefits of NZEHs. Reiterating the original definition of NZEHs—homes that generate as much energy as they consume annually—on average, the net-zero balance of the NZEHs and of the EEHs under investigation are found to be 94% and 61%, respectively, despite the fact that the self-consumption rates of those systems are 25% and 23%, respectively, as demonstrated in Figure 5-3b. However, despite the proven environmental value of solar microgeneration practices due to reduced GHG emissions, the absence of affordable local storage systems in some jurisdictions and the ineffective application of Renewable Energy Credits (RECs) serve to diminish the economic viability of such systems.

One of the key differences between NZEHs and EEHs is that the monthly energy demand pattern of EEHs is relatively uniform compared to that of NZEHs. This can be observed in two examples demonstrated in Figure 5-4. Figure 5-4a and Figure 5-4b represent the monthly profiles (in terms of load, generation, imported energy, and exported energy) of an EEH and an NZEH, respectively. To elaborate on the energy performance patterns, a cumulative energy profile of the EEH and NZEH is presented in Figure 5-4c and Figure 5-4d. Here, the EEH energy demand satisfies a linear regression function while, on the other hand, the NZEH fits a second-degree polynomial function. In this regard, caution must be practiced while considering NZEH community development. The entire utility grid infrastructure should consider the changing demand patterns with the practice of community-scale net-zero energy buildings—not only homes. This non-linearity, as explained earlier, relates to the high energy demand for heating.

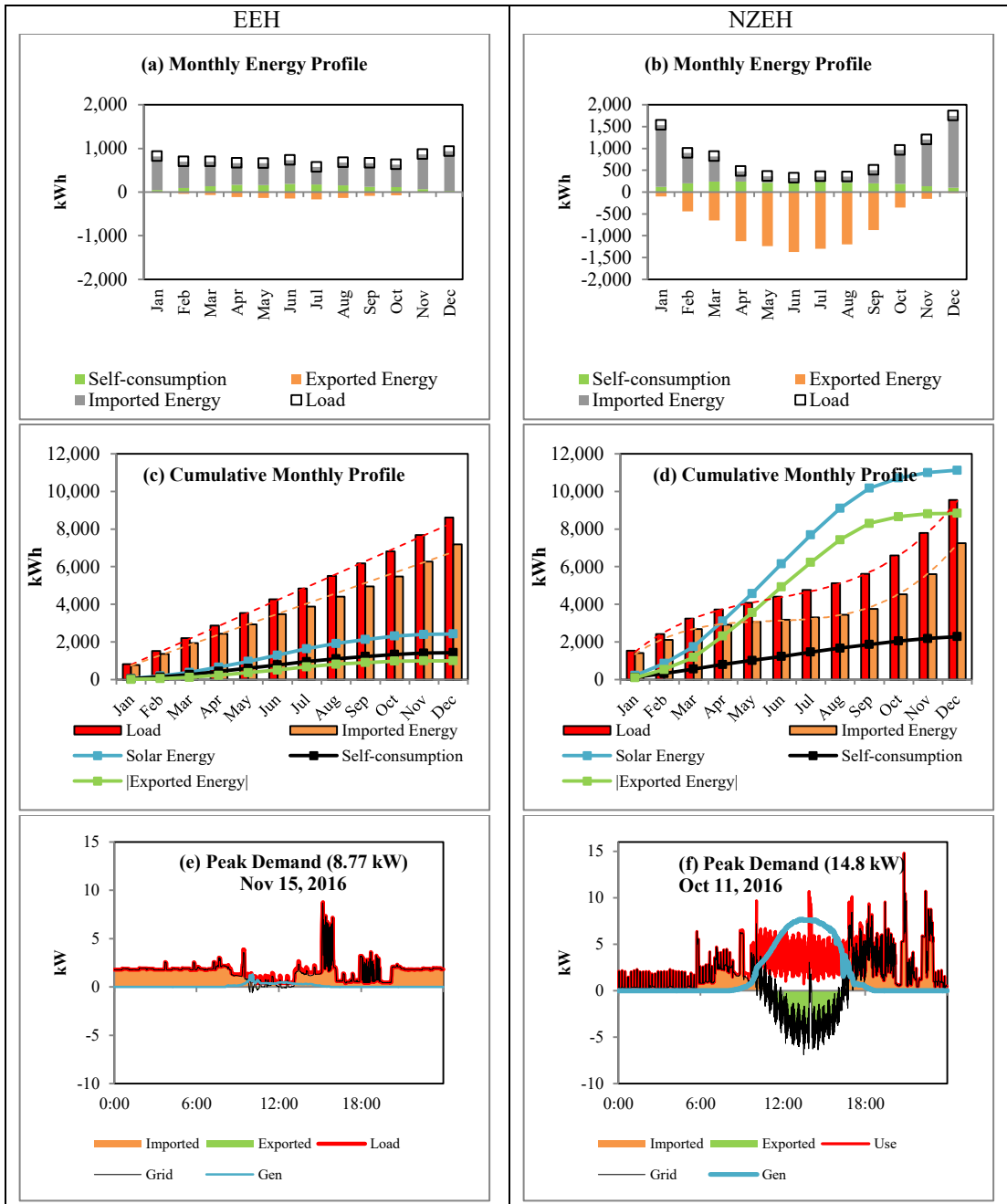


Figure 5-4. Sample energy performance of an EEH's (a) monthly profile, (c) cumulative monthly profile, and (e) daily profile on peak demand, and an NZEH's (b) monthly profile, (d) cumulative monthly profile, and (f) daily profile on peak demand.

It can also be observed that the over-sizing of PV systems can achieve the annual net-zero balance (as presented in Figure 5-4d), but does not necessarily succeed in reducing the real-time energy demand from the electricity grid. From the daily profile perspective, the grid interaction profiles of EEHs and NZEHs differ significantly. Because of space heating and DHW heating loads it is observed from Figure 5-4e and Figure 5-4f that, unlike the EEH, in the NZEH, the energy loads fluctuate with a high frequency within the minutely temporal resolution, which can disturb the grid stability within the community-scale application of such homes. In the case of EEHs, fewer fluctuations are observed in terms of grid interactions.

## **5.5. Framework**

### *5.5.1. Simulation of Energy Demand*

Systems simulation has proven its effectiveness in analysing various dynamic operations (Wales and AbouRizk, 1996). The history of simulation software dates back to 1955-1960, namely “the period of search”, and evolved through five main stages over the succeeding 30 years, as described by Nance (1995). Esfahani (2013) compares the simulation engine developed by Hajjar and Abourizk (1996), which can obtain distributions and conduct several iterations simultaneously, with other methods that can also estimate the desired outputs, but only for one iteration, and concludes that the application of Symphony.NET (Hajjar and Abourizk, 1996) is more accurate. Additionally, this simulation engine is capable of providing histograms and cumulative density function (CDF) charts for the output data. In order to simulate a given process, a significant amount of sample data (model inputs) is needed to generate the proper distribution (Esfahani, 2013). For instance, with respect to the study presented in this thesis, in order to simulate the household energy consumption patterns, the energy consumption records for several years are required to determine an appropriate distribution for each month and each hour.

The collection and analysis of input data are considered a major task in simulation, where one of the first steps is to hypothesise a distributional form for the input data (Banks et al., 2009). There are three primary applications of historical data in this study: (1) to validate the output data from the base simulation model, since it mimics the actual energy consumption pattern; (2) to generate the proper probabilistic distribution of each month of the year and hour of the day; and (3) to fill the gaps that result from the divergence between real situations reflecting its stochastic nature, and theoretical data obtained from simulation, which is based on historical data from examples for each house type (i.e., seven EEHs and four NZEHs).

The general-purpose template (GPT) in the simulation engine is selected to simulate the energy consumption patterns through a discrete-event simulation (DES) model. The selected time unit is hourly intervals, since the model is set to simulate the hourly energy consumption. In the context of energy demand, each event (hourly demand) is considered independent of the preceding and/or succeeding event(s) where each event is simulated by random sampling from a given distribution fit. In this context the use of continuous simulation may not become useful. Unlike the common purpose of using simulation engines, which aim to determine specific complex operation durations, the present research manipulates the simulation engine to calculate the aggregated energy consumption of a community consisting of multiple dwellings using data from one or a few dwellings, while considering the stochasticity and uncertainties incurred from such activities. In future considerations, the energy generation of solar PV systems will be implemented in the simulation model and thus the grid interaction will be quantified within the same model. In such configuration, a combined Continuous-DES simulation framework will be used for this purpose; Continuous simulation will be used to simulate the energy generation which follows pre-defined mathematical equations while DES will be used to simulate the energy demand which is primarily dependent on the user's behavior.

One of the merits of Monte Carlo simulation is its ability to mimic the stochastic nature of random activities by collecting historical data from such activities and

converting them from deterministic instances to probabilistic values, which is also referred to as probabilistic simulation. Monte Carlo simulation, also known as random simulation and random sampling, is defined by Yan and Tian (2012) as follows:

*“... in order to solve these problems of mathematics, physics, engineering technology and production management, a probability model or random process should be established firstly, making its parameters equals the solution of the problem; Then, based on this model or process, through sampling test to calculate the statistical characteristic of parameters; Finally, give out the approximation of the problem, and the solution accuracy can be expressed in the form of standard error of the approximation or other statistical characteristics.”*

Due to the limited availability of data and for the interest of replicability, providing a generalised framework with least dependency on local data, 1-minute data (ongoing since May 2015) from only 11 households, 7 of which are EEHs and 4 of which are NZEHs, are manipulated for simulation. The use of probabilistic simulation supports the running of the several consecutive iterations of the model to mimic the electrical energy demand of as many households as desired by the user. With respect to the stochasticity of demand, the data under investigation is analysed and classified by the hour of the day and the month of the year and sorted into 288 bins ( $24 \text{ hours} \times 12 \text{ months}$ ).

In this regard, energy demand data is collected and inserted into a database in order to perform further data mining and analysis. For simplicity, the one-minute interval instances collected by the eGauge® system (2017) are aggregated to represent hourly intervals (i.e., for each hour of the day 60 samples are collected). Since several years of data is collected from 11 homes, a significantly large population of instances will then be used to determine the probability distribution of each hour of the day and month of the year, which will in turn be used to run the random sampling of several dwellings within the community as presented in Figure 5-5. In Figure 5-5, a sample of

the distribution fit of the energy load in January at 0:00 a.m. is presented. It is found that Beta distribution results in the best fit to the data sample [Beta (1.61, 7.84, 0.21, 2.29)] (Eq. 5-1). This step is performed 288 times for each community to run the load simulation in the next step.

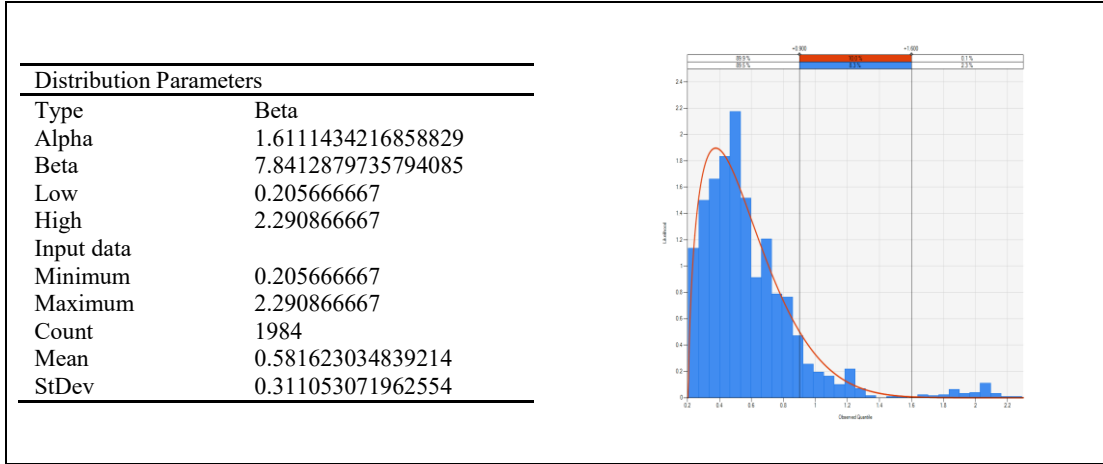


Figure 5-5. Statistical distribution of the energy load in January at 0:00 a.m.

Simphony.NET® (Hajjar and Abourizk, 1996) simulation platform is then used to simulate the load profiles of the 42 dwellings based on the Monte Carlo random sampling technique explained earlier. Figure 5-6 presents a screen shot of the January simulation model in which each of the grey-coloured tasks (squares) represents an hour of the day. Each task runs 42 times to select 42 random samples, and these samples are collected and analysed later. As can be seen in the upper right section of the screen shot, each month is run in a separate scenario and statistics are then collected after all months are simulated. To avoid negative and/or unrealistic values, most of the data bins are fitted into either beta, gamma, or triangular distributions. The probability distribution function of the Beta distribution  $Beta(\rho, \psi, a, b)$  [shape1, shape2, low, high], Gamma distribution  $Gamma(j, \gamma)$  [shape, scale], and Triangular distribution  $Triangular(a, b, c)$  [low, high, mode] are determined by means of Eq. 5-1 to Eq. 5-3 (Abourizk et al., 1993).

$$f_X(x) = \frac{1}{B(\rho, \psi)} x^{\rho-1} (1-x)^{\psi-1} \quad (5-1)$$

$$f_X(x; j, \gamma) = \frac{1}{\Gamma(j)\gamma^j} x^{j-1} e^{-\frac{x}{\gamma}} \quad (5-2)$$

$$f_X(x) = \begin{cases} \frac{2(x-a)}{(b-a)(c-a)} & a \leq x < c \\ \frac{2(b-x)}{(b-a)(b-c)} & c \leq x \leq b \\ 0 & \text{otherwise} \end{cases} \quad (5-3)$$

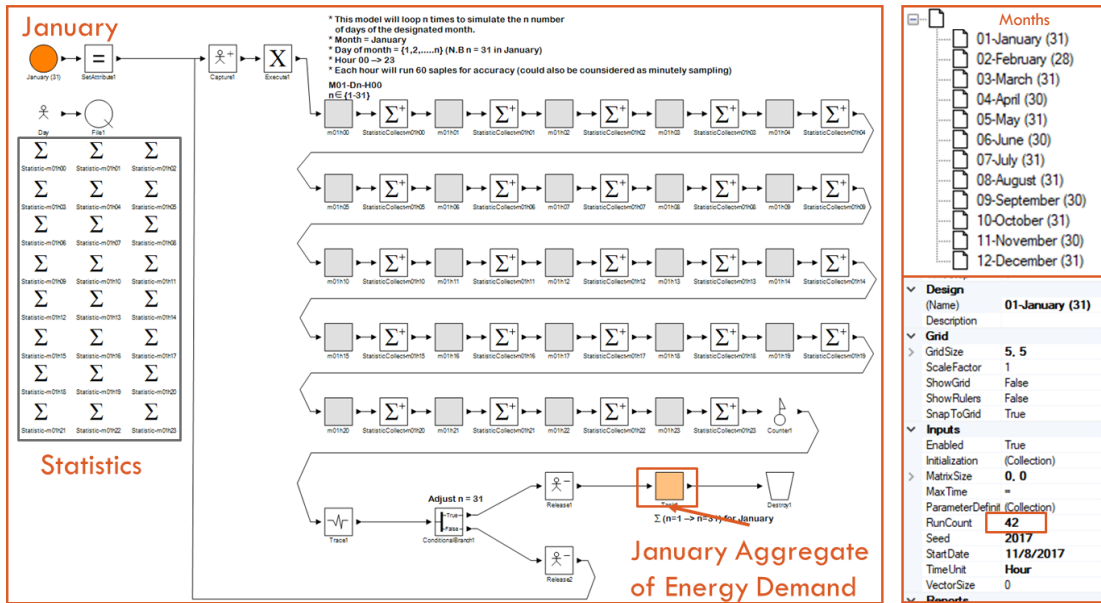


Figure 5-6. Screen shot of the Monte Carlo simulation model for January.

It is observed that in the EEH community 86.81% of the data sample bins fit into Beta distribution, 12.50% into Gamma distribution, and 0.69% into Triangular distribution. In the NZEH community, 62.50% of the data sample bins fit into Beta distribution, 33.33% into Gamma distribution, and 4.17% into Triangular distribution.

### 5.5.2. PV Power Output at a Two-way Tilted Surface

In order to simulate the energy generation of a given solar PV system, an analytical model is developed to determine the power output at any two-way tilted surface. The importance of developing an analytical model for clear-sky global irradiance (and PV power output) is twofold. First, and most importantly, the clear-sky global irradiance model is used in the assessment of the clear-sky index ( $k_t$ ) as the ratio between the

actual power output and the clear-sky PV power output (Eq. 5-4). The purpose of the implementation of  $k_t$  into the optimisation framework is to determine the impact of cloud cover on the power output of the solar PV system under investigation at any two-way tilted surface. In such case, the actual power output can thus be determined with a considerable degree of accuracy. It is worth mentioning that the impact of cloud cover on a given PV system's orientation has been assumed to be fixed. Second, this model is used to support the learning of the optimisation framework since several solar PV systems with varying layouts and locations can be introduced to the generic model. Hence, it is vital to provide the model with sufficient information (i.e., the sun's location and expected angle of incidence on the given PV system at any given time of day). The clear-sky model is used to analytically predict the clear-sky solar PV power output on a two-way tilted surface at the highest possible temporal resolution (i.e., monthly, daily, hourly, or minutely). This information becomes helpful in cases where historical data with high temporal resolution is not available. In the present study, clear-sky PV power output is used to calculate the minutely clear-sky index ( $k_t$ ) as well as to leverage the calculated index later in predicting the solar PV power output at any desired layout placement as a factor of tilt and azimuth angles. Solar geometry calculations for each day of the year (*DOY*), including solar zenith ( $z$ ) (Reno et al., 2012), declination ( $\delta$ ) (Reno et al., 2012; Walter et al., 2012), solar time (*ST*) (Reno et al., 2012; Walter et al., 2012), hour angle ( $\omega$ ) (Kreider et al., 1989; Reno et al., 2012), true zenith ( $z_t$ ) (Reno et al., 2012), extraterrestrial irradiance ( $I_0$ ) (Spencer, 1971), direct normal irradiance (*DNI*) (Eq. 5-5) (Daneshyar, 1978; Paltridge and Proctor, 1976), diffuse irradiance (*diffuse*) (Eq. 5-6) (Daneshyar, 1978; Paltridge and Proctor, 1976), clear-sky global horizontal irradiance ( $GHI_{cs}$ ) (Eq. 5-7) (Badescu, 1998), daylight hours ( $\beta$ ) (Kreider et al., 1989), the sun's degree angle from due south at sunset (*Hourset*) (Kreider et al., 1989), and the sun's azimuth angle ( $\alpha$ ) (Kreider et al., 1989), can be found in the relevant literature.

$$k_t = GHI_{measured}/GHI_{cs} \quad (5-4)$$

$$DNI (W/m^2) = 950.2(1 - \exp(-0.075(90 - z_t))) \quad (5-5)$$

$$Diffuse (W/m^2) = 14.29 + 21.04 \left( \frac{\pi}{2} - z_t \times \pi/180 \right) \quad (5-6)$$

$$GHI_{cs} (W/m^2) = I_0 * 0.70 \times \cos(z_t) \quad (5-7)$$

The angle of incidence of the sun on a two-way tilted surface ( $\theta_i$ ) is defined in Eq. 5-8 as

$$\begin{aligned} \cos \theta_i = & \sin(\delta) \sin(\varphi) \cos(\vartheta) + \sin(\delta) \cos(\varphi) \sin(\vartheta) \cos(\alpha) + \\ & \cos(\delta) \cos(\varphi) \cos(\vartheta) \cos(\omega) - \cos(\delta) \sin(\varphi) \sin(\vartheta) \cos(\alpha) \cos(\omega) - \\ & \cos(\delta) \sin(\vartheta) \sin(\alpha) \sin(\omega) \end{aligned} \quad (5-8)$$

The clear-sky power output is then identified by applying the following equation:

$$P_{cs,o} = \min(MPP, GHI_{cs} \times n_p \times l_p \times w_p \times e_p \times e_s/1000) \quad (5-9)$$

where  $\varphi$  represents the latitude of the site under investigation;  $P_{cs,o}$  represents the clear-sky power output at the original layout placement of the solar PV system;  $MPP$  represents the Maximum Power Point of the PV system;  $n_p$  represents the number of panels in the PV system;  $l_p$  and  $w_p$  represents the length and width of the panel, respectively; and  $e_p$  and  $e_s$  represents the module efficiency and system losses, respectively. The clear-sky index and the clear-sky power output having been determined earlier in this section, the power output at any two-way tilted surface can then be predicted as expressed in Eq. 5-10:

$$P_{p,n} = P_{cs,n} \times k_t \quad (5-10)$$

where  $P_{p,n}$  represents the predicted actual power output at the new layout placement, and  $P_{cs,n}$  represents the clear-sky power output at the new layout placement.

### 5.5.3. Net-zero Balance of Communities

It is essential to quantify the energy performance of NZEHs and EEHs located in cold-climate regions and identify their load-match and grid-interaction (LMGI) indicators in order to achieve the net-zero goal. In this regard, Eq. 5-11 to Eq. 5-19, as per Salom et al. (2014), are applied. In the present study, however, we focus on the

net-zero balance in terms of energy performance only, and thus disregard the weighting factors corresponding to these other aspects. Within the context of this study, the net-zero balance measures are assessed at the community level by aggregating the performance measures from all 42 simulated dwellings as follows:

$$\sum exp - \sum imp = EXP - IMP \geq 0 \quad (5-11)$$

$$\sum g - \sum l = G - L \geq 0 \quad (5-12)$$

$$g_m = \sum_m \max[0, g(m) - l(m)] \quad (5-13)$$

$$l_m = \sum_m \max[0, l(m) - g(m)] \quad (5-14)$$

$$\sum g_m - \sum_i l_m = G_m - L_m \geq 0 \quad (5-15)$$

$$f_{load} = \frac{1}{N} \sum_{year} \min[1, g(t)/l(t)] \quad (5-16)$$

$$f_{grid} = net\ grid / \max|net\ grid| \times 100(\%) \quad (5-17)$$

$$\text{with } net\ grid = exp - imp \quad (5-18)$$

$$f_{grid,yr} = STD(f_{grid,i}) \quad (5-19)$$

where *exp* represents the exported energy to the grid; *imp* represents the imported energy from the grid; *g* represents the generation; *l* represents the load; *m* represents monthly resolution; *i* represents the index; *t* represents the time interval; and *N* represents the number of data samples. The net-zero balance of a given building should be achieved by satisfying the above set of equations. In other words, the exported energy should be greater than or equal to the imported energy (at the yearly and monthly time intervals). Similarly, the generated energy should be greater than or equal to the load of the yearly interval.

#### 5.5.4. Optimisation Framework

Based on the aggregated findings from the previous sub-sections, a generalised reduced gradient (GRG) nonlinear optimisation algorithm (Lasdon et al., 1974) is employed to identify the optimal PV system layout and size. For interested readers, detailed information on the optimisation model structure is given in the study by

Awad et al. (2017b). The optimisation model focuses on finding a solution that maximises the self-consumption of a given solar PV system through the load-match-driven design criterion. In this regard, the optimisation procedure follows four iterations that target (1) optimum tilt and azimuth angles for maximised load-match such as in Eq. 5-20 to Eq. 5-22, (2) net-zero balance achievement, (3) regulatory criterion, and (4) system economics criterion. For example, in the first iteration the objective function is to maximise the load-match index by changing the tilt and azimuth angles of the PV system, as expressed in Eq. 5-20 to Eq. 5-22, in order to maximise the load-match indicator (previously calculated in Eq. 5-16), considering that

$$f_{load} = f(\theta, \alpha_s) \quad (5-20)$$

Here, the objective function, taken from Lasdon et al. (1974), is defined as

$$\text{maximise } f(\theta, \alpha_s) \quad (5-21)$$

and subject to

$$0^\circ \leq \theta_o \leq 90^\circ, 90^\circ \leq \alpha_{s_o} \leq 270^\circ \quad (5-22)$$

where  $\theta_o$  represents the optimum PV system's tilt angle and  $\alpha_{s_o}$  represents the optimum PV system's azimuth angle. It is assumed that the  $0^\circ$  and  $90^\circ$  tilt angles are horizontal and vertical placements, respectively. Similarly,  $90^\circ$  and  $270^\circ$  azimuth angles are east- and west-oriented placements, respectively, while true south is represented as  $180^\circ$ .

#### 5.5.5. Model Validation

The proposed models have been validated by means of the cross-validation technique by applying the percent error technique presented in Eq. 5-23. First, in case of the simulated energy loads, the simulation results are validated by comparing the simulation output with the measured energy loads. Validation results are discussed later in Section 5.6. With regard to the predicted PV power output at a two-wat tilted surface, the model results are validated by comparison with a reliable commercial

solar PV estimating tool developed by the National Renewable Energy Laboratory (NREL) named PVWatts® (Dobos, 2014). Percent error technique is also used for this purpose.

$$\%_{error} = \left| \frac{G_s - G_m}{G_m} \right| \times 100\% \quad (5-23)$$

where  $\%_{error}$  represents the percent error of the modelled energy load,  $G_s$  represents the simulated data, and  $G_m$  represents the measured data. Energy generation validation is carried out by simulating all the given PV systems in the PVWatts® online simulation platform (Dobos, 2014). The system losses are assessed according to the local climatic conditions in Edmonton as summarised in Table 5-2.

Table 5-2. Assessment of estimated system losses in PVWatts®.

Parameter	Loss Factor (%)
Soiling	2
Shading (based on location)	3
Snow	5
Mismatch	2
Wiring	2
Connections	0.5
Light-induced Degradation	1.5
Nameplate Rating	1
Age	0.5
Availability	3
Estimated system losses	18.78 (EEH) / 28.61 (NZEH)

## 5.6. Results

A site under planning and design for a sustainable community located in Edmonton (53.44° N, 113.53° W) is investigated in this section. It is assumed that this future community consists of 42 dwellings and is connected to either a (1) behind-the-meter single rooftop PV system connected to each individual dwelling or (2) larger-sized PV system connected to the entire community as a whole unit. The site location and suggested housing layout is presented in Figure 5-8. In order to further investigate the future implications of net-zero energy communities in comparison with traditional housing practices (i.e., EEHs), the simulation of the given site is considered in two separate scenarios, NZEH community and EEH community, while each scenario is

simulated twice (referred to in Section 5.6.2 as scenario#1 and scenario#2, respectively) to consider the two PV system options mentioned earlier in this paragraph.

### 5.6.1. Energy Demand Simulation Results

As previously mentioned, by collecting historical data and identifying the probability distribution of each hour of the day and month of the year (288 bins of instances), 42 dwellings are simulated by running Monte Carlo simulation technique 42 times, where in each run, random samples are selected according to the distribution of each bin. Figure 5-7 presents the simulated hourly energy demand of the 42 EEH dwellings (Figure 5-7a) and NZEH dwellings (Figure 5-7b).

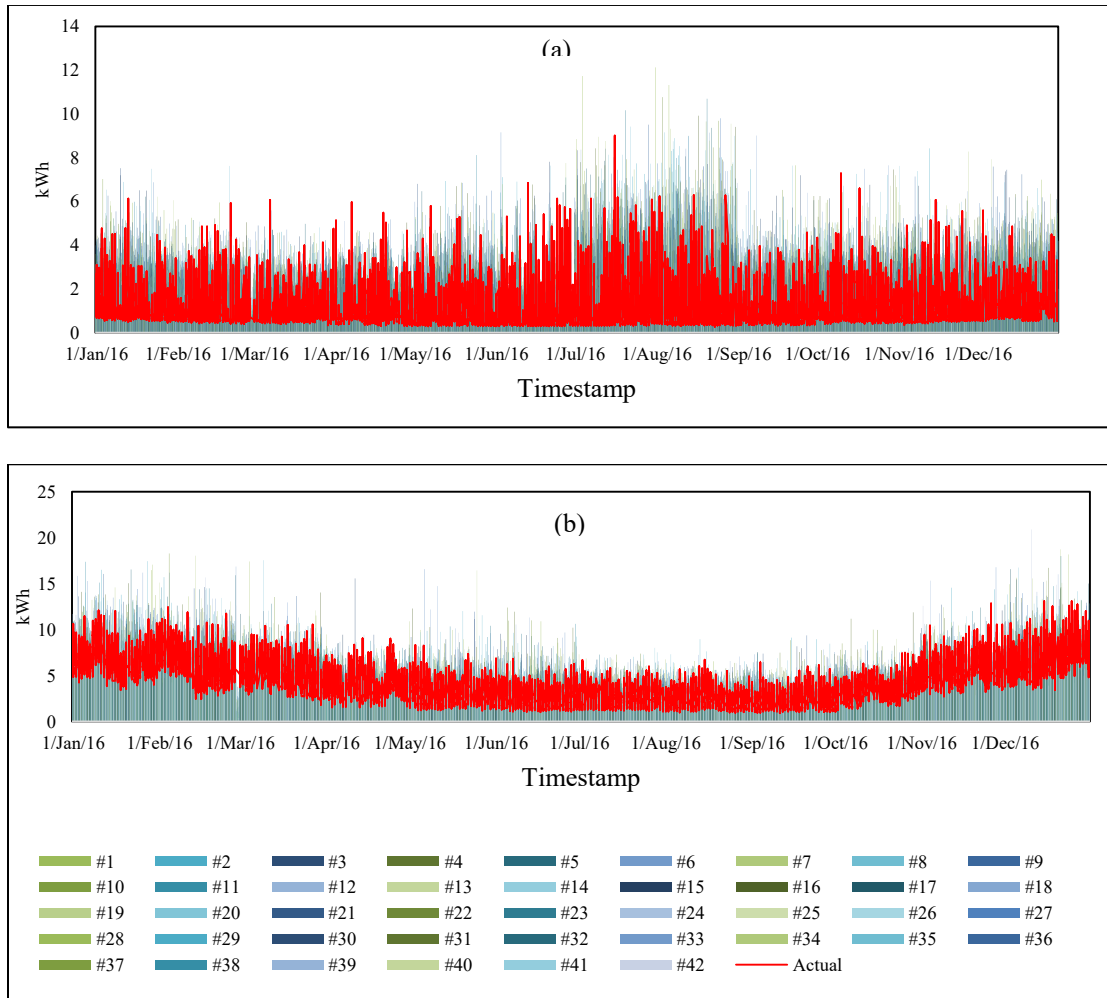


Figure 5-7. Simulation results of energy consumption of 42 (a) EEH and (b) NZEH dwellings.

In Table 5-3, a comparison between the average monthly energy demand from measured data against the statistical results from the simulation model is presented. Based on the percent error calculation, it is found that on average, the error for EEHs and NZEHs is 12% and 8%, respectively. It is noted that the average energy demand of an EEH and an NZEH is 7,712 kWh and 14,817 kWh, respectively.

Table 5-3. Statistical analysis of simulation results and data validation.

Month	Measured Mean (kWh)	Modelled				%error
		Mean (kWh)	St. Dev. (kWh)	Min (kWh)	Max (kWh)	
(a) EEH						
Jan	817.81	744.22	20.91	690.02	803.65	0.09
Feb	696.70	598.07	13.46	576.86	630.34	0.14
Mar	696.97	638.80	15.86	603.80	688.22	0.08
Apr	664.37	560.36	14.67	532.43	602.79	0.16
May	659.73	548.75	15.94	521.91	608.60	0.17
Jun	730.97	690.78	13.21	687.57	713.99	0.16
Jul	574.00	596.21	19.57	559.85	625.32	0.04
Aug	676.99	595.12	20.81	557.36	652.13	0.12
Sep	665.70	543.31	10.66	523.98	574.28	0.18
Oct	632.36	626.31	15.13	592.08	675.25	0.01
Nov	866.21	729.27	13.27	696.36	755.43	0.16
Dec	935.90	841.12	21.49	795.94	895.24	0.10
Annual	8,617.71	7,712.34	16.25	7,338.17	8,225.24	0.12
(b) NZEH						
Jan	1,968.59	2,151.29	63.68	2,030.74	2,267.11	0.09
Feb	1,415.54	1,736.91	47.92	1,613.64	1,856.03	0.23
Mar	1,542.36	1,509.94	45.32	1,373.39	1,606.96	0.02
Apr	1,141.97	1,093.07	29.11	1,025.57	1,145.51	0.04
May	814.60	890.65	25.21	855.03	955.00	0.09
Jun	748.00	727.61	26.17	672.89	788.68	0.03
Jul	822.85	714.13	24.88	669.99	773.83	0.13
Aug	705.48	702.84	22.61	650.53	745.91	0.00
Sep	638.64	659.64	23.08	611.49	707.79	0.03
Oct	1,056.30	988.89	29.89	918.61	1,065.77	0.06

Nov	1,341.21	1,589.48	33.44	1,491.21	1,667.21	0.19
Dec	2,073.16	2,052.72	41.10	1,954.77	2,152.78	0.01
Annual	14,268.68	14,817.15	34.37	13,867.84	15,732.57	0.08

## 5.6.2. Energy Generation Modelling Results

### 5.6.2.1. Behind-the-meter Individual PV System

As presented in Figure 5-8, the site layout consists of several blocks that indicate each house with variable rooftop slope orientations (from top to bottom, right to left of the figure: north-west, north-east, east, west, and south). In this scenario, the current practice for individual solar PV systems is simulated, while aiming to improve this practice in the proposed scenario offered in the next subsection. It is assumed that each dwelling is paired with a rooftop small-sized PV system, which adheres to the rooftop orientation, of approximately 3 kW<sub>p</sub> and 13 kW<sub>p</sub> for EEHs and NZEHs, respectively. This sizing assumption is based on the collected information for the average PV sizing in current practice, which is also summarised in Table 5-1. According to the current construction practices in North America, it is also assumed that the rooftop slope, and consequently the PV system's tilt angle, is approximately 18.43° (4:12). In order to simulate the varying system orientations, each system is modelled individually and coupled with its corresponding household simulated energy consumption as demonstrated in Table 5-4a and Table 5-4b for EEH and NZEH communities, respectively.



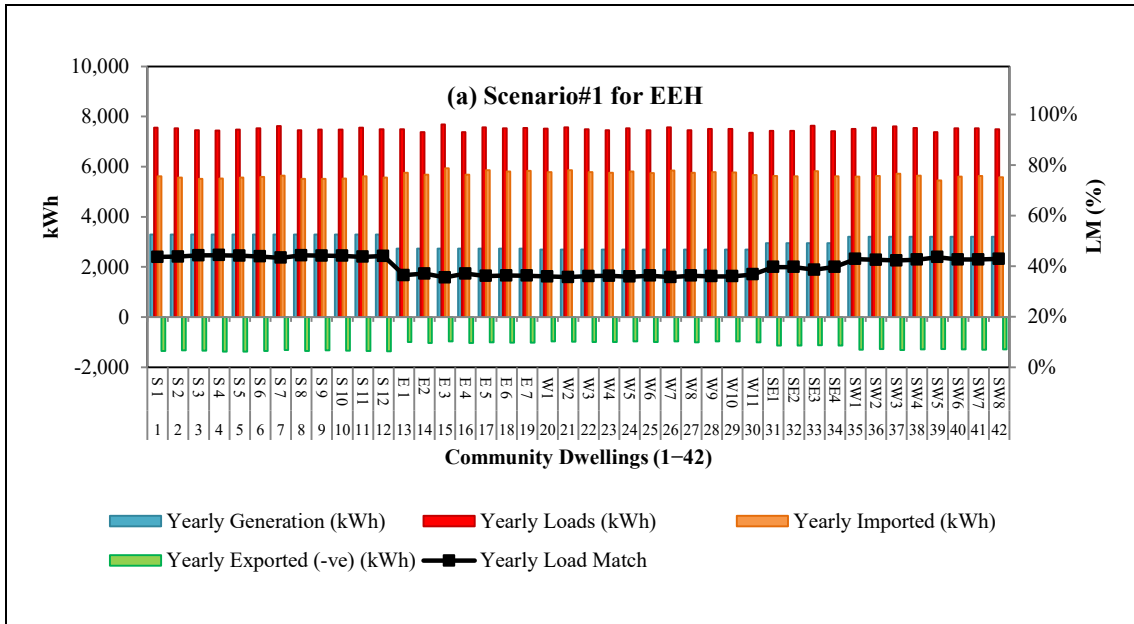
Figure 5-8. Single system dwelling unit setting (green rectangle represents the backyard of each dwelling).

Table 5-4. Single system per unit setting.

Roof Orientation	Tilt (°) (0° H)	Orientation (°) (0° N)	Units /Orientation	System Size (kW <sub>p</sub> )	Annual Generation /Unit (kWh)	Annual Generation /Orientation (kWh)
(a) EEH						
South	18.43	180	12	3.08	3,522	42,275
East	18.43	90	7	3.08	2,878	20,147
West	18.43	270	11	3.08	2,841	31,249
Southeast	18.43	111	4	3.08	3,120	12,479
Southwest	18.43	210	8	3.08	3,423	27,382
Total			42	129.36	133,532	
(b) NZEH						
South	18.43	180	12	13.39	15,159	181,909
East	18.43	90	7	13.39	12,552	87,867
West	18.43	270	11	13.39	12,402	136,421
Southeast	18.43	111	4	14.00	13,529	54,117
Southwest	18.43	210	8	14.00	14,754	118,033
Total			42	588.00	578,348	578,348

Figure 5-9 summarises the simulation results of scenario#1 for individual dwellings of the communities under investigation, where Figure 5-9a and Figure 5-9b represent EEH and NZEH communities. Annual figures are given in this context for brevity;

however, the calculations are carried out at the hourly temporal resolution. Each of the dwellings is assigned a label ([letter] [number]) as seen on the x-axis of Figure 5-9, where the [letter] represents the orientation of the rooftop PV system that is assumed to be installed as per scenario #1, while the [number] represents the index of the dwelling (1,2,...*n*) within its block as presented in Figure 5-8. For the EEH dwellings, each coupled with 3.08 kW<sub>p</sub> systems, the load match (LM) varies between 37.72 and 47.06% with a mean of 42.38% and a standard deviation of 3.77%, indicating that the net-zero balance with such setting is impossible to achieve. On the other hand, although each of the NZEH dwellings are coupled with over-sized PV systems of 13.39 kW<sub>p</sub>, the LM varied between 82.41% and 100% with a mean of 92.22% and a standard deviation of 7.60%. This drop in LM is primarily due to the reduced PV final yield of the PV systems that are east- and west- oriented (in the center of the chart in Figure 5-9b). Readers should note that the axis scale of Figure 5-9a and Figure 5-9b are unequal for the interest of better figure visualisation.



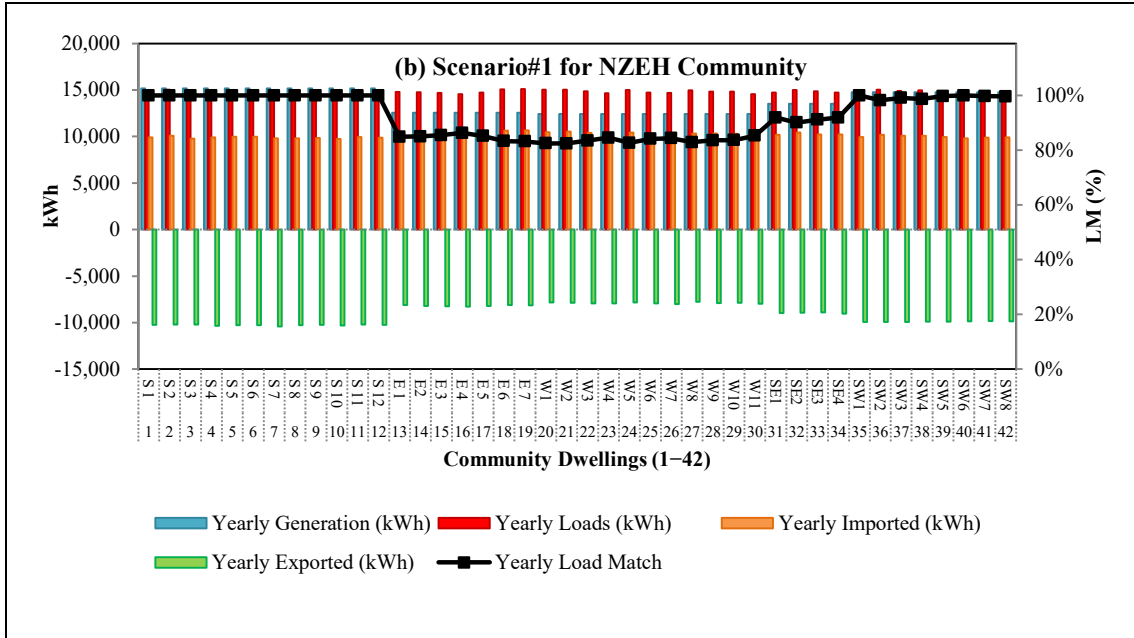


Figure 5-9. Simulation results for individual dwellings based on scenario#1 for the (a) EEH and (b) NZEH community. Labels are assigned to the dwellings according to the orientation of the rooftop PV system; S: south, E: east, W: west, SE: south east, and SW: south west.

#### 5.6.2.2. Community-scale distributed generation PV system

Here, a community-scale PV system connected to the community as a whole and distributed evenly among the individual end-users or dwellings is proposed. The optimisation framework proposed in the previous section is applied to identify the optimum layout placement and sizing of the PV system in order to achieve the maximum possible self-consumption, while energy storage option is not considered within the context of this study. One of the merits of community shared solar is its flexibility in design since it does not necessarily adhere to the rooftop layout or boundaries of a specific building. Another merit is that this system is evenly distributed among the community members; in other words, those dwellings with an east-facing rooftop will receive equal amounts and patterns of energy to those that are south-facing. This setting is difficult to achieve in individual PV application. In this option the size and layout placement of the community shared solar energy system is

left to be determined and will be identified by the optimisation engine for both EEH and NZEH communities.

### 5.6.3. *System Optimisation Results*

Energy performance measures such as household electricity loads, generated energy, imported and exported energy, and LMGI indicators at the hourly temporal resolution are calculated for both of the above-mentioned scenarios by using Eq. 5-8 to Eq. 5-16 in Section 5.5.3. The optimisation model is then run to identify the optimum tilt and azimuth angles and PV sizing in order to maximise the PV system's self-consumption based on the load patterns. Within the context of the present work, due to the novelty of community shared solar applications and the lack of knowledge on the know-how of the smart-metering infrastructure, as well as legal implications of such systems, the entire community is considered as a whole unit. In such case, the energy consumption, generation, and respective grid interaction measures for all 42 dwellings are aggregated in a summation technique.

Simulation results indicate that by implementing the current micro-generation practice (scenario 1), which adheres to rooftop layout and geometric constraints, the PV system's tilt angle is  $18.43^\circ$ , its azimuth angle is variable according to the building's orientation, and its size is  $3.08 \text{ kW}_p$  and  $13.39 \text{ kW}_p$  for EEHs and NZEHs, respectively (with regard to the current practice). From Table 5-3, the mean energy demand of EEHs and NZEHs is  $7,712 \text{ kWh}$  and  $14,817 \text{ kWh}$ , respectively. On the other hand, as presented in Table 5-4, the estimated rooftop generation for EEHs and NZEHs range between  $3,068 \text{ kWh}$ – $3,750 \text{ kWh}$  and  $12,402 \text{ kWh}$ – $15,159 \text{ kWh}$ , respectively. As a result, the load-match (LM) indicator for EEHs and NZEHs does not exceed 45% and 92%, respectively. For the system economics, a fixed electricity rate of  $9.05 \text{ ¢/kWh}$  and a renewable energy credit (REC) of  $3.9 \text{ ¢/kWh}$  is assumed. Administrative and grid-operation fees are also assumed to be at a flat rate of  $\$5.67/\text{month}$  and  $\$18.92/\text{month}$ , respectively, based on the local energy retailer fees. The PV system price is also assumed to be  $\$3.00/W_p$ . Although in the case of EEHs natural gas is used as an energy source for heating, the gas rates are not included in the calculations.

The layout placement solutions provided by the optimisation framework for both cases (EEH and NZEH) are indicative of the nature of the household energy demand for the given community type. For example, NZEHs consume significantly larger amounts of electricity, and, in addition, the high electricity demand is clustered in the winter months to meet mechanical system demand. Because the altitude of the sun in winter is relatively low in Edmonton, a higher-than-typical tilt angle is proposed by the optimisation framework— approximately  $56^\circ$  (about  $3^\circ$  higher than the local latitude). An EEH, as mentioned earlier, consumes natural gas for space heating and DHW heating, but has an energy-efficient building envelope. It is thus easier to achieve net-zero balance for this type of community than for an NZEH, provided that the PV system is sized properly. This explains the layout solution identified by the optimisation framework, which proposes a tilt angle of approximately  $50^\circ$  (about  $3^\circ$  lower than the local latitude). In both cases—EEH and NZEH communities—the azimuth angle is found to be approximately  $195^\circ$ , a value that is considerably similar to the conclusions of Litjens et al. (2017) in a study conducted in the Netherlands where the preferred azimuth angle for maximised self-consumption in residential buildings is deemed to be  $212^\circ$ . The reasoning behind this given solution is that the energy loads peak in the late afternoon hours (especially on weekdays). The given solution also adheres to the research findings previously observed by Awad et al. (2017b), where the optimum tilt angle, azimuth angle, and system size for a single EEH located in Edmonton are concluded to be  $38.9^\circ$  and  $189.8^\circ$ , and  $4.94 \text{ kW}_p$ , respectively. Table 5-5 and Table 5-6 summarise the results from the two given scenarios and the implied changes by considering the proposed solution over the current practice for EEHs and NZEHs, respectively.

First, the optimisation framework suggests increasing the PV system size of the EEH community from  $129.36 \text{ kW}_p$  to  $244.92 \text{ kW}_p$  in order to achieve the entire community's electricity net-zero balance; however, in case of the NZEH community, it is suggested to down-size the PV system from  $560.28 \text{ kW}_p$  to  $479.18 \text{ kW}_p$  while the net-zero balance can still be achieved.

Table 5-5. Total EEH community optimisation results.

Iteration	W/out Solar	Current Practice		Suggested Solution		Implied Changes
State		(Scenario 1)		(Scenario 2)		Suggested Solution vs. Current Practice
		Total	Average	Total	Average	
Index		$S_{1,t}$	$S_{1,\mu}$	$S_{2,t}$	$S_{2,\mu}$	$(S_2 - S_1) / S_1$
System Size (kW <sub>p</sub> )	-	129.36	3.08	244.92	5.83	89.33%
System's Generating Capacity (kWh/kW <sub>p</sub> )		174,636	4,158	330,642	7,872	89.33%
Tilt Angle (°)	-	18.5	18.5	50.1	50.1	
Azimuth Angle (°)	-	Variable	Variable	194	194	
Yearly Exported (kWh)	-	49,023	1,167	221,306	5,269	351.44%
Yearly Imported (kWh)	315,080	238,375	5,676	218,563	5,204	-8.31%
Imported/Exported Balance (kWh)	-315,080	-189,352	-4,508	2,743	65	-101.45%
Yearly Generation (kWh)	-	125,728	2,994	317,823	7,567	152.79%
Yearly Loads (kWh)	315,080	315,080	7,502	317,899	7,569	0.89%
Load/Generation Balance (kWh)	-315,080	-440,808	-10,495	-635,722	-15,136	44.22%
On-site Solar Energy Use (kWh)	-	76,705	1,826	99,336	2,365	29.50%
On-site Solar Energy Use (%)	-	61.01%	61.01%	31.26%	31.26%	-48.77%
Yearly LM	-	39.90%	39.90%	99.98%	99.98%	150.54%
System Initial Cost (\$)	\$0.00	\$388,080	\$9,240	\$734,760	\$17,494	89.33%
Imported Grid Electricity (\$/year)	\$28,514	\$21,573	\$514	\$19,780	\$471	-8.31%
Export Revenue (\$/year)	\$0.00	\$1,912	\$46	\$8,631	\$206	351.44%
Balance (\$/year)	\$28,515	\$19,661	\$468	\$11,149	\$265	-43.29%
Balance Inc. Admin. Fees (%/year)	\$28,810	\$19,956	\$475	\$11,444	\$272	-42.65%

Second, the layout placement has proven its effectiveness in designing a solar PV system on both the individual (Awad et al., 2017b) and the community levels. For example, it can be seen that in the EEH community, increasing the system size by 89.33% while installing the solar PV system at the proper layout placement (50.1°-tilt and 194°-azimuth) can improve the net-zero balance by 101.45% and can also improve the PV system's self-consumption by 29.50%.

On the other hand, in the NZEH community, it is noticed that by reducing the system size by 14.47% while installing the solar PV system at the proper layout placement (55.7°-tilt and 195.8°-azimuth) can achieve net-zero balance, which has not been

achieved with the larger PV system in the first scenario, and can also improve the PV system's energy generation by 8.20%.

Table 5-6. Total NZEH community optimisation results.

Iteration	W/out Solar	Current Practice		Suggested Solution		Implied Changes
		(Scenario 1)		(Scenario 2)		
State		Total	Average	Total	Average	Suggested Solution vs. Current Practice
Index		$S_{1,t}$	$S_{1,\mu}$	$S_{2,t}$	$S_{2,\mu}$	$(S_2 - S_1) / S_1$
System Size (kW <sub>p</sub> )	-	560.28	13.39	479.18	11.41	-14.47%
System's Generating Capacity (kW/kW <sub>p</sub> )	-	756,378	18,009	646,893	15,402	-14.47%
Tilt Angle (°)	-	18.5	18.5	55.7	55.7	
Azimuth Angle (°)	-	Variable	Variable	195.8	195.8	
Yearly Exported (kWh)	-	382,437	9,106	444,308	10,579	16.18%
Yearly Imported (kWh)	315,080	426,244	10,149	440,675	10,492	3.39%
Imported/Exported Balance (kWh)	-315,080	-43,807	-1,043	3,633	87	-108.29%
Yearly Generation (kWh)	-	578,348	13,770	625,789	14,900	8.20%
Yearly Loads (kWh)	315,080	622,156	14,813	622,156	14,813	0.00%
Load/Generation Balance (kWh)	-315,080	-1,200,504	-28,583	-1,247,944	-29,713	3.95%
On-site Solar Energy Use (kWh)	-	195,911	4,665	181,481	4,321	-7.37%
On-site Solar Energy Use (%)	-	33.87%	33.87%	29.00%	29.00%	-14.39%
Yearly LM	-	92.96%	92.96%	100.00%	100.58%	7.57%
System Initial Cost (\$)	\$0.00	\$1,680,840	\$40,020	\$1,437,540	\$34,227	-14.47%
Imported Grid Electricity (\$/year)	\$28,515	\$38,575	\$918	\$39,881	\$950	3.39%
Export Revenue (\$/year)	\$0.00	\$14,915	\$355	\$17,328	\$413	16.18%
Balance (\$/year)	\$28,515	\$23,660	\$563	\$22,553	\$537	-4.68%
Balance Inc. Admin. Fees (%/year)	\$28,810	\$23,955	\$570	\$22,848	\$544	-4.62%

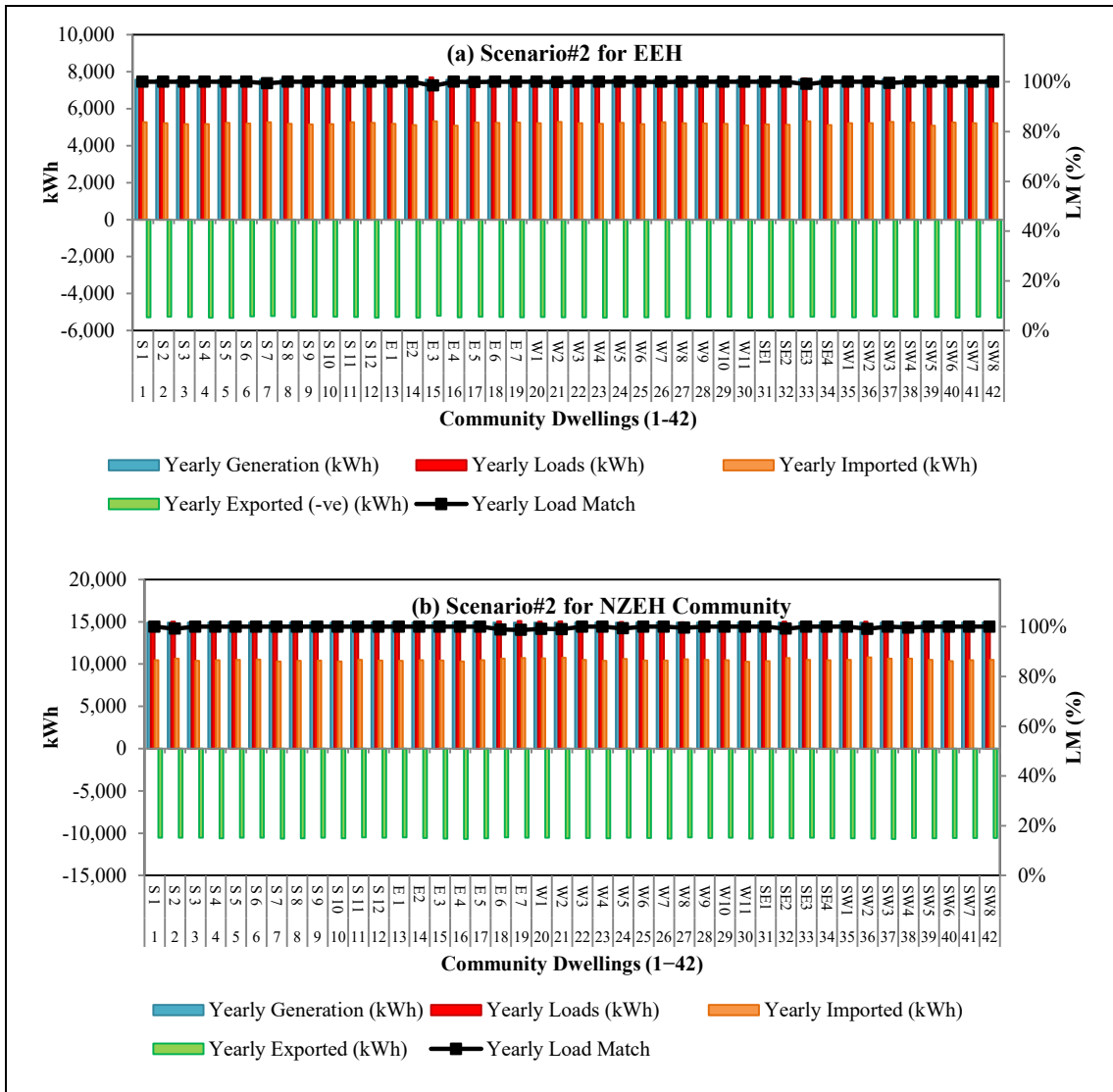


Figure 5-10. Energy profiles of the community dwellings after implementing the suggested solution for community shared solar PV application for the (a) EEH and (b) NZEH community.

Detailed comparisons of the current practice and suggested solutions for EEH and NZEH communities are provided in Table 5-5 and

Table 5-6. In general, it is found that the average PV sizing per dwelling is approximately 5.83 kW<sub>p</sub> and 11.41 kW<sub>p</sub>. Figure 5-10 demonstrates the potential implications on the energy performance of the communities under investigation by

implementing the proposed community shared solar PV solution where Figure 5-10a and Figure 5-10b represent the EEH and the NZEH communities, respectively. One of the advantages that can be observed in this figure is an even distribution of the generated electricity from the entire system. Shading, soiling, and layout constraint challenges can be overcome by such a solution.

## **5.7. Discussion and Conclusion**

### *5.7.1. Summary and Discussion*

The present study aims to investigate the viability of community shared solar application within a community consisting of a large group of dwellings under planning and design. One of the primary challenges for designing the solar PV system for future communities which are not built yet is that the consumption data is not yet available. In this regard, data from 11 dwellings (7 EEHs and 4 NZEHs) located in Edmonton, Alberta are collected in order to utilise this data for simulation purposes. Probability distribution simulation (or Monte Carlo simulation) technique is applied to simulate the statistical data rather than the deterministic values collected from the historical data in a discrete-event simulation (DES) platform. Two types of communities are simulated: NZEH and EEH communities. In order to investigate the viability of community shared solar application, two scenarios for pairwise comparison are considered: (1) the installation of behind-the-meter individual solar PV systems that adhere to the current local microgeneration installation practice, and (2) proposed large-scale community shared solar PV system that serves the entire community as one user and is distributed evenly among all users. Thus, an optimisation framework is developed using a data-driven approach that focuses on maximising the entire community's load-match rather than either maximising the annual solar PV energy production (i.e., south-facing system with the local latitude as a tilt angle) or simply applying the current common practices that conform to the commonly constructed roof-sloping practices (as in the first scenario).

The present study focuses on discovering methods of improvement for the body of knowledge of distributed energy generation practices coupled with residential communities, with the intent that the findings from this research will be addressed in future smart community developments. In the research presented in this thesis, data of a minutely temporal resolution from 7 EEHs and 4 NZEHs is used to feed the proposed framework; however, data of any available temporal resolution can be used. It should be taken into consideration that the greater the population and diversity of data samples, the more accurate the results will be in the sense that data with greater population results in more realistic probability density functions that will, in turn, reflect the most likely energy flow situations rather than the dependency on one or a few households.

Also, by collecting historical data from more households that are significantly diverse in shape, size, type, and age, more concrete conclusions will be determined. It is advisable to also expand the definition of “community” to include commercial and institutional buildings as well as street furniture. This way, the diverse load patterns will compensate the peak generation/load challenges and PV mismatch incurred by “only-residential” community shared solar societies.

Based on the presented research, it can be concluded that, since NZEHs rely on electricity for running the mechanical equipment, energy consumption fluctuations with relatively high frequency are, to a great extent, influenced by outdoor weather conditions, specifically in cold-climate regions. As for the present study, it is found that, on average, NZEHs consume double the electrical energy consumed by EEHs. Intuitively, while regarding the large-scale implementation of net-zero communities, stakeholders should practice caution regarding the hardware installation of the electricity grid and the design of the community shared solar energy system coupled with such communities. Another notable finding is that the self-consumption of individual households does not exceed 25% of the generated energy on average for the homes under investigation. This issue points to the need for future work on reducing as well as flattening the electrical energy demand of NZEHs (Awad et al., 2017b; Freitas et al., 2018).

It is observed that the community shared solar concept can be accompanied with fewer constraints regarding the layout design of the PV system, provided that the community dedicates a considerable area for renewable energy installations, not to mention the creation of a positive stigma among the community members by feeling a greater sense of responsibility towards the sustainable environment they are part of as concluded by Hanger et al. (2016). In the current study, the physical constraints such as space availability are not considered within its context. However, future work will consider the conclusions made by Awad et al. (2016) and Salim (2017) in order to implement the optimisation of solar PV systems in flat limited spaces.

In conformity with Awad et al. (2017b) and Litjens et al. (2017), results from the present study indicate that a properly-sized southwest-oriented PV system improves the load-match indicator by increasing the PV energy utilised on site and reducing the grid power demand for the community.

It should be noted that a PV system's tilt angle is dependent on the local latitude of the site under investigation; however, it is found that a tilt angle that is above or below the local latitude by approximately  $3^\circ$  coupled with a southwest-facing azimuth angle is the optimum scenario satisfying both environmental and economic criteria, regardless of geographic location. In specific, the optimal tilt angles for EEH and NZEH communities are found to be  $50^\circ$  (below the local latitude by  $3^\circ$ ) and  $56^\circ$  (above the local latitude by  $3^\circ$ ), respectively. Since NZEH communities depend solely on electricity (from either the grid or DERs) as the sole source of energy in which case the community demand peaks in winter, a relatively higher tilt angle is determined as the optimal solution for maximised self-consumption. It is also found that proper PV sizing is primarily dependent on the load/generation and import/export balance goals, secondarily taking into consideration criteria such as the given regulatory parameters and the economic feasibility of the system.

Intuitively, in order to ensure economical and environmentally-friendly energy usage in highly efficient self-consuming communities such as EEHs or NZEHs, community members should be actively engaged in the energy-saving process. Several strategies

can be suggested in this context, such as peak-shaving (or avoiding energy consumption at peak hours), applying delay/scheduled programs on wet appliances such as clothes dryers and washing machines and running them during peak generation hours, and considering smart devices such as sensor-based lighting and heating/cooling systems. In the present study, all monitored sites were built in the year 2012 or later and are rated as highly energy-efficient building envelopes; however, it should be noted that, when studying the energy profiles of older communities, the building envelopes of such communities should be investigated as this can be a major driver of high energy demand.

#### 5.7.2. *Conclusion, Limitations, and Recommendations*

In conclusion, it is found that community shared solar PV systems that are distributed evenly among the community members are effective for facilitating a net zero balance for the entire community. Two types of communities are simulated using a data-driven approach. It is found that, in general, the optimum layout placement of the proposed solar PV system for the EEH and NZEH communities is found to be [50.1°-tilt, 194°-azimuth] and [55.7°-tilt, 195.8°-azimuth], respectively, for the location of this study: Edmonton, Canada (53.44° N, 113.53° W). This finding also conforms to the findings found in Awad et al. (2017b) and Litjens et al. (2017). The proposed framework is systematic and can be used for simulations of both individual households and communities of any given size.

The present chapter contributes to the following areas:

- investigating the energy performance of two types of existing homes; energy-efficient homes (EEHs) and net-zero energy homes (NZEHs);
- highlighting the implications of housing type on the design of future sustainable communities;
- analysing the community shared solar design options of EEH and NZEH communities in terms of load match and grid interaction;

- developing a generic framework that simulates the energy demand of an entire community based on historical data from one or more households, with a high degree of accuracy (88% for EEH communities and 92% for NZEH communities);
- developing a generic framework that optimises the load-match-based layout design of community-shared solar PV systems in order to maximise self-consumption and minimise cost while achieving the community's net-zero balance; and
- comparing individual behind-the-meter micro-generating PV systems with community-shared solar practices using a real-life example of a local site under planning and design.

Findings from this study are informative for academics and land developers and can easily be implemented for future research and in practice at the pre-planning phase in order to achieve greener net-zero communities and/or community generation applications. Local storage practices are also highly recommended for consideration as another step toward flattening the load-generation balance and stimulating on-site energy utilisation. As another limitation to the current optimisation framework, the authors have assumed that each dwelling in the community is an independent setting and that neighbouring PV systems (if any) do not incur any significant energy exchange or interference. However, future work will account for this issue.

Future work will focus on multi-array layout placement at multiple orientations for maximised self-consumption. In light of the worldwide endeavors towards mitigating GHG emissions resulting from buildings, other community shared components will be considered in future work such as community energy storage, district heating systems, and plug-in electric vehicles (PEVs).

## Chapter 6: Summary, Conclusions and Recommendations for Future Research

### 6.1. Research Summary

Several challenges accompany solar PV applications on the residential level, such as determining an optimum size and layout design for best on-site self-consumption that conforms to the current local roof-sloping practices, especially in cold-climate regions. In addition, solar PVs installed in high-latitude regions encounter other challenges such as the seasonal variations and snow cover. Furthermore, greater challenges are encountered with the implementation of solar PVs into net-zero energy homes (NZEHS), which aim to provide electricity for the entire household energy demand.

In this context, the research presented in this thesis focuses on reducing the mutual negative impacts exchanged among NZEHs, solar PV microgeneration, and the utility grid by (a) developing a new solar PV design perspective referred to as “load-match-driven” design which, in turn, considers optimising the solar PV design to match the household energy load patterns rather than maximising its aggregated annual generation and (b) investigating the viability of community-scale shared solar PV systems in future sustainable communities. Hence, this study focuses on four key tasks in order to achieve its ultimate goal. First, the long-term performance of solar PV systems and household energy demand patterns of EEHs and NZEHs are investigated and analysed. Historical energy generation data from 85 solar PV sites in Alberta are collected at a five-minute temporal resolution and energy consumption data from 7 EEHs and 4 NZEHs in Edmonton is collected at a one-minute temporal resolution. Findings from this part of the study are summarised and used as input to the succeeding components of the thesis. Second, a prediction model is developed and validated to predict the daily energy generation of solar PV systems using Artificial Neural Network (ANN). The model is structured to predict the energy generation at

any higher latitude geographical location at any size and layout placement (i.e., tilt angle and azimuth angle) and is currently trained for Alberta. Snow adjustment factors are derived empirically and added to the ANN model so that the model can determine the impact of snow cover on the PV system's performance as a function of tilt angle and month of the year. In order to improve the self-consumption of solar PVs, it is essential to understand the household load patterns and, accordingly, design the solar PV to match these patterns. Intuitively, the third objective includes the development of a generic load-match-driven design optimisation framework in order to determine the optimum layout placement and sizing of a solar PV system by maximising the self-consumption rather than maximising the aggregated annual energy generation. Generalised reduced gradient (GRG) non-linear optimisation algorithm is used in this framework, while the framework itself is a hybrid composition of mathematical-based and data-driven approaches. Thus, the proposed framework can be implemented at any geographical location; however, the energy load data should be provided by the end-user since load patterns can differ significantly with the variability of location, weather, culture, and house type. Fourth, in light of society's increasing awareness and prosperous endeavors toward sustainable communities, the final objective of the present research is to investigate the community-scale application of solar PV systems—be it individual rooftop PVs or community shared solar PVs—integrated within EEH and NZEH communities. One of the greatest challenges of this part of the study is the realistic simulation of an entire community to mimic the stochastic nature of energy demand provided that historical data from only 11 homes is collected. Thus, a Monte Carlo simulation model is developed for the purpose of simulating the entire community using the probability distributions of the energy consumption data samples rather than the deterministic values. After simulating the energy consumption of an entire community, simulation output is implemented into the load-match-based optimisation framework in order to identify the optimum design of community-scale solar PV systems.

## **6.2. Research Contributions**

The research presented in this thesis contributes several additions to the body of knowledge of grid-tied solar PV systems integrated into net-zero energy homes and energy-efficient homes. Overall, the work presented in this thesis has contributed to developing new design methods of residential solar PV systems on the individual as well as the community levels from the load-match standpoint. The primary contributions of this research are summarised as follows:

### **Chapter 2:**

- Benchmarking of Solar PV generation and the EPBT and GHG emissions associated with solar PV installations by investigating the long-term performance analysis of 86 solar PV system sites located in 9 cities in Alberta—Edmonton, Calgary, Red Deer, Airdrie, Cochrane, Leduc, Sherwood Park, Sylvan Lake, and Lakeland County.
- Identifying the PV potential of solar PV systems in the above-mentioned cities and identifying the optimal layout placement for maximised aggregated energy generation.
- Quantifying the impacts of tilt angle, azimuth angle, and geographic location on the solar PV performance and GHG emissions in the above-mentioned cities.

### **Chapter 3:**

- Developing an Artificial Neural Network (ANN) model for predicting the energy generation of solar PV systems located in Alberta at large, placed at any two-way tilted surface, and at any time of the year.
- Deriving evidence-based snow adjustment factors empirically to quantify the impact of snow cover on solar PV systems at any given tilt angle at any time of the year. These factors are then fed into the ANN.
- Quantifying relevant performance parameters by conducting a correlation analysis in order to identify the solar PV dependency on such parameters.

#### **Chapter 4:**

- Developing a generic optimisation framework by which to identify a system's optimum layout placement and sizing with respect to maximising the system's self-consumption rather than maximising its aggregated annual generation.
- Quantifying the dependency of the overall performance of solar PV systems on layout placement (tilt angle and azimuth angle) by deriving an empirical polynomial equation using surface-fitting technique.
- Understanding the energy performance of energy-efficient homes (EEHs) and net-zero energy homes (NZEHs) in order to understand the implications of household electrification and to properly develop future net-zero energy communities.
- Quantifying the load-match and grid-interaction (LMGI) indicators of EEHs and NZEHs.

#### **Chapter 5:**

- Developing a generic framework to simulate the energy demand of an entire community based on historical data from one or more households, with a high degree of accuracy (88% for EEH communities and 92% for NZEH communities).
- Developing a generic framework to optimise the load-match-based layout design of community-shared solar PV systems in order to maximise its self-consumption and minimise its cost while achieving the community's net-zero balance.
- Comparing individual behind-the-meter micro-generating PV systems with community-shared solar practices using a real-life example of a local site under planning and design.
- Highlighting the implications of housing type on the design of future sustainable communities.
- Analysing the community shared solar design options of EEH and NZEH communities in terms of load match and grid interaction.

### 6.3. Limitations and Recommendations for Future Work

Despite the successful achievement of its goals, the research presented in this thesis is confronted by the following limitations:

- (1) Availability of historical meteorological data with high temporal and spatial resolution: Major parts of the proposed ANN solar PV prediction model in Chapter 3 are conducted by collecting historical meteorological data from publicly available online sources such as NASA and The Government of Canada at a daily temporal resolution and a  $1^\circ$  longitude by  $1^\circ$  latitude spatial resolution. Therefore, the highest possible prediction interval for the developed model currently is the daily energy generation.
- (2) Availability of historical energy consumption data for houses with variability in type, size, construction material or technology, and age: In Chapter 4 and Chapter 5, the developed optimisation frameworks are tested on detached single-family EEHs and NZEHs (both types built in 2012 or later). However, due to the hardship of obtaining such data, other housing types, such as multi-family apartment buildings, townhouses, semi-attached, modular, etc., are not included in this study.
- (3) Due to the limited availability of meteorological data at the desired temporal and spatial resolutions, clear-sky index and clear-sky PV power output at two-way tilted surface models are offered as a solution: Since the optimisation frameworks developed in Chapter 4 and Chapter 5 are primarily dependent on the data input of energy consumption and energy generation at the one-minute interval, the solar PV prediction model is not able to serve as input to the optimisation model as planned in the early stages of this study. Instead, a mathematical model is developed to estimate the PV power output at the one-minute interval.
- (4) Community simulation: Two communities, one consisting of EEHs and the other of NZEHs, are simulated in Chapter 5 based on data from 7 EEHs and 4

NZEHs. Intrinsicly, the probability distributions used to simulate the community energy demand may be skewed toward the user behaviour patterns of the monitored homes.

- (5) Due to the computational time constraints and for simplicity, historical energy consumption data is grouped by the hour of the day and the month of the year into 288 data sampling bins. Day type, such as weekday, weekend, and holiday, are not accounted for in this study, although the consideration of this attribute could enhance the simulation accuracy.

Based on the conclusions and limitations presented in this research thesis, a list of recommendations for future work are summarised as follows:

- (1) Four generic models are developed in this thesis to (1) predict the energy generation using ANN at the daily interval, (2) optimise the load-match-driven solar PV system's layout placement and sizing by using one-minute temporal resolution data, (3) simulate the community-scale household energy demand of individual dwellings at the hourly interval, and (4) optimise the load-match-driven design of community shared solar PV at the hourly interval. It is recommended that all four models be combined to autonomously carry out the solar PV assessments with minimal interaction from the end user.
- (2) The proposed framework for community energy demand is carried out by using a general-purpose template (GPT) in Symphony® simulation engine, and it is considered a solid foundation that can be expanded upon in order to consider the various components of a community regardless of its size. It is recommended to upgrade the simulation model from the static probabilistic simulation to continuous simulation in order to obtain near-realistic situations that would align with the dynamic complexity of the utility grid interactions. On the other hand, the proposed optimisation model is also generic since it is based on an analytical model and can be applied at any location around the globe.

- (3) Energy demand simulation framework will consider the variability of day type in the sense that weekdays, weekends, and holidays will be considered in the simulations to reflect the real-life energy demand patterns.

#### 6.3.1. *Comments on Building Research in the Context of Smart Grids*

Today, as a result of their integration into buildings and communities, renewable energy sources should be considered an integral part of the building and/or community, the building should be considered as a dynamic system, and the end-user should become a key player in the energy-saving process. Furthermore, as smart grid technology is emerging rapidly, the utility grid will soon transform from centralised to decentralised, accompanied by a transition from fossil-based to renewable-based energy sources. Having said that, these paradigmatic transformations will require advanced technologies integrated with artificial intelligence in order to involve the end-users in a proactive manner. It is expected that the findings from the present thesis will help reduce barriers to smart communities and smart grid infrastructure in the sense that the building- and/or community-integrated renewable energy sources will be designed and operated from a long-term optimised performance perspective. As an approach to future Smart Grid implementation, the research presented in this thesis is expected to contribute to reducing the impacts of residential solar PV microgeneration on the utility grid by means of improving the solar PV design approach and criteria. As a continuation to the current research, future work will focus on adding smart features to building components in order to ensure the end-user's involvement and active participation in the application of Smart Grid technology.

“Smart Grid” is defined as an electricity network that intelligently integrates generators and end-users to efficiently deliver electricity in a sufficient, accessible, safe, economic, reliable, efficient, and sustainable fashion (Banerjee et al., 2013; Phuangpornpitak and Tia, 2013). The key goal of a Smart Grid is to promote active customer participation and decision making and to create a flexible environment where both the utility and end-user can influence one another (Phuangpornpitak and

Tia, 2013). Camacho et al. (2011) study the control of renewable energy and the role of Smart Grids in addressing the problems associated with wind and solar energy applications. Smart Grid systems enable the integration of a wide range of technologies that could not be available in conventional grids such as, and not limited to, Advanced Metering Infrastructure (AMI) and Energy Management Systems (EMSs) (Camacho et al., 2011). Braun et al. (2011) provide a comprehensive review of current grid codes in some countries with high PV penetrations. The results of the present study conclude that the leading PV countries demonstrate diverse approaches regarding the grid interaction with PV integration; according to some countries, PV systems should perform in a highly passive manner, and according to others it is necessary to actively participate in grid control; a situation that, from the author's point of view, needs harmonisation. Phuangpornpitak and Tia (2013) showcase the opportunities and challenges of integrating renewable energy in Smart Grid systems through discussions on the role of renewable energy and distributed generation in Smart Grids, the concept of Smart Grid and its barriers and benefits, and finally pricing as a key factor in the success of renewable energy promotion. Previous studies exploring the renewable energy integration in Smart Grids include presenting the concept as well as the pros and cons of Smart Grids for renewable energy distributed generation (Gaviano et al., 2012; Sutabutr, 2016), Smart Grid technology adoption (Filho et al., 2009; Kohsri and Plangklang, 2011), optimal allocation of renewable energy sources in Smart Grid systems, and challenges of integrating renewable energy in Smart Grid systems (Alonso et al., 2012; Phuangpornpitak et al., 2010). As demonstrated in Table 6-1, in the Smart Grid research, a key role is being carried out by renewable integration, buildings, and control and monitoring in the interaction with end users (or prosumers) (Hovd, 2015). Stoll et al. (2013) investigate the interaction between the so-called "Active House" electricity consumer (resident) and the utility in Stockholm, Sweden. The concept aims at reducing the utilisation of electricity resulting in high CO<sub>2</sub> emissions, involving the customers in consumption control as well as cutting the overall electricity loads and local microgeneration.

Reka and Ramesh (2016) study the demand response modelling for residential consumers in the Smart Grid environment and develop a game-theory-based algorithm as Generalised Tit for Tat Dominant Game based Energy Scheduler. In the demand response concept, both the end-users (consumers) and utility grids become key players and consumers have to become tech-savvy in order to be economically and environmentally friendly (Reka and Ramesh, 2016). In the gaming environment, the user aims at minimising total cost. On the other hand, since utility administrations aims at reducing the demand at peak hours and the peak-to-average ratio, the utility company will announce the peak period, hence users will avoid consuming excessive electricity at peak times using demand response programs.

Table 6-1. Disciplines and domains for Smart Grid research (Source: Hovd, 2015).

Perspectives/Disciplines	Domains						
	Bulk Generation	Transmission	Distribution	Distributed Energy Resources (DER)	End users	Market	Society policies, regulation
Micro grids			x	x	x		x
Renewables integration			x	x	x	x	x
EV integration			x	x	x	x	x
Information and Communication Technologies	x	x	x	x	x	x	x
Buildings			x	x	x	x	x
Thermal energy		x	x	x	x	x	x
Business and services	x			x	x	x	x
User behaviour and acceptance			x	x	x	x	x
Control and monitoring		x	x	x	x	x	
Standardisation			x	x	x	x	x

Future work will include other aspects of the energy system such as local or community energy storage; district heating systems; other renewable energy sources such as geothermal, solar thermal, and wind; plug-in electric vehicles (PEVs); and home energy management systems (HEMS) which are primarily dependent on data-driven decision-making algorithms using the internet of things (IoT).

## References

- Abourizk, B.S.M., Member, A., Halpin, D.W., 1993. Statistical Properties of Construction Duration Data. *J. Constr. Eng. Manag.* 118, 525–544.
- AESO, 2017. *Microgeneration in Alberta*. Calgary, AB, Canada.
- Al-Amoudi, A., Zhang, L., 2000. Application of Radial Basis Function Networks for Solar-Array Modelling and Maximum Power-Point Prediction. *IEE* 147. doi:10.1049/ip-gtd:20000605
- Alberta Government, 2015. Renewable Energy will Power up to 30 Per Cent of Alberta's Electricity Grid by 2030 [WWW Document]. URL <http://www.alberta.ca/release.cfm?xID=389297B6E1245-F2DD-D96D-329E36A4573C598B> (accessed 9.23.16).
- Alluhaidah, B.M., Shehadeh, S.H., El-Hawary, M.E., 2014. Most Influential Variables for Solar Radiation Forecasting Using Artificial Neural Networks. 2014 IEEE Electr. Power Energy Conf. 71–75. doi:10.1109/EPEC.2014.36
- Almonacid, F., Rus, C., Pérez-Higueras, P., Hontoria, L., 2011. Calculation of the Energy Provided by a PV Generator. Comparative Study: Conventional Methods vs. Artificial Neural Networks. *Energy* 36, 375–384. doi:10.1016/j.energy.2010.10.028
- Alonso, M., Amaris, H., Alvarez-Ortega, C., 2012. Integration of Renewable Energy Sources in Smart Grids by Means of Evolutionary Optimization Algorithms. *Expert Syst. Appl.* 39, 5513–5522. doi:10.1016/j.eswa.2011.11.069
- Andrews, R.W., Pearce, J.M., 2012. Prediction of Energy Effects on Photovoltaic Systems due to Snowfall Events. *Conf. Rec. IEEE Photovolt. Spec. Conf.* 3386–3391. doi:10.1109/PVSC.2012.6318297
- Andrews, R.W., Pollard, A., Pearce, J.M., 2013. The Effects of Snowfall on Solar Photovoltaic Performance. *Sol. Energy* 92, 84–97.

doi:10.1016/j.solener.2013.02.014

Andrews, R.W., Pollard, A., Pearce, J.M., 2013. A New Method to Determine the Effects of Hydrodynamic Surface Coatings on the Snow Shedding Effectiveness of Solar Photovoltaic Modules. *Sol. Energy Mater. Sol. Cells* 113, 71–78. doi:10.1016/j.solmat.2013.01.032

Antonanzas, J., Osorio, N., Escobar, R., Urraca, R., Martinez-de-Pison, F.J., Antonanzas-Torres, F., 2016. Review of Photovoltaic Power Forecasting. *Sol. Energy* 136, 78–111. doi:10.1016/j.solener.2016.06.069

Askarzadeh, A., 2013. Voltage Prediction of a Photovoltaic Module using Artificial Neural Networks. *Int. Trans. Electr. Energ. Syst.* 24, 1715–1725. doi:10.1002/etep.1799

Augustine, P., 2015. The Time is Right for Utilities to Develop Community Shared Solar Programs. *Electr. J.* 28, 107–108. doi:10.1016/j.tej.2015.11.010

Awad, H., Gül, M., Ritter, C., Verma, P., Chen, Y., Salim, K.M.E., Al-Hussein, M., Yu, H., Kasawski, K., 2016. Solar Photovoltaic Optimization for Commercial Flat Roof Tops in Cold Regions, in: 4th IEEE Conference on Technologies for Sustainability (SusTech). Phoe.

Awad, H., Gül, M., Salim, K.M.E., Yu, H., 2017a. Predicting the Energy Production by Solar Photovoltaic Systems in Cold-Climate Regions. *Int. J. Sustain. Energy* 1–21. doi:10.1080/14786451.2017.1408622

Awad, H., Gül, M., Yu, H., 2017b. Load-match-Driven Design Improvement of Solar PV Systems and Its Impact on the Grid with a Case Study, in: 5th IEEE Conference on Technologies for Sustainability (SusTech). IEEE Xplore, Phoenix, AZ, USA.

Ayompe, L.M., Duffy, A., McCormack, S.J., Conlon, M., 2011. Measured performance of a 1.72 kW rooftop grid connected photovoltaic system in Ireland. *Energy Convers. Manag.* 52, 816–825. doi:10.1016/j.enconman.2010.08.007

- Azadeh, A., Maghsoudi, A., Sohrabkhani, S., 2009. An Integrated Artificial Neural Networks Approach for Predicting Global Radiation. *Energy Convers. Manag.* 50, 1497–1505. doi:10.1016/j.enconman.2009.02.019
- Badescu, V., 2008. *Modeling Solar Radiation at the Earth ' s Surface*. Springer. doi:10.1007/978-3-540-77455-6
- Badescu, V., 1998. Verification of Some Very Simple Clear and Cloudy Sky Models to Evaluate Global Solar Irradiance. *Sol. Energy* 61, 251–264. doi:10.1016/S0038-092X(97)00057-1
- Banerjee, S., Meshram, A., Swamy, N.K., 2013. Integration of Renewable Energy Sources in Smart Grid : a Review. *Int. J. Sci. Res.* 50, 311–327.
- Banks, J., Carson II, J.S., Nelson, B.L., Nicol, D.M., 2009. *Discrete-Event System Simulation*, 5th editio. ed.
- Barbour, E., Parra, D., Awwad, Z., González, M.C., 2018. Community Energy Storage: A Smart Choice for the Smart Grid? *Appl. Energy* 212, 489–497. doi:10.1016/j.apenergy.2017.12.056
- Becker, G., Schiebelsberger, B., Weber, W., Vodermayr, C., Zehner, M., Kummerle, G., 2006. An Approach to the Impact of Snow on the Yield of Grid Connected PV Systems, in: *21st EU PVSEC*.
- Bernardo, L.R., Perers, B., Håkansson, H., Karlsson, B., 2011. Performance Evaluation of Low Concentrating Photovoltaic/Thermal Systems: A Case Study from Sweden. *Sol. Energy* 85, 1499–1510. doi:10.1016/j.solener.2011.04.006
- Bhandari, K.P., Collier, J.M., Ellingson, R.J., Apul, D.S., 2015. Energy Payback Time (EPBT) and Energy Return on Energy Invested (EROI) of Solar Photovoltaic Systems: A Systematic Review and Meta-analysis. *Renew. Sustain. Energy Rev.* 47, 133–141. doi:10.1016/j.rser.2015.02.057
- Bhargava, A.K., Garg, H.P., Agarwal, R.K., 1991. Study of a Hybrid Solar System— Solar Air Heater Combined with Solar Cells. *Energy Convers. Manag.* 31, 471–

479. doi:10.1016/0196-8904(91)90028-H

Braun, H., 2012. Signal Processing for Solar Array Monitoring , Fault Detection , and Optimization. Morgan & Claypool. doi:10.2200/S00425ED1V01Y201206PEL004

Braun, M., Stetz, T., Bründlinger, R., Mayr, C., Ogimoto, K., Hatta, H., Kobayashi, H., Kroposki, B., Mather, B., Coddington, M., Lynn, K., Graditi, G., Woyte, A., MacGill, I., 2011. Is the Distribution Grid Ready to Accept Large-Scale Photovoltaic Deployment? State of the Art, Progress, and Future Prospects. Prog. Photovolt Res. Appl. 20, 681–697. doi:10.1002/pip

Braunstein, A., Kornfeld, A., 1986. On the Development of the Solar Photovoltaic and Thermal (PVT) Collector. IEEE Trans. Energy Convers. EC-1, 31–33. doi:10.1109/TEC.1986.4765770

Cai, Y.P., Huang, G.H., Tan, Q., Yang, Z.F., 2009a. Planning of Community-Scale Renewable Energy Management Systems in a Mixed Stochastic and Fuzzy Environment. Renew. Energy 34, 1833–1847. doi:10.1016/j.renene.2008.11.024

Cai, Y.P., Huang, G.H., Yang, Z.F., Lin, Q.G., Tan, Q., 2009b. Community-Scale Renewable Energy Systems Planning Under Uncertainty-An Interval Chance-Constrained Programming Approach. Renew. Sustain. Energy Rev. 13, 721–735. doi:10.1016/j.rser.2008.01.008

California Department of Forestry and Fire Protection, 2008. Solar Photovoltaic Installation Guideline. California.

Camacho, E.F., Samad, T., Garcia-Sanz, M., Hiskens, I., 2011. Control for Renewable Energy and Smart Grids. Impact Control Technol. 1, 1–20.

Canadian Solar, 2013. CanadianSolar CS6P-250M. San Ramon, CA.

Casaca de Rocha Vaz, A.G., 2014. Photovoltaic Forecasting with Artificial Neural Network. Fac. CIÊNCIAS\DEPARTAMENTO Eng. GEOGRÁFICA, GEOFÍSICA E Energ.

- CCEMC, 2016. Large Scale Building Integrated Solar PV Demonstration in Production Housing [WWW Document]. URL <http://ccec.ca/project/integrated-solar-pv-demonstration-in-production-housing/> (accessed 9.21.16).
- Celik, I., Philips, A.B., Song, Z., Yan, Y., Ellingson, R.J., Heben, M.J., Apul, D., 2018. Energy Payback Time (EPBT) and Energy Return on Energy Invested (EROI) of Perovskite Tandem Photovoltaic Solar Cells. *IEEE J. Photovoltaics* 8, 305–309. doi:10.1109/JPHOTOV.2017.2768961
- Chan, G., Evans, I., Grimley, M., Ihde, B., Mazumder, P., 2017. Design Choices and Equity Implications of Community Shared Solar. *Electr. J.* 30, 37–41. doi:10.1016/j.tej.2017.10.006
- Chen, C., Duan, S., Cai, T., Liu, B., 2011. Online 24-h Solar Power Forecasting Based on Weather Type Classification Using Artificial Neural Network. *Sol. Energy* 85, 2856–2870. doi:10.1016/j.solener.2011.08.027
- Chow, T.T., 2010. A Review on Photovoltaic/Thermal Hybrid Solar Technology. *Appl. Energy* 87, 365–379. doi:10.1016/j.apenergy.2009.06.037
- Coimbra, C.F.M., Kleissl, J., Marquez, R., 2013. Overview of Solar-Forecasting Methods and a Metric for Accuracy Evaluation. *Sol. Energy Forecast. Resour. Assess.* 171–194. doi:10.1016/B978-0-12-397177-7.00008-5
- Coit, D.W., Jackson, B.T., Smith, A.E., 1998. Static Neural Network Process Models: Considerations and Case Studies. *Int. J. Prod. Res.* 36, 2953–2967. doi:10.1080/002075498192229
- Conergy, 2016. Conergy [WWW Document]. URL <http://www.conergy.com/en> (accessed 9.27.16).
- Cox, C.H., Raghuraman, P., 1985. Design Considerations for Flat-plate-Photovoltaic/Thermal Collectors. *Sol. Energy* 35, 227–241. doi:10.1016/0038-092X(85)90102-1

- da Silva, R.M.M., Fernandes, J.L.M.L.M., 2010. Hybrid Photovoltaic/Thermal (PV/T) Solar Systems Simulation with Simulink/Matlab. *Sol. Energy* 84, 1985–1996. doi:10.1016/j.solener.2010.10.004
- Daneshyar, M., 1978. Solar Radiation Statistics for Iran. *Sol. Energy* 21, 345–349. doi:10.1016/0038-092X(78)90013-0
- Darghouth, N.R., Barbose, G., Wiser, R., 2011. The Impact of Rate Design and Net Metering on the Bill Savings from Distributed PV for Residential Customers in California. *Energy Policy* 39, 5243–5253. doi:10.1016/j.enpol.2011.05.040
- Darhmaoui, H., Lahjouji, D., 2013. Latitude Based Model for Tilt Angle Optimization for Solar Collectors in the Mediterranean Region. *Energy Procedia* 42, 426–435. doi:10.1016/j.egypro.2013.11.043
- De Oliveira Siqueira, A.M., Gomes, P.E.N., Torrezani, L., Lucas, E.O., Da Cruz Pereira, G.M., 2014. Heat Transfer Analysis and Modeling of a Parabolic Trough Solar Collector: An Analysis. *Energy Procedia* 57, 401–410. doi:10.1016/j.egypro.2014.10.193
- Decker, B., Jahn, U., 1997. Performance of 170 Grid Connected PV Plants in Northern Germany - Analysis of Yields and Optimization Potentials. *Sol. Energy* 59, 127–133. doi:10.1016/S0038-092X(96)00132-6
- Delisle, V.V., Kummert, M.M., 2014. A Novel Approach to Compare Building-Integrated Photovoltaics/Thermal Air Collectors to Side-by-Side PV Modules and Solar Thermal Collectors. *Sol. Energy* 100, 50–65. doi:10.1016/j.solener.2013.09.040
- Deng, S., Wang, R.Z., Dai, Y.J., 2014. How to Evaluate Performance of Net Zero Energy Building - A Literature Research. *Energy* 71, 1–16. doi:10.1016/j.energy.2014.05.007
- Denholm, P., O'Connell, M., Brinkman, G., Jorgenson, J., 2015. Overgeneration from Solar Energy in California: A Field Guide to the Duck Chart (NREL/TP-6A20-65023) 46.

- Ding, M., Wang, L., Bi, R., 2011. An ANN-Based Approach for Forecasting the Power Output of Photovoltaic System. *Procedia Environ. Sci.* 11, 1308–1315. doi:10.1016/j.proenv.2011.12.196
- Do, M.-T., Soubdhan, T., Benoît Robyns, 2016. A Study on the Minimum Duration of Training Data to Provide a High Accuracy Forecast for PV Generation Between Two Different Climatic Zones. *Renew. Energy* 85, 959–964. doi:10.1016/j.renene.2015.07.057
- Dobos, A., 2014. PVWatts. doi:10.2172/1158421
- E Knapp, K., L Jester, T., 2000. Initial Empirical Results for the Energy Payback Time of Photovoltaic Modules, in: *Proceedings of the 16th European Photovoltaic Solar Energy Conference*. Glasgow, UK.
- eGauge Systems, 2017. eGauge Systems.
- EIA, 2016. *Annual Energy Outlook 2016 with Projections to 2040*. Washington, DC.
- Elliot, S., 2017. Carbon Emissions and the Canadian Electricity Sector [WWW Document]. *Can. Energy Law*.
- Energy Informative, 2016. How Much do Solar Panels Cost [WWW Document]. URL <http://energyinformative.org/solar-panels-cost/> (accessed 4.4.16).
- Engerer, N.A., Mills, F.P., 2015. KPV: A Clear-Sky Index for Photovoltaics. *Sol. Energy* 1–8.
- “Enphase Energy Inc.,” 2016. Enlighten Enphase Energy [WWW Document]. URL <https://enlighten.enphaseenergy.com/> (accessed 9.27.16).
- Enphase System, 2017. Envoy.
- Environment Canada, 2017. Alberta - Weather Conditions and Forecast by Locations [WWW Document]. Gov. Canada. URL [https://weather.gc.ca/forecast/canada/index\\_e.html?id=AB](https://weather.gc.ca/forecast/canada/index_e.html?id=AB) (accessed 7.11.17).
- Esfahani, M.N., 2013. Carbon Footprint Assessment of the Pre-Panelized Construction Process. University of Alberta.

- Farahbakhsh, H., Ugursal, V.I., Fung, A.S., 1998. A Residential End-Use Energy Consumption Model for Canada. *Int. J. Energy Res.* 22, 1133–1143. doi:10.1002/(SICI)1099-114X(19981025)22:13<1133::AID-ER434>3.0.CO;2-E
- Filho, J.C.R., Affonso, C.M., Oliveira, R.C.L., 2009. Pricing Analysis in the Brazilian Energy Market: a Decision Tree Approach, in: *IEEE Bucharest Power Tech Conference*. Bucharest, Romania, pp. 1–6.
- Freitas, S., Reinhart, C., Brito, M.C., 2018. Minimizing Storage Needs for Large Scale Photovoltaics in the Urban Environment. *Sol. Energy* 159, 375–389. doi:10.1016/j.solener.2017.11.011
- Fthenakis, V., Mason, J.E., Zweibel, K., 2009. The Technical, Geographical, and Economic Feasibility for Solar Energy to Supply the Energy Needs of the US. *Energy Policy* 37, 387–399. doi:10.1016/j.enpol.2008.08.011
- Fujisawa, T., Tani, T., 1997. Annual Exergy Evaluation on Photovoltaic-Thermal Hybrid Collector. *Sol. Energy Mater. Sol. Cells* 47, 135–148. doi:10.1016/S0927-0248(97)00034-2
- Futurism, 2016. Solar Panels Roll-like Carpet Can Save Lives [WWW Document]. URL <http://futurism.com/videos/solar-panels-roll-like-carpet-can-save-lives/> (accessed 4.5.16).
- Gaviano, A., Weber, K., Dirmeier, C., 2012. Challenges and Integration of PV and Wind Energy Facilities from a Smart Grid Point of View. *Energy Procedia* 25, 118–125. doi:10.1016/j.egypro.2012.07.016
- Government of Canada, 2017. Edmonton, Alberta Climate [WWW Document]. Gov. Canada. URL [http://climate.weather.gc.ca/climateData/dailydata\\_e.html?StationID=31427&Month=4&Day=1&Year=2015&timeframe=2](http://climate.weather.gc.ca/climateData/dailydata_e.html?StationID=31427&Month=4&Day=1&Year=2015&timeframe=2) (accessed 2.10.17).
- Grana, P., Gibbs, P., 2015. The 3 Best Ways to Optimize a Commercial PV System [WWW Document]. 3 Best Ways to Optim. a Commer. PV Syst. URL <http://www.greentechmedia.com/articles/read/The-3-Best-Ways-to-Optimize-a->

- Commercial-PV-System (accessed 5.5.16).
- Hachem-Vermette, C., Cubi, E., Bergerson, J., 2016. Energy Performance of a Solar Mixed-Use Community. *Sustain. Cities Soc.* 27, 145–151. doi:10.1016/j.scs.2015.08.002
- Hajjar, D., Abourizk, S., 1996. Building a Special Purpose Simulation Tool for Earth Moving Operations, in: *Winter Simulation Conference*. pp. 1313–1320. doi:10.1145/256562.256955
- Hanger, S., Komendantova, N., Schinke, B., Zejli, D., Ihlal, A., Patt, A., 2016. Community Acceptance of Large-Scale Solar Energy Installations in Developing countries: Evidence from Morocco. *Energy Res. Soc. Sci.* 14, 80–89. doi:10.1016/j.erss.2016.01.010
- Hassan, Q.K., Rahman, K.M., Haque, A.S., Ali, A., 2011. Solar Energy Modelling over a Residential Community in the City of Calgary, Alberta, Canada. *Int. J. Photoenergy* 2011. doi:10.1155/2011/216519
- Heliene Inc., 2017. Heliene 60-Cell 280 Monocrystalline Silicon Module. Ontario.
- Hestnes, A.G., 1999. Building Integration Of Solar Energy Systems. *Sol. Energy* 67, 181–187. doi:10.1016/S0038-092X(00)00065-7
- Hicks, J., Ison, N., 2018. An Exploration of the Boundaries of “Community” in Community Renewable Energy Projects: Navigating Between Motivations and Context. *Energy Policy* 113, 523–534. doi:10.1016/j.enpol.2017.10.031
- Homer Energy, 2015. Hybrid Optimization Model for Electric Renewables [WWW Document]. URL <https://www.homerenergy.com/> (accessed 2.5.18).
- Hovd, M., 2015. Norwegian Smart Grid Research Strategy.
- Huang, B., Lin, T., Hung, W., Sun, F., 2001. Performance Evaluation of Solar Photovoltaic/Thermal Systems. *Sol. Energy* 70, 443–448. doi:10.1016/S0038-092X(00)00153-5
- Hussein, H.M.S., Ahmad, G.E., El-Ghetany, H.H., 2004. Performance evaluation of

- photovoltaic modules at different tilt angles and orientations. *Energy Convers. Manag.* 45, 2441–2452. doi:10.1016/j.enconman.2003.11.013
- Hyundai, 2010. Hyundai Solar Module. Seoul.
- Ibrahim, A., Othman, M.Y., Ruslan, M.H., Mat, S., Sopian, K., 2011. Recent Advances in Flat Plate Photovoltaic/Thermal (PV/T) Solar Collectors. *Renew. Sustain. Energy Rev.* 15, 352–365. doi:10.1016/j.rser.2010.09.024
- IEA, 2014. Canada Final Consumption (2014) [WWW Document]. URL [http://www.iea.org/sankey/#?c=Canada&s=Final consumption](http://www.iea.org/sankey/#?c=Canada&s=Final%20consumption) (accessed 9.21.16).
- Inman, R.H., Pedro, H.T.C., Coimbra, C.F.M., 2013. Solar Forecasting Methods for Renewable Energy Integration. *Prog. Energy Combust. Sci.* 39, 535–576. doi:10.1016/j.pecs.2013.06.002
- International Energy Agency IEA, 2014. World Final Consumption (2014) [WWW Document]. Int. Energy Agency. URL [https://www.iea.org/sankey/#?c=World&s=Final consumption](https://www.iea.org/sankey/#?c=World&s=Final%20consumption) (accessed 2.2.17).
- Iwafune, Y., Yagita, Y., Ogimoto, K., 2010. Estimation of Appliance Electricity Consumption by Monitoring Currents on Residential Distribution Boards. 2010 Int. Conf. Power Syst. Technol. Technol. Innov. Mak. Power Grid Smarter, POWERCON2010 1–6. doi:10.1109/POWERCON.2010.5666076
- JA Solar, 2015. JAM6 60 250-270 Monocrystalline Silicon Module. Shanghai.
- Jahn, U., Nasse, W., 2003. Performance Analysis and Reliability of Grid-connected PV Systems in IEA Countries, in: 3rd World Conference on Photovoltaic Energy Conversion. Osaka, Japan, pp. 3–6.
- Jakica, N., 2018. State-of-the-Art Review of Solar Design Tools and Methods for Assessing Daylighting and Solar Potential for Building-Integrated Photovoltaics. *Renew. Sustain. Energy Rev.* 81, 1296–1328. doi:10.1016/j.rser.2017.05.080
- Jin, Z., Yezheng, W., Gang, Y., 2005. General Formula for Estimation of Monthly

- Average Daily Global Solar Radiation in China. *Energy Convers. Manag.* 46, 257–268. doi:10.1016/j.enconman.2004.02.020
- Jones, K.B., Bennett, E.C., Ji, F.W., Kazerooni, B., 2017. Chapter 4 – Beyond Community Solar: Aggregating Local Distributed Resources for Resilience and Sustainability, in: *Innovation and Disruption at the Grid's Edge*. Elsevier Inc., South Royalton, VT, USA, pp. 65–81. doi:10.1016/B978-0-12-811758-3.00004-8
- Joshi, A.S., Dincer, I., Reddy, B. V., 2009. Performance analysis of photovoltaic systems: A review. *Renew. Sustain. Energy Rev.* 13, 1884–1897. doi:10.1016/j.rser.2009.01.009
- Kacira, M., Simsek, M., Babur, Y., Demirkol, S., 2004. Determining Optimum Tilt Angles and Orientations of Photovoltaic Panels in Sanliurfa, Turkey. *Renew. Energy* 29, 1265–1275. doi:10.1016/j.renene.2003.12.014
- Kaddoura, T.O., Ramli, M.A.M., Al-turki, Y.A., 2016. On the Estimation of the Optimum Tilt Angle of PV Panel in Saudi Arabia. *Renew. Sustain. Energy Rev.* 65, 626–634. doi:10.1016/j.rser.2016.07.032
- Kalogirou, S.A., 2001. Use a TRNSYS for Modelling and Simulation of a Hybrid PV-Thermal Solar System for Cyprus. *Renew. Energy* 23, 247–260. doi:10.1016/S0960-1481(00)00176-2
- Katiraei, F., 2011. Solar PV Integration Challenges. *Ieee Power Energy Mag.* 62–71. doi:10.1109/MPE.2011.940579
- Kato, K., Murata, A., Sakuta, K., 1998. Energy Pay-back Time and Life-cycle CO<sub>2</sub> Emission of Residential PV Power System with Silicon PV Module. *Prog. Photovoltaics Res. Appl.* 6, 105–115. doi:10.1002/(sici)1099-159x(199803/04)6:2<105::aid-pip212>3.3.co;2-3
- Knapp, K., Jester, T., 2001. Empirical Investigation of the Energy Payback Time for Photovoltaic Modules. *Sol. Energy* 71, 165–172. doi:10.1016/S0038-092X(01)00033-0

- Kohsri, S., Plangklang, B., 2011. Energy Management and Control System for Smart Renewable Energy Remote Power Generation. *Energy Procedia* 9, 198–206. doi:10.1016/j.egypro.2011.09.021
- Kraemer, D., Poudel, B., Feng, H.-P., Caylor, J.C., Yu, B., Yan, X., Ma, Y., Wang, X., Wang, D., Muto, A., McEnaney, K., Chiesa, M., Ren, Z., Chen, G., 2011. High-Performance Flat-Panel Solar Thermoelectric Generators with High Thermal Concentration. *Nat. Mater.* 10, 532–538. doi:10.1038/nmat3013
- Kreider, J.F., Hoogendoorn, C.J., Kreith, F., 1989. *Solar Design: Components, Systems, Economics*. Hemisphere Pub. Corp., New York.
- Krenker, A., Bešter, J., Kos, A., 2011. Introduction to the Artificial Neural Networks. *Eur. J. Gastroenterol. Hepatol.* 19, 1046–1054. doi:10.1097/MEG.0b013e3282f198a0
- Krömer, P., Musilek, P., Rodway, J., Reformat, M., Prauzek, M., 2015. Estimating Harvestable Solar Energy from Atmospheric Pressure Using Support Vector Regression. *Proc. - 2015 Int. Conf. Intell. Netw. Collab. Syst. IEEE INCoS 2015*. doi:10.1109/INCoS.2015.58
- Kumar, R., Rosen, M.A., 2011. Performance Evaluation of a Double Pass PV/T Solar Air Heater with and without Fins. *Appl. Therm. Eng.* 31, 1402–1410. doi:10.1016/j.applthermaleng.2010.12.037
- Laleman, R., Albrecht, J., Dewulf, J., 2011. Life Cycle Analysis to Estimate the Environmental Impact of Residential Photovoltaic Systems in Regions with a Low Solar Irradiation. *Renew. Sustain. Energy Rev.* 15, 267–271. doi:10.1016/j.rser.2010.09.025
- Lasdon, L.S., Fox, R.L., Ratner, M.W., 1974. Nonlinear Optimization Using the Generalized Reduced Gradient Method. *Rev. française d'Automatique, Inform. Rech. opérationelle* 3.
- Leach, A., Adams, A., Cairns, S., Coady, L., Lambert, G., 2015. *Climate Leadership: Report to Minister*. Alberta, Canada.

- Leloux, J., Narvarte, L., Trebosc, D., 2012. Review of the Performance of Residential PV Systems in Belgium. *Renew. Sustain. Energy Rev.* 16, 178–184. doi:10.1016/j.rser.2011.07.145
- Leng, G.J., 1998. Renewable Energy Technologies Project Assessment Tool: RETScreen.
- Leuphana University Lüneburg and Trend: research, Institut/Leuphana Universität Lüneburg, 2013. Definition und Marktanalyse von Bürgerenergie in Deutschland. Bremen.
- Lewis, N., 2010. Energy Tutorial : Solar Energy 101.
- Li, H.X., 2016. Analysis of NetZero Energy Homes (NZEHS): Stakeholders, Design, and Performance. University of Alberta.
- Li, H.X., Gül, M., Yu, H., Awad, H., Al-Hussein, M., 2016. An Energy Performance Monitoring, Analysis and Modelling Framework for NetZero Energy Homes (NZEHS). *Energy Build.* 126. doi:10.1016/j.enbuild.2016.05.041
- Li, Y., Wen, Z., Cao, Y., Tan, Y., Sidorov, D., Panasetky, D., 2017. A Combined Forecasting Approach with Model Self-Adjustment for Renewable Generations and Energy Loads in Smart Community. *Energy* 129, 216–227. doi:10.1016/j.energy.2017.04.032
- Linak, 2016. Solar Tracking [WWW Document]. URL <http://www.solar-tracking.com/> (accessed 4.5.16).
- Litjens, G.B.M.A., Worrell, E., van Sark, W.G.J.H.M., 2017. Influence of Demand Patterns on the Optimal Orientation of Photovoltaic Systems. *Sol. Energy* 155, 1002–1014. doi:10.1016/j.solener.2017.07.006
- Louwen, A., Van Sark, W.G.J.H.M., Faaij, A.P.C., Schropp, R.E.I., 2016. Re-assessment of Net Energy Production and Greenhouse Gas Emissions Avoidance after 40 Years of Photovoltaics Development. *Nat. Commun.* 7, 1–9. doi:10.1038/ncomms13728

- Luthander, R., Widén, J., Nilsson, D., Palm, J., 2015. Photovoltaic self-consumption in buildings: A review. *Appl. Energy* 142, 80–94. doi:10.1016/j.apenergy.2014.12.028
- Mahmoud, M., Nabhan, I., 1990. Determination of Optimum Tilt Angle of Single and Multi Rows of Photovoltaic Arrays for Selected Sites in Jordan. *Sol. Wind Technol.* 7, 739–745.
- Mandal, P., Madhira, S.T.S., haque, A.U., Meng, J., Pineda, R.L., 2012. Forecasting Power Output of Solar Photovoltaic System Using Wavelet Transform and Artificial Intelligence Techniques. *Procedia Comput. Sci.* 12, 332–337. doi:10.1016/j.procs.2012.09.080
- Marion, B., Adelstein, J., Boyle, K., Hayden, H., Hammond, B., Fletcher, T., Narang, D., Kimber, A., Mitchell, L., Richter, S., Hadyen, H., Hammond, B., Flechter, T., 2005. Performance Parameters for Grid-Connected PV Systems, in: *Proceedings of Photovoltaic Specialists Conference. IEEE Xplore, Lake Buena Vista, FL, USA*, pp. 1601–1606. doi:10.1109/PVSC.2005.1488451
- Marion, B., Rodri, J., Pruet, J., 2009. Instrumentation for Evaluating PV System Performance Losses from Snow Preprint. *Natl. Sol. Conf. (SOLAR 2009)* 1–6.
- Marion, B., Schaefer, R., Caine, H., Sanchez, G., 2013. Measured and Modeled Photovoltaic System Energy Losses from Snow for Colorado and Wisconsin Locations. *Sol. Energy* 97, 112–121. doi:10.1016/j.solener.2013.07.029
- Marique, A.F., Reiter, S., 2014. A Simplified Framework to Assess the Feasibility of Zero-Energy at the Neighbourhood/Community Scale. *Energy Build.* 82, 114–122. doi:10.1016/j.enbuild.2014.07.006
- Marquez, R., Coimbra, C.F.M., 2012. Proposed Metric for Evaluation of Solar Forecasting Models. *J. Sol. Energy Eng.* 135, 11016. doi:10.1115/1.4007496
- Mathiesen, P., Kleissl, J., 2011. Evaluation of Numerical Weather Prediction for Intra-Day Solar Forecasting in the Continental United States. *Sol. Energy* 85, 967–977. doi:10.1016/j.solener.2011.02.013

- Mellit, A., 2008. Artificial Intelligence Technique for Modelling and Forecasting of Solar Radiation Data: A Review. *Int. J. Artif. Intell. Soft Comput.* 1, 52–76.
- Mellit, A., Pavan, A.M., 2010. A 24-H Forecast of Solar Irradiance Using Artificial Neural Network: Application for Performance Prediction of a Grid-Connected PV Plant at Trieste, Italy. *Sol. Energy* 84, 807–821. doi:10.1016/j.solener.2010.02.006
- Moghadam, H., Tabrizi, F.F., Sharak, A.Z., 2011. Optimization of Solar Flat Collector Inclination. *Desalination* 265, 107–111. doi:10.1016/j.desal.2010.07.039
- Mondol, J.D., Yohanis, Y., Smyth, M., Norton, B., 2006. Long Term Performance Analysis of a Grid Connected Photovoltaic System in Northern Ireland. *Energy Convers. Manag.* 47, 2925–2947. doi:10.1016/j.enconman.2006.03.026
- Mondol, J.D., Yohanis, Y.G., Norton, B., 2007. Comparison of Measured and Predicted Long Term Performance of Grid a Connected Photovoltaic System. *Energy Convers. Manag.* 48, 1065–1080. doi:10.1016/j.enconman.2006.10.021
- Mondol, J.D., Yohanis, Y.G., Smyth, M., Norton, B., 2005. Long-term validated simulation of a building integrated photovoltaic system. *Sol. Energy* 78, 163–176. doi:10.1016/j.solener.2004.04.021
- Mondol, J.D., Yohanis, Y.G., Smyth, M., Norton, B., Commission, I.E., Kisan, M., Sangathan, S., Nehru, J., Mondol, J.D., Yohanis, Y.G., Smyth, M., Norton, B., Ayompe, L.M., Duffy, A., McCormack, S.J., Conlon, M., Sugiura, T., Yamada, T., Nakamura, H., Umeya, M., Sakuta, K., Kurokawa, K., Skoplaki, E., Palyvos, J.A., Chang, Y.P., Moghadam, H., Tabrizi, F.F., Sharak, A.Z., Shariah, A., Al-Akhras, M.A., Al-Omari, I.A., Jahn, U., Nasse, W., Decker, S.E., Gmbh, M., Joshi, A.S., Dincer, I., Reddy, B. V., Hussein, H.M.S., Ahmad, G.E., El-Ghetany, H.H., Pless, S., Deru, M., Torcellini, P., Hayter, S., Drews, A., Beyer, H.G., Rindelhardt, U., 1998. Photovoltaic System Performance Monitoring — Guidelines for Measurement, Data Exchange and Analysis, Solar Photovoltaic

Energy Systems Sectional Committee. Elsevier Ltd.  
doi:10.1016/j.solener.2008.04.009

Nadkarni, K., Hastings-simon, S., 2017. Organizing and Owning Community Solar PV Projects, Alberta Community Solar Guide. Calgary.

NAIT, 2015. Solar Photovoltaic Reference Array Report. Edmonton, Alberta.

Naraghi, M.H., 2016. Optimum Solar Panel Tilt Angle for Maximum Annual Irradiation 1–10.

NASA, 2017. Prediction Of Worldwide Energy Resource. [WWW Document]. URL <http://power.larc.nasa.gov/> (accessed 12.9.15).

Natural Resources Canada, 2015. Electricity Generation GHG Emissions by Energy Source [WWW Document]. URL <http://oee.nrcan.gc.ca/corporate/statistics/neud/dpa/showTable.cfm?type=HB&sector=egen&juris=00&rn=2&page=4&CFID=1981897&CFTOKEN=748f07dda4ee2cdc-13FB87B5-C490-B3E0-BCC64ED34D798496> (accessed 4.6.18).

Neighbour Power Inc., 2014. Solar Payback in Alberta [WWW Document]. URL <http://neighbourpower.com/solar-payback-in-alberta/> (accessed 4.3.15).

Nowak, S., 2015. Photovoltaic Power Systems Technology Collaboration Programme Annual Report 2015.

NRCan, 2016. About Renewable Energy [WWW Document]. URL <http://www.nrcan.gc.ca/energy/renewable-electricity/7295> (accessed 9.21.16).

NREL, 2016. Community Solar Scenario Tool.

NSERC Smart Microgrid Research Network, 2015. Nsmg-Net [WWW Document]. NSERC. URL [www.smart-microgrid.ca](http://www.smart-microgrid.ca) (accessed 4.7.17).

Nugent, D., Sovacool, B.K., 2014. Assessing the Lifecycle Greenhouse Gas Emissions from Solar PV and Wind Energy: A Critical Meta-survey. Energy Policy 65, 229–244. doi:10.1016/j.enpol.2013.10.048

Paltridge, G.W., Proctor, D., 1976. Monthly mean Solar Radiation Statistics for 189

- Australia. *Sol. Energy* 18, 235–243. doi:10.1016/0038-092X(76)90022-0
- Parida, B., Iniyar, S., Goic, R., 2011. A Review of Solar Photovoltaic Technologies. *Renew. Sustain. Energy Rev.* 15, 1625–1636. doi:10.1016/j.rser.2010.11.032
- Parkinson, G., 2015. Solar Costs Will Fall Another 40% in 2 Years. Here's Why [WWW Document]. URL [cleantechnica.com/2015/01/29/solar-costs-will-fall-40-next-2-years-heres/](http://cleantechnica.com/2015/01/29/solar-costs-will-fall-40-next-2-years-heres/) (accessed 8.2.16).
- Peng, J., Lu, L., Yang, H., 2013. Review on Life Cycle Assessment of Energy Payback and Greenhouse Gas Emission of Solar Photovoltaic Systems. *Renew. Sustain. Energy Rev.* 19, 255–274. doi:10.1016/j.rser.2012.11.035
- Phuangpornpitak, N., Prommee, W., Tia, S., Phuangpornpitak, W., 2010. A Study of Particle Swarm Technique for Renewable Energy Power Systems, in: *Proceedings of the International Conference on Energy and Sustainable Development: Issues and Strategies (ESD 2010)*. pp. 1–6. doi:10.1109/ESD.2010.5598791
- Phuangpornpitak, N., Tia, S., 2013. Opportunities and Challenges of Integrating Renewable Energy in Smart Grid System. *Energy Procedia* 34, 282–290. doi:10.1016/j.egypro.2013.06.756
- Poissant, Y., Dignard-bailey, L., Canada, N.R., 2015. Photovoltaic Technology Status and Prospects: Canadian Annual Report 2014 1–4.
- Powers, L., Newmiller, J., Townsend, T., Engineering, B.E.W., Ramon, S., 2010. Measuring and Modeling the Effect of Snow on Photovoltaic System Performance. *Photovolt. Spec. Conf. (PVSC), 2010 35th IEEE* 973–978.
- Purohit, I., Purohit, P., 2018. Performance assessment of grid-interactive solar photovoltaic projects under India's national solar mission. *Appl. Energy* 222, 25–41. doi:10.1016/j.apenergy.2018.03.135
- PVsyst, 2012. PVsyst Photovoltaic Software [WWW Document]. URL <http://www.pvsyst.com/en/> (accessed 2.5.18).

- Raman, V., Tiwari, G.N., 2009. A Comparison Study of Energy and Exergy Performance of a Hybrid Photovoltaic Double-Pass and Single-Pass Air Collector Vivek. *Int. J. energy Res.* 33, 605–617.
- Ramos, F., Cardoso, A., Alcaso, A., 2010. Hybrid Photovoltaic-Thermal Collectors: A review. *IFIP Adv. Inf. Commun. Technol.* 314, 477–484. doi:10.1007/978-3-642-11628-5\_53
- Ramsami, P., Oree, V., 2015. A Hybrid Method for Forecasting the Energy Output of Photovoltaic Systems. *Energy Convers. Manag.* 95, 406–413. doi:10.1016/j.enconman.2015.02.052
- Rana, M., Koprinska, I., Agelidis, V.G., 2015. 2D-Interval Forecasts for Solar Power Production. *Sol. Energy* 122, 191–203. doi:10.1016/j.solener.2015.08.018
- Reka, S.S., Ramesh, V., 2016. A Demand Response Modeling for Residential Consumers in Smart Grid Environment Using Game Theory Based Energy Scheduling Algorithm. *Ain Shams Eng. J.* 7, 835–845. doi:10.1016/j.asej.2015.12.004
- Reno, M.J., Hansen, C.W., Stein, J.S., 2012. Global Horizontal Irradiance Clear Sky Models: Implementation and Analysis. SANDIA Rep. SAND2012-2389 Unltd. Release Print. March 2012 1–66. doi:10.2172/1039404
- Riffat, S.B., Cuce, E., 2011. A Review on Hybrid Photovoltaic/Thermal Collectors and Systems. *Int. J. Low-Carbon Technol.* 6, 212–241. doi:10.1093/ijlct/ctr016
- Rigollier, C., Bauer, O., Wald, L., 2000. On the Clear Sky Model of the ESRA — European Solar Radiation Atlas — with Respect to the Heliosat Method. *Sol. Energy* 68, 33–48.
- Román, E., Martínez, V., Jimeno, J.C., Alonso, R., Ibañez, P., Elorduizapatarietxe, S., 2008. Experimental Results of Controlled PV Module for Building Integrated PV Systems. *Sol. Energy* 82, 471–480. doi:10.1016/j.solener.2007.09.004
- Romero-Rubio, C., de Andrés Díaz, J.R., 2015. Sustainable Energy Communities: A

- Study Contrasting Spain and Germany. *Energy Policy* 85, 397–409. doi:10.1016/j.enpol.2015.06.012
- Salim, K.M.E., 2017. Design Optimization of Grid Tied Solar Photo-Voltaic (PV) Systems for Flat Roofs. University of Alberta.
- Salom, J. (Irec), Widén, J., Candanedo, J. a, Sartori, I., Voss, K., Marszal, A.J., 2011. Understanding Net Zero Energy Buildings: Evaluation of load matching and grid interaction indicators. *Proc. Build. Simul.* 2011 6, 14–16.
- Salom, J., Marszal, A.J., Widén, J., Candanedo, J., Lindberg, K.B., 2014a. Analysis of Load Match and Grid Interaction Indicators in Net Zero Energy Buildings with Simulated and Monitored data. *Appl. Energy* 136, 119–131. doi:10.1016/j.apenergy.2014.09.018
- Salom, J., Widén, J., Candanedo, J., Lindberg, K.B., 2014b. Analysis of Grid Interaction Indicators in Net Zero-Energy Buildings with Sub-Hourly Collected Data. *Adv. Build. Energy Res.* 136, 1–18. doi:10.1080/17512549.2014.941006
- SAM, 2015. System Advisory Model.
- Sanyo, 2014. HIT Photovoltaic Module, Aurus. Munich.
- Sartori, I., Napolitano, A., Voss, K., 2012. Net Zero Energy Buildings: A Consistent Definition Framework. *Energy Build.* 48, 220–232. doi:10.1016/j.enbuild.2012.01.032
- Schlomer, S., Bruckner, T., Fulton, L., Hertwich, E., McKinnon, A., Perczyk, D., Roy, J., Schaeffer, R., Sims, R., Smith, P., Wiser, R., 2014. Annex III: Technology-Specific Cost and Performance Parameters. *Clim. Chang. 2014 Mitig. Clim. Chang. Contrib. Work. Gr. III to Fifth Assess. Rep. Intergov. Panel Clim. Chang.* 1329–1356. doi:http://report.mitigation2014.org/report/ipcc\_wg3\_ar5\_annex-ii.pdf
- Seljom, P., Lindberg, K.B., Tomasgard, A., Doorman, G.L., Sartori, I., 2016. The Impact of Zero Energy Buildings on the Scandinavian Energy System. *Energy*

118, 284–296. doi:10.1016/j.energy.2016.12.008

Shakouri, M., Lee, H.W., Kim, Y.W., 2017. A Probabilistic Portfolio-Based Model for Financial Valuation of Community Solar. *Appl. Energy* 191, 709–726. doi:10.1016/j.apenergy.2017.01.077

Sharma, D.K., Verma, V., Sing, A.P., 2014. Review and Analysis of Solar Photovoltaic Softwares. *Int. J. Curr. Eng. Technol.* 4, 725–731.

Skoplaki, E., Palyvos, J.A., 2009. Operating Temperature of Photovoltaic Modules: A Survey of Pertinent Correlations. *Renew. Energy* 34, 23–29. doi:10.1016/j.renene.2008.04.009

Sopian, K., Liu, H., Kakac, S., Veziroglu, T., 2000. Performance of a Double Pass Photovoltaic Thermal Solar Collector Suitable for Solar Drying Systems. *Energy Convers. Manag.* 41, 353–365. doi:10.1016/S0196-8904(99)00115-6

Spencer, J.W., 1971. Fourier Series Representation of the Sun. *Search* 2, 172.

Statista, 2015. Global Cumulative Solar PV Capacity at the End of 2015, by Country (In Gigawatts) [WWW Document]. URL <https://www.statista.com/statistics/264629/existing-solar-pv-capacity-worldwide/> (accessed 9.21.16).

Statistics Canada, 2017. The Daily — Physical flow accounts: Energy use and greenhouse gas emissions, 2015. Ottawa, ON, Canada.

Stine, W.B., Harrigan, R.W., 1985. *Solar Energy Fundamentals and Design: with Computer Applications, Illustrate.* ed. John Wiley & Sons, Incorporated, Ann Arbor, Michigan.

Stoll, P., Rizvanovic, L., Rossebø, J.E.Y., 2013. Active House Deployment Architecture for Residential Electricity Customers' Active Interaction with the Smart Grid, in: *22nd International Conference on Electricity Distribution*. Stockholm, Sweden, pp. 10–13.

Sugiura, T., Yamada, T., Nakamura, H., Umeya, M., Sakuta, K., Kurokawa, K., 2003.

- Measurements, analyses and evaluation of residential PV systems by Japanese monitoring program. *Sol. Energy Mater. Sol. Cells* 75, 767–779. doi:10.1016/S0927-0248(02)00132-0
- Sulaiman, S.I., Khawa, T.A., Musirin, I., Shaari, S., 2012. Energy Procedia An Artificial Immune-Based Hybrid Multi-Layer Feedforward Neural Network for Predicting Grid-Connected Photovoltaic System Output 14, 260–264. doi:10.1016/j.egypro.2011.12.927
- Sutabutr, T., 2016. Thailand Smart Grid Development Master Plan, in: Franco-Thai Workshop on Smart Grids. Bangkok, Thailand.
- The Weather Network [WWW Document], 2016. . Calgary Stat. URL <https://www.theweathernetwork.com/ca/forecasts/statistics/alberta/calgary> (accessed 9.8.16).
- Torcellini, P.A., Crawley, D.B., 2006. Understanding Zero-Energy Buildings. *ASHRAE J.* 48.
- Tsao, J., Lewis, N., Crabtree, G., 2006. Solar FAQs, US department of Energy.
- U.S. Energy Information Administration, 2017. Renewable Energy Explained [WWW Document]. URL [https://www.eia.gov/energyexplained/?page=renewable\\_home](https://www.eia.gov/energyexplained/?page=renewable_home) (accessed 1.31.18).
- Ueda, Y., Kurokawa, K., Kitamura, K., Yokota, M., Akanuma, K., Sugihara, H., 2009. Performance Analysis of Various System Configurations on Grid-Connected Residential PV Systems. *Sol. Energy Mater. Sol. Cells* 93, 945–949. doi:10.1016/j.solmat.2008.11.021
- Vivar, M., Clarke, M., Pye, J., Everett, V., 2012. A Review of Standards for Hybrid CPV-Thermal Systems. *Renew. Sustain. Energy Rev.* 16, 443–448. doi:10.1016/j.rser.2011.08.008
- Wales, R., AbouRizk, S., 1996. An Integrated Simulation Model for Construction.

- Simul. Pract. Theory 3, 401–420. doi:10.1016/0928-4869(95)00018-6
- Walker, G., Devine-Wright, P., 2008. Community Renewable Energy: What Should it Mean? *Energy Policy* 36, 497–500. doi:10.1016/j.enpol.2007.10.019
- Walter, I.A., Allen, R.G., Elliott, R., Jensen, M.E., Itenfisu, D., Mecham, B., Howell, T.A., Snyder, R., Brown, P., Echings, S., Spofford, T., Hattendorf, M., Cuenca, R.H., Wright, J.L., Martin, D., 2012. The ASCE Standardized Reference Evapotranspiration Equation. *Am. Soc. Civ. Eng.*
- Weniger, J., Bergner, J., Tjaden, T., Quaschnig, V., 2014. Economics of Residential PV Battery Systems in the Self-Consumption Age, in: 29th European Photovoltaic Solar Energy Conference and Exhibition. Berlin, Germany, pp. 2936–2938.
- Widén, J., 2014. Improved Photovoltaic Self-Consumption with Appliance Scheduling in 200 Single-Family Buildings. *Appl. Energy* 126, 199–212. doi:10.1016/j.apenergy.2014.04.008
- Wiseman, H.J., Bronin, S.C., 2013. Community-Scale Renewable Energy 165.
- Wolf, M., 1976. Performance Analyses of Combined Heating and Photovoltaic Power Systems for Residences. *Energy Convers.* 16, 79–90. doi:10.1016/0013-7480(76)90018-8
- Xu, J.L., Yang, Q.R., Du, M., Chang, Z.Q., 2013. The Studies of Optimal Arranging of the Solar Photovoltaic Battery Array and Optimal Matching of Power System for a Parking Garage. *Appl. Mech. Mater.* 283, 99–107. doi:10.4028/www.scientific.net/AMM.283.99
- Yang, D.J., Yuan, Z.F., Lee, P.H., Yin, H.M., 2012. Simulation and Experimental Validation of Heat Transfer in a Novel Hybrid Solar Panel. *Int. J. Heat Mass Transf.* 55, 1076–1082. doi:10.1016/j.ijheatmasstransfer.2011.10.003
- Yang, W., Tian, C., 2012. Monte-Carlo Simulation of Information System Project Performance. *Syst. Eng. Procedia* 3, 340–345. doi:10.1016/j.sepro.2011.11.039

- Yi-da, Y., 2013. PV Panels Laying Method Study. *Appl. Mech. Mater.* 391, 287–290. doi:10.4028/www.scientific.net/AMM.391.287
- Yin, H.M., Yang, D.J., Kelly, G., Garant, J., 2013. Design and Performance of a Novel Building Integrated PV/Thermal System for Energy Efficiency of Buildings. *Sol. Energy* 87, 184–195. doi:10.1016/j.solener.2012.10.022
- Yona, A., Senjyu, T., Funabashi, T., 2013. Decision Technique of Solar Radiation Prediction Applying Recurrent Neural Network for Short-Term Ahead Power Output of Photovoltaic System. *Smart Grid* ....
- Yu, H., 2016. Interview with Dr. Haitao Yu, Senior Researcher at SolarMax Power Inc.
- Zelinka, I., Rössler, O.E., 2013. *Nostradamus 2013 : Prediction , Modeling.*
- Zhang, Y., Beaudin, M., Taheri, R., Zareipour, H., Wood, D., 2015. Day-Ahead Power Output Forecasting for Small-Scale Solar Photovoltaic Electricity Generators. *IEEE Trans. Smart Grid* 6, 2253–2262. doi:10.1109/TSG.2015.2397003
- Zhou, X., Belcher, W., Dastoor, P., 2014. Solar paint: From Synthesis to Printing. *Polymers (Basel)*. 6, 2832–2844. doi:10.3390/polym6112832

## **Appendix A: Commercial Application–Solar Photovoltaic Optimisation for Commercial Flat Rooftops in Cold Regions<sup>5</sup>**

### **A.1 Overview**

Solar photovoltaic systems are becoming increasingly popular as industries try to decrease their carbon footprint. This chapter presents a generic optimisation framework and examines a case study where a flat rooftop located in Edmonton, Alberta is investigated for the installation of a photovoltaic array. The objectives of this study are to maximise power generation while minimising the system cost. This case study represents a proposed generic framework that fulfills this optimisation problem. Solar power generation per month is forecasted using historical generation data. Panels can be installed at different tilt angles and varying inter-row spacing in order to achieve the optimal design. Designing an effective layout is important when installing solar panels, as the increased shade coverage or the wide variation from the normal angle of the sun can result in a loss of energy generation. Both of the capital cost and payback period for the investment are also important factors when determining whether or not a photovoltaic system layout (inter-row spacing, tilt angle, etc.) is considered optimal. Analytic hierarchy process is used to weigh the decision factors and determine the optimal layout.

### **A.2 Introduction**

Solar photovoltaic (PV) systems generate electricity from the sun for use in any residential or commercial applications. The majority of these systems do not have any

---

<sup>5</sup> A version of this appendix has been published in Proceedings of the 4<sup>th</sup> IEEE conference on Technologies for Sustainability (SusTech 2016) as Awad H, Gül M, Ritter C, Verma P, Chen Y, Salim K, Al-Hussein M, Yu H, and Kasawski K, *Solar Photovoltaic Optimization for Commercial Flat Rooftops in Cold Regions*.  
doi: 10.1109/SusTech.2016.7897140

battery backup equipment, but excess power can be sent to the electric utility system (California Department of Forestry and Fire Protection, 2008). Maximising the generation of a fixed solar panel depends on several parameters, some of which are considered fixed for the lifetime of the panel, while others are dynamic or have a degree of stochasticity. This study focuses on the optimisation of the layout of a commercial flat rooftop solar PV system.

The optimisation of solar PV generation on large roofs involves several parameters, including the system size, the panel inter-row spacing, the panel tilt angles, the amount of shading the panels receive due to roof features or other panels, the loss of generation due to precipitation and snow coverage, the cost of the panel installation, and the energy savings received by the installation and use of the panels. This study proposes a generic framework for solar PV optimisation based on the abovementioned parameters. As a demonstration, a case study of a commercial flat rooftop in Edmonton, Canada is presented in this study. The roof area that will be investigated for the installation of a solar panel array is 50 m in length and width. Edmonton's climate is relatively cold, with an average temperature of  $-20^{\circ}\text{C}$  in January and  $-13^{\circ}\text{C}$  in December, and an average monthly snowfall from November to April ranging from 11 cm to 26 cm (Environment Canada, 2017). The potential for snowfall that can cover the panels and consequentially reduce the generation of energy is an important factor when planning the layout for a solar PV system in cold climates.

As the price of solar panels continues to drop, the method and layout used for the installation of photovoltaic arrays is changing. With more expensive panels, it was necessary to obtain the greatest possible generation from each installed panel, which meant eliminating shading and setting up the panels at the optimal angle of incidence with the sun. With the price per panel becoming more affordable, the optimal setup for a photovoltaic array now may involve using smaller tilt angles and closer spacing, which will decrease the energy yield per panel, due to shading and the angle of incidence of the sun not being perpendicular to the panel, but can increase the total power generated by the array, since more panels can be placed (Grana and Gibbs,

2015). This comparison between methods of designing a solar panel array shows that there are several ways that the effectiveness of the array can be measured. The preferred array design will depend on the ultimate goals of the party installing the panels. Effectiveness can be measured based on the generation produced per panel, the generation produced from the entire array, or the generation produced per unit of capital cost of the array.

One study concerning the installation of a solar array on the roof of a parking garage recognises the approach that, while increasing the number of panels may increase the total radiation received by the panels throughout the year, this is not always the best solution to generate power in a cost-effective manner. Though several options were reached for the installation of the array, the study found that, even though the total generation received throughout the year was slightly less for an option with 28 panels than it was for an option with 35 panels, the 28-panel option should be chosen for the economic benefits (Xu et al., 2013). While this study only considers one calculated spacing for each angle of installation for the solar panels, it does show the importance of considering not only the net power generated by an array, but the economic implications that installing an array with a larger number of panels will have on the study.

The payback period plays a vital role in the decision-making process of investing in solar PV system installations. The solar payback mainly depends upon the initial installations costs, return on investments based on energy outsourced (maximised PV system utilisation), and energy savings achieved by the PV system compared to the nominal consumption patterns (Neighbour Power Inc., 2014).

### **A.3 Proposed Methodology**

To optimise the solar PV system design, the objective function is defined in order to determine several layouts that are considered optimal. The objective function is defined as maximising the total generation by either maximising the number of panels or maximising the per-panel generation at the lowest payback period. Models that

satisfy one or more of these goals are created both through an analysis of the spacing and shading to determine the generation, as well as by determining the economic feasibility of each scenario in terms of capital cost, payback period, and cost of electricity unit generated. Analytic hierarchy process (AHP) is then used to make a decision based on experts' judgement. The California Solar Photovoltaic Installation Guideline is used to define the constraints to be used in the optimisation model (California Department of Forestry and Fire Protection, 2008). Figure A-1 presents the framework proposed for flat rooftop optimisation.

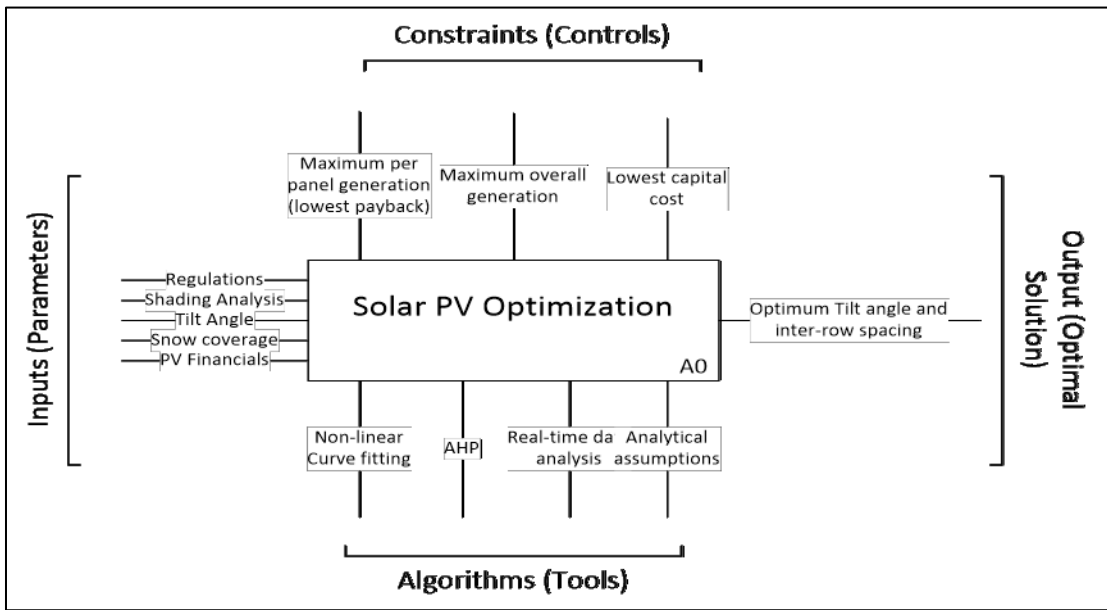


Figure A-1. Proposed framework for the flat rooftop optimisation model.

### A.3.1 *Regulations*

There are many different sets of regulations describing the required access pathways and clearances for solar arrays on varying shapes and sizes of roofs. These regulations will depend on the slope of the roof, the number of residential units contained under the roof or whether it is on a commercial building, and the size of the roof. Since solar PV installation guidelines in Canada have not yet been developed, the California Solar Photovoltaic Installation Guideline was used to define those constraints and plug them into the optimisation model. The strength of the roof must also be

considered, and a plan review is required if a system is to be installed that will occupy more than 50% of the roof area of a residential building (California Department of Forestry and Fire Protection, 2008). In this situation, the panels are to be installed on a flat roof that is 50 m by 50 m in size. The panels may be installed with a tilt angle ranging from 0° to 90° to the roof.

Certain limitations have been implemented by the PV industry for PV installation on roofs due to firefighting suppression techniques. Access and spacing requirements should be observed to provide access to the roof, pathways to specific areas of the roof, emergency egress from the roof, and for an adequate smoke ventilation area. The regulations that apply to the building being investigated in this study include the following: there should be a clear perimeter a minimum of 1.8 m wide around the edges of the roof; the pathways should be straight lines no less than 1.2 m clear of skylights or ventilation hatches, or to roof standpipes; the arrays should be no greater than 45.7 m long in either axis, before a 2.4 m wide pathway (or a 1.2 m wide pathway if it is bordering a skylight or ventilation hatch at least every 6 m on alternating sides of the pathway) is installed. In this study, the array will require a 1.2 m clearance around the edge of the roof, with one 2.4 m wide pathway running in each direction through the center of the roof area.

#### A.3.2 *Shading Analysis and Sun Angles*

There are several parameters that result from the chosen layout of the panels that need to be calculated and used in the design, including the amount of inter-row spacing necessary to result in no shade ( $d$ ), and the shaded length of the panel ( $x$ ), if the desired spacing is closer, in order to calculate the energy lost due to shading. Figure A-2 shows a typical layout for the solar panels and some important parameters. In Figure A-2,  $\theta$  is the tilt angle of the solar panel to the horizontal,  $\gamma$  is shade angle of the sun,  $l$  is the length of the solar panel,  $d$  is the desired spacing of the solar panels (with shading), and  $\delta$  is the footprint of the panel. Eq. A-1 to Eq. A-3 are derived and used to calculate the annual generation for the panels in different layouts (Xu et al., 2013). Due to the unavailability of bypass diodes at each cell of the installed modules,

the shading may highly impact the generation of the overall module due to the fact that all cells are installed in series. Consequently, future field experimentation of shading will be explored and results will be implemented in the proposed framework.

$$d = l * (\cos\theta + \sin\theta * \cot\gamma) \quad (\text{A-1})$$

$$x = [(d - D) * \sin\gamma] / [\sin(180 - \gamma - \theta)] \quad (\text{A-2})$$

$$\text{energy generated} = [1 - (x / l)] * 100\% \quad (\text{A-3})$$

The shade angle of the sun ( $\gamma$ ) varies as the earth revolves around itself every 24 hours and around the sun every 365 days. Kreider et al. (1989) suggest to consider the sun as the moving object with regard to the Earth to better understand the sun declination, azimuth, and altitude. Calculations using Eq. A-4 to Eq. A-7 are applied to derive the shade angle of the sun at different months of the year in Edmonton. The shade angle ( $\gamma$ ) is redefined as *ALT* in Eq. A-4 to represent the sun altitude angle. To simplify the optimisation problem of this research, the altitude angle of the sun at the solar noon on the 21<sup>st</sup> of each month is considered for the following monthly calculations (Kreider et al., 1989; Stine and Harrigan, 1985).

$$ALT = \sin^{-1}[\cos(DEC) \times \cos(LAT) \times \cos(HOUR) + \sin(DEC) + \sin(LAT)] \quad (\text{A-4})$$

$$DEC = -23.45^\circ \times \cos[0.986 \times (DOY + 10.5)] \quad (\text{A-5})$$

$$AZM = \sin^{-1}[\cos(DEC) \times \sin(HOUR) / \cos(ALT)] \quad (\text{A-6})$$

$$INC = \cos^{-1}[\cos(DEC) \times \cos(LAT - TILT) \times \cos(HOUR) + \sin(DEC) \times \sin(LAT - TILT)] \quad (\text{A-7})$$

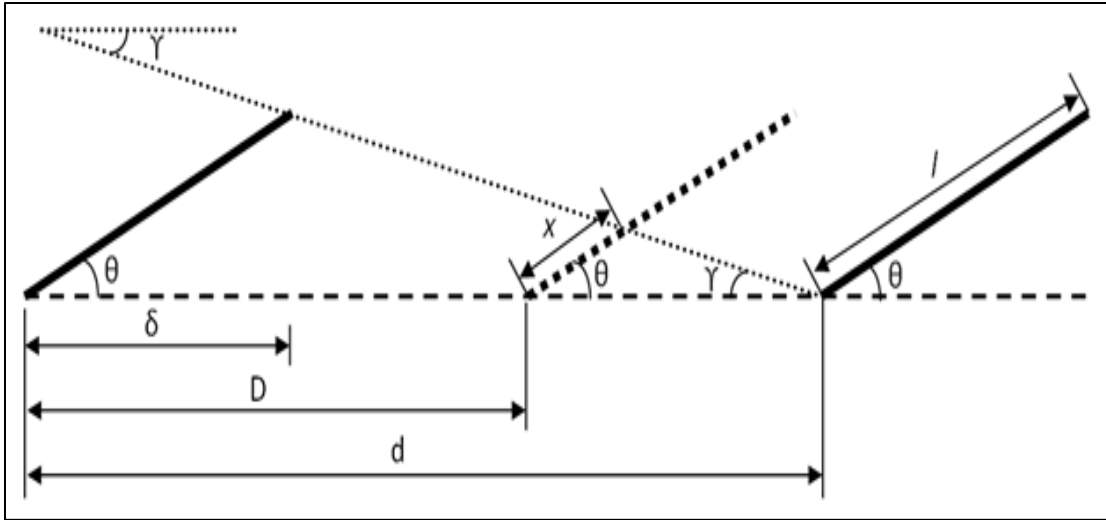


Figure A-2. Solar panel layout and parameters for row spacing.

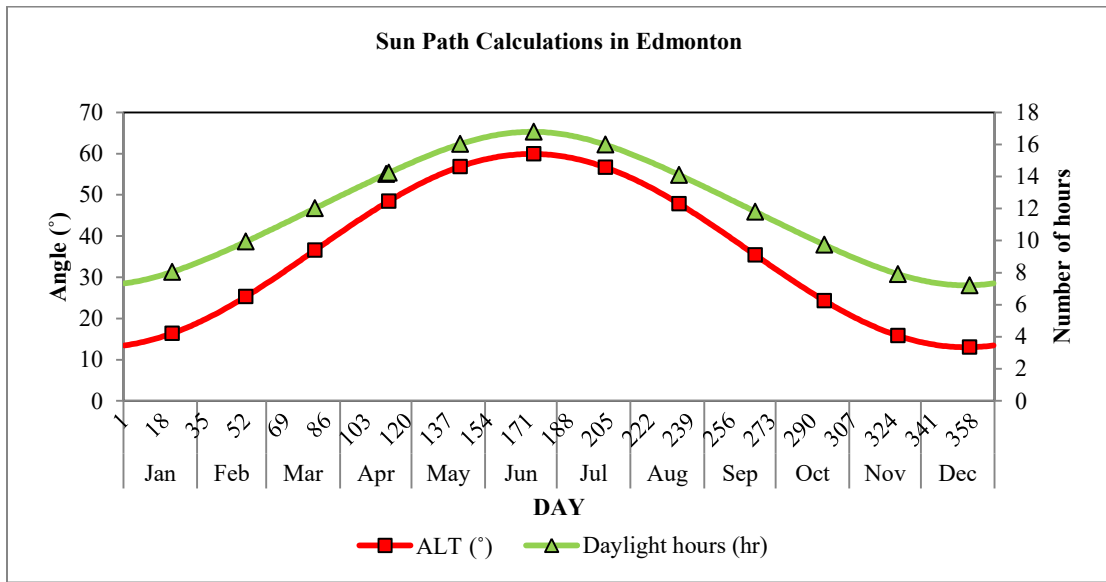


Figure A-3. Solar altitude, declination, and daylight hour calculations in Edmonton over one year.

where, *ALT* is the altitude angle measured above the horizon; *DEC* is the solar declination (derived from Eq. A-5); *LAT* is the latitude; *HOUR* is the solar hour angle; *DOY* is the corresponding day of the year counted from January 1; *AZM* is the solar azimuth angle; *INC* is the inclination angle between beam radiation from the sun

and a line constructed perpendicular to the PV panel surface; and *TILT* is the tilt angle of the PV panel measured from the horizontal.

Figure A-3 shows the diurnal sun altitude angles and daylight hours derived from Eq. A-4 to Eq. A-7. Edmonton is located on the approximate latitude of  $53.53^\circ$  north (and longitude of  $113.5^\circ$  west, yet latitude is not a factor here), thus not only is the severe cold weather a challenge, but also the variance of daylight hours and the sun altitude, which can range from 7.2 hours and  $13.0^\circ$  in the winter solstice and 16.8 hours and  $59.9^\circ$  in the summer solstice.

Due to the wide range of the sun altitude angles and the daylight hours, the decision on the solar PV tilt angle and inter-row spacing to avoid shading and to obtain the highest PV system utilisation (and thus lowest per-panel cost) becomes even more challenging, and the authors have found multiple system configurations where each configuration can serve a specific objective: lowest payback period, lowest per-panel cost, highest generation per panel, or highest generation per area. Details pertaining to each configuration are explained in the following sections.

### A.3.3 *Solar PV Generation in Edmonton*

Real-time, one-minute data of 120 existing solar PV systems in Alberta, 60 of which are in Edmonton, is collected, cleaned, and analysed to determine the optimal tilt and azimuth angles for Alberta in general and Edmonton in particular. It was found that in order to maximise a solar PV generation ( $1,350 \text{ kWh/kW}_p$ ), the panel should be placed facing south ( $180^\circ$ ) at a  $50^\circ$  tilt angle. The real-time values were cross-checked with the commercial PV prediction software, PVWatts (Dobos, 2014) as shown in Figure A-4.

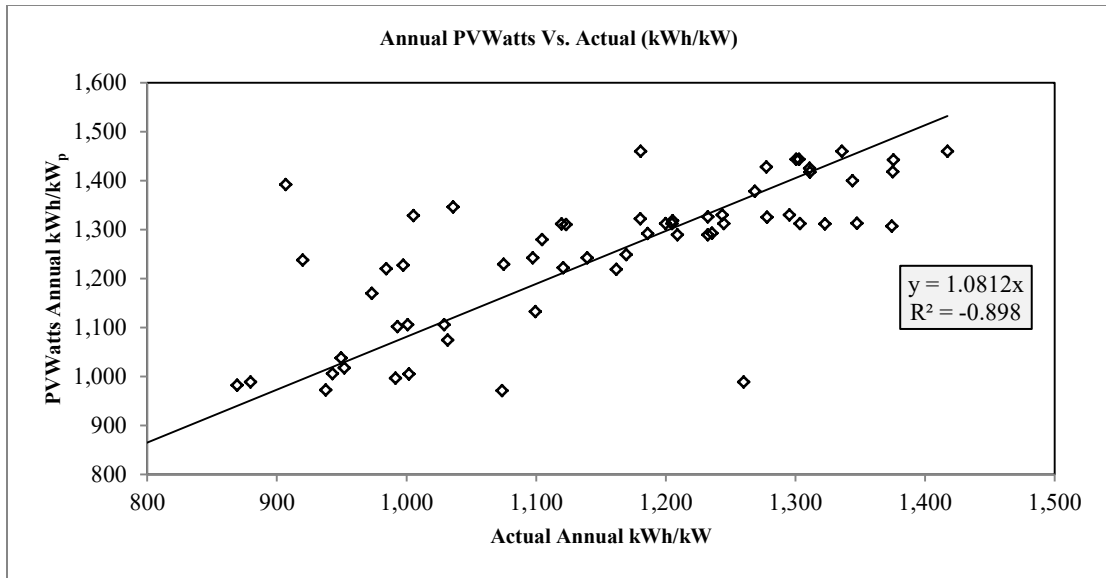


Figure A-4. A comparison between the annual actual PV generation and PVWatts (kWh/kW<sub>p</sub>).

PVWatts	0(0)	10 (0.17)	20(0.36)	30(0.58)	40(0.84)	50(1.19)	60(1.73)	70(2.74)	80(5.67)	90
N	0.759	0.659	0.563	0.476	0.398	0.335	0.298	0.283	0.271	0.261
NNE	0.759	0.667	0.579	0.499	0.428	0.373	0.341	0.320	0.304	0.289
NE	0.759	0.690	0.621	0.559	0.506	0.465	0.433	0.406	0.380	0.355
ENE	0.759	0.723	0.685	0.648	0.614	0.582	0.550	0.517	0.483	0.445
E	0.759	0.760	0.756	0.746	0.729	0.706	0.677	0.640	0.597	0.548
ESE	0.759	0.797	0.823	0.836	0.835	0.823	0.797	0.756	0.708	0.646
SE	0.759	0.827	0.878	0.911	0.923	0.918	0.896	0.854	0.798	0.726
SSE	0.759	0.845	0.913	0.958	0.980	0.980	0.959	0.916	0.853	0.773
S	0.759	0.851	0.924	0.973	0.998	1.000	0.979	0.937	0.872	0.787
SSW	0.759	0.844	0.910	0.954	0.975	0.976	0.955	0.912	0.850	0.770
SW	0.759	0.824	0.871	0.902	0.915	0.910	0.886	0.845	0.789	0.719
WSW	0.759	0.792	0.814	0.826	0.824	0.811	0.784	0.745	0.696	0.637
W	0.759	0.755	0.747	0.733	0.715	0.691	0.661	0.625	0.583	0.536
WNW	0.759	0.718	0.675	0.635	0.599	0.565	0.534	0.502	0.468	0.432
NW	0.759	0.686	0.613	0.547	0.493	0.452	0.420	0.393	0.368	0.344
NNW	0.759	0.665	0.574	0.491	0.419	0.364	0.331	0.312	0.297	0.283

Figure A-5. Solar PV system efficiency at different tilt angles and orientations in Edmonton.

After comparing and validating the field data with PVWatts software the second step is to perform sensitivity analysis on the effect of changing the tilt angle by 10-degree increments from 0° (flat) to 90° (vertical) at different months in a normalised fashion.

Figure A-5 shows that the optimum configuration for installing a PV system for maximised generation is at a tilt angle of 50° and a south facing orientation (180°).

Installing a south facing PV system at a 90° tilt angle results in a PV system efficiency of 79%. Also, it is worth pointing out that if a south (or near south) orientation is not applicable for installation, then, in this case, a flat-mount system at a 76% efficiency would be a considerable solution.

The constant parameters for the array are set first, and include: (i) the minimum inter-row spacing for maintenance and fire safety requirements (California Department of Forestry and Fire Protection, 2008), (ii) the optimum tilt angle for normal incidence of solar radiation, (iii) the maximum system size based on the structural stability of the roof, and (iv) the cost of panel mounting for each panel based on the tilt angle of the installed array. The minimum inter-row spacing is set at 1.245 m to satisfy maintenance requirements, and the installation costs are assumed to be constant, regardless of the tilt angle.

To determine the layouts for the PV array, the likely generation for each panel for each month is forecasted for tilt angles ranging from 0° to 90°. The yearly generation is then calculated for each angle and varying inter-row spacing. Using the forecasted generation per month, and including any generation loss due to shading if the spacing is less than the minimum spacing for no shade for that month, the yearly generation for landscape-oriented panels can be calculated.

#### A.3.4 *Snow Coverage Loss Factors*

Since Edmonton is well known for its severe weather in winter months (assumingly November to February), snow coverage factors should be considered in the optimisation model. A study conducted by Northern Alberta Institute of Technology (NAIT) (2015) showed the effect of snow coverage on solar PV's mounted at different tilt angles.

The study was conducted on two identical PV systems having tilt angles of 14°, 18°, 27°, 45°, 53°, and 90°. Those identical PV systems were monitored for their solar power generation where one system was cleared out after each heavy snow, and the other system was kept covered with snow. The results have shown that the system

loss factors due to snow coverage were 5.18%, 5.24%, 4.15%, 1.92%, 1.53%, and 0.82% for the solar PV systems at 14°, 18°, 27°, 45°, 53°, and 90°, respectively.

Because these angles investigated at NAIT were different from the angles used in the optimisation model, a forecasting model was developed to determine the snow coverage factors on the tilt angles in 10-degree intervals by applying a non-linear curve-fitting technique as shown in Figure A-6.

#### **A. 4 Photovoltaic Array Layout Models**

Of the parameters that are involved in setting up a solar PV panel system on a flat rooftop, some can be set as constants by either the owner of the building, the installation company, or the team designing the array layout. These constant parameters include the minimum inter-row spacing for maintenance and fire safety requirements, the optimum tilt angle for normal incidence of solar radiation (50° angle), the maximum system size based on the structural stability of the roof, and the cost of panel mounting for each panel based on the tilt at which it will be installed. These known values will help set either constants or constraints in the optimisation model. For this particular roof area, it was assumed that the strength would be able to handle as many panels as were desired. The minimum panel spacing was set at 1.245 m (California Department of Forestry and Fire Protection, 2008) to satisfy maintenance requirements, and the installation costs were assumed to be constant, regardless of the tilt angle.

To determine the layouts for the PV array, the likely generation for each panel for each month of the year was forecasted for tilt angles ranging from 0° to 90°, as was discussed earlier. The yearly generation was then calculated for each angle and varying row spacing. Using the forecasted generation per month, and including any generation loss due to shading if the spacing was less than the minimum spacing for no shade for that month, the yearly generation can be calculated. It was assumed that the generation loss was directly proportional to the length of the panel that was shaded. Figure A-7 shows the yearly generation, for varying row spacing and tilt

angles, for the entire array that will fit on the roof space if the panels are installed with a landscape orientation. Figure A- 8 shows the per panel generation for panels installed with a landscape orientation for varying row spacing and tilt angles.

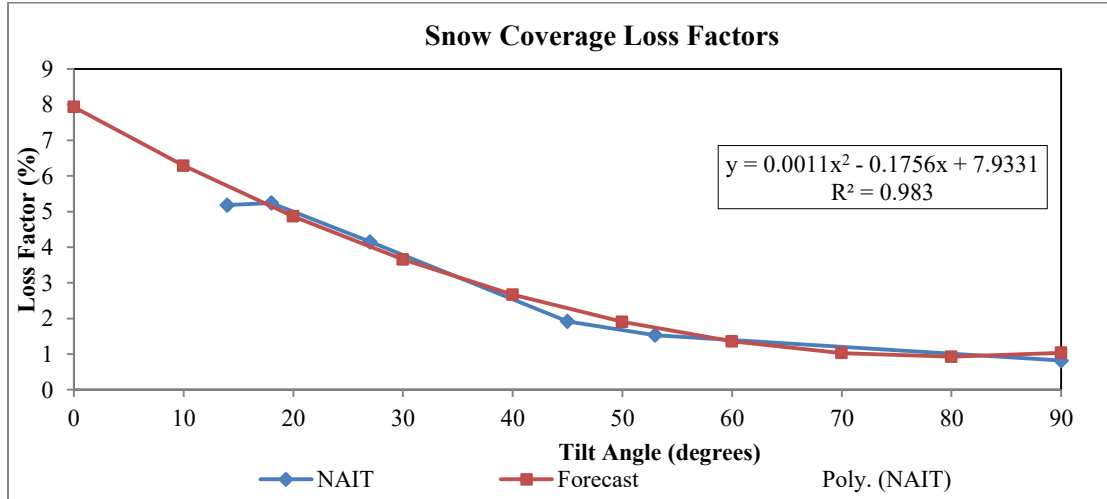


Figure A-6. Actual and forecasted snow coverage efficiency factors of solar PV generation on different tilt angles.

It can be seen that even though the yearly per-panel generation for closely spaced panels placed at a 90° angle is quite low compared to that of relatively widely spaced panels placed at a 50° angle, the total array generation is highest because of the increased number of panels that can be fit on the roof. The per-panel generation is highest at a tilt angle of 50°, as was expected, and at a spacing of 4 m, which provides no shade during any month of the year.

Figure A-9 shows the yearly generation, for varying row spacing and tilt angles, for the entire array that will fit on the roof space if the panels are installed with a portrait orientation. Figure A-10 shows the per panel generation for panels installed with a portrait orientation for varying row spacing and tilt angles. As was true for the landscape panels, the highest array generation results from the panels installed with a 90° tilt and at the minimum spacing, and the highest per panel generation is for the panels installed at a 50° tilt at a row spacing that results in no shade in any month of the year. There were four array layouts that were considered to be optimal based on

the amount of power that they generated. The optimal array layouts in terms of power generation are summarised in Table A-1.

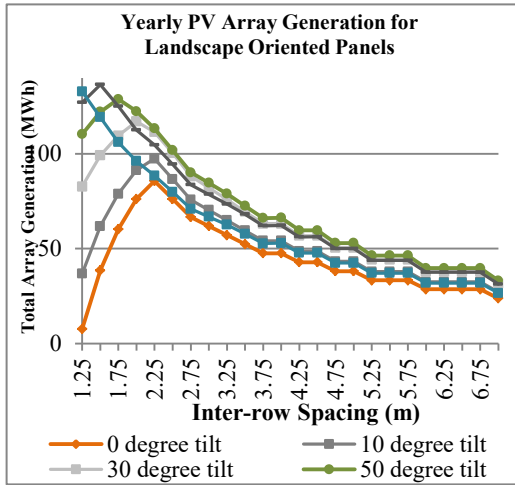


Figure A-7. Yearly total array generation based on panel tilt and row spacing for landscape-oriented panels.

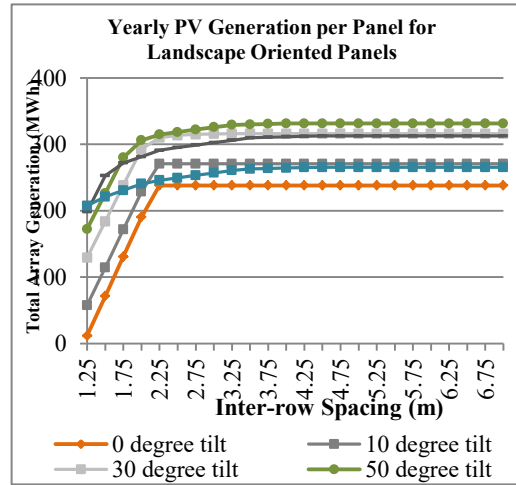


Figure A-8. Yearly generation per panel based on panel tilt and row spacing for landscape-oriented panels.

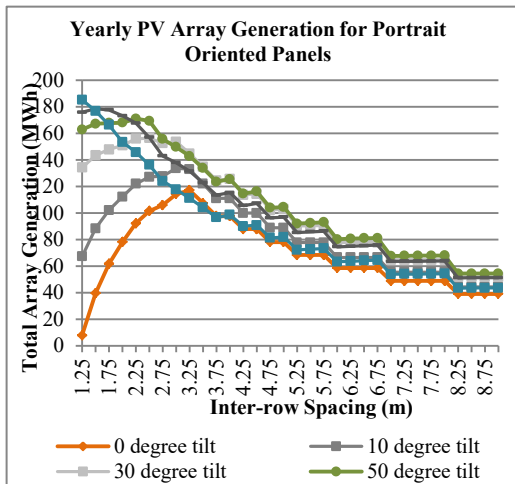


Figure A-9. Yearly total array generation based on panel tilt and row spacing for portrait-oriented panels.

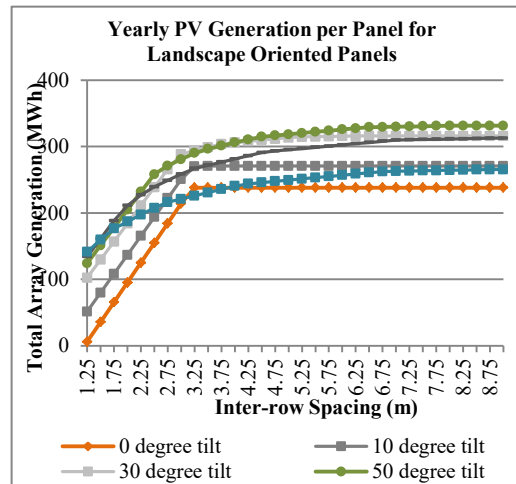


Figure A-10. Yearly generation per panel based on panel tilt and row spacing for portrait-oriented panels.

## A. 5 Payback Period Analysis

The integral factors affecting the solar payback period are the cost of energy from the grid and the cost of solar power installation. The province of Alberta has a good combination of high sun exposure, low temperatures, and very expensive electricity billing rates, which makes Alberta a prime location for solar PV installation, as investors are likely to receive returns within a short span of time (Neighbour Power Inc., 2014).

By using these costs and revenues associated with solar panel installation and operation, the savings per year can be obtained based on some assumptions. It was assumed that self-consumption from the solar grid in Alberta would be 75% of the generation, the grid export would be 25% of the generation, and the electricity consumption would be 25% of the generation. The panels in the array were assumed to be 5 kW solar panels with a panel capacity of 250 W. The following equations (Eq. A-8 to Eq. A-10) can then be derived to calculate the costs and savings associated with the varying solar panel array layouts, characterised by the number of panels, panel tilt, and row spacing:

$$\begin{aligned} Savings_{Yr,n} = & Generation_{Yr,n} \times (Self\ Consumption\ Factor \times \\ & C/100 + Grid\ Export\ Factor \times \\ & E/100 - Electricity\ Consumption\ Factor \times C/100) \end{aligned} \quad (A-8)$$

$$I_t = No.\ of\ Panels \times Panel\ Capacity \times I_w \quad (A-9)$$

$$Payback\ Period = I_t / Savings\ per\ year \quad (A-10)$$

where,  $C$  is the total consumption cost,  $I_t$  is the total installation cost,  $I_w$  is the installation cost per watt, and  $E$  is the export revenue. As was stated in the assumptions, the self-consumption factor is 75%, the grid export factor is 25%, and the electricity consumption factor is 25%. It is also assumed that a degradation rate of 0.5% would impact the solar PV system generation each year.

In order to determine the payback period over the lifetime of a solar PV system, which lasts for an average of 20–25 years, it is important to determine the long-term economic feasibility of that system. As explained in Table A-2, the total consumption cost is 12.43 ¢/kWh and the export revenue is 8 ¢/kWh, while the inflation rate for the electricity price in general is 3.5% (Neighbour Power Inc., 2014). According to the standard test conditions (STC) of most solar PV’s the degradation rate of power generation is 0.5%.

Table A-1. Summary of optimal array layouts.

Layout	No. of Panels	Tilt Angle	Inter-Row Spacing	Array Generation per Annum	Generation per Panel per Annum	Capital Cost	Payback Period
		°	m	MWh	kWh	\$k	year
1 <sup>a</sup>	600	90	1.25	137	207	495	44
2 <sup>b</sup>	1,353	90	1.25	190	140	1,015	65
3 <sup>c</sup>	200	50	4	66	331	150	28
4 <sup>d</sup>	205	50	8	68	331	154	28

<sup>a</sup>Layout 1 provides the maximum array generation with landscape-oriented panels

<sup>b</sup>Layout 2 provides the maximum array generation with portrait-oriented panels

<sup>c</sup>Layout 3 provides the maximum generation per panel with landscape-oriented panels

<sup>d</sup>Layout 4 provides the maximum generation per panel with portrait-oriented panels

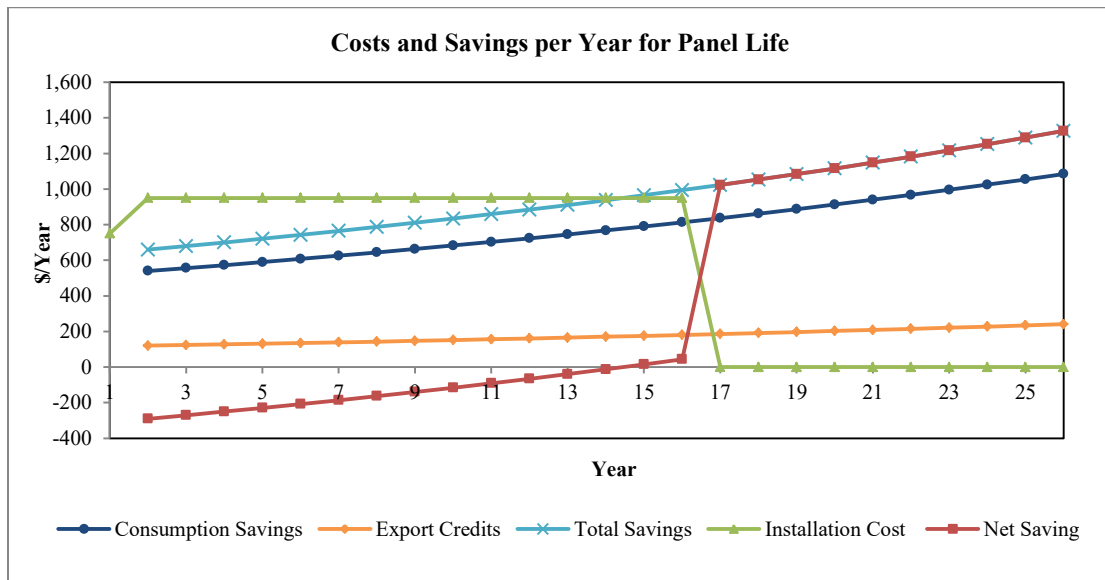


Figure A-11. Associated yearly costs and savings over 25 years of a photovoltaic system’s life (Energy Informative, 2016).

Table A-2. Summary of solar panel costs and revenue (Energy Informative, 2016).

Variable Charges for Grid Energy		Revenue for Exporting to Grid	
Energy Cost	8.35 ¢/kWh	Export Revenue (E)	8 ¢/kWh
Delivery Cost	2.84 ¢/kWh		
Local Access Fee	1.24 ¢/kWh	Installation Cost (I)	\$3/W <sub>p</sub>
Total Consumption Cost (C)	12.43 ¢/kWh		

Figure A-11 demonstrates the costs and savings for a PV system’s life over 25 years. A relaxed model of a small system ( $250 \text{ W} \times 20 \text{ panels} \times 1,200 \text{ kWh/kW}_p = 6,000 \text{ kW}_p$ ) was used for the purpose of demonstration. It is also assumed that the payback period is 15 years, where aftermath net saving jumps to \$1,000 in year 16, and \$1,300 in year 25.

Payback period analysis is conducted for Solar PV's installed in landscape and portrait orientations for different panel spacing and the results for payback period are depicted in Figure A-12 and Figure A-13. It can be seen in these graphs that the payback period is the shortest for the array layouts that have the highest generation per panel, which have a panel angle of  $50^\circ$  and a row spacing of 4 m for the landscape-oriented layout, and 8 m for the portrait-oriented layout. The optimal layouts in terms of the shortest payback period, while still fully utilising the available space on the rooftop, are the same as the layouts for the maximum generation per panel.

It is observed that the minimum payback depends significantly on the generation in a particular year and the installation cost for the panels at various panel spacing. The analysis of payback period for different row spacing and panel angle shows that the payback period reduces with increased spacing between the row panels and a minimum payback period of 27.6 years can result for both the landscape and portrait-oriented panels. The optimal layouts for the shortest payback periods have a panel angle of  $50^\circ$  and spacing of 4 m and 8 m for the landscape and portrait orientations, respectively.

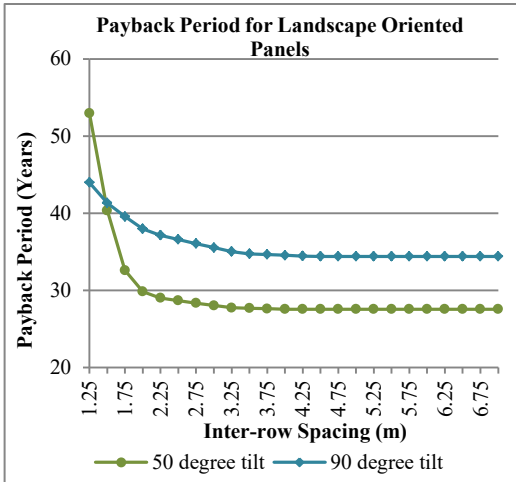


Figure A-12. Payback period for different array layouts for landscape-oriented panels.

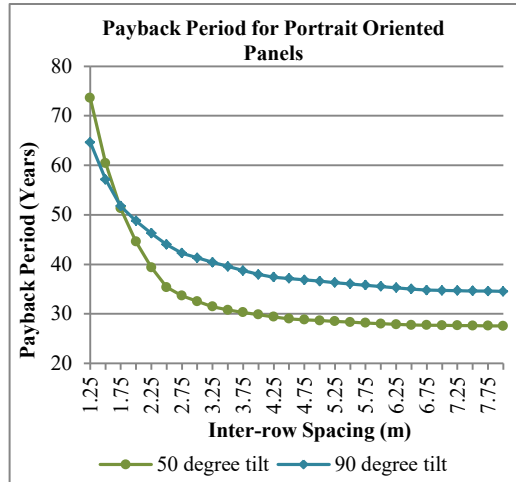


Figure A-13. Payback period for different array layouts for portrait-oriented panels.

The payback period is dependent upon the year of installation as shown in Figure A-14. From 2014 to 2017, the payback period is decreasing for all the layout configurations as the solar costs are estimated to fall by 40% from 2015 to 2017 (Parkinson, 2015).

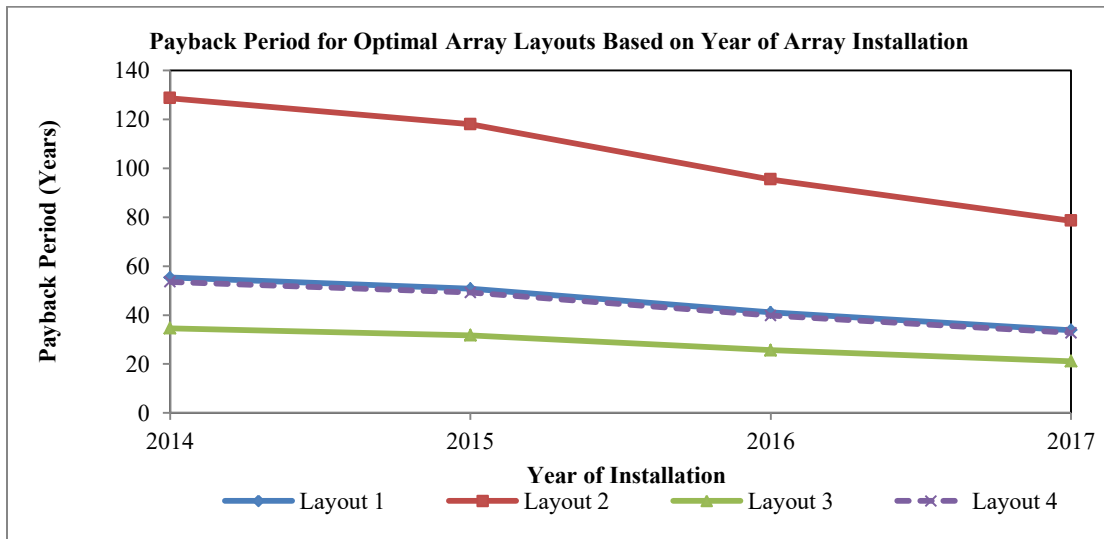


Figure A-14. Payback period for the four optimal layouts previously determined, based on the year that the array is installed and the initial investment is made.

As shown in Figure A-14, the payback period reduces from 26.0 years in 2016 to 21.1 years in 2017 based on the year of panel installation. As the costs for installation reduce due to polysilicon price reductions and government subsidies, it is eminent that the payback period will continue to reduce in the future.

#### **A. 6 Analytic Heirarchy Process**

Several criteria are used to determine the ideal layout, including the length of the payback period, the capital cost of the array and its installation, the total array generation, and the generation per panel in the array. These criteria are ranked in a pairwise comparison, and then each model is ranked on how well it satisfies the desired requirements as summarised previously in Table A-1. The pairwise comparison between the different criteria is reached based on the judgement of a group of experts (Yu, 2016) and ranks the payback period as the most important metric followed by the per panel generation, the capital cost of the entire array, and finally the total array generation. The consistency index is calculated for each matrix to ensure that it is less than 0.1, to indicate that the rankings are consistent. The weighted rankings are then found for each model, and can be seen in Table A-3.

#### **A. 7 Discussion and Conclusion**

Several models are created, all of which represent different solutions which could be considered optimal, depending on how the goal for the study is defined. The first set of models find optimal layouts based on the generation (either the total generation or the per-panel generation). The payback period for each possible array layout is then calculated, and it is found that the shortest payback periods are for the same layouts as those which produce the maximum per-panel generation. To determine which solution provides the best outcome based on the requirements that an optimal system must meet, analytic hierarchy process is used. This process results in the conclusion that the landscape oriented panels installed with a tilt angle of 50° and an inter-row spacing of 4 m are the optimal layout for the solar PV array.

Table A-3. AHP rankings for the four optimal array layouts.

	Weight	Layout 1 <sup>a</sup> .	Layout 2 <sup>b</sup> .	Layout 3 <sup>c</sup> .	Layout 4 <sup>d</sup> .
Payback Period	0.492	0.108	0.039	0.427	0.427
Capital Cost	0.143	0.091	0.039	0.509	0.361
Total Array Generation	0.049	0.234	0.557	0.105	0.105
Generation Per Panel	0.316	0.130	0.105	0.382	0.382
Total Weighted Score		0.546	0.553	0.649	0.640

<sup>a</sup>Layout 1 provides the maximum array generation with landscape oriented panels

<sup>b</sup>Layout 2 provides the maximum array generation with portrait oriented panels

<sup>c</sup>Layout 3 provides the maximum generation per panel with landscape oriented panels

<sup>d</sup>Layout 4 provides the maximum generation per panel with portrait oriented panels

Since the proposed PV system is very large, ranging between 200 and 1,353 panels, and since no incentives are considered in this study, it is observed that the payback period is very long, averaging 27 to 28 years. Adding more credits such as renewable energy credits (REC) at a rate of 2.5 c/kWh generated, tax benefits of up to 50%, and other subsidy options can significantly reduce installation cost and thus reduce the payback period.

## A. 8 Future Recommendations

To optimise the solar PV system design, the objective may vary according to the decision maker's perception, which in turn may result in more than one objective. This is called multi-criteria optimisation (Zelinka and Rössler, 2013), but for the time constraints of this study, an analytical hierarchy process (AHP) is employed to make a decision based on experts' judgement. In the future, a multi-objective model using Particle Swarm Optimisation (PSO) algorithm will be developed to identify the best solution. It is also recommended to use a combination of different tilt angles and inter-row spacing in the search for maximised generation and reduced cost. PV rows that are backed with a parapet, chimneys, and stairwell towers can be mounted at higher tilt degrees since shading will not be a constraint in this case.

The PSO model will include detailed cost analysis that involves a breakdown of PV system item costs, maintenance cost, real-time electricity cost, and other applicable

incentives such as renewable energy credit (REC), subsidies, etc. In addition, based on the monitored historical data of energy generation in five cities in Alberta, the model will be generalised for applicability to cities other than Edmonton. Field experimentation of partial shading and diffuse irradiance effect on series-connected solar PV modules will be carried out in search for more model validation and more accurate objective criteria for the future optimisation model. Other types of solar PV's can be used in the future, such as roll-out solar panels (Futurism, 2016), panels on one- or two-directional sun-tracking systems (Linak, 2016), concave solar panels (also known as concentrating solar power (CSP) collectors) (De Oliveira Siqueira et al., 2014), and solar paint (Zhou et al., 2014); however, these systems are new to the market and may cause significant increase in payback periods and maintenance issues, except for the roll-out panels, which incur less installation cost and time and thereby reduce the payback period greatly.

## Appendix B: List of Publications

### B.1 Journal papers

- (1) **Awad, H.**, Gül, M., and Al-Hussein, M. “Long-term Performance and GHG Emission Offset Analysis of Small-scale Grid-tied Residential Solar PV Systems in Northerly Latitudes.” Submitted for publication in *Applied Energy Journal*.
- (2) **Awad, H.** and Gül, M. “Optimisation of Community Shared Solar Application in Energy Efficient Communities using Monte Carlo Simulation.” Submitted for publication in *Sustainable Cities and Society Journal*.
- (3) **Awad, H.** and Gül, M. “Load-match-driven design improvement of solar PV systems and its impact on the grid.” Under review for publication in *Solar Energy Journal*.
- (4) **Awad, H.**, Gül, M., Salim, K.M.E., and Yu, H. (2017) "Predicting the energy production by solar photovoltaic systems in cold-climate regions." *International Journal of Sustainable Energy*, doi: 10.1080/14786451.2017.1408622
- (5) Li, H.X., Gül, M., Yu, H., **Awad, H.**, and Al-Hussein, M. (2016). “An energy performance monitoring, analysis and modelling framework for NetZero Energy Homes (NZEHS).” *Energy and Buildings*, 126, 353-364.
- (6) Li, Y., Yu, H., Sharmin, T., **Awad, H.**, and Gül, M. (2016). “Towards energy-efficient homes: Evaluating the hygrothermal performance of different wall assemblies through long-term field monitoring. *Energy and Buildings*, 121, 43-56.
- (7) **Awad, H.**, Gul, M., Zaman, H., Yu, H., and Al-Hussein, M. (2014) “Evaluation of the thermal and structural performance of potential energy

efficient wall systems for mid-rise wood-frame buildings.” *Energy and Buildings*, 82, 416-427.

## **B. 2 Conference papers**

- (1) Secchi L., **Awad, H.**, Salim, K.M.E., Gul, M., and Knudson R. (2018). “Hygrothermal field testing of multi-functional wood fibre panels for residential buildings.” *Proceedings, 1<sup>st</sup> International Conference on New Horizons in Green Civil Engineering (NHICE-01)*, Victoria, BC, Canada, April 25–27, 2018.
- (2) **Awad, H.**, Gül, M., and Yu, H. (2017). “Load-match-driven design improvement of solar PV systems and its impact on the grid with a case study.” *Proceedings, 5<sup>th</sup> IEEE Conference on Technologies for Sustainability*, Phoenix, AZ, USA, Nov. 12-14.
- (3) **Awad, H.**, Gül, M., Ritter, C., Verma, P., Chen, Y., Yu, H., Kasawski, K., Salim, K. E., and Al-Hussein, M. (2016). “Solar photovoltaic optimization for commercial flat rooftops in cold regions.” *Proceedings, 4<sup>th</sup> IEEE Conference on Technologies for Sustainability*, Phoenix, AZ, USA, Oct. 9-11.
- (4) Salim, K.M.E., **Awad, H.**, Gül, M., Knudson, R., and Al-Hussein, M. (2016). “An experimental framework for investigating the hygrothermal properties of multi-functional wood fibre and XPS panels for residential buildings.” *Proceedings, Modular and Offsite Construction (MOC) Summit*, Edmonton, AB, Canada, Sep. 29-Oct. 1, pp. 266-273.
- (5) **Awad, H.**, Gul, M., Zaman, H., Yu, H., and Al-Hussein, M. (2014) “Evaluation of the thermal and structural performance of potential energy efficient wall systems for mid-rise wood-frame buildings.” *Proceedings, Construction Research Congress*, 2255-2265.